Functional Data Analysis in Orthogonal Designs with Applications to Gait Patterns

Bairu Zhang

School of Mathematical Sciences

Queen Mary, University of London

Queen Mary
University of London

Submitted in partial fulfillment of the requirements of the Degree of

Doctor of Philosophy

Statement of originality

I, Bairu Zhang, confirm that the research included within this thesis is my own work or that where it has been carried out in collaboration with, or supported by others, that this is duly acknowledged below and my contribution indicated. Previously published material is also acknowledged below.

I attest that I have exercised reasonable care to ensure that the work is original, and does not to the best of my knowledge break any UK law, infringe any third party's copyright or other Intellectual Property Right, or contain any confidential material.

I accept that the College has the right to use plagiarism detection software to check the electronic version of the thesis.

I confirm that this thesis has not been previously submitted for the award of a degree by this or any other university.

Signature:

Date:

Abstract

This thesis presents a contribution to the active research area of functional data analysis (FDA) and is concerned with the analysis of data from complex experimental designs in which the responses are curves. High resolution, closely correlated data sets are encountered in many research fields, but current statistical methodologies often analyse simplistic summary measures and therefore limit the completeness and accuracy of conclusions drawn. Specifically the nature of the curves and experimental design are not taken into account. Mathematically, such curves can be modelled either as sample paths of a stochastic process or as random elements in a Hilbert space. Despite this more complex type of response, the structure of experiments which yield functional data is often the same as in classical experimentation. Thus, classical experimental design principles and results can be adapted to the FDA setting.

More specifically, we are interested in the functional analysis of variance (ANOVA) of experiments which use orthogonal designs. Most of the existing functional ANOVA approaches consider only completely randomised designs. However, we are interested in more complex experimental arrangements such as, for example, split-plot and row-column designs. Similar to univariate responses, such complex designs imply that the response curves for different observational units are correlated.

We use the design to derive a functional mixed-effects model and adapt the classical projection approach in order to derive the functional ANOVA. As a main result, we derive new functional F tests for hypotheses about treatment effects in the appropriate strata of the design. The approximate null distribution of these tests is derived by applying the Karhunen-Loève expansion to the covariance functions in the relevant strata. These results extend

existing work on functional F tests for completely randomised designs.

The methodology developed in the thesis has wide applicability. In particular, we consider novel applications of functional F tests to gait analysis. Results are presented for two empirical studies. In the first study, gait data of patients with cerebral palsy were collected during barefoot walking and walking with ankle-foot orthoses. The effects of ankle-foot orthoses are assessed by functional F tests and compared with pointwise F tests and the traditional univariate repeated-measurements ANOVA. The second study is a designed experiment in which a split-plot design was used to collect gait data from healthy subjects. This is commonly done in gait research in order to better understand, for example, the effects of orthoses while avoiding confounded analysis from the high variability observed in abnormal gait. Moreover, from a technical point of view the study may be regarded as a real-world alternative to simulation studies. By using healthy individuals it is possible to collect data which are in better agreement with the underlying model assumptions.

The penultimate chapter of the thesis presents a qualitative study with clinical experts to investigate the utility of gait analysis for the management of cerebral palsy. We explore potential pathways by which the statistical analyses in the thesis might influence patient outcomes.

The thesis has six chapters. After describing motivation and introduction in Chapter 1, mathematical representations of functional data are presented in Chapter 2. Chapter 3 considers orthogonal designs in the context of functional data analysis. New functional F tests for complex designs are derived in Chapter 4 and applied in two gait studies. Chapter 5 is devoted to a qualitative study. The thesis concludes with a discussion which details the extent to which the research question has been addressed, the limitations of the work and the degree to which it has been answered.

Acknowledgements

I would like to express my greatest gratitude to my supervisors Dr Heiko Großmann and Dr Dylan Morrissey for their support throughout my PhD. The story started with a casual chat outside the Engineering Building, at Queen Mary University of London, where two supervisors had the initial idea of this fascinating PhD project. Over the last four years, they have provided consistent guidance and inspiration to my work. I would also like to thank Dr Richard Twycross-Lewis, who acted as the third supervisor, helped me a lot with the lab training, gait analysis and writing.

Many thanks to my colleagues and PhD fellows in the School of Mathematical Sciences and Centre for Sports and Exercise Medicine. Many research ideas emerged during interesting discussions with them. Particular thanks goes to Dr Lawrence Pettit and Dr Hugo Maruri-Aguilar, who are assessors of my PhD project, and Dr Aleksandra Birn-Jeffery, Dr Wolfram Just, Dr Steve Coad, Dr Zakir Hossain, Dr Wenyu Liu, Mr Shaoxiong Hu and Mr Jack Tu, from whom I gained many help and support.

Without the high-quality data, I would not have been able to complete the application part of this thesis. Gait data of patients with cerebral palsy were provided by Dr Richard Twycross-Lewis; Professor Roger Woledge generously shared a database of normal gait data and Matlab programs to process gait data; Mr Yousuf Khan helped me to collect gait data from healthy subjects; and Mr Augustine Adu-Amankwah and Ms Anna Hebda-Boon helped me to collect qualitative data.

Finally, I would like to express my sincerest gratitude to my family and friends. Their love and encouragement inspire me not to give up at every difficult moment.

Publications and conference presentations

Publications:

(1) Zhang, B., Twycross-Lewis, R., Großmann, H., and Morrissey, D. (2017). Testing gait with ankle-foot orthoses in children with cerebral palsy by using functional mixed-effects analysis of variance. *Scientific Reports*, 7:11081.

(2) Zhang, B. and Großmann, H. (2016). Functional data analysis in designed experiments. In *mODa 11-Advances in Model-Oriented Design and Analysis*, pages 235-242. Springer.

Conference presentations:

(1) Zhang, B. and Großmann, H. Functional F tests for orthogonal designs. The Design and Analysis of Experiments Conference, October 2017, Los Angeles, USA

(2) Zhang, B., Großmann, H., Morrissey, D., and Twycross-Lewis, R. Functional mixed-effects analysis of variance for human movement patterns. The 10th International Chinese Statistical Association Conference, December 2016, Shanghai, China

(3) Zhang, B. and Großmann, H. Mixed-effects analysis of variance for functional data: an exploration of gait patterns in cerebral palsy patients. The 38th Research Students' Conference in Probability and Statistics, August 2015, Leeds, UK

Contents

List of Figures

List of Tables

Glossary

Notation	Description	Page number (first used)
FDA	functional data analysis	p. 1
ANOVA	analysis of variance	p. 3
AFO	ankle-foot orthoses	p. 5
T	closed interval in $\mathbb{R}$	p. 19
$\mathbb{L}^2(T,\mathscr{B}(T),\mu)$	Hilbert space of functions f for which $\int_T \lvert f\rvert^2 d\mu < \infty$	p. 19
$\mathbb{R}$	set of real numbers	p. 21
$(\Omega,\mathscr{A},P)$	probability space, with Ω as a set of possible outcomes, $\mathscr{A}$ as a σ-field on Ω, and P as a probability measure over $\mathscr{A}$	p. 21
$(R_t : t \in T)$, $(S_t : t \in T)$	stochastic processes	p. 21
$\eta(t)$, $\theta(s,t)$, $\theta_{R,S}(s,t)$	mean function, covariance function, cross-covariance function	p. 25
GP	Gaussian process	p. 25
$\mathscr{R}$	covariance operator	p. 27

Continued on next page

Table – *Continued from previous page*

Notation	**Description**	**Page number (first used)**
λ, ϕ	eigenvalue, eigenfunction of the covariance operator	p. 27
$\{y_1(t) : t \in T\}, \ldots,$ $\{y_N(t) : t \in T\}$	N stochastic processes	p. 33
$\mathbb{V}$, $\mathbb{W}$	$\mathbb{V}$-subspace, $\mathbb{W}$-subspace	p. 34
$\mathscr{I}$, $\mathscr{T}$	set of observational units, set of treatments	p. 35
$\mathscr{B}$, $\mathscr{G}$, $\mathscr{U}$, $\mathscr{E}$	block factor, treatment factor, universal factor, equality factor	p. 35
$\mathscr{F}$, $\mathscr{H}$	general factors	p. 36
$n_{\mathscr{F}}$, $q_{\mathscr{B}}$, $p_{\mathscr{G}}$	levels of a factor, levels of a block factor, levels of a treatment factor	p. 36
$\mathfrak{B}$, $\mathfrak{T}$, ϕ	block structure, treatment structure, design function	p. 39
$\mathscr{G}^{\phi}$, $\mathscr{H}^{\phi}$	induced block factor	p. 39
$\mathfrak{T}^{\phi}$	set of induced block factors	p. 40
$d_{\mathbb{W}}$	dimension of the $\mathbb{W}$-subspace, degrees of freedom of a factor	p. 41
q_k, p_u	levels of a block factor, levels of a treatment factor	p. 42
$\mathbf{X}$, $\mathbf{Z}$,	design matrices	p. 49

Continued on next page

Table – *Continued from previous page*

Notation	Description	Page number (first used)
$y(t)$, $\beta(t)$, $\delta(t)$, $\varepsilon(t)$	functional response, fixed-effect function, random-effect function, error term	p. 49
$\mathbf{I}$, $\mathbf{J}$, $\mathbf{1}$	identity matrix, all-1 matrix, all-1 vector	p. 49
C	column space	p. 51
$\mathbf{P}$	orthogonal projection	p. 52
$SS(t)$, SS^*	functional sum of squares, integrated sum of squares	p. 57
$\Lambda(s,t)$	stratum-based covariance function	p. 58
ξ, $\mathbf{u}$	eigenvalue, eigenvector of the orthogonal projection $\mathbf{P}$	p. 59
$EMS(t)$	functional expected mean square	p. 63
F	F statistic in the functional F test (or univariate F test)	p. 80
df	degrees of freedom of the functional F test	p. 81

Chapter 1

Introduction

1.1 Motivation

It is increasingly common to encounter experiments in which the individual responses are not real numbers but curves or surfaces which are observed over some continuous domain due to advances in laboratory equipment and imaging technology. Mathematically, responses of this kind can be regarded as functions and the relatively new and thriving area of statistics which is known as *functional data analysis* (FDA) is concerned with developing methods for analysing data that are functions.

Functional data not only arise in experiments and generalisations of classical multivariate statistical techniques (Johnson and Wichern, 2007), such as principal component analysis, have attracted considerable attention. However, in this thesis we will be concerned with experiments and explore how well-established principles of experimental design can be adapted to the FDA setting. The applications that will be considered come from the field of gait research and the responses of interest are typically curves depicting the movements of lower limb joints over time. Despite the complexity of functional responses, the scientific questions an experiment is supposed to answer are often similar to those in classical experi-

ments with univariate responses and often amount to comparing different treatments, where, as usual in the statistical literature, the generic term "treatment" refers to all conditions of interest that can be actively varied by the experimenter (Hinkelmann and Kempthorne, 1994, p. 26).

In the simplest case, one may be interested in investigating if there is a difference in the "mean responses" of two independent groups of patients of which one is treated with a placebo and one with an active treatment. A main challenge in this situation is that contrary to classical experiments the "mean response" is now a function itself rather than a single parameter. Moreover, comparing entire functions and deriving appropriate statistical tests for this purpose is more involved than testing hypothesis which only involve real parameters.

The analysis becomes increasingly complicated in experiments where, in addition to the functional responses, the units, for example patients, to which treatments are applied and for which observations are being taken possess some structure. Such structure may be inherent, such as the fact that a person's legs "reside" within that person and cannot necessarily be regarded as independent entities. Likewise, when each person is observed under different conditions, the repeated measurements taken for this person form a group of observations which needs to be distinguished from the groups of observations that are obtained for other individuals in the same experiment. Moreover, structure of the units in an experiment may also be a consequence of administrative, logistic or other aspects of the how the experiment is conducted (Bailey, 2008, p. 55). For example, if an experiment includes data recorded at various times over several days, then both the day and the time of the data collection impose some structure on the data. Likewise, if in preparation for data recordings people are equipped with marker sets by, say, one of two assistants, then this again adds some structure to the experiment since the data may be grouped under the different assistants.

The reason why the structure of the units is important is that the factors which impose structure are associated with sources of variation which can influence the comparison of

the treatments which is the primary goal of the experiment. For this reason it is important to reflect the structure of the units properly in the analysis of the experiment. Failing to do so may result in incorrect conclusions being drawn. In classical experimentation with univariate responses this problem occurs, for instance, when there are large units to which a treatment is applied and responses are measured on smaller sub-units. Often the sub-units are then mistakenly regarded as providing independent observations with the consequence that "significant" treatment effects are found by using incorrect residual sums of squares and degrees of freedom in the analysis of variance (ANOVA). More technically, this problem typically arises when an experiment with a complex design, that is structure of the units, is analysed as a completely randomised design.

Similar issues occur in structured experiments with functional responses. Despite the more complex type of response such experiments often have a structure which is the same as in a classical experiment. Accounting for the structure of the experiment in the analysis is a problem that can largely be dealt with without having to worry about the fact that the responses are functions. In particular, it is possible to attribute variation to different sources in an ANOVA. Some of these sources are associated with factors that determine the structure of the units while others are associated with the treatment comparisons of primary interest. Formally, the division of the variation is accomplished by decomposing a total sum of squares into sums of squares for structural and treatment factors. This is achieved by using established theory for so-called orthogonal designs which will be presented later.

By using the theory of orthogonal designs, for experiments with univariate responses it is possible to allocate every treatment factor to a unique stratum of the design (Bailey, 2008, p. 198), that is, a specific part of the experimental structure, and to derive F tests for testing whether the treatment factor affects the responses. In this process, residual sums of squares and corresponding degrees of freedom are derived which determine the distribution of the F statistic under the null hypothesis of no treatment effect.

Generalising this approach to functional data poses however new challenges. Although the allocation of treatment factors to strata can be done as in the ANOVA for univariate responses, the derivation of a suitable test statistic is more complicated. First, the sums of squares that are typically used to define the F statistic become random functions themselves. In order to turn these functions into real random variables, integrated sums of squares are computed by integrating the sums of squares over the domain on which the responses are collected. Appropriate ratios of integrated sums of squares, divided by degrees of freedom, for treatments and residuals in the relevant strata of the design are then used to define a test statistic which is similar to a classical F statistic in the ANOVA for orthogonal designs. Secondly, determining the distribution of the test statistic thus defined under the null hypothesis of no treatment effect requires the use of some results for stochastic processes, in particular the so-called Karhunen-Loève expansion.

The idea to derive functional F tests for the ANOVA of functional data by using integrated sums of squares and the Karhunen-Loève expansion was originally proposed by Shen and Faraway (2004) and subsequently used by Zhang (2013) for one-way and two-way ANOVA problems. However, in this earlier work only completely randomised designs with independent response curves were considered. Likewise, the univariate theory for orthogonal designs with complex unit structures was developed by Nelder (1965a,b), Tjur (1984) and Bailey (2008). The main methodological contribution of the current thesis is to link these two approaches in order to produce novel methods for analysing complex experiments with functional responses. Figure 1.1 summarises the research question, the two main areas on which the methodological research in the thesis is based and more specific topics which will be presented in subsequent chapters.

The work presented in the thesis is the outcome of an interdisciplinary project and applying the methods developed here to data from real experiments is of particular interest. We will consider two applications in which the response curves represent measurements of dynamic 3-dimensional 'joint' angles between lower limb segments during gait. In the first

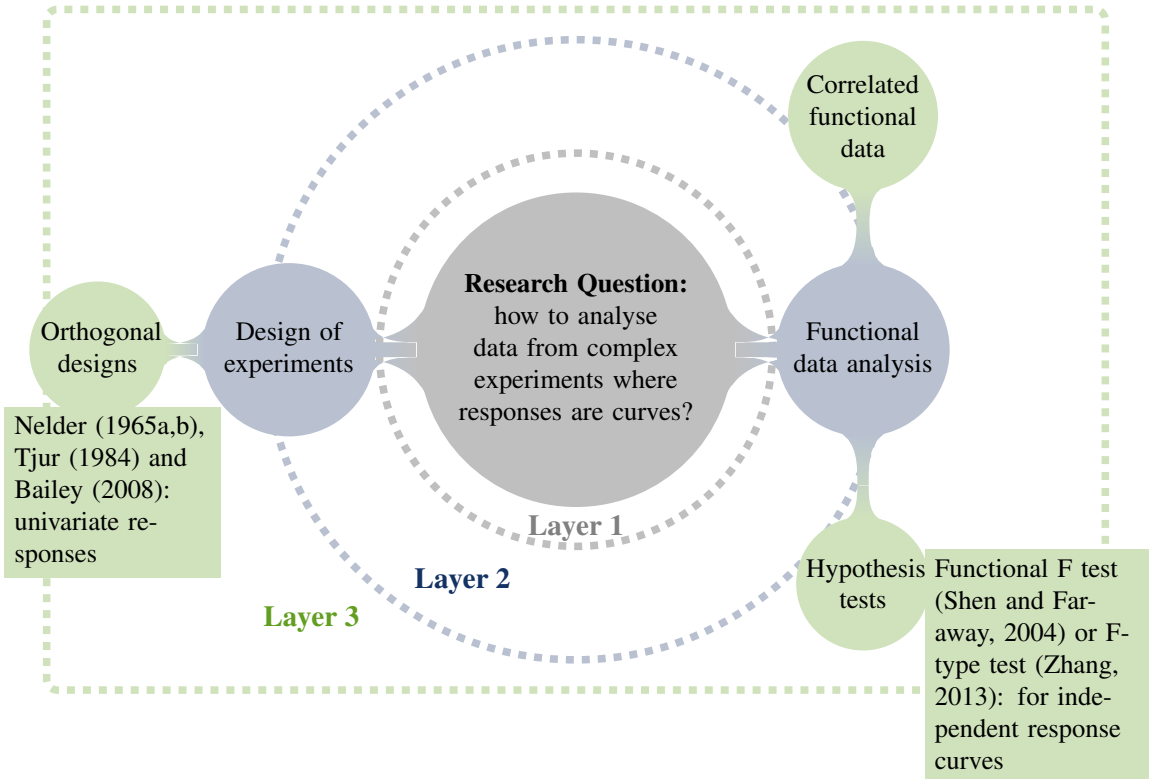

Figure 1.1: Research question (Layer 1), relevant topics (Layer 2) and existing techniques (Layer 3, where boxes show the literature of existing techniques)

study, data were collected from both legs of 14 patients with cerebral palsy while walking both barefoot and wearing prescribed ankle-foot orthoses (AFO). One objective of such gait studies is to assess the effect of an AFO on the response gait curves, which may be grouped with respect to both patients and legs within patients. Because of this structure, the different response curves should not be regarded as being independent and the functional F test for a completely randomised design should not be used. Instead, by using the theory of orthogonal designs and applying it to existing data, we identify the appropriate stratum for testing the effect of wearing (or respectively not wearing) an AFO and use the new functional F test from Chapter 4 to test the treatment effect in the appropriate stratum of the design.

In the second study, the functional F tests from Chapter 4 are applied to another gait study where a split-plot design was used to collect data from 9 healthy subjects whilst walking on an instrumented treadmill at different speeds and under different orthosis conditions:

a control condition (barefoot), a unilateral orthosis condition and a bilateral orthoses condition. Experiments with healthy subjects avoid the weak ambulatory capability of patients with cerebral palsy and high variability of pathological gait data and thus are expected to generate data which are in better agreement with the underlying model assumptions. Specifically, it can be expected that participants with cerebral palsy would have greater variance than those without cerebral palsy between individuals (units) and the sub-units of limbs within a subject. This would therefore introduce extra variability which could obscure the comparison of statistical approaches.

Human gait data is interesting in that it is quasi-cyclic, repeatable and an easily recognisable pattern, while at the same time providing sufficient complexity to allow for a functional approach to data analysis. Having tested a new approach in participants with essentially normal gait, the added complexity of stochasticity present in pathological gait patters found in cerebral palsy gait provides a fertile ground for statistical analysis with clinical applications which may ultimately benefit patient care. Clinicians play an intermediate role in the clinical application of quantitative gait analysis and in the thesis their experiences with and opinions about the method have been explored by using semi-structured interviews. The results of this qualitative investigation will be presented in Chapter 5.

In the remainder of this chapter, I first present a review of the relevant literature, including hypothesis tests and correlated functional data in the field of FDA, orthogonal designs and previous applications of FDA to gait studies, in Section 1.2. Aims and the potential impact of my research are described in Section 1.3 and a more detailed outline of the thesis is provided in Section 1.4.

1.2 Literature review

1.2.1 Functional data analysis

In 1982, Ramsay proposed the idea of extending the statistical techniques to functional data (Ramsay, 1982), and Ramsay and Silverman (2005) explored both the theory and application of FDA, which has been applied in many other fields, such as biomedicine (Song et al., 2008), biomechanics (Crane et al., 2010) and linguistics (Koenig et al., 2008). There is a wide range of topics in FDA, which have been reviewed by Ullah and Finch (2013), Cuevas (2014), Morris (2015) and Wang et al. (2016) from different perspectives, including applications of FDA, models and statistical inference for functional data. In my thesis, two topics of FDA are particularly important for experiments with functional responses - hypothesis tests for functional data and correlated functional data.

Hypothesis tests for functional data

A straightforward approach to testing hypotheses for functional data is the pointwise approach (Ramsay and Silverman, 2005). With this approach, the domain over which the response curves are observed is discretised into a set of points and a univariate statistical test is performed at each of these points. However, the pointwise approach has two disadvantages. Significant differences at some or even all of these points do not necessarily imply a significant difference between two entire curves over the whole domain (Górecki and Smaga, 2015). Moreover, multiple simultaneous tests cause the common problem of multiplicity. As a consequence, the (uncontrolled) overall Type I error of pointwise tests can be unacceptably high (Abramovich and Angelini, 2006). Although, in principle, this issue could be addressed by using the well-known Bonferroni correction, this approach is not recommended for functional data because of the correlation within functions (Vsevolozhskaya et al., 2015).

As an alternative, global tests for functional data have been proposed. These tests treat

the response curves as entities and summarise information over the whole domain on which the curves are observed. To test two nested functional regression models, Faraway (1997) presented a bootstrap-based method, and Shen and Faraway (2004) developed a functional F test. Under the assumption that the error terms in the regression model are independent realisations of a Gaussian process, the numerator and denominator of the test statistic can be transformed into linear combinations of independent χ^2 random variables. By using the Welch-Satterthwaite approximation (Satterthwaite, 1941, 1946; Welch, 1947), the null distribution of the functional F test can be approximated by an F distribution with adjusted degrees of freedom. Zhang (2013) used a similar test, which he called an F-type test, to explore one-sample, two-sample, one-way and two-way ANOVA problems. Furthermore, Zhang (2005), Zhang and Chen (2007), Zhang (2013) and Zhang and Liang (2014) considered an L^2-norm-based test and a bootstrap test.

Górecki and Smaga (2015) reviewed the statistical tests mentioned above for the one-way ANOVA problem for comparing means of several independent groups of random functions. They further discussed tests proposed by Fan and Lin (1998) and Cuevas et al. (2004) and presented a new test where functional data were fitted by B-splines and multivariate tests were applied to the coefficients of the spline functions. Furthermore, a hypothesis test for a functional fixed-effects ANOVA was developed by Cuesta-Albertos and Febrero-Bande (2010) where the response functions were assumed to belong to the separable Hilbert space of square-integrable functions.

Correlated functional data

In the literature on FDA, the term correlated functional data refers to correlations among entire functions. Such correlations arise from experimental structures, such as nested or crossed designs (Morris and Carroll, 2006; Di et al., 2009; Aston et al., 2010; Crainiceanu et al., 2012; Staicu et al., 2014; Shou et al., 2015), or spatial locations where data are measured (Baladandayuthapani et al., 2008; Staicu et al., 2010, 2015). Spatial-temporal data are

sometimes analysed as spatially correlated functional data, for example, electroencephalographic signals from various parts of the brain (Staicu et al., 2010) or data on waste production from various locations in Venice Province produced between 1991 and 2011 (Bernardi et al., 2017).

The structure of correlated functional data is complicated due to correlations within and between functions. Staicu et al. (2010) proposed a multi-level framework for correlated functional data and in the current work I use a similar framework to illustrate the structure of data that are generated in a complex design as follows: (1) subject groups, (2) subjects, (3) functions within the subject, and (4) measurements within the function. This multi-level framework has a wide scope of application. For example, Pataky et al. (2013) described a dataset which contains curves of muscle forces of 16 healthy subjects and 27 patients with Patello-Femoral Pain. The data were collected from each subject during walking and running and can be described by the multi-level framework. At level (1), two groups contained healthy subjects and patients respectively; at level (2), all subjects were independent; at level (3), two curves (functions) within each subject were correlated; and at level (4), data were measured at 101 time points for each curve and were correlated.

Most studies of FDA limit their scope to level (4) in the above structure under the assumption of independent functions. However, for correlated functional data, at least one of the preceding levels (1) - (3) needs to be taken into account. Correlation at level (4) results from the nature of functional data, that is, the fact that, for instance, measurements are taken over time, whereas correlations at levels (1) - (3) are determined by the experimental structure. The structure of a dataset may differ from the framework given above, according to the specific structure of an experiment.

A useful tool to study correlated functional data is the functional mixed-effects model, where correlations between functions can be modelled by random-effect terms. Although Guo (2002) proposed the term *functional mixed-effects model*, the random-effect term was

used to represent the curve-specific deviation, that is the variability of measurements within the curve, and correlations between curves were not accounted for. A more general functional mixed-effects model for correlated functional data was developed by Morris and Carroll (2006), where functions were represented by linear combinations of wavelet basis functions and the model was estimated using a Bayesian approach.

Several studies have extended hypothesis tests to correlated functional data. To compare two correlated groups of functions, Crainiceanu et al. (2012) employed a bootstrap method, whereas Staicu et al. (2014) used a likelihood ratio test. Staicu et al. (2015) proposed a global L^2-norm based test to compare mean functions of multiple groups of correlated functional data, along with a block bootstrap method which can be applied to a study with a small sample size. Zhang and Großmann (2016) extended the F-type test of Shen and Faraway (2004) to examine treatment effects in a split-plot design with functional responses.

1.2.2 Orthogonal designs

The systematic study of the univariate analysis of variance for orthogonal designs was initiated by Nelder (1965a,b). Subsequently, these ideas were extended and refined by Tjur (1984) and Bailey (2008).

Nelder (1965a) emphasized the distinction between the block structure and the treatment structure in the analysis of designs. Block structure derives from the internal structure of observational units regardless of treatments, while treatment structure describes the structure on the set of treatments and how treatment factors are allocated to observational units. Nelder (1965a,b) presented a framework to analyse both block structure and treatment structure of the design with an orthogonal block structure. Orthogonality induces a set of mutually orthogonal idempotent matrices, which are fundamental to the ANOVA of block structures (Nelder, 1965a). However, a formal definition for orthogonal designs was not provided in Nelder (1965a,b).

Tjur (1984) generalised the approach proposed by Nelder (1965a,b) to more general orthogonal designs, where all factors are orthogonal. Moreover, Tjur (1984) clarified the definition of orthogonality, that is, two factors are orthogonal if the corresponding subspaces are *geometrically orthogonal*, as will be explained later in Chapter 3. For an orthogonal design, the vector space where responses are observed can be uniquely decomposed into a direct sum of orthogonal subspaces, each of which is associated with one factor in the design. Projection matrices onto the subspaces that are associated with block factors are equivalent to "a set of mutually orthogonal idempotent matrices" in Nelder (1965a). The concept of orthogonality in Tjur (1984) is also applicable to treatment factors.

A precise mathematical definition of orthogonal designs was provided by Bailey (2008) and in this thesis we only consider designs that fulfill all three conditions of an orthogonal design (Bailey, 2008, p. 198). Briefly, an orthogonal design is determined by the orthogonal block structure, the orthogonal treatment structure and the design function which is used to allocate treatments to observational units. These conditions are composed of twelve specific conditions (Bailey, 2008), which can be checked by using a Mathematica package of Großmann (2014).

Apart from the definition of orthogonal designs, some classical design tools can also be applied to functional data. For instance, a null experiment which ignores treatments can be used to study the block structure and results be summarised in a null ANOVA table (Nelder, 1965a); projection matrices onto the corresponding orthogonal subspaces can be used to derive sums of squares in the ANOVA (Tjur, 1984); a skeleton ANOVA table describes the structure of a design without taking responses into account and Hasse diagrams are used to display the treatment structure and block structure (Bailey, 2008).

1.2.3 Applications of FDA to gait analysis

Gait analysis

Data collected from gait analysis typically results in curves that provide a measure of the gait cycle, which indicates the time interval between two consecutively repetitive events during walking (Whittle, 2007, p. 52), e.g. between the initial foot contact to the next initial contact by the same foot. In gait analysis, the stance phase lasts from initial contact to toe off, whereas the swing phase starts from toe off until the next initial contact, as shown in Figure 1.2.

Perry (1992, p. 11) identified the following gait phases for normal gait patterns: initial contact (0-2% of gait cycle), loading response (0-10% of gait cycle), mid-stance (10-30% of gait cycle), terminal stance (30-50% of gait cycle), pre-swing (50-60% of gait cycle), initial swing (60-73% of gait cycle), mid-swing (73-87% of gait cycle) and terminal swing (87-100% of gait cycle). The initial contact, when the foot just touches the floor, is sometimes not considered as a gait phase. Both the start (loading response) and the end (pre-swing) of the stance phase are periods when two feet have contact with the floor, and, hence regarded as double support. The stance phase accounts for the first 60% of the gait cycle, while the

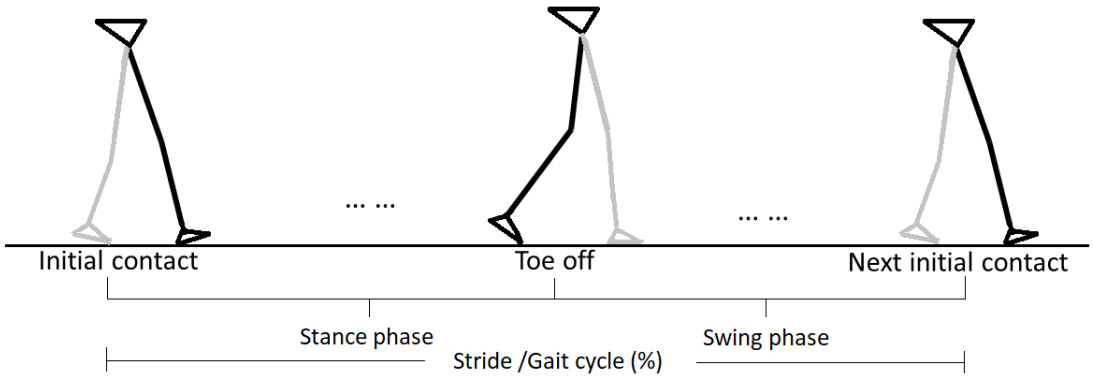

Figure 1.2: Positions of the leg (black) and the contralateral leg (grey) when major gait events (initial contact, toe off and the next initial contact) occur during the gait cycle

swing phase during which the foot is propelled forward ready for the next step accounts for approximately 40% of the gait cycle (Richards, 2008, p. 52).

Common measurements in gait laboratories include joint angles, joint moments and ground reaction forces. In the thesis, I focus on 3-dimensional joint angles and segmental position of the lower limbs, including pelvis, hip joint, knee joint, ankle joint and foot. In gait analysis, joint angles (which are also called joint rotations) in the coronal plane, sagittal plane and horizontal plane are commonly reported. Reference planes are explained by Whittle (2007, p. 3). More specifically, the sagittal plane divides the body into right and left portions; the coronal plane divides the body into front and back portions; and the horizontal plane divides the body into upper and lower portions. In a gait report, gait curves are usually plotted against the percentage of the gait cycle, not real time.

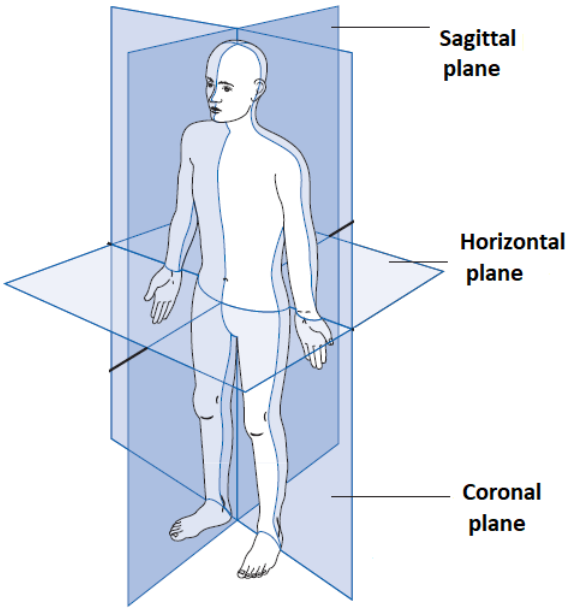

Figure 1.3: Reference planes (Whittle, 2007, p. 3)

FDA in gait analysis

Statistical methods used to analyse single data points may not be adequate for curves and some studies have applied more advanced FDA techniques to analyse gait data. As summarised by Duhamel et al. (2004), statistical tools in clinical gait analysis are used to identify whether gait data of a new subject should be classified into a clinically normal group or not, or to compare differences of gait data from different groups. FDA has been applied for both gait classification (Sutherland et al., 1988; Olshen et al., 1989; Lenhoff et al., 1999) and gait comparison (Duhamel et al., 2006; Ryan et al., 2006; Donoghue et al., 2008).

Sutherland et al. (1988) and Olshen et al. (1989) proposed bootstrap prediction regions to classify gait patterns. Joint rotations were represented as functions of the percentage of the gait cycle using a Fourier basis system. Data collected from 38 children, who were five years old and had clinically 'normal' gait, were used as a training set and bootstrap prediction regions were constructed based on the training set. The gait curve of a test subject was displayed together with the bootstrap prediction region and it was examined whether the test curve was covered by the prediction region or not. In addition, bootstrap distribution percentiles were used to identify the abnormality of joint movements for a test subject. This bootstrap method was compared with pointwise prediction bands by Lenhoff et al. (1999) with an application to knee flexion angles of 28 healthy subjects. The bootstrap bands covered more gait curves than the pointwise bands, but required intensive computations. To improve the efficacy, pointwise prediction bands were adjusted by a Bonferroni correction. However, as pointed out by Lenhoff et al. (1999), a typical gait curve with at least 100 data points results in a conservative evaluation, since the width of Bonferroni corrected prediction bands increases with the number of points. Furthermore, the bootstrap approach takes the correlation between measurements within a curve into account, which is neglected by the pointwise approach.

Functional principal component analysis (PCA) developed by Ramsay and Silverman (2005) is commonly used for gait comparison. By using functional PCA, main features of gait curves are represented by principal components and then classical statistical tools can be applied to principal component scores. In order to compare gait patterns of 12 Parkinsonian patients under different treatment conditions, Duhamel et al. (2006) applied functional PCA to gait data smoothed by cubic B-splines to reduce the dimension and then principal component scores were analysed by a linear discriminant analysis to measure the differences between treatment groups. Similarly, Ryan et al. (2006) used F tests of principal component scores to compare knee joint angles of children at different developmental stages. Donoghue et al. (2008) applied ANOVA models to principal component scores, in order to assess the

effects of orthoses on running kinematics of patients with chronic Achilles tendon injury. Despite the advanced FDA techniques used to extract the information from these curves, univariate statistical methods, such as ANOVA models and F tests, were still used in these papers. Therefore, Donoghue et al. (2008) pointed out the need for an extension of experimental analysis to functional data, such as the work presented in this thesis.

1.3 Aims and impact

The overarching aim of this thesis was to develop statistical methodology for functional data that are collected from complex orthogonal designs and to explore applications of FDA to gait analysis. The potential impact of this research would be to provide tools to analyse correlated functional data, where the correlation stems from the experimental structure. Such methods will be applied to gait data, with the ultimate goal of improving gait analysis by considering the entire curve in the analysis, rather than single values.

The following list summarises secondary aims and specific objectives:

(1) To explore links between existing techniques of FDA and design of experiments. The specific objective is to explore the mathematical concepts of functional data and orthogonal designs.

(2) To analyse orthogonal designs with functional responses. The specific objective is to construct ANOVA for functional data. We consider an experiment where responses are time-dense curves. Despite the complicated responses, the structure of the experiment does not depend on time. Therefore, we will start with a skeleton ANOVA, where responses are not taken into account and then develop a full ANOVA, which contains calculations of functional responses, such as, sums of squares.

(3) To develop hypothesis tests for functional data. The specific objective is to examine the treatment effects of an orthogonal design with functional responses. Previous sta-

tistical tests have not yet considered functional data and the complicated structure of the design together.

(4) To explore novel applications of FDA in gait analysis. The specific objective is to analyse gait data using the proposed statistical methods. We will test the effects of AFO on 3-dimensional joint angles of patients with cerebral palsy. Moreover, we will analyse gait data of healthy subjects in a split-plot design.

(5) To investigate the potential utilisation of our approach in clinical gait assessment. The specific objective is to explore how clinicians perceive quantitative gait analysis in the management of cerebral palsy.

1.4 Outline of thesis

This thesis consists of 6 chapters including this introductory chapter and the remainder of this thesis is organised as follows.

Chapter 2 introduces mathematical background of functional data. Two different perspectives exist to explain functional data. The first representation of functional data is as sample paths of a stochastic process and under the second perspective, functional data are realisations of a random element defined on a probability space and taking values in a Hilbert space. Existing FDA theories are developed respectively from these two perspectives. However, these two perspectives are not always equivalent. In this chapter, conditions under which a stochastic process is also a random element of a Hilbert space are clarified. Under such conditions, the Karhunen-Loève expansion is introduced and two theorems are subsequently proposed, which will be used later in the functional ANOVA to derive distributions of sums of squares.

Chapter 3 explores the analysis of orthogonal designs with functional responses. Since the experimental structure is time-independent, we introduce orthogonal designs without

taking responses into account and then construct a functional mixed-effects model where responses are functions. In this thesis, design matrices of the functional mixed-effects model are determined by the experimental structure, and thus are the same as in a general linear model. The random-effect terms of the model are associated with the block structure, whereas the fixed-effect terms are associated with the treatment structure of the design. Moreover, the result that the column space of a design matrix is equal to the $\mathbb{V}$-subspace (Bailey, 2008) of the corresponding factor of the design links FDA and orthogonal designs. Orthogonal projections calculated from design matrices are used to derive functional sums of squares. The ANOVA table for an orthogonal design with functional responses consists of the analysis of the block and treatment structures, and functional sums of squares.

Chapter 4 covers the theory and practice of functional F tests in orthogonal designs. According to the block and treatment structure given in Chapter 3, a functional F test is derived to examine treatment effects. Under the null hypothesis that a treatment factor has no effect, the integrated sums of squares for both the treatment factor and the corresponding residual can be represented as linear combinations of independent χ^2 random variables. It can then be shown that under the null hypothesis the F statistic of the functional F test is approximately distributed as an F distribution. Two applications of functional F tests to gait data are introduced in Section 4.2 and Section 4.3, respectively. The gait study of patients with cerebral palsy aims to examine the effects of AFO on kinematics in lower limbs. However, there are limitations in this study concerning the experimental design. In particular, treatments were not randomised since the children with cerebral palsy are fatigue prone during walking. This issue becomes further exacerbated during barefoot walking. In order to explore more applications of functional F tests, we designed a split-plot experiment to collect gait data from healthy subjects. Functional F tests are used to examine effects of AFO, walking speeds and their interaction.

Chapter 5 explores clinical gait analysis. Although gait data are analysed by the proposed approach in Chapter 4 for a research purpose, the ultimate purpose of gait analysis

is to improve patient outcomes. Therefore, this chapter reports a qualitative study which aims to explore clinicians' experience and opinions of using 3-dimensional gait data and gait analysis in the management of cerebral palsy. We recruited clinicians who had frequently conducted gait assessment in clinical routine for semi-structured interviews and participants included physiotherapists, orthotists, a specialist orthopaedic surgeon and clinical scientists. Based on their understanding and needs of gait analysis, we explore the potential that our study can be utilised in the assessment or treatment of patients with movement disorders.

Chapter 6 summarises the main findings of the thesis and draws conclusions from the current study. In this chapter, the utility and possible application of the approach is considered.

Chapter 2

Functional data

This chapter describes the conceptual background of functional data. The chapter starts with an example of functional data in Section 2.1. Mathematically, functional data may be regarded as either the sample paths of a stochastic process (*stochastic process perspective*) or realisations of a random element (*random element perspective*). These two perspectives are not always equivalent. We consider conditions to ensure a stochastic process to be a random element in the Hilbert space $\mathbb{L}^2(T, \mathscr{B}(T), \mu)$, as will be explained in Section 2.2. In Section 2.3 mean-square continuous stochastic processes, of which the mean and covariance functions are well-defined and continuous, are of particular interest, since the Karhunen-Loève expansion expressed in Section 2.4 is applied to mean-square continuous stochastic processes with zero mean to represent a stochastic process by a series of random variables and functions.

Moreover, a mean-square continuous stochastic process, which is also a random element in $\mathbb{L}^2(T, \mathscr{B}(T), \mu)$, is square integrable referring to both the interval T and the probability space Ω. Thus, the square integration of the stochastic process with respect to the Lebesgue measure μ is a real-value random variable. In particular, if the stochastic process is Gaussian distributed, the random variable derived from Lebesgue integral of the squared process

has the identical distribution to a linear combination of χ^2 random variables (Zhang, 2013, Theorem 4.2, p. 86) by applying the Karhunen-Loève expansion. A similar theorem, where multiple Gaussian processes are considered, is stated as Theorem 2.4, which is the basis to derive distributions of sums of squares in ANOVA and functional F tests in Chapters 3 and 4.

2.1 An example of functional data

This study is motivated by data which consist of gait curves and a simple example of gait data is shown in Figure 2.1 as a prototype for functional data. In this example, gait data were collected from healthy adults (age: 18 - 50, free from lower limb injury and musculoskeletal disease in the past 6 months) in the Human Performance Laboratory at Queen Mary University of London. We focus on angles that are formed by segments of lower limbs, including the angles of pelvis, hip, knee, ankle and foot.

In Figure 2.1, knee angles of two subjects (subject 3 and subject 6) are plotted against the percentage of gait cycle as an example. Gait curves collected at the fast, medium and slow speeds are indicated by the solid, dashed and dotted curves, respectively. Since each participant walked at all three speeds, it is necessary to consider the correlation between different gait curves from the same participant when we assess the effects of walking speeds on gait patterns.

More details of this example will be introduced in Section 4.3, where the structure of data is more complicated than what is shown in Figure 2.1, since we analyse gait data that were collected when participants walked barefoot and wearing orthoses which are commonly prescribed to patients with movement disorders. To analyse such gait data, each curve can be viewed as a continuous function of the percentage of the gait cycle. Before we explore statistical analysis for functional data, we first discuss how to represent functional data mathematically.

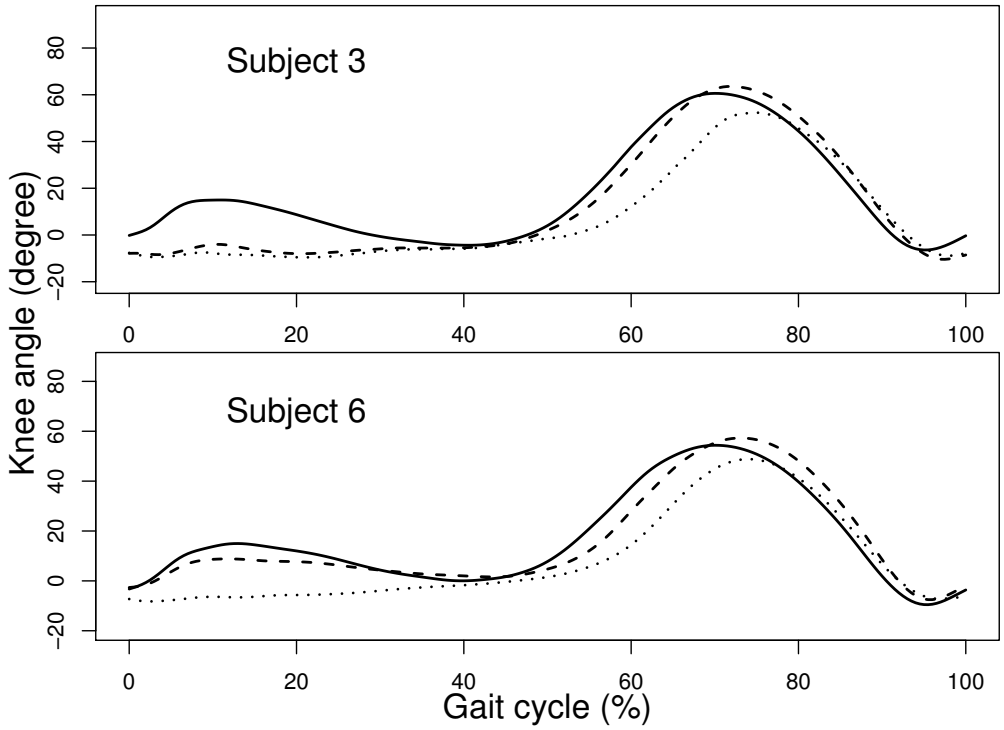

Figure 2.1: Angles of knee joints in the sagittal plane of two healthy subjects during their barefoot walking on an instrumented treadmill at the fast speed (solid curves), the medium speed (dashed curves) and the slow speed (dotted curves).

2.2 Two perspectives of functional data

In FDA, every observation is regarded as a (real) function $f : T \to \mathbb{R}$ with $t \mapsto f(t)$ (e.g. curves in Figure 2.1). In what follows, T is a closed interval in $\mathbb{R}$. There are two main approaches to modelling random observations that are curves.

One possibility is to start with a stochastic process $(R_t : t \in T)$ on a probability space $(\Omega, \mathscr{A}, P)$, where R_t is a real random variable for every $t \in T$. In other words, $R_t : \Omega \to \mathbb{R}$ is an $\mathscr{A}$-$\mathscr{B}(\mathbb{R})$-measurable function which for every $\omega \in \Omega$ yields the value $R_t(\omega)$, where $\mathscr{B}(\mathbb{R})$ is the Borel σ-field on $\mathbb{R}$. For every $\omega \in \Omega$ the sample path at ω is the mapping $r_\omega : T \to \mathbb{R}$ where $r_\omega(t) := R_t(\omega)$. Observed functions f can then be regarded as sample

paths. This is called the *stochastic process perspective* (Hsing and Eubank, 2015, p. 175).

Alternatively, one may start with the probability space $(\Omega, \mathscr{A}, P)$ and a measurable space $(\mathbb{E}, \mathscr{M})$, where $\mathbb{E} \subset \mathbb{R}^T$ is a subset of the set $\mathbb{R}^T$ of all function $f : T \to \mathbb{R}$ and $\mathscr{M}$ is a suitable σ-field on $\mathbb{E}$. Every $\mathscr{A}$-$\mathscr{M}$-measurable function $R : \Omega \to \mathbb{E}$ is then the analogue of a (real) random variable and, due to the more complicated image space, called a random function (Bosq, 2000, p. 16) or a random element, if $\mathbb{E}$ is a Hilbert space which is equipped with the Borel σ-field $\mathscr{B}(\mathbb{E})$ (Hsing and Eubank, 2015, p. 176). In this setting, every observed function f may be regarded as a realisation $R(\omega)$ of R. This is called the *random element perspective* (Hsing and Eubank, 2015, p. 175).

If one starts with a stochastic process $(R_t : t \in T)$ and the corresponding sample paths $r_\omega : T \to \mathbb{R}$ for $\omega \in \Omega$, then the two perspectives can be linked by defining $R : \Omega \to \mathbb{R}^T$ through $R(\omega) := r_\omega$ for every $\omega \in \Omega$. The function R defined in this way obviously produces functions from T to $\mathbb{R}$ as its "values". However, the mapping $R : \Omega \to \mathbb{R}^T$ is not always measurable. As indicated in Bosq (2000, p. 21), $\mathbb{R}^T$ is generally a too large space, such that there are irregular functions in this space. For R to be a random function or element, one also needs to specify a suitable measurable space $(\mathbb{E}, \mathscr{M})$ where $\mathbb{E} \subset \mathbb{R}^T$ and to show that R is $\mathscr{A}$-$\mathscr{M}$-measurable and, hence, a random element.

Often, $\mathbb{E} = \mathbb{L}^2(T, \mathscr{B}(T), \mu)$ is the Hilbert space of functions f for which the integral of f^2 with respect to the Lebesgue measure μ is finite, that is, $\int_T |f|^2 d\mu < \infty$ (f is said to be square integrable). The corresponding σ-field is the Borel σ-field $\mathscr{B}(\mathbb{E})$ on $\mathbb{E}$, which is the smallest σ-field containing all open subsets of $\mathbb{E}$ (Karatzas and Shreve, 1998, p. 1). It is then natural to ask which properties the stochastic process $(R_t : t \in T)$ and its paths r_ω need to possess in order to ensure that R, where $R(\omega) = r_\omega$, is $\mathscr{A}$-$\mathscr{B}(\mathbb{E})$-measurable, and, hence, a random element.

We consider the condition that was proposed by Bosq (2000, p. 23). For a stochastic

process $(R_t : t \in T)$ with sample paths in $\mathbb{E} = \mathbb{L}^2(T, \mathscr{B}(T), \mu)$, if the mapping

$$(t, \omega) \mapsto R_t(\omega) : \quad (T \times \Omega, \mathscr{B}(T) \otimes \mathscr{A}) \to (\mathbb{R}, \mathscr{B}(\mathbb{R})) \tag{2.1}$$

is measurable (say, R is *jointly measurable* with respect to the product σ-field $\mathscr{B}(T) \otimes \mathscr{A}$), then R is $\mathscr{A}$-$\mathscr{B}(\mathbb{E})$-measurable. Hence, R is a random element in $\mathbb{L}^2(T, \mathscr{B}(T), \mu)$.

A sufficient condition to derive the joint measurability is the continuity of sample paths. If every sample path is right-continuous, the stochastic process is jointly measurable (Karatzas and Shreve, 1998, p. 5). Moreover, the sample path continuity implies the property of indistinguishability. Two stochastic processes $(R_t : t \in T)$ and $(S_t : t \in T)$ defined on the same probability space are modifications of each other, such that

$$P(R_t = S_t) = 1, \quad \text{for all } t \in T.$$

However, modification does not imply

$$P(\cap_{t \in T} \{R_t = S_t\}) = 1,$$

which is referred to as indistinguishability and two indistinguishable stochastic processes almost surely have the same sample paths. If two stochastic processes $(R_t : t \in T)$ and $(S_t : t \in T)$ with right-continuous sample paths are modification of each other, they are indistinguishable (Karatzas and Shreve, 1998, p. 2; Bosq, 2000, p. 17). All results also hold for left-continuity.

In FDA, it is convenient to consider a jointly measurable stochastic process which takes values in $\mathbb{L}^2(T, \mathscr{B}(T), \mu)$, i.e., the stochastic process is also a random element in $\mathbb{L}^2(T, \mathscr{B}(T), \mu)$.

If the stochastic process $(R_t : t \in T)$ is joint measurable, sample paths $t \mapsto R_t(\omega)$ for

$\omega \in \Omega$ are $\mathscr{B}(T)$-measurable; and if random variables R_t have well-defined expectations for $t \in T$, the mean function $\eta : t \mapsto E(R_t)$, which will be discussed more later, is also $\mathscr{B}(T)$-measurable with E being the expectation with respect to a probability measure P on $(\Omega, \mathscr{A})$.

Moreover, for a stochastic process which is also a random element in $\mathbb{L}^2(T, \mathscr{B}(T), \mu)$, it is an immediate consequence of Fubini's theorem (Saks and Banach, 1937, p. 77) that

$$E\Big(\int_T (R_t)^2 d\mu(t)\Big) = \int_T \Big(E(R_t)^2\Big) d\mu(t), \tag{2.2}$$

where $\int_T (R_t)^2 d\mu(t)$ indicates the random variable $\omega \mapsto \int_T \big(R_t(\omega)\big)^2 d\mu(t)$ taking nonnegative values.

In particular, if the following condition

$$E\Big(\int_T (R_t)^2 d\mu(t)\Big) < \infty \tag{2.3}$$

is satisfied, the stochastic process $(R_t : t \in T)$ is regarded as an $\mathbb{L}^2$-*stochastic process* (Wang et al., 2016) or the random element R is said to be square integrable with integration referring to the probability space $(\Omega, \mathscr{A}, P)$ (Kokoszka and Reimherr, 2017, p. 40). Condition (2.3) is desirable in FDA from both the stochastic process perspective and random element perspective. Under the condition (2.3), the expectation of the random variable $\int_T (R_t)^2 d\mu(t)$ exists and is finite, which is important to derive the distributions for sums of squares in functional ANOVA, as will be introduced in the following chapter.

In Chapter 3 and 4, observed functional data are viewed as sample paths of stochastic processes $(y_t^{(1)} : t \in T), (y_t^{(2)} : t \in T), \ldots, (y_t^{(N)} : t \in T)$, where $i = 1, 2, \ldots, N$ for $(y_t^{(i)} : t \in T)$ are indices of stochastic processes. Moreover, to analyse the experiment where functional data are collected, we are interested in sums of squares, which are calculated by the orthogonal projections of responses onto the corresponding subspaces. The sum of squares for a factor can be represented by a sum of squared independent stochastic processes

$(R_t^{(1)} : t \in T), (R_t^{(2)} : t \in T), \ldots, (R_t^{(d)} : t \in T)$ with d being the degrees of freedom of this factor, as will be explained in Chapter 3. Definitions that are related to stochastic processes in Section 2.3 are applicable to responses and sums of squares, while theorems in Section 2.4 will be applied to $(R_t^{(1)} : t \in T), (R_t^{(2)} : t \in T), \ldots, (R_t^{(d)} : t \in T)$ in the following study.

2.3 Mean-square continuous stochastic process

Suppose $(R_t : t \in T)$ is a stochastic process. Then, the *mean function* is defined by:

$$\eta(t) := E(R_t), \quad \text{for } t \in T, \tag{2.4}$$

and the *covariance function* is defined by:

$$\theta(s,t) := Cov(R_s, R_t) = E\Big(\big(R_s - \eta(s)\big)\Big)\Big(\big(R_t - \eta(t)\big)\Big), \quad \text{for } s,t \in T. \tag{2.5}$$

According to the *mean function* and *covariance function*, we can define the following stochastic processes.

Definition 2.1 A stochastic process $(R_t : t \in T)$ is a *second-order process*, if $E\Big((R_t)^2\Big) < \infty$ for every $t \in T$.

Definition 2.2 A second-order process $(R_t : t \in T)$ is a *Gaussian process*, if for any k points $t_1, \ldots, t_k \in T$, $(R_{t_1}, \ldots, R_{t_k})$ follows a multivariate Gaussian distribution.

In what follows, a Gaussian process $(R_t : t \in T)$ with mean function η and covariance function θ will be denoted by $R \sim GP(\eta, \theta)$.

Definition 2.3 A second-order process $(R_t : t \in T)$ is *mean-square continuous*, if its mean and covariance functions are continuous, that is, the mean function $\eta : T \to \mathbb{R}$ with $\eta(t) = E(R_t)$ and the covariance function $\theta : T \times T \to \mathbb{R}$ with $\theta(s,t) = Cov(R_s, R_t)$ are continuous.

The stochastic processes which are mean-square continuous can be studied by using the Karhunen-Loève expansion, which is a useful tool in FDA, and details will be introduced in the next section.

Now, we consider two stochastic processes $(R_t : t \in T)$ and $(S_t : t \in T)$. The *cross-covariance function* of two stochastic processes is defined by:

$$\theta_{R,S}(s,t) := Cov(R_s, S_t) = E\Big(\big(R_s - \eta_R(s)\big)\Big)\Big(\big(S_t - \eta_S(t)\big)\Big), \quad \text{for } s,t \in T, \tag{2.6}$$

where $\eta_R(s) = E(R_s)$ and $\eta_S(t) = E(S_t)$.

Two stochastic processes $(R_t : t \in T)$ and $(S_t : t \in T)$ on a common set T are *independent*, if for all finite subset $T_1, T_2 \subset T$,

$$P(\{R_{t_i} \leq r_{t_i} : t_i \in T_1\} \cap \{S_{t_j} \leq s_{t_j} : t_j \in T_2\}) = P(\{R_{t_i} \leq r_{t_i} : t_i \in T_1\})P(\{S_{t_j} \leq s_{t_j} : t_j \in T_2\}).$$

Independent stochastic processes $(R_t : t \in T)$ and $(S_t : t \in T)$ imply that each random variable R_s for $s \in T$ is independent to the random variable S_t for $t \in T$. Thus, $Cov(R_s, S_t) = 0$ for all $s,t \in T$.

2.4 Karhunen-Loève expansion

In this section, we will introduce the Karhunen-Loève expansion of a mean-square continuous stochastic process, as will be applied in Chapters 3 and 4. To state the Karhunen-Loève expansion, we first need definitions of the covariance operator, eigenvalues and eigenfunctions.

The covariance function $\theta(s,t)$ of a mean-square continuous process $(R_t : t \in T)$ is continuous, nonnegative definite and symmetric. Suppose $\int_T \int_T \theta^2(s,t) d\mu(s) d\mu(t) < \infty$. The

integral operator $\mathscr{R} : \mathbb{L}^2(T, \mathscr{B}(T), \mu) \to \mathbb{L}^2(T, \mathscr{B}(T), \mu)$, defined by

$$(\mathscr{R}f)(t) := \int_T \theta(s,t) f(s) d\mu(s), \quad \text{for all } t \in T \tag{2.7}$$

with $f \in \mathbb{L}^2(T, \mathscr{B}(T), \mu)$, is referred to as the *covariance operator* of the stochastic process $(R_t : t \in T)$.

Suppose there exist $\lambda \in \mathbb{R}$ and nonzero $\phi \in \mathbb{L}^2(T, \mathscr{B}(T), \mu)$, such that

$$\int_T \theta(s,t)\phi(s) d\mu(s) = (\mathscr{R}\phi)(t) = \lambda\phi(t), \quad t \in T.$$

Then λ is an *eigenvalue* of the covariance operator $\mathscr{R}$ with the corresponding *eigenfunction* ϕ. Moreover, if all eigenfunctions satisfy

$$\int_T \phi_r(t)^2 d\mu(t) = 1, \quad \int_T \phi_r(t)\phi_l(t) d\mu(t) = 0, \quad \text{for} \quad r, l \geq 1, \text{ and } r \neq l,$$

then $\phi_1, \phi_2, \ldots$ are called a system of *orthonormal eigenfunctions* of the covariance operator.

Since the covariance operator $\mathscr{R}$ is compact (Hsing and Eubank, 2015, Theorem 4.6.2, p. 117), the set of nonzero eigenvalues for $\mathscr{R}$ is either finite or consists of a sequence which tends to zero (Hsing and Eubank, 2015, Theorem 4.2.4, p. 98). Therefore, we can arrange all eigenvalues in a nonincreasing order, such that $\lambda_1 \geq \lambda_2 \geq \cdots \geq 0$.

These definitions are applied in the following Mercer's theorem (Mercer, 1909; Riesz and Szökefalvi-Nagy, 1955, p. 245), which is needed to derive the Karhunen-Loève expansion.

Theorem 2.1 (Mercer's theorem) *Let $\theta(s,t)$ be a continuous, nonnegative definite and symmetric covariance function with the corresponding covariance operator $\mathscr{R}$ defined by Equation (2.7). Then there exists a sequence of eigenvalues and orthonormal eigenfunctions*

$(\lambda_r, \phi_r)_{r=1}^{\infty}$ *for* $\mathscr{R}$. *The covariance function* $\theta(s,t)$ *has the representation*

$$\theta(s,t) = \sum_{r=1}^{\infty} \lambda_r \phi_r(s) \phi_r(t), \quad s,t \in T,$$

with the series converging absolutely and uniformly.

The proof of Mercer's theorem can be found in Hsing and Eubank (2015, p. 122).

As mentioned in Hsing and Eubank (2015, p. 122) and Gohberg and Kreĭn (1969, Corollary 10.1, p. 117) that the covariance operator $\mathscr{R}$ is trace class (or say nuclear), that is,

$$\sum_{r=1}^{\infty} \lambda_r = \int_T \theta(t,t) d\mu(t) < \infty.$$

Hence, if a stochastic process $(R_t : t \in T)$ with zero mean function and continuous covariance function $\theta(s,t)$ is also a random element in $\mathbb{L}^2(T, \mathscr{B}(T), \mu)$, then $\theta(t,t) = E(R_t)^2$ and by applying Equation (2.2) we have that

$$E\Big(\int_T (R_t)^2 d\mu(t) \Big) = \int_T \Big(E(R_t)^2 \Big) d\mu(t) = \int_T \theta(t,t) d\mu(t) < \infty. \tag{2.8}$$

Now we are ready to state the Karhunen-Loève expansion (Loève, 1977, p. 151), which represents a stochastic process to a linear combination of uncorrelated random variables and functions in $\mathbb{L}^2(T, \mathscr{B}(T), \mu)$ space.

Theorem 2.2 (Karhunen-Loève expansion) *Let* $(R_t : t \in T)$ *be a stochastic process with zero mean function and continuous covariance function* $\theta(s,t)$. *Then, with* $(\lambda_r, \phi_r)_{r=1}^{\infty}$ *defined in the Mercer's theorem, we have that*

$$R_t = \sum_{r=1}^{\infty} u_r \phi_r(t), \quad t \in T,$$

where the series converges uniformly with respect to the $\mathbb{L}^2(\Omega, \mathscr{A}, P)$*-distance and* $(u_r)_{r=1}^{\infty}$

are uncorrelated random variables with $E(u_r) = 0$ *and* $E(u_r^2) = \lambda_r$.

The Karhunen-Loève expansion is proved by applying the Mercer's theorem and the proof can be found in Bosq (2000, p. 25) and Hsing and Eubank (2015, p. 188).

In addition, if R is also a random element in $\mathbb{L}^2(T, \mathscr{B}(T), \mu)$, then $\int_T R_t \phi_r(t) d\mu(t)$ is an $\mathbb{L}^2(\Omega, \mathscr{A}, P)$ random variable (Ash and Gardner, 1975, p. 34; Hsing and Eubank, 2015, p. 187). In this case, we have

$$u_r = \int_T R_t \phi_r(t) d\mu(t) \tag{2.9}$$

for the Karhunen-Loève expansion.

As explained by Hsing and Eubank (2015, p. 193) that Karhunen-Loève expansion does not depend on the condition that R a random element in $\mathbb{L}^2(T, \mathscr{B}(T), \mu)$ space, since we can always find an $\mathbb{L}^2(\Omega, \mathscr{A}, P)$ random variable to play the role of $\int_T R_t \phi_r(t) d\mu(t)$. However, Equation (2.9) only works when the mean-square continuous stochastic process $(R_t : t \in T)$ is also a random element in $\mathbb{L}^2(T, \mathscr{B}(T), \mu)$, which we will use in this thesis.

Moreover, if $(R_t : t \in T)$ is also a Gaussian process, u_r defined by Equation (2.9) for $r = 1, 2, \ldots$ are independent random variables, each of which follows a normal distribution $N(0, \lambda_r)$.

Next, we consider the Karhunen-Loève expansions for two stochastic processes.

Theorem 2.3 *Let* $(R_t : t \in T)$ *and* $(S_t : t \in T)$ *be two stochastic processes with zero mean function and continuous covariance functions. Moreover, R and S are random elements in* $\mathbb{L}^2(T, \mathscr{B}(T), \mu)$ *space.*

If the cross-covariance function $\theta_{R,S}(s,t) = 0$ *for* $s,t \in T$, *then* $R_t = \sum_{r=1}^{\infty} u_{1r} \phi_{1r}(t)$ *and* $S_t = \sum_{l=1}^{\infty} u_{2l} \phi_{2l}(t)$, *where* $(u_{1r})_{r=1}^{\infty}$ *and* $(u_{2l})_{l=1}^{\infty}$ *are all uncorrelated.*

Proof. By applying the Karhunen-Loève expansion along with that R is a random element

in $\mathbb{L}^2(T,\mathscr{B}(T),\mu)$ space, $u_{1r} = \int_T R_t \phi_{1r}(t) d\mu(t)$ for $r = 1,2,\ldots$ are uncorrelated.

Likewise, $u_{2l} = \int_T S_t \phi_{2l}(t) d\mu(t)$ for $l = 1,2,\ldots$ are uncorrelated. In what follows, we prove each pair of u_{1r} and u_{2l} for $r, l = 1,2,\ldots$ from Karhunen-Loève expansions of different stochastic processes are uncorrelated.

Since $(R_t : t \in T)$ and $(S_t : t \in T)$ have zero mean function, the cross-covariance function is

$$\theta_{R,S}(s,t) = E(R_s S_t) = 0 \quad s,t \in T.$$

From the Karhunen-Loève expansion in Theorem 2.2, we have that

$$\begin{aligned} E(u_{1r}u_{2l}) &= E\Big(\big(\int_T R_s \phi_{1r}(s) d\mu(s)\big)\Big)\Big(\big(\int_T S_t \phi_{2l}(t) d\mu(t)\big)\Big) \\ &= E\Big(\int_T \int_T R_s \phi_{1r}(s) S_t \phi_{2l}(t) d\mu(s) d\mu(t)\Big) \\ &= \int_T \int_T E(R_s S_t) \phi_{1r}(s) \phi_{2l}(t) d\mu(s) d\mu(t) \\ &= \int_T \int_T \theta_{R,S}(s,t) \phi_{1r}(s) \phi_{2l}(t) d\mu(s) d\mu(t) \\ &= 0, \end{aligned}$$

where $E(u_{1r}u_{2l}) \leq \big(E(u_{1r}^2)\big)^{1/2}\big(E(u_{2l}^2)\big)^{1/2} < \infty$ by applying the Cauchy-Schwarz inequality allows us to exchange the order of the expectation and integrals (Fubini's theorem). Therefore, all $(u_{1r})_{r=1}^{\infty}$ and $(u_{2l})_{l=1}^{\infty}$ are uncorrelated. □

Mercer's theorem and Karhunen-Loève expansion are commonly applied in FDA. In this thesis, we will not apply them directly, but need the following theorem which is derived from the Karhunen-Loève expansions for independent stochastic processes and similar to Zhang (2013, Theorem 4.10, p. 90).

Throughout this thesis, $A_1, A_2, \ldots \overset{i.i.d.}{\sim} \mathbb{D}$ denotes that $A_1, A_2, \ldots$ are independent random

variables or functions, which are identically distributed as $\mathbb{D}$, and $A \overset{d.}{=} B$ denotes that random variables or functions A and B have the same distribution.

Theorem 2.4 *Let $(R_t^{(1)} : t \in T), \ldots, (R_t^{(d)} : t \in T)$ be d independent Gaussian processes with zero mean function and the continuous covariance function $\theta(s,t)$, that is, $R^{(1)}, \ldots, R^{(d)} \overset{i.i.d.}{\sim} GP(0,\theta)$. If $R^{(1)}, \ldots, R^{(d)}$ are also random elements in $\mathbb{L}^2(T, \mathscr{B}(T), \mu)$, we have*

$$\sum_{i=1}^{d} \int_T (R_t^{(i)})^2 d\mu(t) \overset{d.}{=} \sum_{r=1}^{\infty} \lambda_r A_r,$$

where $(A_r)_{r=1}^{\infty} \overset{i.i.d.}{\sim} \chi_d^2$ as a χ^2 distribution with the degrees of freedom being equal to d. Moreover, $\lambda_1 \geq \lambda_2 \geq \cdots \geq 0$ are the eigenvalues of the covariance operator with the corresponding covariance function $\theta(s,t)$.

Proof. Suppose $(\lambda_r, \phi_r)_{r=1}^{\infty}$ are the eigenvalues and orthonormal eigenfunctions of the covariance operator that is associated with $\theta(s,t)$. By using the Karhunen-Loève expansion expressed in Theorem 2.2, we have that $R_t^{(i)} = \sum_{r=1}^{\infty} u_{ir}\phi_r(t)$ with $u_{ir} = \int_T R_t^{(i)} \phi_r(t) d\mu(t)$ for $r = 1, 2, \ldots$ and $i = 1, \ldots, d$.

Recall that the inner product of the Hilbert space $\mathbb{L}^2(T, \mathscr{B}(T), \mu)$ is usually defined by $\langle f, g \rangle = \int_T f(t)g(t)d\mu(t)$ and the norm is $||f|| = \langle f, f \rangle^{1/2}$ for $f, g \in \mathbb{L}^2(T, \mathscr{B}(T), \mu)$. By applying Hsing and Eubank (2015, Theorem 4.2.4, p. 98), the system of orthonormal eigenfunctions $\{\phi_r\}$ is a complete orthonormal system for $\mathbb{L}^2(T, \mathscr{B}(T), \mu)$; and hence for $i = 1, 2, \ldots, d$,

$$\int_T (R_t^{(i)})^2 d\mu(t) = \sum_{r=1}^{\infty} \Big(\int_T R_t^{(i)} \phi_r(t) d\mu(t) \Big)^2,$$

which is directly from Parseval's theorem

$$||R^{(i)}||^2 = \sum_{r=1}^{\infty} \langle R^{(i)}, \phi_r \rangle^2 \quad \text{(Kokoszka and Reimherr, 2017, p. 218).}$$

Then,

$$\begin{aligned}\sum_{i=1}^{d}\int_T (R_t^{(i)})^2 d\mu(t) &= \sum_{i=1}^{d}\sum_{r=1}^{\infty}\Big(\int_T R_t^{(i)}\phi_r(t)d\mu(t)\Big)^2 \\ &= \sum_{i=1}^{d}\sum_{r=1}^{\infty} u_{ir}^2 \\ &= \sum_{r=1}^{\infty}\sum_{i=1}^{d} u_{ir}^2.\end{aligned}$$

Due to the independence between Gaussian processes, all random variables $u_{ir} \sim N(0,\lambda_r)$ for $r = 1,2,\ldots$ and $i = 1,\ldots,d$ are independent by applying Theorem 2.3. We standardise the random variable $u_{ir}^2 = \lambda_r(\frac{u_{ir}}{\sqrt{\lambda_r}})^2$, where $\frac{u_{ir}}{\sqrt{\lambda_r}} \sim N(0,1)$. Then, we have

$$\begin{aligned}\sum_{i=1}^{d}\int_T (R_t^{(i)})^2 d\mu(t) &= \sum_{r=1}^{\infty}\sum_{i=1}^{d} u_{ir}^2 \\ &= \sum_{r=1}^{\infty}\sum_{i=1}^{d} \lambda_r(\frac{u_{ir}}{\sqrt{\lambda_r}})^2 \\ &= \sum_{r=1}^{\infty}\lambda_r\Big(\sum_{i=1}^{d}(\frac{u_{ir}}{\sqrt{\lambda_r}})^2\Big) \\ &= \sum_{r=1}^{\infty}\lambda_r A_r,\end{aligned}$$

with $A_r = \sum_{i=1}^{d}(\frac{u_{ir}}{\sqrt{\lambda_r}})^2$. Since $((\frac{u_{ir}}{\sqrt{\lambda_r}})_{i=1}^{d})_{r=1}^{\infty} \overset{i.i.d.}{\sim} N(0,1)$, we have $(A_r)_{r=1}^{\infty} \overset{i.i.d.}{\sim} \chi_d^2$ and hence

$$\sum_{i=1}^{d}\int_T (R_t^{(i)})^2 d\mu(t) \sim \sum_{r=1}^{\infty}\lambda_r\chi_d^2,$$

where $\lambda_1 \geq \lambda_2 \geq \cdots \geq 0$ are the eigenvalues of the covariance operator that is associated with the covariance function $\theta(s,t)$. □

As in (2.8), for $R_t^{(i)}$ with $i = 1,2,\ldots,d$ in Theorem 2.4, we have

$$E\Big(\int_T (R_t^{(i)})^2 d\mu(t)\Big) < \infty,$$

which implies the random variable $\int_T (R_t^{(i)})^2 d\mu(t)$ has a well-defined expectation. Similarly, the random variable $\sum_{i=1}^{d} \int_T (R_t^{(i)})^2 d\mu(t)$ also have a finite expectation, which is actually equal to $\sum_{r=1}^{\infty} \lambda_r \times d < \infty$.

Theorem 2.4 shows that the sum of squared integrals with respects to the Lebesgue measure μ of independent Gaussian processes has the same distribution as a linear combination of random variables, all of which follow a χ^2 distribution with the degrees of freedom being equal to the number of processes. However, according to Theorem 2.3 and the proof of Theorem 2.4, we have the same result if processes are not independent but the cross-covariance of each two Gaussian processes is zero.

We have used $(y_t^{(i)} : t \in T)$ with $i = 1, 2, \ldots, N$ for stochastic processes. However, this is not commonly used in the literature of FDA. A more straightforward way to express stochastic process is $\{y_i(t) : t \in T\}$ for $i = 1, 2, \ldots, N$, where $y_i(t) : \omega \mapsto y_i(t, \omega)$ is a random variable and the same as $y_t^{(i)} : \omega \mapsto y_t^{(i)}(\omega)$ at fixed $t \in T$. In the following chapters, we will use the latter expression $\{y_i(t) : t \in T\}$.

Moreover, in the remainder of this thesis we will only consider stochastic processes which are jointly measurable, mean-square continuous and with sample paths in $\mathbb{L}^2(T, \mathscr{B}(T), \mu)$ space, that is, all stochastic processes are also random elements in $\mathbb{L}^2(T, \mathscr{B}(T), \mu)$ space, unless otherwise stated. $\mathbb{L}^2(T, \mathscr{B}(T), \mu)$ will be simplified to $\mathbb{L}^2(T)$ without stating the corresponding Borel σ field and Lebesgue measure μ.

Chapter 3

Functional analysis of variance

In this chapter, we consider orthogonal designs where the responses are curves. In spite of functional responses, the experimental structure is not affected by time, which allows us to apply well-known principles to analyse experiments. Functional data collected from a completely randomised design are viewed as sample paths of independent stochastic processes. The functional ANOVA for such data has been proposed by Zhang (2013), and in this chapter we consider the functional ANOVA for more general orthogonal designs, which allow correlations between stochastic processes.

As for non-functional data, where we investigate the effects of explanatory or independent variables on responses in a regression model or ANOVA model, we apply a functional mixed-effects model to study functional data. Since the experimental structure is time-independent, design matrices of the functional mixed-effects model are the same as those in a traditional ANOVA model with a univariate response variable though the effect of a factor is a function. Moreover, the column spaces of design matrices are equal to the $\mathbb{V}$-subspaces of the factors, which links the functional mixed-effects model and orthogonal designs. In functional ANOVA, sums of squares are calculated by using the orthogonal projections onto the corresponding subspaces and we summarise all calculations in the ANOVA table.

3.1 Orthogonal designs

Suppose N functions of $t \in T$ are observed from an orthogonal design, each of which is mathematically viewed as a sample path of a stochastic process. In practice, functional data are usually observed discretely over a large number of points. In this study, we suppose functional data are collected from a design, where the experimental structure is fixed across all time points. For instance, data are collected over a fine grid of m equally spaced points $t_1, t_2, \ldots, t_m$ in a closed interval T. At each time point t_ℓ, for $\ell = 1, 2, \ldots, m$, values $y_1(t_\ell), \ldots, y_N(t_\ell)$ can be viewed as observations of an experiment with univariate responses and the experimental structure for all time points is the same. Therefore, methods from classical orthogonal designs can be applied.

An *observational unit* is the smallest unit in an experiment where a response is measured (Bailey, 2008, p. 8), while *treatments* are the conditions that are actively varied and applied to *experimental units* and which are under comparison in the experiment (Cheng, 2014, p. 1). Usually, the experimental and observational coincide but sometimes every experimental unit consists of or contains several observational units.

Observational units are also called *plots* in this thesis. Bailey (2008) used Greek letters, such as ω, to denote observational units and the set of all observational units is denoted by Ω with the total number of observational units being equal to N. In order to avoid potential confusion of notation between the probability space and the set of observational units, $\mathscr{I}$ is used here to denote the set of observational units. Accordingly, functional responses are denoted by $\mathbf{y}(t) = \{y_i(t)\}_{i=1}^N$, rather than $\{y_\omega(t)\}_{\omega \in \Omega}$. At each fixed time point, the vector space for the design with univariate responses is $\mathbb{R}^N$.

3.1.1 Factors

The experimental structure is described by the set of factors which are defined on the observational units (*block structure*) or treatments (*treatment structure*). A mapping $\mathscr{I} \to \mathscr{B}$,

where $\mathscr{I}$ is the set of observational units, is called a *block factor*. Following the notational convention in Tjur (1984), $\mathscr{B}$ is also used to denote the block factor. Likewise, a mapping $\mathscr{T} \to \mathscr{G}$, where $\mathscr{T}$ is the set of treatments, is called a *treatment factor*, which as in Tjur (1984) is also denoted by $\mathscr{G}$.

Since the following results in this section are applicable to both block factors and treatment factors, we will use $\mathscr{F}$ to indicate a general factor, which can either be a block factor or a treatment factor. A factor $\mathscr{F}$ with $n_{\mathscr{F}}$ levels can be viewed as a partition of the set of observational units, respectively the set of treatments $\mathscr{T}$ into $n_{\mathscr{F}}$ mutually disjoint subsets. Each subset consists of the observational units, respectively treatments, to which the same level of $\mathscr{F}$ is allocated, and these subsets are called $\mathscr{F}$-classes (Bailey, 2008, p. 169). If for a factor $\mathscr{F}$ all $\mathscr{F}$-classes have the same size, $\mathscr{F}$ is called a uniform factor (Bailey, 2008, p. 175; Cheng, 2014, p. 39) or a balanced factor (Tjur, 1984). In what follows, the number of levels of a block factor $\mathscr{B}$ is denoted by $q_{\mathscr{B}}$ and the number of levels of a treatment factor $\mathscr{G}$ is denoted by $p_{\mathscr{G}}$.

Two factors $\mathscr{F}$ and $\mathscr{F}'$ which are defined on the same set are equivalent ($\mathscr{F} \equiv \mathscr{F}'$), if they induce the same partition of the set. Otherwise, $\mathscr{F}$ and $\mathscr{F}'$ are said to be inequivalent. We say that $\mathscr{F}$ is finer than $\mathscr{F}'$ ($\mathscr{F} \prec \mathscr{F}'$), or say $\mathscr{F}'$ is coarser than $\mathscr{F}$ ($\mathscr{F}' \succ \mathscr{F}$), if every $\mathscr{F}$-class is contained within one $\mathscr{F}'$-class. Usually, if $\mathscr{F} \prec \mathscr{F}'$, then $\mathscr{F}$ is said to be nested in $\mathscr{F}'$ (Cheng, 2014, p. 39). Following Bailey (2008), we use $\mathscr{F} \preceq \mathscr{F}'$ to indicate that $\mathscr{F}$ is finer than or equivalent to $\mathscr{F}'$. The relation $\preceq$ is reflexive, antisymmetric (with equality replaced by equivalence) and transitive and, hence, a partial order on the set of factors (Tjur, 1984; Cheng, 2014, p. 40). Note that it is possible that for some factors $\mathscr{F}$ and $\mathscr{F}'$ neither $\mathscr{F} \preceq \mathscr{F}'$ nor $\mathscr{F}' \preceq \mathscr{F}$ may hold, for example, when every level of $\mathscr{F}$ occurs together with every level of $\mathscr{F}'$, in which case $\mathscr{F}$ and $\mathscr{F}'$ are said to be crossed.

Two special factors

On both, $\mathscr{I}$ and $\mathscr{T}$, there are two special factors (Tjur, 1984; Bailey, 2008) . The universal factor $\mathscr{U}$ is a constant mapping from the set (either $\mathscr{I}$ or $\mathscr{T}$) to an arbitrary set with a single element and hence this factor makes no difference between observational units or treatments. The equality factor $\mathscr{E}$ is an identity mapping (on either $\mathscr{I}$ or $\mathscr{T}$). The universal factor $\mathscr{U}$ is the coarsest, while the equality factor $\mathscr{E}$ is the finest factors among all factors in a design. Thus, for any factor $\mathscr{F}$ in an experiment, we have

$$\mathscr{E} \preceq \mathscr{F} \preceq \mathscr{U}.$$

Infimum and supremum of two factors

The infimum and supremum of two factors $\mathscr{F}$ and $\mathscr{F}'$ are defined by Bailey (2008, Chapter 10). The infimum of two factors $\mathscr{F}$ and $\mathscr{F}'$ is the factor denoted by $\mathscr{F} \wedge \mathscr{F}'$ which satisfies:

(i) $(\mathscr{F} \wedge \mathscr{F}') \preceq \mathscr{F}$ and $(\mathscr{F} \wedge \mathscr{F}') \preceq \mathscr{F}'$;

(ii) any factor $\mathscr{H}$, that is finer than or equivalent to both $\mathscr{F}$ and $\mathscr{F}'$, is also finer than or equivalent to $\mathscr{F} \wedge \mathscr{F}'$, that is, $\mathscr{H} \preceq (\mathscr{F} \wedge \mathscr{F}')$.

The supremum of two factors $\mathscr{F}$ and $\mathscr{F}'$ is the factor denoted by $\mathscr{F} \vee \mathscr{F}'$ which satisfies:

(i) $\mathscr{F} \preceq (\mathscr{F} \vee \mathscr{F}')$ and $\mathscr{F}' \preceq (\mathscr{F} \vee \mathscr{F}')$;

(ii) any factor $\mathscr{H}$, that is coarser than or equivalent to both $\mathscr{F}$ and $\mathscr{F}'$, is also coarser than or equivalent to $\mathscr{F} \vee \mathscr{F}'$, that is, $(\mathscr{F} \vee \mathscr{F}') \preceq \mathscr{H}$.

Then, we have

$$(\mathscr{F} \wedge \mathscr{F}') \preceq \mathscr{F} \preceq (\mathscr{F} \vee \mathscr{F}') \quad \text{and} \quad (\mathscr{F} \wedge \mathscr{F}') \preceq \mathscr{F}' \preceq (\mathscr{F} \vee \mathscr{F}').$$

The infimum of two factors may be regarded as being similar to a "largest lower bound" and the supremum to a "least upper bound" which relates the terms for factors to the corresponding terms in calculus.

$\mathbb{V}$-subspace and orthogonal factors

Definition 3.1 The $\mathbb{V}$-*subspace* of a factor $\mathscr{F}$ consists of those vectors that take a constant value for each level of $\mathscr{F}$ and is denoted by $\mathbb{V}(\mathscr{F})$.

Suppose, for example, that $\mathscr{B}$ is a block factor with $q_{\mathscr{B}}$ levels and that the components of the vectors in $\mathbb{V}(\mathscr{B})$ are indexed by the observational units in $\mathscr{I}$, then all components of $v \in \mathbb{V}(\mathscr{B})$ will be equal for which the corresponding subscripts are in the same $\mathscr{B}$-class.

For two factors in an experiment: (1) if $\mathscr{F} \equiv \mathscr{F}'$, then $\mathbb{V}(\mathscr{F}) = \mathbb{V}(\mathscr{F}')$; (2) if $\mathscr{F} \prec \mathscr{F}'$, then $\mathbb{V}(\mathscr{F}) \supset \mathbb{V}(\mathscr{F}')$ (see, e.g., Bailey, 2008, p. 178).

Now, we are ready to define *orthogonal factors*, similar to Tjur (1984).

Definition 3.2 Two factors $\mathscr{F}$ and $\mathscr{F}'$ are said to be *orthogonal*, if the corresponding $\mathbb{V}$-subspaces are geometrically orthogonal.

In Tjur (1984, p. 40), two $\mathbb{V}$-subspaces $\mathbb{V}_1$ and $\mathbb{V}_2$ are said to be *geometrically orthogonal*, if the following conditions

(i) $\mathbb{V}_1 = V_0 \oplus V_1$ and $\mathbb{V}_2 = V_0 \oplus V_2$ with $V_0 = \mathbb{V}_1 \cap \mathbb{V}_2$, $V_1 = \mathbb{V}_1 \cap V_0^{\perp}$ and $V_2 = \mathbb{V}_2 \cap V_0^{\perp}$

(ii) $V_1 \perp V_2$, that is, for any vectors $v_1 \in V_1$ and $v_2 \in V_2$, $v_1^T v_2 = 0$,

are satisfied, where $\oplus$ denotes the direct sum of vector spaces; $V_0^{\perp}$ is the orthogonal complement of V_0; $V_1 \perp V_2$ means that V_1 and V_2 are orthogonal; and the superscript T denotes the transposition of vectors and matrices.

The definitions of orthogonal factors in Cheng (2014, p. 47) and Bailey (2008, p. 179) are equivalent to the above. In the latter case, this follows from the fact that for any two factors on the same set the $\mathbb{V}$-space for the supremum is equal to the intersection of the individual $\mathbb{V}$-spaces for the factors (Bailey, 2008, p. 178).

3.1.2 Definition of orthogonal designs

As defined by Bailey (2008, p. 198) an *orthogonal design* has three components: an *orthogonal block structure* $\mathfrak{B}$, an *orthogonal treatment structure* $\mathfrak{T}$, and a *design function* $\phi : \mathscr{I} \to \mathscr{T}$ from the set of observational units to the set of treatments which links the block and treatment structures $\mathfrak{B}$ and $\mathfrak{T}$. Throughout the thesis we make the mild assumption that ϕ is surjective. Note that, here, the notation ϕ in Cheng (2014, p. 279) is used for the design function since in this thesis the symbol T used by Bailey is used for the interval on which the functional responses are collected.

In total, twelve conditions must be satisfied for the triple $(\mathfrak{B}, \mathfrak{T}, \phi)$ to be an orthogonal design. The first six of these define the orthogonal block structure $\mathfrak{B}$ as a set of mutually inequivalent block factors which satisfies: (i) $\mathscr{U} \in \mathfrak{B}$, (ii) $\mathscr{E} \in \mathfrak{B}$, (iii) $\mathscr{B}, \mathscr{B}' \in \mathfrak{B} \Rightarrow \mathscr{B} \vee \mathscr{B}' \in \mathfrak{B}$, (iv) $\mathscr{B}, \mathscr{B}' \in \mathfrak{B} \Rightarrow \mathscr{B} \wedge \mathscr{B}' \in \mathfrak{B}$, (v) if $\mathscr{B}, \mathscr{B}' \in \mathfrak{B}$ then $\mathscr{B}$ and $\mathscr{B}'$ are orthogonal on $\mathscr{I}$ and (vi) all factors $\mathscr{B} \in \mathfrak{B}$ are uniform. The next three conditions define the orthogonal treatment structure $\mathfrak{T}$ in a similar way as a set of mutually inequivalent treatment factors which satisfies: (vii) $\mathscr{U} \in \mathfrak{T}$, (viii) $\mathscr{G}, \mathscr{G}' \in \mathfrak{T} \Rightarrow \mathscr{G} \vee \mathscr{G}' \in \mathfrak{T}$ and (ix) if $\mathscr{G}, \mathscr{G}' \in \mathfrak{T}$ then $\mathscr{G}$ and $\mathscr{G}'$ are orthogonal on $\mathscr{T}$. It should be clear from the context that the universal factors which, in (i) and (vii), are denoted by the same symbol $\mathscr{U}$ are defined on different sets.

The final three conditions can be better understood by noting that for every treatment factor $\mathscr{G} \in \mathfrak{T}$ the design function ϕ induces a block factor $\mathscr{G}^\phi := \mathscr{G} \circ \phi$, that is $\mathscr{G}^\phi$ is the composition "$\mathscr{G}$ after ϕ" (cf. Cheng, 2014, p. 279). This block factor indicates for every observational unit the level of $\mathscr{G}$ that is applied to the unit. By using the block factors that are induced by ϕ the conditions of Bailey (2008, p. 198) which refer to the design function

can be rephrased as follows: (x) if $\mathscr{G}, \mathscr{H} \in \mathfrak{T}$ then $\mathscr{G}^\phi$ and $\mathscr{H}^\phi$ are orthogonal on $\mathscr{I}$, (xi) if $\mathscr{B} \in \mathfrak{B}$ and $\mathscr{G} \in \mathfrak{T}$ then $\mathscr{B}$ and $\mathscr{G}^\phi$ are orthogonal on $\mathscr{I}$, (xii) if $\mathscr{B} \in \mathfrak{B}$ and $\mathscr{G} \in \mathfrak{T}$ then $\mathscr{B} \vee \mathscr{G}^\phi \equiv \mathscr{H}^\phi$ for some treatment factor $\mathscr{H} \in \mathfrak{T}$.

It is worthwhile to note that in most of his exposition of orthogonal designs Cheng (2014) does not work with the set $\mathfrak{T}$ of treatment factors defined on $\mathscr{T}$ but uses the set $\mathfrak{T}^\phi := \{\mathscr{G}^\phi : \mathscr{G} \in \mathfrak{T}\}$. As a consequence, most of his results are stated in terms of two sets of block factors which correspond to the orthogonal block structure $\mathfrak{B}$ and the set $\mathfrak{T}^\phi$. Nevertheless, the resulting analysis of variance is the same as in Bailey (2008).

At the core of the analysis of variance of orthogonal designs for univariate responses is a decomposition of the space $\mathbb{R}^N$ into the direct sum of mutually disjoint subspaces which is exclusively derived from the orthogonal block structure $\mathfrak{B}$ and which uses the properties (i), (ii), (iii) and (v). By using the properties (xi) and (xii) it is possible to identify for every treatment factor a unique block factor such that a subspace for the treatment factor (or, more precisely, for the corresponding induced block factor) is a subset of the subspace, the so-called stratum, for the block factor. Strata that contain treatment factors other than the universal factor can be decomposed further into the direct sum of mutually orthogonal subspaces and a residual subspace by using the orthogonal treatment structure and the design function where the properties (vii), (viii), (ix) and (x) are used. Finally, by also using the remaining properties (iv) and (vi) and assuming normal distributions, it is possible to test the effect of every treatment factor in the corresponding stratum.

Sections 3.1.3 and 3.1.4 summarize the underlying mathematical results and give several examples of orthogonal designs.

3.1.3 Block structure

To analyse the block structure, we use a *null experiment* (Nelder, 1965a), where all observational units receive the same treatment and thus the experimental structure depends only on

how the observational units are grouped. Tjur (1984) called the analysis of variance without treatments the *null ANOVA*.

Suppose that the orthogonal block structure of an orthogonal design is given by $\mathfrak{B} = \{\mathscr{B}_0, \ldots, \mathscr{B}_{K+1}\}$ where $\mathscr{B}_0 = \mathscr{U}$ is the universal factor on $\mathscr{I}$ and $\mathscr{B}_{K+1} = \mathscr{E}$ is the equality factor on $\mathscr{I}$.

Definition 3.3 The $\mathbb{W}$-*subspace* for $\mathscr{B}_k \in \mathfrak{B}$, $k = 0, \ldots, K+1$, is the subspace of $\mathbb{R}^N$ defined by

$$\mathbb{W}(\mathscr{B}_k) = \mathbb{V}(\mathscr{B}_k) \cap [\sum_{\mathscr{B}_{k'} \in \mathfrak{B}: \mathscr{B}_k \prec \mathscr{B}_{k'}} \mathbb{V}(\mathscr{B}_{k'})]^{\perp} \tag{3.1}$$

where the summation symbol denotes the sum of subspaces. Moreover, $\mathbb{W}(\mathscr{B}_k)$ is called the *stratum* for $\mathscr{B}_k \in \mathfrak{B}$.

Notice that the $\mathbb{W}$-subspace of a block factor can be defined in the same way for sets of block factors which do not possess all six properties of an orthogonal block structure. For example, there is also a $\mathbb{W}$-subspace for every block factor in the set $\mathfrak{T}^{\phi}$ of block factors that are induced by the design function ϕ and the orthogonal treatment structure $\mathfrak{T}$ of an orthogonal design. The $\mathbb{W}$-subspace of a block factor is determined within the block structure and not affected by any treatment factor.

For every $\mathscr{B}_k \in \mathfrak{B}$ let $q_{\mathscr{B}_k}$ be the number of levels as before, and $d_{\mathbb{W}(\mathscr{B}_k)}$ the dimension of $\mathbb{W}(\mathscr{B}_k)$. In an orthogonal design, we have the following properties for $\mathbb{W}$-subspaces of block factors; see Bailey (2008, pp. 182–183) and Cheng (2014, pp. 236–237).

Theorem 3.1 *Let $\mathfrak{B}$ be an orthogonal block structure. Then:*

(1) $\mathbb{W}$-subspaces for any two different block factors are orthogonal, i.e., $\mathbb{W}(\mathscr{B}_k) \perp \mathbb{W}(\mathscr{B}_{k'})$ for all $\mathscr{B}_k, \mathscr{B}_{k'} \in \mathfrak{B}$ with $k \neq k'$.

(2) For every $\mathscr{B}_k \in \mathfrak{B}$ it holds that

$$\mathbb{V}(\mathscr{B}_k) = \bigoplus_{\mathscr{B}_{k'} \in \mathfrak{B}: \mathscr{B}_k \preceq \mathscr{B}_{k'}} \mathbb{W}(\mathscr{B}_{k'}).$$

In particular, $\mathbb{R}^N = \mathbb{V}(\mathscr{E}) = \mathbb{W}(\mathscr{U}) \oplus \mathbb{W}(\mathscr{B}_1) \oplus \cdots \oplus \mathbb{W}(\mathscr{B}_K) \oplus \mathbb{W}(\mathscr{E})$.

(3) For every $\mathscr{B}_k \in \mathfrak{B}$ we have

$$d_{\mathbb{W}(\mathscr{B}_k)} = q_{\mathscr{B}_k} - \sum_{\mathscr{B}_{k'} \in \mathfrak{B}: \mathscr{B}_k \prec \mathscr{B}_{k'}} d_{\mathbb{W}(\mathscr{B}_{k'})}. \tag{3.2}$$

Proof. For part *(1)*, let $\mathscr{B}_k$ and $\mathscr{B}_{k'}$ be different factors in $\mathfrak{B}$. Since the factors are orthogonal, we have $\mathbb{V}(\mathscr{B}_k) \cap [\mathbb{V}(\mathscr{B}_k) \cap \mathbb{V}(\mathscr{B}_{k'})]^\perp$ is orthogonal to $\mathbb{V}(\mathscr{B}_{k'}) \cap [\mathbb{V}(\mathscr{B}_k) \cap \mathbb{V}(\mathscr{B}_{k'})]^\perp$. Moreover, as was noted earlier, $\mathbb{V}(\mathscr{B}_k) \cap \mathbb{V}(\mathscr{B}_{k'}) = \mathbb{V}(\mathscr{B}_k \vee \mathscr{B}_{k'})$, and $\mathscr{B}_k \vee \mathscr{B}_{k'} \in \mathfrak{B}$.

At least one of $\mathscr{B}_k$ and $\mathscr{B}_{k'}$ is not equivalent to $\mathscr{B}_k \vee \mathscr{B}_{k'}$. Suppose without loss of generality $\mathscr{B}_k \prec (\mathscr{B}_k \vee \mathscr{B}_{k'})$. Since $[\sum_{\mathscr{B}_{k'} \in \mathfrak{B}: \mathscr{B}_k \prec \mathscr{B}_{k'}} \mathbb{V}(\mathscr{B}_{k'})]^\perp = \bigcap_{\mathscr{B}_{k'} \in \mathfrak{B}: \mathscr{B}_k \prec \mathscr{B}_{k'}} \mathbb{V}(\mathscr{B}_{k'})^\perp$ (Bailey, 2008, p. 183), we have $\mathbb{W}(\mathscr{B}_k) \subseteq \mathbb{V}(\mathscr{B}_k) \cap \mathbb{V}(\mathscr{B}_k \vee \mathscr{B}_{k'})^\perp = \mathbb{V}(\mathscr{B}_k) \cap [\mathbb{V}(\mathscr{B}_k) \cap \mathbb{V}(\mathscr{B}_{k'})]^\perp$.

From $\mathbb{V}(\mathscr{B}_{k'}) = (\mathbb{V}(\mathscr{B}_{k'}) \cap [\mathbb{V}(\mathscr{B}_k) \cap \mathbb{V}(\mathscr{B}_{k'})]^\perp) \oplus (\mathbb{V}(\mathscr{B}_k) \cap \mathbb{V}(\mathscr{B}_{k'}))$ it follows that $\mathbb{W}(\mathscr{B}_k)$ is orthogonal to $\mathbb{V}(\mathscr{B}_{k'})$. The proof is completed by noting that $\mathbb{W}(\mathscr{B}_{k'}) \subseteq \mathbb{V}(\mathscr{B}_{k'})$.

Part *(2)* is proved by mathematical induction (Bailey, 2008, p. 183) and part *(3)* follows immediately from part (2) by using the well-known formula for the dimension of the direct sum of vector spaces. □

The dimension of the $\mathbb{W}$-subspace $d_{\mathbb{W}(\mathscr{B}_k)}$ is also called the *degrees of freedom* for the factor $\mathscr{B}_k$ and thus we will use $d_{\mathscr{B}_k}$ for simplicity in the remainder of this thesis. Also, q_k will be used instead of $q_{\mathscr{B}_k}$.

The block structure of a design can be visualised by using a Hasse diagram (Bailey, 2008). To draw a Hasse diagram, we first order all factors from the coarsest (at the top in

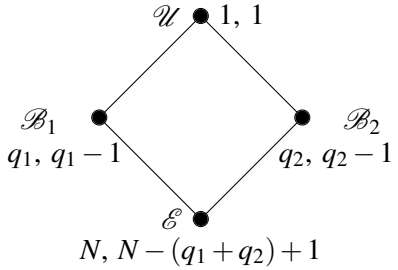

Figure 3.1: Hasse diagram for the block structure of the row-column design in Example 3.1

Table 3.1: Table for the block structure of the row-column design in Example 3.1

Stratum	Source	$\mathbb{W}$-subspace	$d_{\mathbb{W}}$
mean	$\mathscr{U}$	$\mathbb{V}(\mathscr{U})$	1
rows	$\mathscr{B}_1$	$\mathbb{V}(\mathscr{B}_1)\cap\mathbb{V}(\mathscr{U})^{\perp}$	q_1-1
columns	$\mathscr{B}_2$	$\mathbb{V}(\mathscr{B}_2)\cap\mathbb{V}(\mathscr{U})^{\perp}$	q_2-1
plots	$\mathscr{E}$	$[\mathbb{V}(\mathscr{B}_1)+\mathbb{V}(\mathscr{B}_2)]^{\perp}$	$N-(q_1+q_2)+1$
Total		$\mathbb{R}^N$	N

a Hasse diagram) to the finest (at the bottom in a Hasse diagram) and then link two nested factors by a straight line. Factors $\mathscr{B}$ and $\mathscr{B}'$ for which neither $\mathscr{B} \prec \mathscr{B}'$ nor $\mathscr{B}' \prec \mathscr{B}$ are represented at the same level in the diagram. The number of levels and degrees of freedom for each factor are also provided in the Hasse diagram. Moreover, we also use a table to display the block structure.

Example 3.1 (Row-column design) In a row-column design with q_1 rows and q_2 columns, each of, in total, $N = q_1 \times q_2$ observational units belongs to one row and one column. Any two observational units will belong to either different rows or different columns.

We use $\mathscr{B}_1$ and $\mathscr{B}_2$ to indicate the row factor and the column factor. Then, we have $\mathscr{E} \prec \mathscr{B}_1 \prec \mathscr{U}$ and $\mathscr{E} \prec \mathscr{B}_2 \prec \mathscr{U}$. Degrees of freedom can be calculated by using part *(3)* of Theorem 3.1 as:

$$
\begin{aligned}
d_{\mathscr{U}} &= q_0 = 1, \\
d_{\mathscr{B}_1} &= q_1 - d_{\mathscr{U}} = q_1 - 1, \\
d_{\mathscr{B}_2} &= q_2 - d_{\mathscr{U}} = q_2 - 1, \\
d_{\mathscr{E}} &= q_1 q_2 - d_{\mathscr{U}} - d_{\mathscr{B}_1} - d_{\mathscr{B}_2} = N - q_1 - q_2 + 1.
\end{aligned}
$$

Notice that $d_{\mathscr{E}} = d_{\mathscr{B}_1} d_{\mathscr{B}_2}$. The Hasse diagram and the table for the block structure of this row-column design are shown in Figure 3.1 and Table 3.1.

From Example 3.1, we can see the Hasse diagram displays the relationships between factors by linking the dots for factors and it is convenient to calculate degrees of freedom in the diagram following Equation (3.2). Therefore, to analyse an orthogonal design, we start with a Hasse diagram for the orthogonal block structure $\mathfrak{B}$ and summarise the calculations of the degrees of freedom in an ANOVA table. This table represents the null ANOVA of the experiment. The table for the block structure can be expanded into a full ANOVA table by adding calculations for the treatment structure and hypothesis tests as will be shown later.

3.1.4 Treatment structure

Suppose the orthogonal treatment structure of an orthogonal design is given by $\mathfrak{T} = \{\mathscr{G}_0, \mathscr{G}_1, \ldots, \mathscr{G}_U\}$, where $\mathscr{G}_0 = \mathscr{U}$. Then we use calculations similar to those for the block structure. The $\mathbb{V}$-subspace $\mathbb{V}(\mathscr{G}_u)$ of any treatment factor $\mathscr{G}_u \in \mathfrak{T}$ is obtained by using Definition 3.1 and the $\mathbb{W}$-subspace for $\mathscr{G}_u$ is $\mathbb{W}(\mathscr{G}_u) = \mathbb{V}(\mathscr{G}_u) \cap [\sum_{\mathscr{G}_{u'} \in \mathfrak{T}: \mathscr{G}_u \prec \mathscr{G}_{u'}} \mathbb{V}(\mathscr{G}_{u'})]^{\perp}$. Notice, however, that these spaces are subspaces of $\mathbb{R}^t$, where t is the number of treatments.

By using the same arguments as in the proof of Theorem 3.1 it can be shown that the $\mathbb{W}$-subspaces for any two different treatment factors are orthogonal. Moreover, as in part (2) of the theorem $\mathbb{V}(\mathscr{G}_u)$ is equal to the direct sum of the $\mathbb{W}(\mathscr{G}_{u'})$ for the factors $\mathscr{G}_{u'} \in \mathfrak{T}$ with $\mathscr{G}_u \preceq \mathscr{G}_{u'}$. From this decomposition, and using the simpler notation p_u instead of $p_{\mathscr{G}_u}$ for the number of levels of $\mathscr{G}_u$, one obtains the formula $d_{\mathscr{G}_u} = p_u - \sum_{\mathscr{G}_{u'} \in \mathfrak{T}: \mathscr{G}_u \prec \mathscr{G}_{u'}} d_{\mathscr{G}_{u'}}$ for the dimension $d_{\mathscr{G}_u}$ of $\mathbb{W}(\mathscr{G}_u)$, which is similar to Equation (3.2).

Similar to block factors, the degrees of freedom for a treatment factor are the dimension of the $\mathbb{W}$-subspace for the factor. The above formula shows that for treatment factors the degrees of freedom can also be calculated by using a Hasse diagram. We consider the block structure and treatment structure of the following split-plot design as an example.

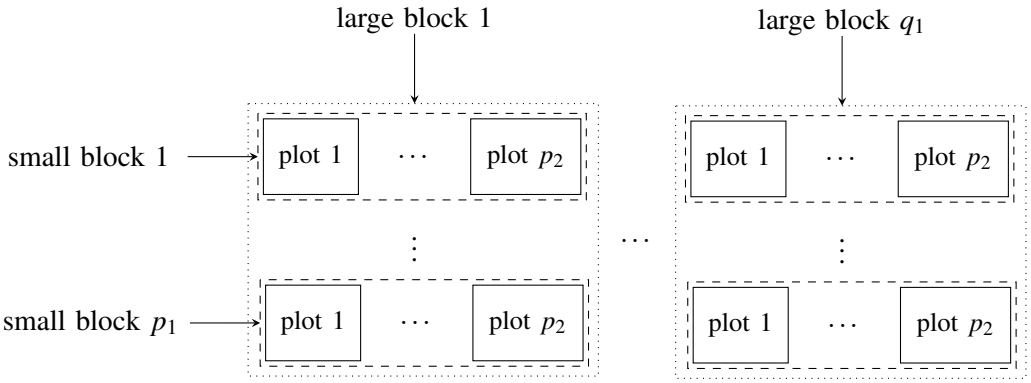

Example 3.2 (Split-plot design) We consider a split-plot design with q_1 large blocks. Each large block contains p_1 small blocks (whole-plots) and each small block contains p_2 plots (split-plots). Thus, there are $q_2 = q_1 p_1$ small blocks in total and $N = q_1 p_1 p_2 = q_2 p_2$ plots in the design. Two treatment factors A and B are applied to whole-plots and split-plots respectively. Each of the p_1 levels of the treatment factor A (whole-plot factor) is randomly allocated to one small block per large block and each of the p_2 levels of the treatment factor B (split-plot factor) is randomly allocated to one plot per small block.

Factors for the large block and the small block are denoted by $\mathscr{B}_1$ and $\mathscr{B}_2$, whereas factors A and B are denoted by $\mathscr{G}_1$ and $\mathscr{G}_2$. The infimum $\mathscr{G}_3 = \mathscr{G}_1 \wedge \mathscr{G}_2$ represents the interaction of the factors A and B. Hasse diagrams for the block structure and the treatment structure of this split-plot design are shown in Figure 3.2.

Separate Hasse diagrams are used to visualise the block structure and treatment structure, as shown in Figure 3.2. In order to distinguish the treatment structure and the block structure, following Bailey (2008), we use a dot to indicate a block factor, whereas a circle is used to indicate a treatment factor.

These diagrams are useful to illustrate the block structure and the treatment structure. However, from separate Hasse diagrams, it is not clear which stratum a specific treatment factor belongs to. We use the following result of Bailey (2008, p. 198) to locate a treatment

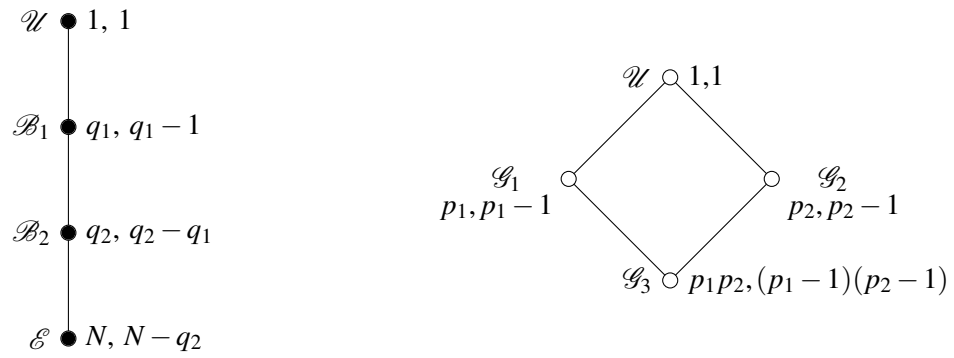

Figure 3.2: Hasse diagrams for the block structure (left) and the treatment structure (right) of the split-plot design in Example 3.2

factor to a stratum. Contrary to the original statement of the result, we refer however explicitly to the induced block factors $\mathscr{G}_u^\phi$ where $\mathscr{G}_u \in \mathfrak{T}$ and ϕ is the design function of the orthogonal design as before. Moreover, $\mathbb{W}(\mathscr{G}_u^\phi)$ is the $\mathbb{W}$-subspace for $\mathscr{G}_u^\phi$ which is defined as in Definition 3.3 with $\mathfrak{B}$ being replaced by the set $\mathfrak{T}^\phi$ of induced block factors.

Theorem 3.2 *Let $\mathscr{G}_u$ be a treatment factor in an orthogonal design with orthogonal block structure $\mathfrak{B}$, orthogonal treatment structure $\mathfrak{T}$ and design function ϕ. Then there exists a unique block factor $\mathscr{B}_k \in \mathfrak{B}$ such that*

(1) $\mathscr{B}_k \preceq \mathscr{G}_u^\phi$,

(2) $\mathscr{B}_k$ is the coarsest factor among all block factors in $\mathfrak{B}$ that are finer than or equivalent to $\mathscr{G}_u^\phi$.

Moreover, $\mathscr{G}_u$ belongs to the stratum for $\mathscr{B}_k$ in the sense that $\mathbb{W}(\mathscr{G}_u^\phi) \subseteq \mathbb{W}(\mathscr{B}_k)$.

In Example 3.2, the whole-plot treatment factor is allocated to small blocks and the split-plot treatment factor is allocated to plots.

Thus, the whole-plot treatment factor $\mathscr{G}_1$ belongs to the stratum $\mathbb{W}(\mathscr{B}_2)$, while the split-plot treatment factor $\mathscr{G}_2$ and the interaction term $\mathscr{G}_3 = \mathscr{G}_1 \wedge \mathscr{G}_2$ belong to the stratum $\mathbb{W}(\mathscr{E})$. All factors, including both block factors and treatment factors, can be visualised together by using a combined Hasse diagram (Bailey, 2008). The combined Hasse diagram of Example 3.2 is shown in Figure 3.3.

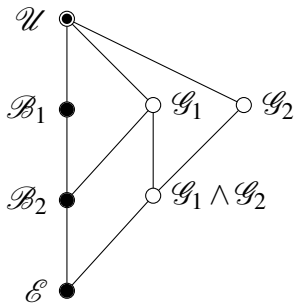

Figure 3.3: Combined Hasse diagram for the split-plot design in Example 3.2

For simplicity, the number of levels and degrees of freedom for each factor are not shown in this diagram. We can see that the universal factor is represented by a dot within a circle, which indicates that the universal factor is considered as both a block factor and a treatment factor.

The properties (vii), (viii) and (ix) which characterise the orthogonal treatment structure $\mathfrak{T}$ of an orthogonal design carry over, with the obvious changes of notation, and by also using property (x) to the set $\mathfrak{T}^\phi$ of induced block factors. This implies that a result which is analogous to Theorem 3.1 also holds for the $\mathbb{V}$-subspaces and the $\mathbb{W}$-subspaces that are associated with the induced block factors in $\mathfrak{T}^\phi$ since the prove of Theorem 3.1 only uses the properties (viii) and (ix), that is, the fact that the supremum of any two factors in the relevant set of block factors is in that set and that any two block factors in the set are orthogonal. Moreover, it can be shown that for any $\mathscr{G}_u \in \mathfrak{T}$ the dimension of $\mathbb{W}(\mathscr{G}_u) \subseteq \mathbb{R}^t$ is equal to the dimension of $\mathbb{W}(\mathscr{G}_u^\phi) \subseteq \mathbb{R}^N$. For these reasons, for practical purposes, such as calculations of degrees of freedom for treatment factors, the orthogonal treatment structure $\mathfrak{T}$ can be identified with the set of induced block factors $\mathfrak{T}^\phi$.

As a consequence of these considerations and of Theorem 3.2 it follows that a stratum $\mathbb{W}(\mathscr{B}_k)$ for $\mathscr{B}_k \in \mathfrak{B}$ that contains the treatment factors $\mathscr{G}_{1^*}, \ldots, \mathscr{G}_{V^*} \in \mathfrak{T}$ in the sense that

$\mathbb{W}(\mathscr{G}_{j^*}^{\phi}) \subseteq \mathbb{W}(\mathscr{B}_k)$ for $j = 1, \ldots, V$ can be decomposed as

$$\mathbb{W}(\mathscr{B}_k) = \mathbb{W}(\mathscr{G}_{1^*}^{\phi}) \oplus \cdots \oplus \mathbb{W}(\mathscr{G}_{V^*}^{\phi}) \oplus \mathbb{W}(res_k), \tag{3.3}$$

where $\mathbb{W}(res_k) := \mathbb{W}(\mathscr{B}_k) \cap [\mathbb{W}(\mathscr{G}_{1^*}^{\phi}) \oplus \cdots \oplus \mathbb{W}(\mathscr{G}_{V^*}^{\phi})]^{\perp}$ is the orthogonal complement of the direct sum of the $\mathbb{W}$-subspaces for the induced block factors in the stratum for $\mathscr{B}_k$.

The subspace $\mathbb{W}(res_k)$ is called the *residual subspace in the stratum*. In the full ANOVA table to be presented later, within any stratum that contains treatment factors other than the universal factor this space will be represented by a line for the *residual* (cf. Bailey, 2008, p. 27) which is indicated by using the notation res_k. The corresponding degrees of freedom are the dimension of $\mathbb{W}(res_k)$ which can be calculated by subtracting from the degrees of freedom for $\mathscr{B}_k \in \mathfrak{B}$ the sum of the degrees of freedom for the treatment factors $\mathscr{G}_{1^*}, \ldots, \mathscr{G}_{V^*} \in \mathfrak{T}$.

Therefore, in the decomposition $\mathbb{R}^N = \mathbb{W}(\mathscr{U}) \oplus \mathbb{W}(\mathscr{B}_1) \oplus \cdots \oplus \mathbb{W}(\mathscr{B}_K) \oplus \mathbb{W}(\mathscr{E})$ from the null ANOVA, some of the strata can be decomposed further. If a stratum contains treatment factors other than the universal factor, it is decomposed as shown in Equation (3.3). If a stratum $\mathbb{W}(\mathscr{B}_k)$ contains no treatment factor or only the universal factor, it remains in the decomposition.

The statement "an orthogonal design determines a unique decomposition on the observation space as a direct sum of orthogonal subspaces, one for each factor of the design" in Tjur (1984) refers to this decomposition. With respect to terminology it should be noted that the "orthogonal subspace" in Tjur (1984) for each treatment factor is in this thesis the $\mathbb{W}$-subspace for the treatment factor (or, more precisely, for the corresponding induced block factor), whereas the "orthogonal subspace" in Tjur (1984) for each block factor is the residual subspace $\mathbb{W}(res_k)$ in the stratum.

3.2 Functional mixed-effects model for orthogonal designs

3.2.1 Functional mixed-effects model

A functional mixed-effects model was introduced by Guo (2002) and then further developed by Morris and Carroll (2006). Moreover, the model constructed by Morris and Carroll (2006) is applicable to more general functional data than those considered by Guo (2002).

We consider the following mixed-effects model for functional responses $\mathbf{y}(t) = [y_1(t),\ldots,y_N(t)]^T, t \in T$:

$$\mathbf{y}(t) = \mathbf{X}\boldsymbol{\beta}(t) + \mathbf{Z}\boldsymbol{\delta}(t) + \boldsymbol{\varepsilon}(t), \quad t \in T, \tag{3.4}$$

where $\mathbf{y}$ is a vector of N stochastic processes; $\mathbf{X}$ and $\mathbf{Z}$ are $N \times p$ and $N \times q$ matrices; $\boldsymbol{\beta} = [\beta_1,\ldots,\beta_p]^T$ is a vector of fixed-effect functions and $\beta_a \in \mathbb{L}^2(T)$ for $a = 1,\ldots,p$; $\boldsymbol{\delta} = [\delta_1,\ldots,\delta_q]^T$ is a vector of stochastic processes with $\delta_1,\ldots,\delta_q \overset{i.i.d.}{\sim} GP(0,\theta)$ for random-effect terms; and $\boldsymbol{\varepsilon} = [\varepsilon_1,\ldots,\varepsilon_N]^T$ is also a vector of stochastic processes with $\varepsilon_1,\ldots,\varepsilon_N \overset{i.i.d.}{\sim} GP(0,\theta_e)$ for error terms. In the terminology of Chapter 2, δ_b for $b = 1,\ldots,q$ and ε_i for $i = 1,\ldots,N$ are also random elements in $\mathbb{L}^2(T)$. Moreover, all random-effect terms and error terms are independent. Then we have that

$$\boldsymbol{\eta} := \boldsymbol{\eta}(t) = E[\mathbf{y}(t)] = \mathbf{X}\boldsymbol{\beta}(t), \quad t \in T,$$

is a vector of mean functions and

$$\boldsymbol{\Gamma} := \boldsymbol{\Gamma}(s,t) = Cov[\mathbf{y}(s),\mathbf{y}(t)] = \mathbf{Z}\mathbf{Z}^T\theta(s,t) + \mathbf{I}\theta_e(s,t), \quad s,t \in T,$$

is a matrix of covariance functions, where $\mathbf{I}$ is an $N \times N$ indentity matrix.

Model equation (3.4) was proposed by Morris and Carroll (2006). By removing the

random-effect term $\mathbf{Z}\boldsymbol{\delta}(t)$, the model is reduced to the functional regression model with independent functional responses in Shen and Faraway (2004).

3.2.2 Design matrices

The mixed-effects model can be used to study an orthogonal design with functional responses. Suppose for an orthogonal design, all factors in the orthogonal treatment structure $\mathfrak{T} = \{\mathscr{G}_0, \ldots, \mathscr{G}_U\}$ have fixed effects, while all factors in the orthogonal block structure $\mathfrak{B} = \{\mathscr{B}_0, \ldots, \mathscr{B}_{K+1}\}$ have random effects. As before, we assume that $\mathscr{G}_0 = \mathscr{U}$ is the universal factor on $\mathscr{T}$, $\mathscr{B}_0 = \mathscr{U}$ is the universal factor on $\mathscr{I}$, and $\mathscr{B}_{K+1} = \mathscr{E}$ is the equality factor on $\mathscr{I}$.

Then, for a treatment factors $\mathscr{G}_u \in \mathfrak{T}$ with p_u levels, the corresponding design matrix $\mathbf{X}_u = [x_{(i,a)}]$ is an $N \times p_u$ matrix with elements:

$$x_{(i,a)} = \begin{cases} 1 & \text{if the level } a \text{ of } \mathscr{G}_u \text{ is assigned to the } i\text{-th observational unit} \\ 0 & \text{otherwise,} \end{cases} \tag{3.5}$$

where $i = 1, \ldots, N$ and $a = 1, \ldots, p_u$. The vector $\boldsymbol{\beta}_u(t) = [\beta_{u,1}(t), \ldots, \beta_{u,p_u}(t)]^T$ indicates the main effect of $\mathscr{G}_u$ for $u = 0, \ldots, U$.

Likewise, for a block factor $\mathscr{B}_k \in \mathfrak{B}$ with q_k levels, the corresponding design matrix $\mathbf{Z}_k = [z_{(i,b)}]$ is an $N \times q_k$ matrix with elements:

$$z_{(i,b)} = \begin{cases} 1 & \text{if the } i\text{-th observational unit belongs to the level } b \text{ of } \mathscr{B}_k \\ 0 & \text{otherwise,} \end{cases} \tag{3.6}$$

where $i = 1, \ldots, N$ and $b = 1, \ldots, q_k$. The vector $\boldsymbol{\delta}_k(t) = [\delta_{k,1}(t), \ldots, \delta_{k,q_k}(t)]^T$ indicates the random effect of $\mathscr{B}_k$ and $\delta_{k,1}, \ldots, \delta_{k,q_k} \overset{i.i.d.}{\sim} GP(0, \theta_k)$ for $k = 0, \ldots, K+1$.

Therefore, the complete model equation for the orthogonal design is:

$$\mathbf{y}(t) = \sum_{u=0}^{U} \mathbf{X}_u \boldsymbol{\beta}_u(t) + \sum_{k=0}^{K} \mathbf{Z}_k \boldsymbol{\delta}_k(t) + \boldsymbol{\varepsilon}(t), \quad t \in T, \tag{3.7}$$

where each of terms $\{\boldsymbol{\beta}_u(t)\}_{u=0}^{U}$, $\{\boldsymbol{\delta}_k(t)\}_{k=0}^{K}$ represents the effect of one factor in the design, while $\boldsymbol{\varepsilon}(t)$ is related to the equality factor $\mathscr{E} = \mathscr{B}_{K+1} \in \mathfrak{B}$. All other assumptions for this model are the same as those in Equation (3.4).

In what follows, for every matrix $\mathbf{M}$, let $C(\mathbf{M})$ be the column space of the matrix.

Proposition 3.1 *In an orthogonal design with block structure $\mathfrak{B}$, treatment structure $\mathfrak{T}$, design function ϕ and design matrices as in Equations (3.5) and (3.6) we have:*

(1) if $\mathscr{B}_k \in \mathfrak{B}$ then $C(\mathbf{Z}_k) = \mathbb{V}(\mathscr{B}_k)$,

(2) if $\mathscr{G}_u \in \mathfrak{T}$ then $C(\mathbf{X}_u) = \mathbb{V}(\mathscr{G}_u^{\phi})$.

Proposition 3.1 is an immediate consequence of the definitions of the design matrices in Equations (3.5) and (3.6) and the definition of the $\mathbb{V}$-subspace (Definition 3.1). This result links functional mixed-effects models and orthogonal designs. See also Cheng (2014, pp. 234–236) for a similar mixed-effects model for orthogonal designs with a univariate response variable which does however not explicitly show the treatment factors.

3.2.3 Orthogonal projections

In order to analyse an orthogonal design, we will use a projection approach. A convenient possibility to define orthogonal projections (Christensen, 2011, p. 426) will be introduced first. We then consider the orthogonal projections onto the $\mathbb{V}$-subspace and the $\mathbb{W}$-subspace, respectively.

Definition 3.4 Let V be an arbitrary subspace of $\mathbb{R}^N$. Then $\mathbf{P}_V : \mathbb{R}^N \to \mathbb{R}^N$ is the *orthogonal projection* from $\mathbb{R}^N$ onto V, if and only if the following two conditions hold:

(i) for any $v \in V$, we have $\mathbf{P}_V(v) = v$;

(ii) for any $w \in V^{\perp}$, we have $\mathbf{P}_V(w) = 0$.

It is well-known that for any subspace V of $\mathbb{R}^N$ the orthogonal projection $\mathbf{P}_V$ yields vectors in V, that is, $\mathbf{P}_V(v) \in V$ for every $v \in \mathbb{R}^N$. Moreover, $\mathbf{P}_V$ is a linear mapping.

In what follows, we will also use $\mathbf{P}_V$ to denote the matrix that represents this mapping. Hence, for $\mathbf{P}_V(v)$ where $\mathbf{P}_V$ is the mapping we can also writ $\mathbf{P}_V v$ where $\mathbf{P}_V$ is the matrix which represents the orthogonal projection.

Orthogonal projection onto the $\mathbb{V}$-subspace

Consider an orthogonal design with orthogonal block structure $\mathfrak{B}$, orthogonal treatment structure $\mathfrak{T}$ and design function ϕ. By applying Proposition 3.1, for a block factor $\mathscr{B}_k \in \mathfrak{B}$, the matrix representing the orthogonal projection from $\mathbb{R}^N$ onto the $\mathbb{V}$-subspace for $\mathscr{B}_k$ can be easily shown to be equal to

$$\mathbf{P}_{\mathbb{V}(\mathscr{B}_k)} = \mathbf{Z}_k(\mathbf{Z}_k^T\mathbf{Z}_k)^{-1}\mathbf{Z}_k^T = \frac{1}{r_{\mathscr{B}_k}}\mathbf{Z}_k\mathbf{Z}_k^T, \tag{3.8}$$

where $r_{\mathscr{B}_k} = N/q_{\mathscr{B}_k}$ is the replication of each level of $\mathscr{B}_k$. Notice that $r_{\mathscr{B}_k}$ is the common size of the $\mathscr{B}_k$-classes.

Similarly, for a treatment factor $\mathscr{G}_u \in \mathfrak{T}$ the matrix representing the orthogonal projection from $\mathbb{R}^N$ onto the $\mathbb{V}$-subspace for the induced block factor $\mathscr{G}_u^{\phi} \in \mathfrak{T}^{\phi}$ is equal to

$$\mathbf{P}_{\mathbb{V}(\mathscr{G}_u^{\phi})} = \mathbf{X}_u(\mathbf{X}_u^T\mathbf{X}_u)^{-1}\mathbf{X}_u^T. \tag{3.9}$$

A simplification of the matrix $\mathbf{P}_{\mathbb{V}(\mathscr{G}_u^{\phi})}$ which is similar to that for $\mathbf{P}_{\mathbb{V}(\mathscr{B}_k)}$ is not possible in

general since the the treatment factors and the corresponding induced block factors are not necessarily uniform. Even when all treatments are applied to the same number of levels, for $\mathscr{G}_u \in \mathfrak{T}$ the induced block factor $\mathscr{G}_u^{\phi} \in \mathfrak{T}^{\phi}$ does not have to be uniform.

Let $\mathscr{B}$ be a block factor, which can be either in $\mathfrak{B}$ or $\mathfrak{T}^{\phi}$ and $\mathscr{I} = \{1,\ldots,N\}$. The orthogonal projection $\mathbf{P}_{\mathbb{V}(\mathscr{B})}$ onto the corresponding $\mathbb{V}$-subspace transforms the vector $[y_1(t),\ldots,y_N(t)]^T$ into a vector of averages:

$$[y_1(t),\ldots,y_N(t)]^T \longrightarrow [\bar{y}_{\mathscr{B}(1)}(t),\ldots,\bar{y}_{\mathscr{B}(N)}(t)]^T, \quad t \in T, \tag{3.10}$$

that is, each $y_i(t)$ for $i = 1,2,\ldots,N$ is replaced by $\bar{y}_{\mathscr{B}(i)}(t)$ with $\mathscr{B}(i) \in \{1,\ldots,q_{\mathscr{B}}\}$, where $\mathscr{B}(i)$ is the level of the factor $\mathscr{B}$ which occurs on plot i and $\bar{y}_{\mathscr{B}(i)}(t)$ is the average of responses belonging to the same level of the factor $\mathscr{B}$ as the plot i.

For instance, suppose N is even and $\mathscr{B}_k \in \mathfrak{B}$ is a block factor with two levels 1 and 2 such that, for simplicity of exposition, the first half of the observational units in the experiment have the first level and the second half of the observational units have the second level. Then the design matrix $\mathbf{Z}_k$ can be expressed as

$$\mathbf{Z}_k = \begin{bmatrix} 1 & \ldots & 1 & 0 & \ldots & 0 \\ 0 & \ldots & 0 & 1 & \ldots & 1 \end{bmatrix}^T$$

and the orthogonal projection onto $\mathbb{V}(\mathscr{B}_k)$ is the mapping

$$\mathbf{P}_{\mathbb{V}(\mathscr{B}_k)}: \quad [y_1(t),\ldots,y_N(t)]^T \mapsto [\bar{y}_{\mathscr{B}_k(1)}(t),\ldots,\bar{y}_{\mathscr{B}_k(N)}(t)]^T, \quad t \in T,$$

where $\mathscr{B}_k(1) = \cdots = \mathscr{B}_k(N/2) = 1$ and $\mathscr{B}_k(N/2+1) = \cdots = \mathscr{B}_k(N) = 2$ and the averages of the responses for the two levels of $\mathscr{B}_k$ are equal to $\bar{y}_1(t) = 2(y_1(t) + \cdots + y_{N/2}(t))/N$ and $\bar{y}_2(t) = 2(y_{N/2+1}(t) + \cdots + y_N(t))/N$, respectively.

Orthogonal projection onto the $\mathbb{W}$-subspace

We continue to consider an orthogonal design with orthogonal block structure $\mathfrak{B}$, orthogonal treatment structure $\mathfrak{T}$ and design function ϕ. As before it is assumed that $\mathfrak{B} = \{\mathscr{B}_0, \ldots, \mathscr{B}_{K+1}\}$ where $\mathscr{B}_0 = \mathscr{U}$ is the universal factor on $\mathscr{I}$, and $\mathscr{B}_{K+1} = \mathscr{E}$ is the equality factor on $\mathscr{I}$ and that $\mathfrak{T} = \{\mathscr{G}_0, \ldots, \mathscr{G}_U\}$ where $\mathscr{G}_0 = \mathscr{U}$ is the universal factor on $\mathscr{T}$.

For $\mathscr{B}_k \in \mathfrak{B}$, the matrix representing the orthogonal projection from $\mathbb{R}^N$ onto $\mathbb{W}(\mathscr{B}_k)$ is denoted by $\mathbf{P}_{\mathbb{W}(\mathscr{B})}$. Similarly, for $\mathscr{G}_u \in \mathfrak{T}$ the matrix for the orthogonal projection from $\mathbb{R}^N$ onto the $\mathbb{W}$-subspace for the induced block factor $\mathscr{G}_u^\phi$ is $\mathbf{P}_{\mathbb{W}(\mathscr{G}_u^\phi)}$.

We first consider properties of $\mathbf{P}_{\mathbb{W}(\mathscr{B})}$.

Theorem 3.3 *Let $\mathscr{B} \in \mathfrak{B}$. Then:*

(1) For every factor $\mathscr{B}' \in \mathfrak{B}$

$$\mathbf{P}_{\mathbb{V}(\mathscr{B})}\mathbf{P}_{\mathbb{W}(\mathscr{B}')} = \begin{cases} \mathbf{P}_{\mathbb{W}(\mathscr{B}')} & \text{if } \mathscr{B} \preceq \mathscr{B}', \\ 0 & \text{otherwise.} \end{cases}$$

(2) $\mathbf{P}_{\mathbb{V}(\mathscr{B})} = \sum_{\mathscr{B}' \in \mathfrak{B}: \mathscr{B} \preceq \mathscr{B}'} \mathbf{P}_{\mathbb{W}(\mathscr{B}')}$.

Proof. (1) Suppose first that $\mathscr{B} \preceq \mathscr{B}'$. Then $\mathbb{W}(\mathscr{B}') \subseteq \mathbb{V}(\mathscr{B}') \subseteq \mathbb{V}(\mathscr{B})$. For every $v \in \mathbb{R}^N$, since $\mathbf{P}_{\mathbb{W}(\mathscr{B}')}v \in \mathbb{W}(\mathscr{B}') \subseteq \mathbb{V}(\mathscr{B})$, it follows from property (i) of the orthogonal projection that $\mathbf{P}_{\mathbb{V}(\mathscr{B})}\mathbf{P}_{\mathbb{W}(\mathscr{B}')}v = \mathbf{P}_{\mathbb{W}(\mathscr{B}')}v$ which implies $\mathbf{P}_{\mathbb{V}(\mathscr{B})}\mathbf{P}_{\mathbb{W}(\mathscr{B}')} = \mathbf{P}_{\mathbb{W}(\mathscr{B}')}$.

Secondly, if $\mathscr{B} \preceq \mathscr{B}'$ does not hold, then $\mathscr{B}' \neq \mathscr{B}$ and $\mathscr{B}'$ is, in particular, not coarser than $\mathscr{B}$. Hence, $\mathbb{W}(\mathscr{B}')$ does not occur in the decomposition $\mathbb{V}(\mathscr{B}) = \bigoplus_{\mathscr{B}'' \in \mathfrak{B}: \mathscr{B} \preceq \mathscr{B}''} \mathbb{W}(\mathscr{B}'')$ of $\mathbb{V}(\mathscr{B})$ which is obtained by applying part *(2)* of Theorem 3.1. Since, by part *(1)* of Theorem 3.1, $\mathbb{W}$-subspaces for different block factors in $\mathfrak{B}$ are orthogonal it follows that $\mathbb{W}(\mathscr{B}')$ is orthogonal to $\mathbb{V}(\mathscr{B})$, that is $\mathbb{W}(\mathscr{B}') \subseteq \mathbb{V}(\mathscr{B})^\perp$.

Since $\mathbf{P}_{\mathbb{W}(\mathscr{B}')}v \in \mathbb{W}(\mathscr{B}')$ for every $v \in \mathbb{R}^N$, it follows by using property (ii) of the orthogonal projection that $\mathbf{P}_{\mathbb{V}(\mathscr{B})}\mathbf{P}_{\mathbb{W}(\mathscr{B}')}v = 0$ for every $v \in \mathbb{R}^N$. Hence, $\mathbf{P}_{\mathbb{V}(\mathscr{B})}\mathbf{P}_{\mathbb{W}(\mathscr{B}')}$ must be the zero matrix.

(2) Part *(2)* follows immediately from part *(2)* of Theorem 3.1 since $\mathbb{V}(\mathscr{B}) = \bigoplus_{\mathscr{B}' \in \mathfrak{B}: \mathscr{B} \preceq \mathscr{B}'} \mathbb{W}(\mathscr{B}')$.

□

It follows from part *(2)* of Theorem 3.3 that $\mathbf{P}_{\mathbb{W}(\mathscr{B})} = \mathbf{P}_{\mathbb{V}(\mathscr{B})} - \sum_{\mathscr{B}' \in \mathfrak{B}: \mathscr{B} \prec \mathscr{B}'} \mathbf{P}_{\mathbb{W}(\mathscr{B}')}$ for every $\mathscr{B} \in \mathfrak{B}$. Hence, like for degrees of freedom, it is possible to calculate orthogonal projections starting at the top of the Hasse diagram for $\mathfrak{B}$ where $\mathbf{P}_{\mathbb{W}(\mathscr{U})} = \mathbf{P}_{\mathbb{V}(\mathscr{U})}$ and then to work down the Hasse diagram using the above equation at each dot.

Although it is not used in this thesis, there is an alternate method to compute orthogonal projections from $\mathbb{R}^N$ onto $\mathbb{W}$-subspaces due to Tjur (1984, p. 44) who proved that $\mathbf{P}_{\mathbb{W}(\mathscr{B})} = \mathbf{P}_{\mathbb{V}(\mathscr{B})} \prod_{\mathscr{B}' \in \mathfrak{B}: \mathscr{B} \prec \mathscr{B}'} [\mathbf{P}_{\mathbb{V}(\mathscr{B})} - \mathbf{P}_{\mathbb{V}(\mathscr{B}')}]$ for every $B \in \mathfrak{B}$. The advantage of this method is that by using only the $\mathbb{V}$-subspaces, which can be easily determined, it avoids the more complicated calculation of the $\mathbb{W}$-subspaces for all factors in $\mathfrak{B}$ that are coarser than $\mathscr{B}$.

Since $\mathbf{P}_{\mathbb{V}(\mathscr{E})} = \mathbf{I}$ for the equality factor in $\mathfrak{B}$, where $\mathbf{I}$ is the $N \times N$ identity matrix, part *(2)* of Theorem 3.3 yields the following result for every orthogonal block structure $\mathfrak{B} = \{\mathscr{U}, \mathscr{B}_1, \ldots, \mathscr{B}_k, \mathscr{E}\}$ that includes the equality factor $\mathscr{E}$:

$$\mathbf{P}_{\mathbb{W}(\mathscr{U})} + \mathbf{P}_{\mathbb{W}(\mathscr{B}_1)} + \cdots + \mathbf{P}_{\mathbb{W}(\mathscr{B}_K)} + \mathbf{P}_{\mathbb{W}(\mathscr{E})} = \mathbf{I} \tag{3.11}$$

As was already mentioned before, the set $\mathfrak{T}^\phi$ of block factors which are induced by the design function ϕ and the orthogonal treatment structure $\mathfrak{T}$ inherits, by also using (x), the properties that are necessary for proving Theorem 3.1, i.e. being closed under forming suprema and orthogonality of factors, from $\mathfrak{T}$. Since only Theorem 3.1 was used to

prove Theorem 3.3, there is also a version of the latter theorem, with the obvious notational changes, which applies to $\mathfrak{T}^{\phi}$. Hence, for every $\mathscr{G}_u^{\phi} \in \mathfrak{T}^{\phi}$ the orthogonal projection $\mathbf{P}_{\mathbb{W}(\mathscr{G}_u^{\phi})}$ from $\mathbb{R}^N$ onto $\mathbb{W}(\mathscr{G}_u^{\phi})$ can be calculated in a similar way as for the factors in the orthogonal block structure $\mathfrak{B}$. Notice however that $\mathfrak{T}^{\phi}$ does usually not contain the equality factor $\mathscr{E}$ on $\mathscr{I}$.

The orthogonal projections onto the $\mathbb{W}$-subspaces play a key role in ANOVA. In an orthogonal design, the sum of squares for each factor can be calculated by using the orthogonal projection onto the corresponding $\mathbb{W}$-subspace, as will be discussed later.

3.3 Analysis of block structure

The general model for a null experiment with the orthogonal block structure $\mathfrak{B} = \{\mathscr{U}, \mathscr{B}_1, \ldots, \mathscr{B}_K, \mathscr{E}\}$ is expressed as:

$$\mathbf{y}(t) = \boldsymbol{\delta}_0(t) + \sum_{k=1}^{K} \mathbf{Z}_k \boldsymbol{\delta}_k(t) + \boldsymbol{\varepsilon}(t), \quad t \in T, \tag{3.12}$$

where $\boldsymbol{\delta}_0$ and $\boldsymbol{\varepsilon}$ are associated with the universal and equality factors, while $\boldsymbol{\delta}_1, \ldots, \boldsymbol{\delta}_K$ are associated with other block factors. We assume all block factors have random effects. Thus, the block structure does not affect the expectation but determines the covariance structure. More specifically, $\boldsymbol{\delta}_0(t) = [\delta_0(t), \ldots, \delta_0(t)]^T$ with $\delta_0(t)$ indicating the random effect for the universal factor and $\delta_0 \sim GP(0, \theta_0)$; $\boldsymbol{\delta}_k(t) = [\delta_{k,1}(t), \ldots, \delta_{k,q_k}(t)]^T$ with $\delta_{k,b}(t)$, for $b = 1, \ldots, q_k$ and $k = 1, \ldots, K$, indicating the random effect for the level b of the k-th block factor, and $\delta_{k,1}, \ldots, \delta_{k,q_k} \overset{i.i.d.}{\sim} GP(0, \theta_k)$; and $\boldsymbol{\varepsilon}(t) = [\varepsilon_1(t), \ldots, \varepsilon_N(t)]^T$ with $\varepsilon_1, \ldots, \varepsilon_N \overset{i.i.d.}{\sim} GP(0, \theta_e)$.

According to Equation (3.12), the mean function is $E[\mathbf{y}(t)] = \mathbf{0}$ and the covariance function is

$$Cov[\mathbf{y}(s), \mathbf{y}(t)] = \mathbf{J}\theta_0(s,t) + \sum_{k=1}^{K} \mathbf{Z}_k \mathbf{Z}_k^T \theta_k(s,t) + \mathbf{I}\theta_e(s,t), \quad s,t \in T, \tag{3.13}$$

where $\mathbf{J}$ is an $N \times N$ all-1 matrix and $\mathbf{I}$ is an $N \times N$ identity matrix.

3.3.1 Sum of squares of a block factor

Since the experimental structure is time-fixed, at each specific time point t_ℓ, for $t_\ell \in T$ and $\ell = 1,\ldots,m$, the sum of squares $SS(t_\ell)$ is calculated as in a traditional ANOVA. When t traverses an interval T, the sum of squares $SS(t)$ becomes a function of t and is called the *functional sum of squares*. In this section, we use a projection approach to derive functional sums of squares.

According to Equation (3.12), the functional sum of squares for the stratum $\mathbb{W}(\mathscr{B}_k)$, or say for the factor $\mathscr{B}_k \in \mathfrak{B}$, is calculated by

$$SS_{\mathscr{B}_k}(t) = \mathbf{y}(t)^T \mathbf{P}_{\mathbb{W}(\mathscr{B}_k)} \mathbf{y}(t), \quad t \in T. \tag{3.14}$$

According to Equation (3.11), the total functional sum of squares of a design can be partitioned as follows:

$$\begin{aligned} \mathbf{y}(t)^T \mathbf{y}(t) &= SS_{\mathscr{U}}(t) + SS_{\mathscr{B}_1}(t) + \cdots + SS_{\mathscr{B}_K}(t) + SS_{\mathscr{E}}(t) \\ &= \mathbf{y}(t)^T \mathbf{P}_{\mathbb{W}(\mathscr{U})} \mathbf{y}(t) + \mathbf{y}(t)^T \mathbf{P}_{\mathbb{W}(\mathscr{B}_1)} \mathbf{y}(t) + \ldots \\ &\quad + \mathbf{y}(t)^T \mathbf{P}_{\mathbb{W}(\mathscr{B}_K)} \mathbf{y}(t) + \mathbf{y}(t)^T \mathbf{P}_{\mathbb{W}(\mathscr{E})} \mathbf{y}(t). \end{aligned}$$

Definition 3.5 The integral

$$SS^*_{\mathscr{B}} = \int_T SS_{\mathscr{B}}(t)dt = \int_T \mathbf{y}(t)^T \mathbf{P}_{\mathbb{W}(\mathscr{B})} \mathbf{y}(t)dt$$

of the functional sum of squares over $t \in T$ is called the *integrated sum of squares*.

The functional sum of squares is a random function, while the integrated sum of squares

is a random variable. The distribution of the integrated sum of squares will be derived in the following subsection.

3.3.2 Stratum-based covariance function

In order to further analyse the sum of squares of a block factor, the functional sum of squares in Equation (3.14) can be transformed into the sum of squared functions, which are sample paths of Gaussian processes. These Gaussian processes have zero mean function, a common covariance function and zero cross-covariance function. I will call the covariance function of these Gaussian processes the *stratum-based covariance function*.

Theorem 3.4 *The functional sum of squares for $\mathscr{B}_k \in \mathfrak{B}$ in Equation (3.14) can be expressed as:*

$$SS_{\mathscr{B}_k}(t) = \sum_{i=1}^{d_{\mathscr{B}_k}} R_i(t)R_i(t), \quad t \in T,$$

where $R_1,\ldots,R_{d_{\mathscr{B}_k}} \sim GP(0,\Lambda_{\mathscr{B}_k})$ and the cross-covariance between each two Gaussian processes is zero. Furthermore, $\Lambda_{\mathscr{B}_k}$ is called the stratum-based covariance function and calculated by

$$\Lambda_{\mathscr{B}_k}(s,t) = Cov[R_i(s),R_i(t)] = \sum_{\mathscr{B}_{k'} \in \mathfrak{B}:\mathscr{B}_{k'} \preceq \mathscr{B}_k} r_{\mathscr{B}_{k'}}\theta_{k'}(s,t), \quad s,t \in T,$$

where $\mathscr{B}_{k'}$ is every factor that is finer than or equivalent to $\mathscr{B}_k$ in $\mathfrak{B}$; $r_{\mathscr{B}_{k'}}$ is the number of observational units in each level of $\mathscr{B}_{k'}$ and $\theta_{k'}(s,t)$ is the covariance function of random-effect functions that are associated with the block factor $\mathscr{B}_{k'}$.

Proof. For a block factor $\mathscr{B}_k \in \mathfrak{B}$, the orthogonal projection $\mathbf{P}_{\mathbb{W}(\mathscr{B}_k)}$ onto the $\mathbb{W}$-subspace is a symmetric and idempotent matrix with the rank being equal to the degree of freedom $d_{\mathscr{B}_k}$. Hence, $\mathbf{P}_{\mathbb{W}(\mathscr{B}_k)}$ has the following singular value decomposition (SVD):

$$\mathbf{P}_{\mathbb{W}(\mathscr{B}_k)} = \mathbf{UDU}^T,$$

where $\mathbf{D} = diag(\xi_1, \ldots, \xi_N)$ is a diagonal matrix with $\xi_1 = \cdots = \xi_{d_{\mathscr{B}_k}} = 1$ and $\xi_{d_{\mathscr{B}_k}+1} = \cdots = \xi_N = 0$ being the eigenvalues of $\mathbf{P}_{\mathbb{W}(\mathscr{B}_k)}$ and $\mathbf{U} = [\mathbf{u}_1, \ldots, \mathbf{u}_N]$ is a matrix with $\mathbf{u}_1, \ldots, \mathbf{u}_N$ being the corresponding orthonormal eigenvectors.

Therefore, $SS_{\mathscr{B}_k}(t)$ can be re-expressed by using the SVD of $\mathbf{P}_{\mathbb{W}(\mathscr{B}_k)}$ as follows:

$$SS_{\mathscr{B}_k}(t) = \mathbf{y}(t)^T \mathbf{P}_{\mathbb{W}(\mathscr{B}_k)} \mathbf{y}(t) = \mathbf{y}(t)^T \mathbf{U}\mathbf{D}\mathbf{U}^T \mathbf{y}(t) = \mathbf{R}(t)^T \mathbf{D}\mathbf{R}(t),$$

where $\mathbf{R}(t) = \mathbf{U}^T \mathbf{y}(t) = [R_1(t), \ldots, R_N(t)]^T$ with $R_i(t) = \mathbf{u}_i^T \mathbf{y}(t)$ for $i = 1, \ldots, N$. The functional sum of squares can be transformed into:

$$SS_{\mathscr{B}_k}(t) = \sum_{i=1}^{d_{\mathscr{B}_k}} R_i(t) R_i(t). \tag{3.15}$$

Then, we will derive the distribution of $R_i(t)$. The model for a null experiment is given in Equation (3.12) with the mean and covariance functions shown as follows:

$$E[\mathbf{y}(t)] = \mathbf{0} \quad \text{and} \quad Cov[\mathbf{y}(s), \mathbf{y}(t)] = \mathbf{J}\theta_0(s,t) + \sum_{k'=1}^{K} \mathbf{Z}_{k'} \mathbf{Z}_{k'}^T \theta_{k'}(s,t) + \mathbf{I}\theta_e(s,t).$$

We know that $R_i(t) = \mathbf{u}_i^T \mathbf{y}(t)$, and hence we have the following calculations.

(1) **Mean function**

The mean function of $R_i(t)$ is calculated by:

$$E[R_i(t)] = E[\mathbf{u}_i^T \mathbf{y}(t)] = \mathbf{u}_i^T E[\mathbf{y}(t)] = \mathbf{u}_i^T \mathbf{0} = 0.$$

(2) **Covariance function**

The covariance function of $R_i(t)$ is derived from:

$$\begin{aligned} Cov[R_i(s),R_i(t)] &= Cov[\mathbf{u}_i^T\mathbf{y}(s),\mathbf{u}_i^T\mathbf{y}(t)] \\ &= \mathbf{u}_i^T Cov[\mathbf{y}(s),\mathbf{y}(t)]\mathbf{u}_i \\ &= \mathbf{u}_i^T[\mathbf{J}\theta_0(s,t)+\sum_{k'=1}^{K}\mathbf{Z}_{k'}\mathbf{Z}_{k'}^T\theta_{k'}(s,t)+\mathbf{I}\theta_e(s,t)]\mathbf{u}_i. \end{aligned}$$

Since $\mathbf{Z}_{k'}\mathbf{Z}_{k'}^T = r_{\mathscr{B}_{k'}}\mathbf{P}_{\mathbb{V}(\mathscr{B}_{k'})}$, we have

$$Cov[R_i(s),R_i(t)] = \mathbf{u}_i^T[\sum_{k'=0}^{K+1} r_{\mathscr{B}_{k'}}\mathbf{P}_{\mathbb{V}(\mathscr{B}_{k'})}\theta_{k'}(s,t)]\mathbf{u}_i,$$

where $\mathbf{u}_i$ is an orthonormal eigenvector of $\mathbf{P}_{\mathbb{W}(\mathscr{B}_k)}$, $\mathbf{P}_{\mathbb{V}(\mathscr{B}_{K+1})} = \mathbf{P}_{\mathbb{V}(\mathscr{E})} = \mathbf{I}$ and $\theta_{K+1}(s,t) = \theta_e(s,t)$. By applying part *(1)* of Theorem 3.3, for $\mathscr{B}_{k'} \in \mathfrak{B}$

$$\mathbf{P}_{\mathbb{V}(\mathscr{B}_{k'})}\mathbf{P}_{\mathbb{W}(\mathscr{B}_k)} = \begin{cases} \mathbf{P}_{\mathbb{W}(\mathscr{B}_k)} & \text{if } \mathscr{B}_{k'} \preceq \mathscr{B}_k, \\ 0 & \text{otherwise;} \end{cases}$$

and since $\mathbf{P}_{\mathbb{W}(\mathscr{B}_k)}\mathbf{u}_i = \mathbf{u}_i$,

$$\mathbf{u}_i^T\mathbf{P}_{\mathbb{V}(\mathscr{B}_{k'})}\mathbf{u}_i = \begin{cases} \mathbf{u}_i^T\mathbf{P}_{\mathbb{V}(\mathscr{B}_{k'})}\mathbf{P}_{\mathbb{W}(\mathscr{B}_k)}\mathbf{u}_i = \mathbf{u}_i^T\mathbf{P}_{\mathbb{W}(\mathscr{B}_k)}\mathbf{u}_i = \mathbf{u}_i^T\mathbf{u}_i = 1 & \text{if } \mathscr{B}_{k'} \preceq \mathscr{B}_k, \\ 0 & \text{otherwise;} \end{cases}$$

Finally, we derive the covariance function as:

$$Cov[R_i(s),R_i(t)] = \sum_{\mathscr{B}_{k'}\in\mathfrak{B}:\mathscr{B}_{k'}\preceq\mathscr{B}_k} r_{\mathscr{B}_{k'}}\theta_{k'}(s,t), \quad s,t \in T.$$

(3) **Cross-covariance function**

The cross-covariance function of $R_i(t) = \mathbf{u}_i^T\mathbf{y}(t)$ and $R_j(t) = \mathbf{u}_j^T\mathbf{y}(t)$ for $i \neq j$ and

$i, j = 1, \ldots, d_{\mathscr{B}_k}$ is derived from:

$$
\begin{aligned}
Cov[R_i(s), R_j(t)] &= \mathbf{u}_i^T [\mathbf{J}\theta_0(s,t) + \sum_{k'=1}^{K} \mathbf{Z}_{k'} \mathbf{Z}_{k'}^T \theta_{k'}(s,t) + \mathbf{I}\theta_e(s,t)] \mathbf{u}_j \\
&= \mathbf{u}_i^T [\sum_{k'=0}^{K+1} r_{\mathscr{B}_{k'}} \mathbf{P}_{\mathbb{V}(\mathscr{B}_{k'})} \theta_{k'}(s,t)] \mathbf{u}_j \\
&= \sum_{k'=0}^{K+1} r_{\mathscr{B}_{k'}} \theta_{k'}(s,t) \mathbf{u}_i^T \mathbf{P}_{\mathbb{V}(\mathscr{B}_{k'})} \mathbf{u}_j \\
&= \sum_{\mathscr{B}_{k'} \in \mathfrak{B}: \mathscr{B}_{k'} \preceq \mathscr{B}_k} r_{\mathscr{B}_{k'}} \theta_{k'}(s,t) \mathbf{u}_i^T \mathbf{P}_{\mathbb{W}(\mathscr{B}_k)} \mathbf{u}_j \\
&= \sum_{\mathscr{B}_{k'} \in \mathfrak{B}: \mathscr{B}_{k'} \preceq \mathscr{B}_k} r_{\mathscr{B}_{k'}} \theta_{k'}(s,t) \mathbf{u}_i^T \mathbf{u}_j \\
&= 0,
\end{aligned}
$$

since the eigenvectors are mutually orthogonal.

Therefore, we can see that $\{R_i(t) : t \in T\}$ for $i = 1, \ldots, d_{\mathscr{B}_k}$ are stochastic processes with zero mean function and common covariance function. The cross-covariance function of each two stochastic processes is a zero function. Due to the Gaussian process assumption in Equation (3.12) and the notation of $R_i(t)$ which is a linear combination of $y_1(t), \ldots, y_N(t)$, $\{R_i(t) : t \in T\}$ for $i = 1, \ldots, d_{\mathscr{B}_k}$ are also Gaussian processes.

Finally, $R_1, \ldots, R_{d_{\mathscr{B}_k}} \sim GP(0, \Lambda_{\mathscr{B}_k})$ with the cross-covariance function of each two Gaussian processes being zero is proved. □

Now, we are ready to derive the distribution of the integrated sum of squares.

Theorem 3.5 *The distribution of the integrated sum of squares is:*

$$
SS^*_{\mathscr{B}_k} \stackrel{d.}{=} \sum_{r=1}^{\infty} \lambda_r A_r,
$$

where $(A_r)_{r=1}^{\infty} \overset{i.i.d.}{\sim} \chi^2_{d_{\mathscr{B}_k}}$ *and* $\lambda_1 \geq \lambda_2 \geq \cdots \geq 0$ *are the eigenvalues of the covariance operator associated with the stratum-based covariance function* $\Lambda_{\mathscr{B}_k}(s,t) = \sum_{\mathscr{B}_{k'} \in \mathfrak{B}: \mathscr{B}_{k'} \preceq \mathscr{B}_k} r_{\mathscr{B}_{k'}} \theta_{k'}(s,t)$, *for* $s,t \in T$.

Proof. Theorem 3.5 is straightforward by applying Theorem 2.4 to the following result:

$$SS^*_{\mathscr{B}_k} = \int_T SS_{\mathscr{B}_k}(t)dt = \int_T \sum_{i=1}^{d_{\mathscr{B}_k}} R_i(t)R_i(t)dt = \sum_{i=1}^{d_{\mathscr{B}_k}} \int_T R_i(t)^2 dt,$$

where $R_1, \ldots, R_{d_{\mathscr{B}_k}} \sim GP(0, \Lambda_{\mathscr{B}_k})$ with the cross-covariance function of each two Gaussian processes being zero follows by Theorem 3.4. □

Similar to the role that sums of squares play in the classical ANOVA, both functional sum of squares and integrated sum of squares are useful to develop the functional ANOVA. Functional sums of squares will be displayed in the null ANOVA table. By integrating the functional sum of squares into the integrated sum of squares, information of observed functional responses is concentrated. Furthermore, distributions of integrated sums of squares will be used to derive functional F tests in Chapter 4.

3.3.3 Null ANOVA table

In this section, we summarise the analysis of the block structure by using a null ANOVA table, which contains the structure of strata, functional sums of squares and functional expected mean squares.

Similar to the sum of squares, the pointwise expected mean square $EMS(t_\ell)$ can be calculated at each time point $t_\ell \in T$ for $\ell = 1, \ldots, m$. When calculating over $t \in T$, the

functional expected mean square $EMS(t)$ is a function of t, which is derived by:

$$\begin{aligned} EMS_{\mathscr{B}_k}(t) &= \frac{E[SS_{\mathscr{B}_k}(t)]}{d_{\mathscr{B}_k}} = \frac{1}{d_{\mathscr{B}_k}} E[\sum_{i=1}^{d_{\mathscr{B}_k}} R_i(t) R_i(t)] \\ &= \frac{1}{d_{\mathscr{B}_k}} d_{\mathscr{B}_k} E[R_1(t) R_1(t)] \\ &= Cov[R_1(t), R_1(t)] \\ &= \Lambda_{\mathscr{B}_k}(t,t), \quad t \in T, \end{aligned}$$

by using the previous result that $R_1(t), \ldots, R_{d_{\mathscr{B}_k}}(t) \sim GP(0, \Lambda_{\mathscr{B}_k})$ with zero cross-covariance function in Theorem 3.4. The functional expected mean square of a stratum is equal to the main diagonal of the stratum-based covariance function.

We consider the split-plot design that was described in Example 3.2.

Example 3.3 (Example 3.2 continued: split-plot design) The model for the null experiment is expressed as follows:

$$\mathbf{y}(t) = \boldsymbol{\delta}_0(t) + \mathbf{Z}_1 \boldsymbol{\delta}^L(t) + \mathbf{Z}_2 \boldsymbol{\delta}^S(t) + \boldsymbol{\varepsilon}(t), \quad t \in T, \tag{3.16}$$

where $\delta_0 \sim GP(0, \theta_0)$, $\delta_1^L, \ldots, \delta_{q_1}^L \overset{i.i.d.}{\sim} GP(0, \theta_1)$, $\delta_1^S, \ldots, \delta_{q_1 p_1}^S \overset{i.i.d.}{\sim} GP(0, \theta_2)$ and $\varepsilon_1, \ldots, \varepsilon_N \overset{i.i.d.}{\sim} GP(0, \theta_e)$ indicate the random effects of $\mathscr{U}$, $\mathscr{B}_1$, $\mathscr{B}_2$ and $\mathscr{E}$. We calculate the functional

sums of squares for block factors by:

$$\begin{aligned}
SS_{\mathscr{U}}(t) &= \mathbf{y}(t)^T\mathbf{P}_{\mathbb{W}(\mathscr{U})}\mathbf{y}(t) = \mathbf{y}(t)^T\mathbf{P}_{\mathbb{V}(\mathscr{U})}\mathbf{y}(t) = \tfrac{1}{N}\mathbf{y}(t)^T\mathbf{J}\mathbf{y}(t) \\
SS_{\mathscr{B}_1}(t) &= \mathbf{y}(t)^T\mathbf{P}_{\mathbb{W}(\mathscr{B}_1)}\mathbf{y}(t) = \mathbf{y}(t)^T\mathbf{P}_{\mathbb{V}(\mathscr{B}_1)}\mathbf{y}(t) - SS_{\mathscr{U}}(t) \\
&= \mathbf{y}(t)^T[\tfrac{1}{r_{\mathscr{B}_1}}\mathbf{Z}_1\mathbf{Z}_1^T - \tfrac{1}{N}\mathbf{J}]\mathbf{y}(t) \\
SS_{\mathscr{B}_2}(t) &= \mathbf{y}(t)^T\mathbf{P}_{\mathbb{W}(\mathscr{B}_2)}\mathbf{y}(t) = \mathbf{y}(t)^T\mathbf{P}_{\mathbb{V}(\mathscr{B}_2)}\mathbf{y}(t) - SS_{\mathscr{U}}(t) - SS_{\mathscr{B}_1}(t) \\
&= \mathbf{y}(t)^T[\tfrac{1}{r_{\mathscr{B}_2}}\mathbf{Z}_2\mathbf{Z}_2^T - \tfrac{1}{r_{\mathscr{B}_1}}\mathbf{Z}_1\mathbf{Z}_1^T]\mathbf{y}(t) \\
SS_{\mathscr{E}}(t) &= \mathbf{y}(t)^T\mathbf{P}_{\mathbb{W}(\mathscr{E})}\mathbf{y}(t) = \mathbf{y}(t)^T\mathbf{P}_{\mathbb{V}(\mathscr{E})}\mathbf{y}(t) - SS_{\mathscr{U}}(t) - SS_{\mathscr{B}_1}(t) - SS_{\mathscr{B}_2}(t) \\
&= \mathbf{y}(t)^T[\mathbf{I} - \tfrac{1}{r_{\mathscr{B}_2}}\mathbf{Z}_2\mathbf{Z}_2^T]\mathbf{y}(t),
\end{aligned}$$

where $r_{\mathscr{B}_1} = p_1p_2$ and $r_{\mathscr{B}_2} = p_2$, since in this split-plot design each small block has p_2 observational units and each large block has p_1 small blocks. Furthermore, the stratum-based covariance functions are derived by:

$$\begin{aligned}
\Lambda_{\mathscr{U}}(s,t) &= N\theta_0(s,t) + p_1p_2\theta_1(s,t) + p_2\theta_2(s,t) + \theta_e(s,t) \\
\Lambda_{\mathscr{B}_1}(s,t) &= p_1p_2\theta_1(s,t) + p_2\theta_2(s,t) + \theta_e(s,t) \\
\Lambda_{\mathscr{B}_2}(s,t) &= p_2\theta_2(s,t) + \theta_e(s,t) \\
\Lambda_{\mathscr{E}}(s,t) &= \theta_e(s,t).
\end{aligned}$$

All above calculations for the split-plot design are summarised in the null ANOVA table (Table 3.2). The first three columns of the table summarise the strata structure, while degrees of freedom are shown in the fourth column. Functional sums of squares and functional expected mean squares are displayed in the last two columns. The null ANOVA table can be

Table 3.2: Null ANOVA table for the split-plot design in Example 3.2

Stratum	Source	$\mathbb{W}$-subspace	$d_{\mathbb{W}}$	$SS(t)$	$EMS(t)$
mean	$\mathscr{U}$	$\mathbb{V}(\mathscr{U})$	1	$\frac{1}{N}\mathbf{y}(t)^T\mathbf{J}\mathbf{y}(t)$	$N\theta_0(t,t)+p_1p_2\theta_1(t,t)+$ $p_2\theta_2(t,t)+\theta_e(t,t)$
large blocks	$\mathscr{B}_1$	$C(\mathbf{Z}_1)\cap\mathbb{V}(\mathscr{U})^\perp$	q_1-1	$\mathbf{y}(t)^T[\frac{1}{p_1p_2}\mathbf{Z}_1\mathbf{Z}_1^T-$ $\frac{1}{N}\mathbf{J}]\mathbf{y}(t)$	$p_1p_2\theta_1(t,t)+$ $p_2\theta_2(t,t)+\theta_e(t,t)$
small blocks	$\mathscr{B}_2$	$C(\mathbf{Z}_2)\cap C(\mathbf{Z}_1)^\perp$	q_2-q_1	$\mathbf{y}(t)^T[\frac{1}{p_2}\mathbf{Z}_2\mathbf{Z}_2^T-$ $\frac{1}{p_1p_2}\mathbf{Z}_1\mathbf{Z}_1^T]\mathbf{y}(t)$	$p_2\theta_2(t,t)+\theta_e(t,t)$
plots	$\mathscr{E}$	$C(\mathbf{Z}_2)^\perp$	$N-q_2$	$\mathbf{y}(t)^T[\mathbf{I}-$ $\frac{1}{p_2}\mathbf{Z}_2\mathbf{Z}_2^T]\mathbf{y}(t)$	$\theta_e(t,t)$
Total		$\mathbb{R}^N$	N	$\mathbf{y}(t)^T\mathbf{y}(t)$	

extended to a general ANOVA, which summarises both the block structure and the treatment structure, as will be shown in the next section.

From this example, we can see that the null ANOVA is applied to analyse the null experiment (or the block structure) based on the decomposition of the whole space: $\mathbb{R}^N = \mathbb{W}(\mathscr{U})\oplus\mathbb{W}(\mathscr{B}_1)\oplus\cdots\oplus\mathbb{W}(\mathscr{B}_K)\oplus\mathbb{W}(\mathscr{E})$, as introduced in part *(2)* of Theorem 3.1.

3.4 Analysis of treatment structure

In an orthogonal design with the block structure $\mathfrak{B}$ and the treatment structure $\mathfrak{T}$, by applying Theorem 3.2, we can determine the stratum that a treatment factor belongs to. If one stratum contains no treatment factor, the analysis remains the same as in the null ANOVA. Otherwise, the stratum is decomposed into treatment $\mathbb{W}$-subspaces and the corresponding residual $\mathbb{W}$-subspace by applying Equation (3.3).

3.4.1 Functional treatment and residual sums of squares

In order to derive the general ANOVA, we calculate the functional sum of squares and functional expected mean square for a treatment factor in the similar way to a block factor, however, based on the set $\mathfrak{T}^{\phi}$ of induced block factors. According to Equation (3.7), for a treatment factor $\mathscr{G}_u \in \mathfrak{T}$ the functional sum of squares is:

$$SS_{\mathscr{G}_u}(t) = \mathbf{y}(t)^T \mathbf{P}_{\mathbb{W}(\mathscr{G}_u^{\phi})} \mathbf{y}(t), \quad t \in T, \tag{3.17}$$

since the induced block factor $\mathscr{G}_u^{\phi}$ describes how to assign levels of the treatment factor $\mathscr{G}_u$ to observational units. Moreover, $\mathbf{P}_{\mathbb{V}(\mathscr{G}_u^{\phi})} = \mathbf{X}_u(\mathbf{X}_u^T\mathbf{X}_u)^{-1}\mathbf{X}_u^T$ in Equation (3.9) implies that the treatment sum of squares in Equation (3.17) is the same as that commonly used in the linear regression.

The functional expected mean square is derived by the following theorem.

Theorem 3.6 *The functional expected mean square for $\mathscr{G}_u$, which belongs to a stratum $\mathbb{W}(\mathscr{B}_k)$, is equal to:*

$$EMS_{\mathscr{G}_u}(t) = \frac{E[SS_{\mathscr{G}_u}(t)]}{d_{\mathscr{G}_u}} = \Lambda_{\mathscr{B}_k}(t,t) + \frac{1}{d_{\mathscr{G}_u}} \boldsymbol{\eta}(t)^T \mathbf{P}_{\mathbb{W}(\mathscr{G}_u^{\phi})} \boldsymbol{\eta}(t), \quad t \in T,$$

where $\Lambda_{\mathscr{B}_k}(t,t)$ is the functional expected mean square of the stratum and $\boldsymbol{\eta}(t) = E[\mathbf{y}(t)]$.

Proof. In Theorem 3.6, $d_{\mathscr{G}_u}$ is the degrees of freedom for treatment factor $d_{\mathscr{G}_u}$, which also denotes the dimension of $\mathbb{W}(\mathscr{G}_u)$ and is equal to the dimension of $\mathbb{W}(\mathscr{G}_u^{\phi})$ as explained in Section 3.1.4.

The mean and covariance functions for $\mathbf{y}(t)$ are calculated by using Equation (3.7) as:

$$\boldsymbol{\eta}(t) = E[\mathbf{y}(t)] = \sum_{u=0}^{U} \mathbf{X}_u \boldsymbol{\beta}_u(t) \quad \text{and} \quad Cov[\mathbf{y}(s), \mathbf{y}(t)] = \sum_{k=0}^{K} \mathbf{Z}_k \mathbf{Z}_k^T \theta_k(s,t) + \mathbf{I}\theta_e(s,t),$$

where $\mathbf{I}$ is an $N \times N$ identity matrix.

The functional sum of squares can be transformed to:

$$SS_{\mathscr{G}_u}(t) = \sum_{i=1}^{d_{\mathscr{G}_u}} R_i(t) R_i(t),$$

which can be proved in the way similar to the proof of Theorem 3.4. In addition, $R_i(t) = \mathbf{u}_i^T \mathbf{y}(t)$ and $\mathbf{u}_i$ is an orthonormal eigenvector of $\mathbf{P}_{\mathbb{W}(\mathscr{G}_u^{\phi})}$ with the corresponding eigenvalue being equal to 1, for $i = 1, \ldots, d_{\mathscr{G}_u}$. The mean and covariance functions for $R_i(t)$ are calculated by:

$$E[R_i(t)] = \mathbf{u}_i^T E[\mathbf{y}(t)] = \mathbf{u}_i^T \boldsymbol{\eta}(t)$$

and

$$Cov[R_i(s), R_i(t)] = \mathbf{u}_i^T [\sum_{k=0}^{K} \mathbf{Z}_k \mathbf{Z}_k^T \theta_k(s,t) + \mathbf{I}\theta_e(s,t)] \mathbf{u}_i = \Lambda_{\mathscr{B}_k}(s,t),$$

since $\mathbf{u}_i \in \mathbb{W}(\mathscr{G}_u^{\phi}) \subseteq \mathbb{W}(\mathscr{B}_k)$. Then, the functional expected mean square is derived by:

$$\begin{aligned} EMS_{\mathscr{G}_u}(t) &= \frac{E[SS_{\mathscr{G}_u}(t)]}{d_{\mathscr{G}_u}} = \frac{1}{d_{\mathscr{G}_u}} \sum_{i=1}^{d_{\mathscr{G}_u}} E[R_i(t) R_i(t)] \\ &= \frac{1}{d_{\mathscr{G}_u}} \sum_{i=1}^{d_{\mathscr{G}_u}} \left(\Lambda_{\mathscr{B}_k}(t,t) + \left(E[R_i(t)] \right)^2 \right) \\ &= \Lambda_{\mathscr{B}_k}(t,t) + \frac{1}{d_{\mathscr{G}_u}} \sum_{i=1}^{d_{\mathscr{G}_u}} [\mathbf{u}_i^T \boldsymbol{\eta}(t)]^2, \end{aligned}$$

and by applying the SVD of $\mathbf{P}_{\mathbb{W}(\mathscr{G}_u^{\phi})}$, $\boldsymbol{\eta}(t)^T \mathbf{P}_{\mathbb{W}(\mathscr{G}_u^{\phi})} \boldsymbol{\eta}(t) = \sum_{i=1}^{d_{\mathscr{G}_u}} [\mathbf{u}_i^T \boldsymbol{\eta}(t)]^2$ can be proved.

Thus, $EMS_{\mathscr{G}_u}(t) = \Lambda_{\mathscr{B}_k}(t,t) + \frac{1}{d_{\mathscr{G}_u}} \boldsymbol{\eta}(t)^T \mathbf{P}_{\mathbb{W}(\mathscr{G}_u^{\phi})} \boldsymbol{\eta}(t)$ is proved. □

Similarly, the functional sum of squares for the residual term in the stratum $\mathbb{W}(\mathscr{B}_k)$ is calculated by:

$$SS_{res_k}(t) = \mathbf{y}(t)^T \mathbf{P}_{\mathbb{W}(res_k)} \mathbf{y}(t), \quad t \in T$$

and the functional expected mean square is derived by the following theorem.

Theorem 3.7 *The functional expected mean square for the residual term in the stratum* $\mathbb{W}(\mathscr{B}_k)$ *is calculated by*

$$EMS_{res_k}(t) = \frac{E[SS_{res_k}(t)]}{d_{\mathbb{W}(res_k)}} = \Lambda_{\mathscr{B}_k}(t,t).$$

Proof. In an orthogonal design, $\mathbb{W}(res_k) \perp C(\mathbf{X}_u)$ for $u = 0, \ldots, U$. By using the same notations as in the proof of Theorem 3.6, we have $\mathbf{u}_i^T E[\mathbf{y}(t)] = \mathbf{u}_i^T \sum_{u=0}^{U} \mathbf{X}_u \boldsymbol{\beta}_u(t) = 0$ with $\mathbf{u}_i$ as an eigenvector of $\mathbf{P}_{\mathbb{W}(res_k)}$ and $EMS_{res_k}(t) = \Lambda_{\mathscr{B}_k}(t,t)$ can be proved by the similar method as Theorem 3.6. □

3.4.2 General ANOVA table

All above calculations for an orthogonal design can be summarised in a general ANOVA table, which is obtained from the null ANOVA table by adding the analysis of the treatment structure. We use the split-plot design continued from Example 3.2 and Example 3.3 as an example.

Example 3.4 (Example 3.3 continued: split-plot design) The general ANOVA is shown in Table 3.3, where details of orthogonal projections and stratum-based covariance functions are not given.

In a null ANOVA table (e.g. Table 3.2) each stratum is summarised in one row, whereas in a general ANOVA table (e.g. Table 3.3) the stratum which contains treatment factors are shown in several rows.

The general ANOVA table can be viewed as the pointwise analysis of variance without the hypothesis test. Although pointwise F tests can be easily derived from this ANOVA table by performing univariate F tests at discrete points independently, we are more interested in

Table 3.3: General ANOVA table for the split-plot design in Example 3.2

Stratum	Source	$d_{\mathbb{W}}$	$SS(t)$	$EMS(t)$
mean	$\mathscr{U}$	1	$\mathbf{y}(t)^T\mathbf{P}_{\mathbb{W}(\mathscr{U})}\mathbf{y}(t)$	$\Lambda_{\mathscr{U}}(t,t)+\boldsymbol{\eta}(t)^T\mathbf{P}_{\mathbb{W}(\mathscr{U})}\boldsymbol{\eta}(t)$
large blocks	$\mathscr{B}_1$	q_1-1	$\mathbf{y}(t)^T\mathbf{P}_{\mathbb{W}(\mathscr{B}_1)}\mathbf{y}(t)$	$\Lambda_{\mathscr{B}_1}(t,t)$
small blocks	$\mathscr{G}_1$	p_1-1	$\mathbf{y}(t)^T\mathbf{P}_{\mathbb{W}(\mathscr{G}_1)}\mathbf{y}(t)$	$\Lambda_{\mathscr{B}_2}(t,t)+\frac{\boldsymbol{\eta}(t)^T\mathbf{P}_{\mathbb{W}(\mathscr{G}_1^{\phi})}\boldsymbol{\eta}(t)}{p_1-1}$
	res_2	$q_2-q_1-p_1+1$	$\mathbf{y}(t)^T\mathbf{P}_{\mathbb{W}(res_2)}\mathbf{y}(t)$	$\Lambda_{\mathscr{B}_2}(t,t)$
	total	q_2-q_1	$\mathbf{y}(t)^T\mathbf{P}_{\mathbb{W}(\mathscr{B}_2)}\mathbf{y}(t)$	
plots	$\mathscr{G}_2$	p_2-1	$\mathbf{y}(t)^T\mathbf{P}_{\mathbb{W}(\mathscr{G}_2^{\phi})}\mathbf{y}(t)$	$\Lambda_{\mathscr{E}}(t,t)+\frac{\boldsymbol{\eta}(t)^T\mathbf{P}_{\mathbb{W}(\mathscr{G}_2^{\phi})}\boldsymbol{\eta}(t)}{p_2-1}$
	$\mathscr{G}_3$	$(p_1-1)(p_2-1)$	$\mathbf{y}(t)^T\mathbf{P}_{\mathbb{W}(\mathscr{G}_3^{\phi})}\mathbf{y}(t)$	$\Lambda_{\mathscr{E}}(t,t)+\frac{\boldsymbol{\eta}(t)^T\mathbf{P}_{\mathbb{W}(\mathscr{G}_3^{\phi})}\boldsymbol{\eta}(t)}{(p_1-1)(p_2-1)}$
	res_e	$N-q_2-p_1(p_2-1)$	$\mathbf{y}(t)^T\mathbf{P}_{\mathbb{W}(res_e)}\mathbf{y}(t)$	$\Lambda_{\mathscr{E}}(t,t)$
	total	$N-q_2$	$\mathbf{y}(t)^T\mathbf{P}_{\mathbb{W}(\mathscr{E})}\mathbf{y}(t)$	
Total		N	$\mathbf{y}(t)^T\mathbf{y}(t)$	

a global statistical test which takes the entire response functions into account, as will be explored in the next chapter.

3.5 Conclusions

The main result of this chapter is the ANOVA for orthogonal designs with functional responses, which has been developed on the basis of orthogonal designs (Bailey, 2008) and the functional mixed-effects model (Morris and Carroll, 2006). Although responses that we are interested in are functions, the structure of experiments where functional data are collected can be analysed in a similar way to classical experiments with univariate responses. More specifically, at each time point, the univariate ANOVA is applied to study the experimental structure and we assume the structures are the same across different time points. There-

fore, we apply a functional mixed-effects model with time-independent covariates (design matrices) in this thesis. The equivalence between the column space of a design matrix and the $\mathbb{V}$-subspace of the corresponding factor in the design enables us to develop functional ANOVA based on the model.

The simplest orthogonal design is a completely randomised design, where observational units are unstructured and treatments are allocated randomly. One-way ANOVA and two-way ANOVA for functional data from a completely randomised design was introduced in Zhang (2013). In a classical completely randomised design, treatments are studied depending on the overall variability of observational units, while in a more complex orthogonal design, treatments may be studied in different strata, that is, depending on different error terms or different sources of error (Cheng, 2014). Similarly, in a completely randomised design with functional responses, the functional ANOVA is derived based on the covariance function of functional responses, whereas in a more complex design, the functional ANOVA is derived based on the *stratum-based covariance function*, that is the covariance function of the corresponding error term (or residual) in each stratum.

Although we have extended the classical orthogonal design principles to functional data and used the terminology of comparative experiments, it is necessary to distinguish between classical methods and our proposed method with respect to the meaning of *stratum*. In Bailey (2008, p. 40), it is defined that *"A stratum is an eigenspace of* $Cov(\mathbf{Y})$*"*, where $\mathbf{Y}$ is the vector of responses. Furthermore, $Cov(\mathbf{Y}) = \sum_{\text{all}\,\mathscr{B}_k} \xi_{\mathscr{B}_k} \mathbf{P}_{\mathbb{W}(\mathscr{B}_k)}$, where $\mathscr{B}_k$ is a block factor and $\mathbb{W}(\mathscr{B}_k)$ is an eigenspace of $Cov(\mathbf{Y})$ with the corresponding eigenvalue $\xi_{\mathscr{B}_k}$. In addition, $\xi_{\mathscr{B}_k}$ is the expected mean square of the stratum in a null experiment. However, the covariance structure of functional responses can be viewed as a matrix with covariance functions as diagonal elements and cross-covariance functions as off-diagonal elements. Hence the spectral decomposition of the covariance matrix is not appropriate for functional responses and strata are no longer eigenspaces. Moreover, we define expected mean square for each stratum as a function of time and it is not an eigenvalue of the covariance matrix.

At the end of this chapter, we place particular emphasis on ANOVA, which can be viewed from two different perspectives. Under the first perspective, studies focus on model equations, which can be either linear regression models or ANOVA models. By contrast, under the second perspective, the emphasis is on the experimental structure, that is the relationship between factors, although model equations are sometimes used as a supplementary tool. Nelder (1965a,b), Tjur (1984) and Bailey (2008) all studied orthogonal designs under the second perspective.

The functional ANOVA in this study is developed under the second perspective, although some of our results are derived by using the functional mixed-effects models. For functional data measured from a design with many factors or a complicated structure, there is no need to express the model equation and our proposed functional ANOVA and hypothesis tests can be applied independently of model equations.

Chapter 4

Functional F tests in orthogonal designs

The comparison of treatments is usually considered in the design of experiment. In a classical ANOVA, it is common to apply an F test to assess whether there is a treatment effect or not. However, it is more complicated to test functional data. A functional F test (Shen and Faraway, 2004; Zhang, 2013) has been proposed for independent functional data, which imply data are generated from a completely randomised design. In this chapter, we extend the functional F test to orthogonal designs. A complete version of the functional ANOVA can be constructed by taking functional F tests for treatments and interaction terms into account.

The proposed functional ANOVA is applied to gait data collected at the Human Performance Laboratory, Queen Mary University of London. Two examples are considered in this chapter. In the first example, gait data of 14 patients with cerebral palsy are analysed, to examine the effects of ankle-foot orthoses (AFO). Functional F tests are applied to gait kinematics, in comparison with pointwise F tests and univariate F tests. However, this retrospective study has limitations, such as the lack of randomisation. Patients always walked barefoot before walking with AFO during the data collection. Another limitation is the high variability in gait of patients with cerebral palsy. In order to avoid these problems and to achieve better statistical interpretation of gait analysis, the second study was designed to col-

lect gait data from 9 healthy subjects. Gait data were collected from a split-plot experiment with two treatment factors: AFO and the walking speeds. The treatment factors and their interaction are examined by functional F tests.

In this chapter, functional F tests are introduced in Section 4.1. Gait data of patients with cerebral palsy are analysed in Section 4.2, while healthy gait data collected from a split-plot design are analysed in Section 4.3.

4.1 Functional F tests for treatments

4.1.1 Treatment comparisons

In a designed experiment with functional responses, the main effect of a treatment factor is indicated by the corresponding vector of fixed-effect functions. For instance, in order to examine the effect of a treatment factor $\mathscr{G}_u$ with p_u levels in an orthogonal design, as expressed in Equation (3.7), we test the null hypothesis:

$$H_0 : \beta_{u,1}(t) = \beta_{u,2}(t) = \cdots = \beta_{u,p_u}(t).$$

This null hypothesis can be viewed from different perspectives, depending on whether $\beta(t)$ indicates a function across $t \in T$ or the value of a function at a specific point t. Therefore, in what follows, we distinguish between the pointwise test problem

(1) $$H_0 : \beta_{u,1}(t_\ell) = \beta_{u,2}(t_\ell) = \cdots = \beta_{u,p_u}(t_\ell)$$

versus

$$H_1 : \text{ at least two parameters are different,}$$

for $t_\ell \in T$ being the fixed time point, and the functional test problem

(2) $$H_0 : \beta_{u,1}(t) = \beta_{u,2}(t) = \cdots = \beta_{u,p_u}(t) \text{ for all } t \in T$$

versus

$$H_1: \text{ at least two functions are different for some } t \in T.$$

The hypotheses (1) lead to the development of pointwise F tests, which will be applied and discussed in Section 4.2 and Section 4.3. However, Ramsay and Silverman (2005) pointed out that the pointwise ANOVA problem at each specific time point was the same as the univariate ANOVA problem, and thus the pointwise approach is not technically new. Therefore, we focus more on global tests based on the hypotheses (2). We will derive the null distributions of functional sums of squares and develop a functional F test in the rest of this section.

4.1.2 Null distribution of functional sum of squares

Consider an orthogonal design with the block structure $\mathfrak{B}$ and the treatment structure $\mathfrak{T}$. Suppose Equation (3.7) is the model for this orthogonal design. As introduced in Section 3.4, the set $\mathfrak{T}^{\phi}$ of induced block factors is used to derive the treatment sum of squares.

We will derive the null distributions of the sums of squares for both a treatment factor and the corresponding residual in the same stratum.

Theorem 4.1 *If a treatment factor $\mathscr{G}_u \in \mathfrak{T}$ belongs to the stratum $\mathbb{W}(\mathscr{B}_k)$, $\mathscr{B}_k \in \mathfrak{B}$, with the corresponding stratum-based covariance function $\Lambda_{\mathscr{B}_k}(s,t)$, the functional treatment sum of squares for $\mathscr{G}_u$ can be expressed as:*

$$SS_{\mathscr{G}_u}(t) = \mathbf{y}(t)^T \mathbf{P}_{\mathbb{W}(\mathscr{G}_u^{\phi})} \mathbf{y}(t) = \sum_{i=1}^{d_{\mathscr{G}_u}} R_i(t) R_i(t), \tag{4.1}$$

where $R_1, \ldots, R_{d_{\mathscr{G}_u}}$ are Gaussian processes with the common covariance function being equal to $\Lambda_{\mathscr{B}_k}(s,t)$. Moreover, the mean function is calculated by

$$E[R_i(t)] = \sum_{\mathscr{G}_{u'}^{\phi} \in \mathfrak{T}^{\phi}: \mathscr{G}_{u'}^{\phi} \preceq \mathscr{G}_u^{\phi}} \mathbf{u}_i^T \mathbf{X}_{u'} \boldsymbol{\beta}_{u'}(t), \tag{4.2}$$

where $\mathbf{u}_i$ *is an orthonormal eigenvector of* $\mathbf{P}_{\mathbb{W}(\mathscr{G}_u^\phi)}$.

Proof. Equation (4.1) and the corresponding covariance function were proved in Theorem 3.6. Here, we concentrate on the mean function of $R_i(t)$ for $i = 1, \ldots, d_{\mathscr{G}_u}$.

According to the proof of Theorem 3.6, for $\mathscr{G}_u \in \mathfrak{T}$ the mean function of $R_i(t)$ in Equation (4.1) is $E[R_i(t)] = \mathbf{u}_i^T \boldsymbol{\eta}(t)$, where $\mathbf{u}_i$ is an orthonormal eigenvector of $\mathbf{P}_{\mathbb{W}(\mathscr{G}_u^\phi)}$. By applying Equation (3.7), we have

$$E[R_i(t)] = \mathbf{u}_i^T \boldsymbol{\eta}(t) = \mathbf{u}_i^T E[\mathbf{y}(t)] = \sum_{u'=0}^{U} \mathbf{u}_i^T \mathbf{X}_{u'} \boldsymbol{\beta}_{u'}(t).$$

Similar to part *(1)* of Theorem 3.3, for $\mathscr{G}_u^\phi, \mathscr{G}_{u'}^\phi \in \mathfrak{T}^\phi$

$$\mathbf{P}_{\mathbb{V}(\mathscr{G}_{u'}^\phi)} \mathbf{P}_{\mathbb{W}(\mathscr{G}_u^\phi)} = \begin{cases} \mathbf{P}_{\mathbb{W}(\mathscr{G}_u^\phi)} & \text{if } \mathscr{G}_{u'}^\phi \preceq \mathscr{G}_u^\phi, \\ 0 & \text{otherwise,} \end{cases}$$

which implies that $\mathbf{u}_i^T \mathbf{X}_{u'} = 0$ if $\mathscr{G}_{u'}^\phi$ is neither finer than nor equivalent to $\mathscr{G}_u^\phi$. Thus, we have the following result:

$$E[R_i(t)] = \mathbf{u}_i^T \boldsymbol{\eta}(t) = \sum_{\mathscr{G}_{u'} \in \mathfrak{T}^\phi : \mathscr{G}_{u'}^\phi \preceq \mathscr{G}_u^\phi} \mathbf{u}_i^T \mathbf{X}_{u'} \boldsymbol{\beta}_{u'}(t),$$

where $\mathscr{G}_{u'}^\phi$ is every treatment factor that is finer than or equivalent to $\mathscr{G}_u^\phi$ in $\mathfrak{T}^\phi$. □

In what follows, we will calculate $E[R_i(t)]$ in Equation (4.2) under the null hypothesis $H_0 : \beta_{u,1}(t) = \beta_{u,2}(t) = \cdots = \beta_{u,p_u}(t)$. Similar to the traditional ANOVA, a constraint is needed for functional ANOVA.

Alternatively, we can also use the null hypothesis $H_0 : \mathbf{P}_{\mathbb{W}(\mathscr{G}_u^\phi)} \boldsymbol{\eta}(t) = \mathbf{0}$, as in Bailey (2008). It is not difficult to prove that if $\mathbf{P}_{\mathbb{W}(\mathscr{G}_u^\phi)} \boldsymbol{\eta}(t) = \mathbf{0}$ then $E[R_i(t)]$ in Equation (4.2) is

equal to zero. If $\mathbf{P}_{\mathbb{W}(\mathscr{G}_u^\phi)}\boldsymbol{\eta}(t) = \mathbf{0}$, then we have

$$\begin{aligned}\mathbf{P}_{\mathbb{W}(\mathscr{G}_u^\phi)}\boldsymbol{\eta}(t) &= \mathbf{P}_{\mathbb{W}(\mathscr{G}_u^\phi)}\sum_{u'=0}^{U}\mathbf{X}_{u'}\boldsymbol{\beta}_{u'}(t) = \sum_{u'=0}^{U}\mathbf{P}_{\mathbb{W}(\mathscr{G}_u^\phi)}\mathbf{X}_{u'}\boldsymbol{\beta}_{u'}(t)\\ &= \sum_{\mathscr{G}_{u'}^\phi\in\mathfrak{T}^\phi:\mathscr{G}_{u'}^\phi\preceq\mathscr{G}_u^\phi}\mathbf{P}_{\mathbb{W}(\mathscr{G}_u^\phi)}\mathbf{X}_{u'}\boldsymbol{\beta}_{u'}(t) = \mathbf{0}.\end{aligned} \tag{4.3}$$

In Equation (4.2), since $\mathbf{u}_i$ is an eigenvector of $\mathbf{P}_{\mathbb{W}(\mathscr{G}_u^\phi)}$ with the corresponding eigenvalue being equal to 1,

$$E[R_i(t)] = \sum_{\mathscr{G}_{u'}^\phi\in\mathfrak{T}^\phi:\mathscr{G}_{u'}^\phi\preceq\mathscr{G}_u^\phi}\mathbf{u}_i^T\mathbf{X}_{u'}\boldsymbol{\beta}_{u'}(t) = \sum_{\mathscr{G}_{u'}^\phi\in\mathfrak{T}^\phi:\mathscr{G}_{u'}^\phi\preceq\mathscr{G}_u^\phi}\mathbf{u}_i^T\mathbf{P}_{\mathbb{W}(\mathscr{G}_u^\phi)}\mathbf{X}_{u'}\boldsymbol{\beta}_{u'}(t) = 0.$$

Moreover, $\mathbf{P}_{\mathbb{W}(\mathscr{G}_u^\phi)}\boldsymbol{\eta}(t) = \sum_{\mathscr{G}_{u'}^\phi\in\mathfrak{T}^\phi:\mathscr{G}_{u'}^\phi\preceq\mathscr{G}_u^\phi}\mathbf{P}_{\mathbb{W}(\mathscr{G}_u^\phi)}\mathbf{X}_{u'}\boldsymbol{\beta}_{u'}(t) = \mathbf{0}$, if $\beta_{u,1}(t) = \beta_{u,2}(t) = \cdots = \beta_{u,p_u}(t)$ together with the constraint, which will be given later in Equation (4.4).

We will first prove that for every treatment factor $\mathscr{G}_{u'}^\phi \in \mathfrak{T}^\phi$ that is finer than $\mathscr{G}_u^\phi$, if $\beta_{u,1}(t) = \beta_{u,2}(t) = \cdots = \beta_{u,p_u}(t)$ and the constraint in Equation (4.4) holds, $\mathbf{P}_{\mathbb{W}(\mathscr{G}_u^\phi)}\mathbf{X}_{u'}\boldsymbol{\beta}_{u'}(t) = \mathbf{0}$. Suppose $\boldsymbol{\beta}_u(t) = [\beta_{u,1}(t),\ldots,\beta_{u,p_u}(t)]^T$ with $\beta_{u,a}(t)$ being the effect of the a-th level of the treatment factor $\mathscr{G}_u$ for $a = 1,\ldots,p_u$. For $\mathscr{G}_{u'}^\phi \prec \mathscr{G}_u^\phi$, let n_a be the number of levels of $\mathscr{G}_{u'}^\phi$ that are nested within the same a-th level of $\mathscr{G}_u^\phi$. The vector $\boldsymbol{\beta}_{u'}(t) = [\beta_{u',1}(t),\ldots,\beta_{u',p_{u'}}(t)]^T$ can be re-expressed as

$$[\beta_{u',1(1)}(t),\ldots,\beta_{u',n_1(1)}(t),\ldots,\beta_{u',1(p_u)}(t),\ldots,\beta_{u',n_{p_u}(p_u)}(t)]^T,$$

where $\beta_{u',b(a)}(t)$ is the effect of $\mathscr{G}_{u'}$ with the b-th level nested within the a-th level of $\mathscr{G}_u$, for $a = 1,\ldots,p_u$ and $b = 1,\ldots,n_a$. Like the traditional ANOVA, we consider the following constraint:

$$\sum_{b=1}^{n_a}\beta_{u',b(a)}(t) = 0 \text{ for every } a \text{ and for all } t \in T. \tag{4.4}$$

The design matrices $\mathbf{X}_u$ and $\mathbf{X}_{u'}$ can be re-expressed as:

$$\mathbf{X}_u = [\mathbf{v}_{u,1}, \ldots, \mathbf{v}_{u,p_u}] \quad \text{and} \quad \mathbf{X}_{u'} = [\mathbf{v}_{u',1(1)}, \ldots, \mathbf{v}_{u',n_1(1)}, \ldots, \mathbf{v}_{u',1(p_u)}, \ldots, \mathbf{v}_{u',n_{p_u}(p_u)}],$$

where $\mathbf{v}_{u,a}$ and $\mathbf{v}_{u',b(a)}$ for $a = 1, \ldots, p_u$ and $b = 1, \ldots, n_a$ are column vectors of the design matrices $\mathbf{X}_u$ and $\mathbf{X}_{u'}$, respectively. Recall the description of the orthogonal projection onto the $\mathbb{V}$-subspace $\mathbf{P}_{\mathbb{V}}$ shown in (3.10). Then, for $a = 1, \ldots, p_u$,

$$\mathbf{P}_{\mathbb{V}(\mathscr{G}_u^{\phi})}\mathbf{v}_{u',1(a)} = \cdots = \mathbf{P}_{\mathbb{V}(\mathscr{G}_u^{\phi})}\mathbf{v}_{u',n_a(a)}.$$

Since $\mathbf{P}_{\mathbb{W}(\mathscr{G}_u^{\phi})}\mathbf{v}_{u',b(a)} = \mathbf{P}_{\mathbb{W}(\mathscr{G}_u^{\phi})}\mathbf{P}_{\mathbb{V}(\mathscr{G}_u^{\phi})}\mathbf{v}_{u',b(a)}$, we have

$$\mathbf{P}_{\mathbb{W}(\mathscr{G}_u^{\phi})}\mathbf{v}_{u',1(a)} = \cdots = \mathbf{P}_{\mathbb{W}(\mathscr{G}_u^{\phi})}\mathbf{v}_{u',n_a(a)}.$$

By using the constraint in Equation (4.4), we derive the following result:

$$\begin{aligned}
\mathbf{P}_{\mathbb{W}(\mathscr{G}_u^{\phi})}\mathbf{X}_{u'}\boldsymbol{\beta}_{u'}(t) =& \mathbf{P}_{\mathbb{W}(\mathscr{G}_u^{\phi})}[\mathbf{v}_{u',1(1)}, \ldots, \mathbf{v}_{u',n_1(1)}, \ldots, \mathbf{v}_{u',1(p_u)}, \ldots, \mathbf{v}_{u',n_{p_u}(p_u)}]\boldsymbol{\beta}_{u'}(t) \\
=& [\mathbf{P}_{\mathbb{W}(\mathscr{G}_u^{\phi})}\mathbf{v}_{u',1(1)}, \ldots, \mathbf{P}_{\mathbb{W}(\mathscr{G}_u^{\phi})}\mathbf{v}_{u',n_1(1)}, \ldots, \\
& \mathbf{P}_{\mathbb{W}(\mathscr{G}_u^{\phi})}\mathbf{v}_{u',1(p_u)}, \ldots, \mathbf{P}_{\mathbb{W}(\mathscr{G}_u^{\phi})}\mathbf{v}_{u',n_{p_u}(p_u)}]\boldsymbol{\beta}_{u'}(t) \\
=& [\mathbf{P}_{\mathbb{W}(\mathscr{G}_u^{\phi})}\mathbf{v}_{u',1(1)}, \ldots, \mathbf{P}_{\mathbb{W}(\mathscr{G}_u^{\phi})}\mathbf{v}_{u',1(1)}, \ldots, \\
& \mathbf{P}_{\mathbb{W}(\mathscr{G}_u^{\phi})}\mathbf{v}_{u',1(p_u)}, \ldots, \mathbf{P}_{\mathbb{W}(\mathscr{G}_u^{\phi})}\mathbf{v}_{u',1(p_u)}]\boldsymbol{\beta}_{u'}(t) \\
=& \mathbf{P}_{\mathbb{W}(\mathscr{G}_u^{\phi})}\mathbf{v}_{u',1(1)}[\beta_{u',1(1)}(t) + \cdots + \beta_{u',n_1(1)}(t)] + \ldots \\
& + \mathbf{P}_{\mathbb{W}(\mathscr{G}_u^{\phi})}\mathbf{v}_{u',1(p_u)}[\beta_{u',1(p_u)}(t) + \cdots + \beta_{u',n_{p_u}(p_u)}(t)] \\
=& \sum_{a=1}^{p_u} \mathbf{P}_{\mathbb{W}(\mathscr{G}_u^{\phi})}\mathbf{v}_{u',1(a)} \sum_{b=1}^{n_a} \beta_{u',b(a)}(t) \\
=& \sum_{a=1}^{p_u} \mathbf{P}_{\mathbb{W}(\mathscr{G}_u^{\phi})}\mathbf{v}_{u',1(a)} \times 0 = \mathbf{0}.
\end{aligned}$$

We will then prove that for $\mathscr{G}_u^{\phi} \in \mathfrak{T}^{\phi}$, $\mathbf{P}_{\mathbb{W}(\mathscr{G}_u^{\phi})}\mathbf{X}_u\boldsymbol{\beta}_u(t) = \mathbf{0}$ under the null hypoth-

esis $H_0 : \beta_{u,1}(t) = \cdots = \beta_{u,p_u}(t)$. If $\mathscr{G}_u$ is not a universal factor and $\beta_{u,1}(t) = \cdots = \beta_{u,p_u}(t)$, then $\mathbf{X}_u\boldsymbol{\beta}_u(t) = \mathbf{1}_{N\times 1}\beta_{u,1}(t)$ where $\mathbf{1}_{N\times 1}$ is an $N \times 1$ all-1 vector. We have $\mathbf{P}_{\mathbb{W}(\mathscr{G}_u^\phi)}\mathbf{X}_u\boldsymbol{\beta}_u(t) = \mathbf{P}_{\mathbb{W}(\mathscr{G}_u^\phi)}\mathbf{1}_{N\times 1}\beta_{u,1}(t) = \mathbf{0}$, since $\mathbf{P}_{\mathbb{W}(\mathscr{G}_u^\phi)} \perp \mathbf{1}_{N\times 1}$. To test the universal factor $\mathscr{G}_0$ in $\mathfrak{T}$, $\mathbf{P}_{\mathbb{W}(\mathscr{G}_0^\phi)}\mathbf{X}_0\boldsymbol{\beta}_0(t) = \mathbf{P}_{\mathbb{W}(\mathscr{G}_0^\phi)}\mathbf{1}_{N\times 1} \times 0 = \mathbf{0}$ holds under the null hypothesis $H_0 : \beta_0(t) = 0$.

Therefore, under the null hypothesis $H_0 : \beta_{u,1}(t) = \cdots = \beta_{u,p_u}(t)$ together with the constraint in Equation (4.4), $\mathbf{P}_{\mathbb{W}(\mathscr{G}_u^\phi)}\boldsymbol{\eta}(t) = \sum_{\mathscr{G}_{u'}^\phi \in \mathfrak{T}^\phi : \mathscr{G}_{u'}^\phi \preceq \mathscr{G}_u^\phi} \mathbf{P}_{\mathbb{W}(\mathscr{G}_u^\phi)}\mathbf{X}_{u'}\boldsymbol{\beta}_{u'}(t) = \mathbf{0}$; and hence $E[R_i(t)] = 0$ in Equation (4.2). Functional treatment sum of squares can be transformed to

$$SS_{\mathscr{G}_u}(t) = \sum_{i=1}^{d_{\mathscr{G}_u}} R_i(t)R_i(t) \text{ with } R_1, \ldots, R_{d_{\mathscr{G}_u}} \sim GP(0, \Lambda_{\mathscr{B}_k}).$$

In addition, the cross-covariance function is zero, the proof of which is similar to Theorem 3.4.

By applying Theorem 2.4, we have the following result for the integrated treatment sum of squares:

$$\begin{aligned} SS^*_{\mathscr{G}_u} &= \int_T SS_{\mathscr{G}_u}(t)dt = \int_T \mathbf{y}(t)^T \mathbf{P}_{\mathbb{W}(\mathscr{G}_u^\phi)}\mathbf{y}(t)dt \\ &= \int_T \sum_{i=1}^{d_{\mathscr{G}_u}} R_i(t)R_i(t)dt \\ &= \sum_{i=1}^{d_{\mathscr{G}_u}} \int_T R_i(t)^2 dt \\ &\overset{d.}{=} \sum_{r=1}^{\infty} \lambda_r A_r, \end{aligned} \tag{4.5}$$

where $(A_r)_{r=1}^{\infty} \overset{i.i.d.}{\sim} \chi^2_{d_{\mathscr{G}_u}}$ and $\lambda_1 \geq \lambda_2 \geq \cdots \geq 0$ are the eigenvalues of the covariance operator that is associated with the stratum-based covariance function $\Lambda_{\mathscr{B}_k}(s,t)$.

Similarly, for the corresponding residual in the stratum $\mathbb{W}(\mathscr{B}_k)$, we have the following

result:

$$\begin{aligned} SS^*_{res_k} &= \int_T SS_{res_k}(t)dt = \int_T \mathbf{y}(t)^T \mathbf{P}_{\mathbb{W}(res_k)} \mathbf{y}(t)dt \\ &= \int_T \sum_{i=1}^{d_{res_k}} \tilde{R}_i(t)\tilde{R}_i(t)dt \\ &= \sum_{i=1}^{d_{res_k}} \int_T \tilde{R}_i(t)^2 dt \\ &\stackrel{d.}{=} \sum_{r=1}^{\infty} \lambda_r \tilde{A}_r, \end{aligned} \tag{4.6}$$

where $\tilde{R}_1, \ldots, \tilde{R}_{d_{res_k}} \sim GP(0, \Lambda_{\mathscr{B}_k})$ with the cross-covariance function of every two processes being zero and $(\tilde{A}_r)_{r=1}^{\infty} \overset{i.i.d.}{\sim} \chi^2_{d_{res_k}}$ and $\lambda_1 \geq \lambda_2 \geq \cdots \geq 0$ are the eigenvalues of the covariance operator that is associated with the stratum-based covariance function $\Lambda_{\mathscr{B}_k}(s,t)$.

So far we have derived distributions for the integrated treatment and residual sums of squares. We also need to confirm the independence between sums of squares before presenting the functional F test in the next subsection.

Since for a treatment factor $\mathscr{G}_u$ and the corresponding residual $\mathbb{W}(\mathscr{G}_u) \perp \mathbb{W}(res_k)$, any eigenvector $\mathbf{u}_i$ of $\mathbf{P}_{\mathbb{W}(\mathscr{G}_u)}$ for $i = 1, \ldots, d_{\mathscr{G}_u}$ is orthogonal to any eigenvector $\tilde{\mathbf{u}}_j$ of $\mathbf{P}_{\mathbb{W}(res_k)}$ for $j = 1, \ldots, d_{res_k}$. Therefore, it is obvious that the cross-covariance function of

$$R_i(t) = \mathbf{u}_i^T \mathbf{y}(t) \quad \text{and} \quad \tilde{R}_j(t) = \tilde{\mathbf{u}}_j^T \mathbf{y}(t)$$

is $Cov[R_i(s), \tilde{R}_j(t)] = 0$ for all $s,t \in T$ and each pair of i and j; and hence $(A_r)_{r=1}^{\infty}$ in Equation (4.5) and $(\tilde{A}_r)_{r=1}^{\infty}$ in Equation (4.6) are independent, according to Theorem 2.3. Thus, $SS^*_{\mathscr{G}_u}$ which is a linear combination of $(A_r)_{r=1}^{\infty}$ is independent of $SS^*_{res_k}$ which is a linear combination of $(\tilde{A}_r)_{r=1}^{\infty}$.

To summarise, under the null hypothesis $H_0 : \beta_{u,1}(t) = \beta_{u,2}(t) = \cdots = \beta_{u,p_u}(t)$ for all $t \in T$, we have

$$SS^*_{\mathscr{G}_u} \stackrel{d.}{=} \sum_{r=1}^{\infty} \lambda_r A_r \quad \text{and} \quad SS^*_{res_k} \stackrel{d.}{=} \sum_{r=1}^{\infty} \lambda_r \tilde{A}_r,$$

where $A_1, A_2, \ldots$ and $\tilde{A}_1, \tilde{A}_2, \ldots$ are independent random variables that all follow χ^2 distributions. Moreover, the integrated treatment and residual sums of squares $SS^*_{\mathscr{G}_u}$ and $SS^*_{res_k}$ are independent.

4.1.3 Functional F test

In order to test the treatment effects in an orthogonal design with functional responses, we consider a functional F test. For each treatment factor, the functional F test is conducted within the stratum where the treatment factor is located. We test the hypotheses (2) in Section 4.1.1 by using the following functional F test:

$$F = \frac{SS^*_{\mathscr{G}_u}/d_{\mathscr{G}_u}}{SS^*_{res_k}/d_{res_k}}. \tag{4.7}$$

We have proved that under the null hypothesis both the integrated treatment and residual sums of squares can be transformed into linear combinations of independent random variables which follow χ^2 distributions.

However, the exact distribution of a linear combination of χ^2 random variables is complicated. As suggested by Shen and Faraway (2004) and Zhang (2013), the Welch-Satterthwaite approximation (Satterthwaite, 1941, 1946; Welch, 1947) can be applied to derive the approximate distribution of the statistic in the functional F test.

Suppose $\mathscr{X} = c_1 x_1 + \cdots + c_n x_n$, where $x_1, \ldots, x_n$ are independent random variables and x_i follows a χ^2 distribution with degrees of freedom d_i, for $i = 1, \ldots, n$. Then $\mathscr{X}/\kappa$ can be approximated by a χ^2 distribution with degrees of freedom being equal to df. Welch (1947) proposed that the first two moments (mean and variance) of the approximating χ^2 distribution should agree with $\mathscr{X}$. Thus we have

$$E(\mathscr{X}) = \kappa \times df = c_1 d_1 + \cdots + c_n d_n,$$
$$var(\mathscr{X}) = \kappa^2 \times 2df = 2c_1^2 d_1 + \cdots + 2c_n^2 d_n,$$

and parameters in the approximate distribution are calculated by:

$$df = \frac{(c_1 d_1 + \cdots + c_n d_n)^2}{c_1^2 d_1 + \cdots + c_n^2 d_n},\ \kappa = \frac{c_1^2 d_1 + \cdots + c_n^2 d_n}{c_1 d_1 + \cdots + c_n d_n}.$$

By using a simulation approach, Zhang (2013, p. 97) showed that the χ^2-approximation works well when all coefficients $c_1, \ldots, c_n$ are positive. Under the functional null hypothesis (2),

$$SS^*_{\mathscr{G}_u} \overset{d.}{=} \sum_{r=1}^{\infty} \lambda_r A_r \sim \sum_{r=1}^{\infty} \lambda_r \chi^2_{d_{\mathscr{G}_u}}$$

with $\lambda_1 \geq \lambda_2 \geq \cdots \geq 0$. Thus, $SS^*_{\mathscr{G}_u}$ can be approximated by $\kappa\chi^2_{df_1}$, where

$$df_1 = \frac{(\sum_{r=1}^{\infty} \lambda_r)^2}{\sum_{r=1}^{\infty} {\lambda_r}^2} \times d_{\mathscr{G}_u} \quad \text{and} \quad \kappa = \frac{\sum_{r=1}^{\infty} {\lambda_r}^2}{\sum_{r=1}^{\infty} \lambda_r}. \tag{4.8}$$

Similarly, $SS^*_{res_k} \overset{d.}{=} \sum_{r=1}^{\infty} \lambda_r \tilde{A}_r$ can be approximated by $\kappa\chi^2_{df_2}$, where κ is the same as in Equation (4.8) and $df_2 = \frac{(\sum_{r=1}^{\infty} \lambda_r)^2}{\sum_{r=1}^{\infty} {\lambda_r}^2} \times d_{res_k}$.

Now we are ready to derive the approximate distribution of the statistic F in Equation (4.7) as follows:

$$\begin{aligned} F = \frac{SS^*_{\mathscr{G}_u}/d_{\mathscr{G}_u}}{SS^*_{res_k}/d_{res_k}} &\overset{approx.}{\sim} \frac{\kappa\chi^2_{df_1}/d_{\mathscr{G}_u}}{\kappa\chi^2_{df_2}/d_{res_k}} = \frac{\chi^2_{df_1}/d_{\mathscr{G}_u}}{\chi^2_{df_2}/d_{res_k}} \\ &= \frac{\chi^2_{df_1} \Big/ \{d_{\mathscr{G}_u} \times \frac{(\sum_{r=1}^{\infty} \lambda_r)^2}{\sum_{r=1}^{\infty} {\lambda_r}^2}\}}{\chi^2_{df_2} \Big/ \{d_{res_k} \times \frac{(\sum_{r=1}^{\infty} \lambda_r)^2}{\sum_{r=1}^{\infty} {\lambda_r}^2}\}} \\ &= \frac{\chi^2_{df_1}/df_1}{\chi^2_{df_2}/df_2}. \end{aligned}$$

Furthermore, since $SS^*_{\mathscr{G}_u}$ and $SS^*_{res_k}$ are independent, the null distribution of F can be approximated by an F distribution:

$$F \overset{approx.}{\sim} F(df_1, df_2).$$

Summary of functional F test

In order to test the functional null hypothesis $H_0 : \beta_{u,1}(t) = \beta_{u,2}(t) = \cdots = \beta_{u,p_u}(t)$ for all $t \in T$, we use the functional F test as follows:

$$F = \frac{\int_T SS_{\mathscr{G}_u}(t)dt / d_{\mathscr{G}_u}}{\int_T SS_{res_k}(t)dt / d_{res_k}} \overset{approx.}{\sim} F(df_1, df_2),$$

where df_1 and df_2 are called as the adjusted degrees of freedom and calculated by

$$df_1 = d_{\mathscr{G}_u} \times \frac{(\sum_{r=1}^{\infty} \lambda_r)^2}{\sum_{r=1}^{\infty} {\lambda_r}^2} \quad \text{and} \quad df_2 = d_{res_k} \times \frac{(\sum_{r=1}^{\infty} \lambda_r)^2}{\sum_{r=1}^{\infty} {\lambda_r}^2} \tag{4.9}$$

with $\lambda_1 \geq \lambda_2 \geq \cdots \geq 0$ as the eigenvalues of the covariance operator that is associated with the stratum-based covariance function $\Lambda_{\mathscr{B}_k}(s,t)$.

Adjusted degrees of freedom calculated by Equation (4.9) are not always integers. Thus, Shen and Faraway (2004) used an alternative distribution $F([df_1],[df_2])$, where $[df_1]$ and $[df_2]$ indicate the closest integers to df_1 and df_2. A similar issue of non-integer degrees of freedom in Welch's test has been discussed in Derrick et al. (2016). Although integer degrees of freedom, which are calculated by rounding down to the nearest integers, are required when using the statistical table for critical values, commonly-used statistical software, such as R, SPSS and Matlab, would conduct the test with non-integer degrees of freedom. Therefore, we will still use df_1 and df_2 calculated by Equation (4.9), as suggested in Zhang (2013, p. 98).

In a practical application of the functional F test, we need to derive the integrals in the numerator and denominator of F and to calculate the eigenvalues of the corresponding covariance operator.

More specifically, the interval $T = [0,1]$ is discretised by superimposing a fine grid of m equally spaced points $t_1, \ldots, t_m$, where $t_1 = 0 < t_2 < \cdots < t_{m-1} < t_m = 1$. The integral

$\int_T SS_{\mathscr{G}_u}(t)dt$ is approximated by the sum $\sum_{\ell=1}^{m} SS_{\mathscr{G}_u}(t_\ell)$. Likewise, as an approximation to the integral $\int_T SS_{res_k}(t)dt$, the sum $\sum_{\ell=1}^{m} SS_{res_k}(t_\ell)$ is used. To calculate the eigenvalues, the covariance function is estimated by:

$$\hat{\Lambda}_{\mathscr{B}_k}(t_\ell, t_v) = \mathbf{y}(t_\ell)^T \mathbf{P}_{\mathbb{W}(res_k)} \mathbf{y}(t_v),$$

where $\mathbf{y}(t_\ell) = [y_1(t_\ell), \ldots, y_N(t_\ell)]^T$ and $\mathbf{y}(t_v) = [y_1(t_v), \ldots, y_N(t_v)]^T$ are vectors of observed values at specific time points t_ℓ, t_v for $\ell, v = 1, \ldots, m$. Thus, $\hat{\Lambda}_{\mathscr{B}_k}$ is an $m \times m$ matrix and the eigenvalue $\hat{\lambda}_r$ for $r = 1, \ldots, m$ can be calculated.

4.2 Functional F test for gait data of patients with cerebral palsy

4.2.1 Introduction

In this section, we apply functional F tests to examine the effects of AFO on 3-dimensional kinematic gait data of children with cerebral palsy, which is a childhood condition with impaired motor function caused by lesion of the brain (Miller, 2005, p. 3). Patients with cerebral palsy usually have abnormal gait patterns leading to the prescription of fixed AFO. Generally, AFO are expected to enhance the ambulatory function and to improve motions of lower limb segments during the gait cycle (Wingstrand et al., 2014).

The effects of AFO on kinematics of patients with cerebral palsy have been examined by several studies (Abel et al., 1998; Buckon et al., 2004; Abd El-Kafy, 2014; Kerkum et al., 2015; Danino et al., 2016). However, without a proper statistical tool to analyse curves, different kinematic variables were chosen in different studies. As a result, it is difficult to summarise findings from different studies. It has been recommended to consider the effects of AFO throughout the entire gait cycle to ensure that important findings are not neglected (Hsu et al., 2008, p. 307). The FDA approach which can be applied to analyse whole gait

curves would solve these problems.

In this retrospective study, the effect of wearing AFO on the gait kinematics of patients with cerebral palsy was assessed. We aim to explore how the functional F test improves gait analysis, compared to some other statistical tests, such as univariate F tests and pointwise F tests. Material in this section is from the published paper by Zhang et al. (2017), which is enclosed in Appendix A.

4.2.2 Data collection

The original clinical study was designed in accordance with the ethical guidelines of the Declaration of Helsinki and was approved by East London NHS Research Ethics Committee (Ethics REF 09/H0806/56). Written informed assent and consent, from all children and parents respectively, was collected.

Time-dense gait data were collected from 14 patients with cerebral palsy (mean age $12.3 \pm 2.88\,years$, mean height $1.44 \pm 0.15\,m$, mean weight $39.57 \pm 11.78\,kg$) by Dr Richard Twycross-Lewis between 2010 to 2013 in Human Performance Laboratory. All recruited children had been diagnosed with spastic cerebral palsy and prescribed fixed AFO (see Figure 4.1) for a minimum of six months. Children were initially assessed by a paediatric orthopaedic consultant and only included if they were independently ambulatory and considered to have sufficient muscular endurance for gait measurements. Most recruited children were classified to the Gross Motor Function Classification System (GMFCS) (Palisano et al., 1997) level II and III and few children were classified at level IV.

Data collection followed the commonly used protocol (Ounpuu et al., 1991; Abel et al., 1998; Brehm et al., 2008) whereby each patient was instructed to perform a series of walks both barefoot and wearing AFO placed within shoes. Order was not randomised and barefoot walking was conducted first (Abel et al., 1998; Brehm et al., 2008). While walking with AFO, patients were shod, owing to the importance of footwear in the orthotic prescription that AFO modify kinematics of segments only with appropriate footwear (Hsu et al., 2008, p. 306).

Figure 4.1: Bespoke, fixed AFO for children with cerebral palsy

More specifically, anthropometric information, including pelvic width and depth and bilateral knee and ankle width, was obtained. Then kinetic data were collected while the patient walked barefoot at a self selected pace along a 6-meter walkway with two ground embedded force plates (Type 9281B Multicomponent Force Plate, Kistler Instruments Ltd, Winterthur, Switzerland) that measured 3-dimensional ground reaction force. After 10 - 20 walks, patients then repeated walking tests whilst wearing their AFO over the same force plates.

Kinematic data were collected using four 3D Cartesian Optoelectric Dynamics Anthropometer systems (Charnwood Dynamics, Rotheley, Leicestershire, UK) that were placed at distances of 2 - 3 meters from the force plates, oblique to the centre of the laboratory in order to create a data collection volume. A modified Helen Hayes marker set protocol (Richards, 2008) was used, whereby active infra-red markers were placed bilaterally on the anterior sacro-iliac spine (ASIS); posterior sacro-iliac spine (PSIS); lateral epicondyle of the knee and the lateral malleolus; lateral aspect of the calcaneous and the 5th metatarsal. Instrumented marker wand sets were also placed superior and inferior to the knees (see Figure 4.2). Joint centres for the pelvis, hips, knees and ankles were calculated using Codamotion

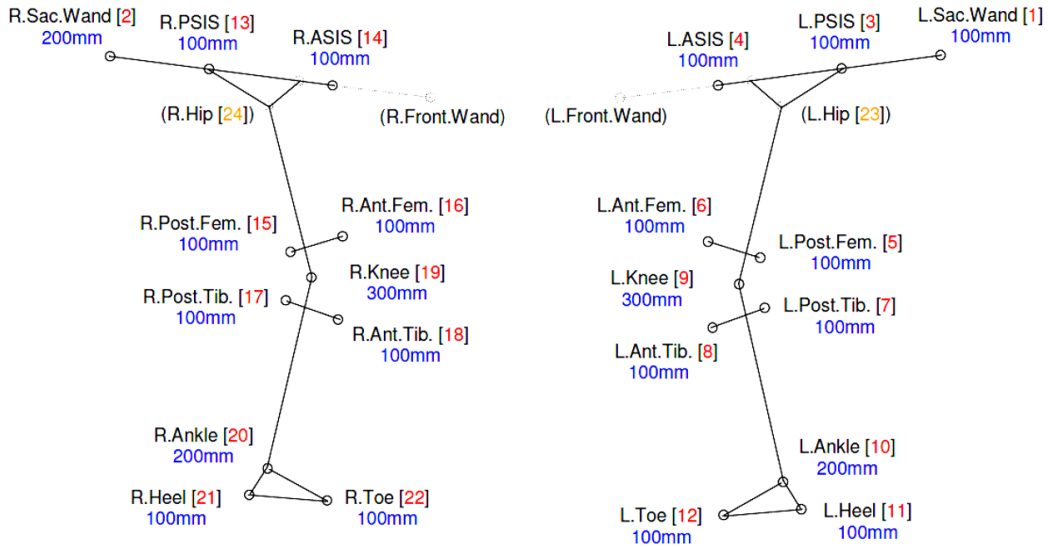

Figure 4.2: Modified Helen Hayes protocol for the gait data collection (Codamotion User Guide, 2005)

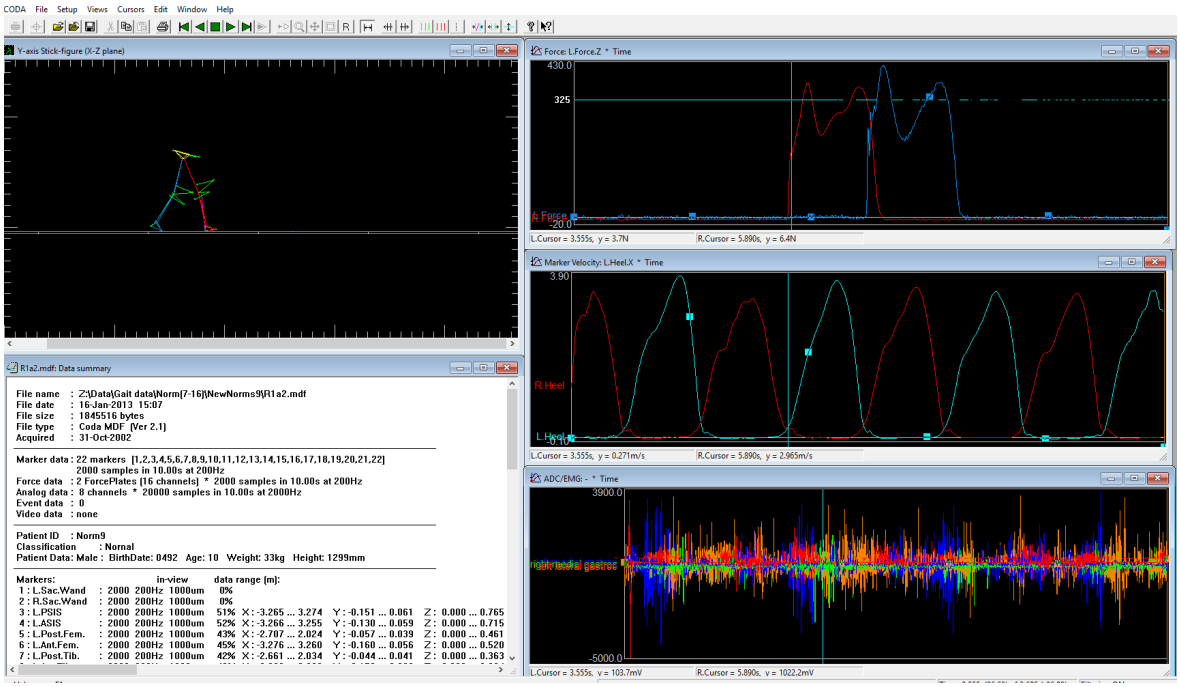

Figure 4.3: Codamotion Analysis software for the gait data collection (version 6.76.2-CX1/mpx30, Charnwood Dynamics, Rotheley, Leicestershire, UK)

Analysis software (see Figure 4.3) based on subject specific anthropometric data.

Gait events in each trial, from initial contact to toe off to the following initial contact (see Figure 1.2), were marked using the vertical component of ground reaction force and velocity of the calcaneous marker for both the ipsilateral and contralateral limbs. Standardised gait graphs were then extracted by analysing the kinematic data offline using Matlab (version 2009a, The Mathworks, Natick, MA, USA). Furthermore, a standardised gait graph usually contains 3×5 panels, where columns show the pelvis, hip joint, knee joint, ankle joint and foot and rows are the coronal plane, sagittal plane and horizontal plane respectively.

4.2.3 Statistical analysis

The structure of gait data

For each subject, four gait curves were observed from two legs (left and right) and two walking conditions (barefoot and wearing AFO). Figure 4.4 shows the rotations of knee joints in the sagittal plane as an example. Each curve represents the gait of one leg in one patient during walking under one condition. More specifically, the top and bottom panels in Figure 4.4 display the gait data from barefoot walking and walks with AFO respectively. Moreover, angles of the left and right knees are displayed in the left and right panels.

Model

In total 56 gait curves were obtained from 14 patients for each segment in each plane, which can be indicated by $\mathbf{y}(t) = [y_1(t), \ldots, y_N(t)]^T$ for $N = 56$ and $t \in [0,1]$. Hasse diagrams (see Figure 4.5) and a skeleton ANOVA table (see Table 4.1) are used to illustrate the experimental structure. We can see that the treatment factor AFO is located in the *walks*-stratum.

The functional mixed-effects model to test the effects of AFO can be expressed as:

$$\mathbf{y}(t) = \boldsymbol{\beta}_0(t) + \mathbf{X}_1\boldsymbol{\beta}_1(t) + \sum_{k=0}^{3} \mathbf{Z}_k\boldsymbol{\delta}_k(t) + \boldsymbol{\varepsilon}(t), \quad t \in [0,1], \tag{4.10}$$

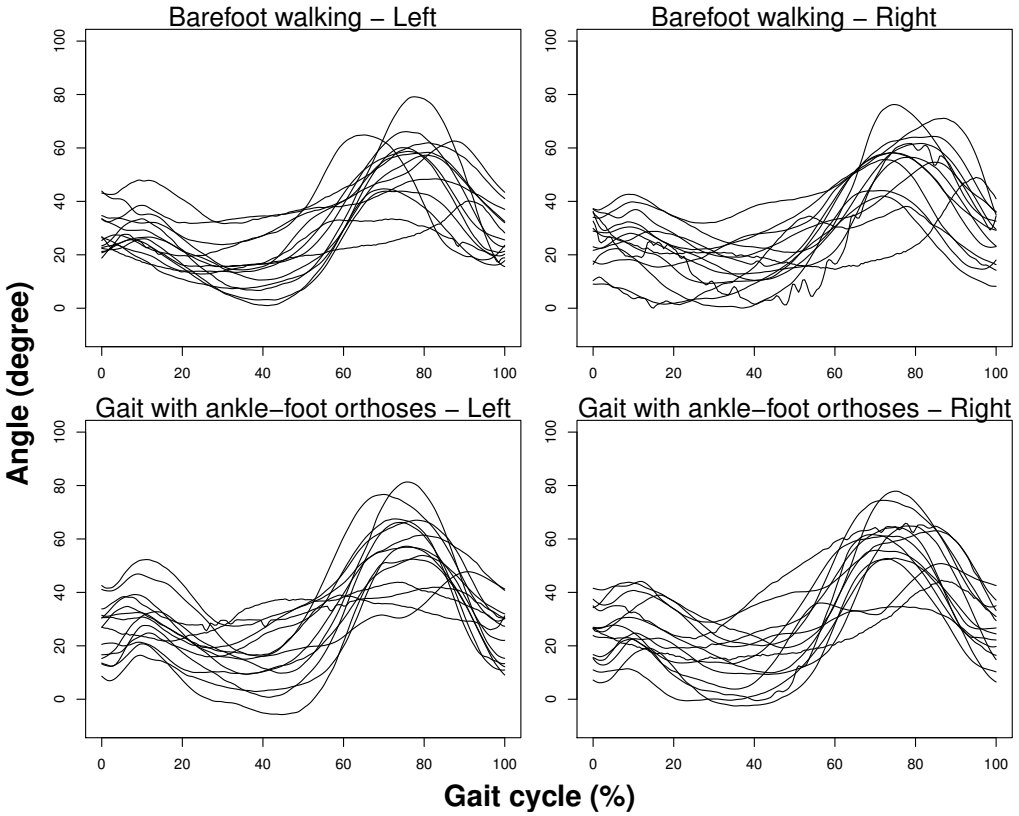

Figure 4.4: Angles of knee joints in the sagittal plane of 14 children with cerebral palsy

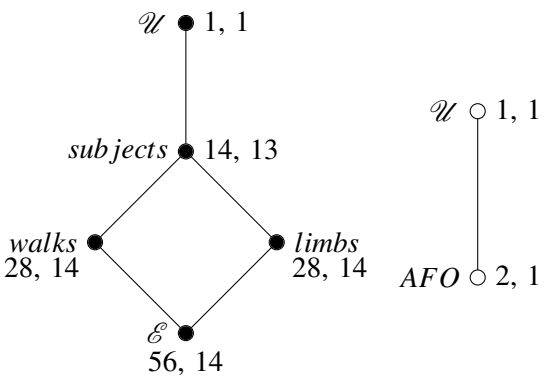

Figure 4.5: Hasse diagrams for the block structure (left) and the treatment structure (right) of the experiment where gait data of patients with cerebral palsy were collected

Table 4.1: Skeleton ANOVA table for the experiment where gait data of patients with cerebral palsy were collected

Stratum	Source	$d_{\mathbb{W}}$
$\mathscr{U}$	$\mathscr{U}$	1
subjects	*subjects*	13
walks	*AFO*	1
	residual	13
	total	14
limbs	*limbs*	14
$\mathscr{E}$	$\mathscr{E}$	14
Total		56

where $\boldsymbol{\beta}_0(t) = \mathbf{1}_{56\times1}\beta_0(t)$ with $\mathbf{1}_{56\times1}$ being an all-1 vector and $\beta_0(t)$ indicating the overall mean function; $\boldsymbol{\beta}_1(t) = [\beta_{1,1}(t), \beta_{1,2}(t)]^T$ indicates the main effect of wearing and respectively not wearing AFO; $\boldsymbol{\delta}_1(t) = [\delta_{1,1}(t), \ldots, \delta_{1,14}(t)]^T$ indicates the random effects for the subjects; $\boldsymbol{\delta}_2(t) = [\delta_{2,1(1)}(t), \ldots, \delta_{2,2(14)}(t)]^T$ indicates the random effects for the walks nested within subjects, and due to the experiment without randomisation, the first walk is barefoot and the second walk is with AFO for each subject; $\boldsymbol{\delta}_3(t) = [\delta_{3,1(1)}(t), \ldots, \delta_{3,2(14)}(t)]^T$ indicates the random effects for the limbs nested within subjects; all other terms are similar to those in Equation (3.7). In addition, $\delta_0 \sim GP(0, \theta_0)$, $\delta_{1,1}, \ldots, \delta_{1,14} \overset{i.i.d.}{\sim} GP(0, \theta_1)$, $\delta_{2,1(1)}, \ldots, \delta_{2,2(14)} \overset{i.i.d.}{\sim} GP(0, \theta_2)$, $\delta_{3,1(1)}, \ldots, \delta_{3,2(14)} \overset{i.i.d.}{\sim} GP(0, \theta_3)$ and $\varepsilon_1, \ldots, \varepsilon_N \overset{i.i.d.}{\sim} GP(0, \theta_e)$.

In order to test if the treatment factor AFO has an effect or not, we concentrate on the *walks*-stratum. Functional sums of squares in this stratum are calculated by:

$$SS_{walks}(t) = \mathbf{y}(t)^T \mathbf{P}_{walks}\mathbf{y}(t), \quad SS_{AFO}(t) = \mathbf{y}(t)^T \mathbf{P}_{AFO}\mathbf{y}(t), \quad SS_{residual}(t) = SS_{walks}(t) - SS_{AFO}(t), \tag{4.11}$$

where the corresponding orthogonal projections are

$$\mathbf{P}_{walks} = \frac{1}{2}\mathbf{Z}_2\mathbf{Z}_2^T - \frac{1}{4}\mathbf{Z}_1\mathbf{Z}_1^T \quad \text{and} \quad \mathbf{P}_{AFO} = \frac{1}{28}\mathbf{X}_1\mathbf{X}_1^T - \frac{1}{56}\mathbf{1}_{56\times1}\mathbf{1}_{56\times1}^T.$$

Functional sums of squares in Equation (4.11) are used by both pointwise F tests and functional F tests. However, whereas the pointwise F tests also use the degrees of freedom $d_{\mathbb{W}}$ in Table 4.1 in order to assess the significance of the results, this is not the case for the functional F test.

Pointwise F tests

The effect of AFO may be tested by adopting a multiple testing approach. However, this does not take the functional nature of the data into account. This amounts to performing a

series of separate F tests of

$$H_0 : \beta_{1,1}(t_\ell) = \beta_{1,2}(t_\ell) \quad \text{versus} \quad H_1 : \beta_{1,1}(t_\ell) \neq \beta_{1,2}(t_\ell)$$

at each of m equally spaced points $t_\ell \in [0,1]$, $\ell = 1,\ldots,m$, in the gait cycle. The test statistic of the pointwise F test at t_ℓ and its distribution under the null hypothesis H_0 are given by

$$F(t_\ell) = \frac{SS_{AFO}(t_\ell)/1}{SS_{residual}(t_\ell)/13} \sim F(1,13).$$

The resulting values $F(t_\ell)$ are plotted against t_ℓ for $\ell = 1,\ldots,m$ and can be assessed for statistical significance at every time point.

Pointwise F tests face the usual problems surrounding multiple testing. In particular, the familywise error probability (Hochberg and Tamhane, 1987, p. 7) can be much higher than the nominal significance level of the individual tests, as will be illustrated later.

Functional F test

Alternatively, the functional F test summarises information across the whole gait cycle by integrating the functional sums of squares $SS_{AFO}(t)$ and $SS_{residual}(t)$ over $[0,1]$. Contrary to the pointwise F tests, the hypotheses tested by the functional F test are given by

$$H_0 : \beta_{1,1}(t) = \beta_{1,2}(t) \text{ for all } t \in [0,1] \quad \text{versus} \quad H_1 : \beta_{1,1}(t) \neq \beta_{1,2}(t) \text{ for some } t \in [0,1],$$

and the functional F test uses the single statistic

$$F = \frac{\int_0^1 SS_{AFO}(t)dt/1}{\int_0^1 SS_{residual}(t)dt/13}. \tag{4.12}$$

We have already proved in Section 4.1 that under H_0 the distribution of the above F can be approximated by an F distribution as follows

$$F \overset{approx.}{\sim} F(df_{AFO}, df_{residual}),$$

with the adjusted degrees of freedom equal to

$$df_{AFO} = \frac{(\sum_{r=1}^{\infty} \lambda_r)^2}{\sum_{r=1}^{\infty} \lambda_r^2} \quad \text{and} \quad df_{residual} = 13 \times \frac{(\sum_{r=1}^{\infty} \lambda_r)^2}{\sum_{r=1}^{\infty} \lambda_r^2},$$

where $\lambda_1 \geq \lambda_2 \geq \cdots \geq 0$ are the eigenvalues of the covariance operator that is associated with the *walks*-stratum-based covariance function $\Lambda_{walks}(s,t)$. Furthermore, $\Lambda_{walks}(s,t) = 2\theta_2(s,t) + \theta_e(s,t)$, according to Theorem 3.4.

An attractive feature of the functional F test is that the integration over $[0,1]$ can be replaced with integration over subsets of $[0,1]$. This opens up the possibility to test the effects of AFO in specific phases of the gait cycle as will be illustrated below.

4.2.4 Results

Observational results

Figures 4.6 and 4.7 show descriptive information for 3-dimensional segmental rotations of lower limbs in patients during both barefoot and shod with AFO walking. Differences can be seen in the overall kinematics with the application of the AFO: there is an overall increase in maximal dorsiflexion from 10° to 15° of the ankle joint in the sagittal plane in gait with AFO, however the magnitude of joint rotation does not change. Differences in the mean curves shown in Figures 4.6 and 4.7 are not immediately apparent.

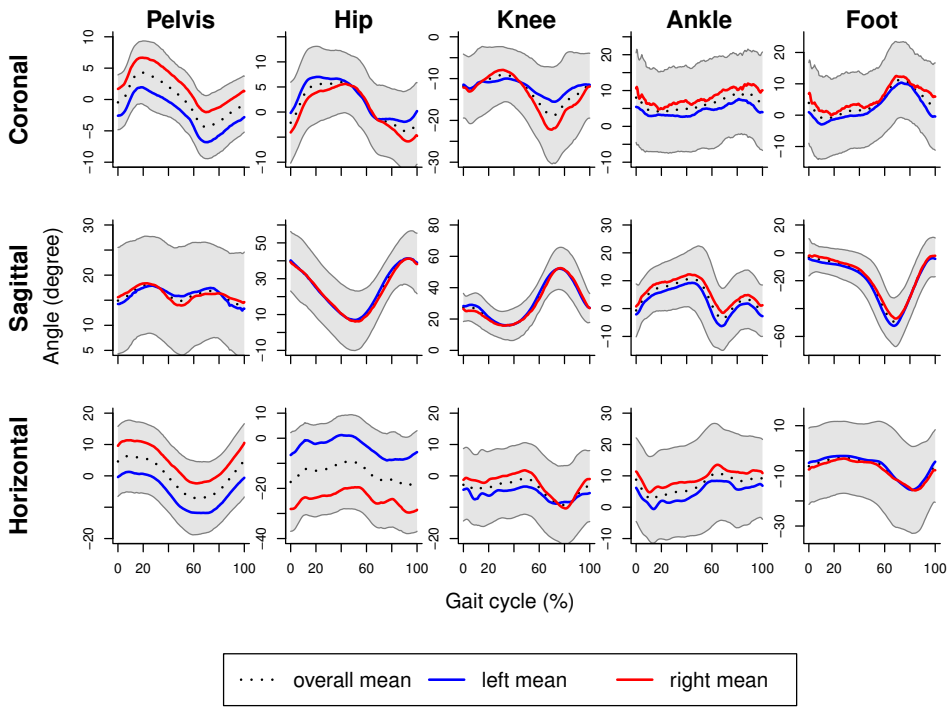

Figure 4.6: Barefoot walking in 14 children with cerebral palsy. Data are normalised to percentage (%) of the gait cycle and grey areas represent intervals [mean−s.d., mean+s.d.] at every point.

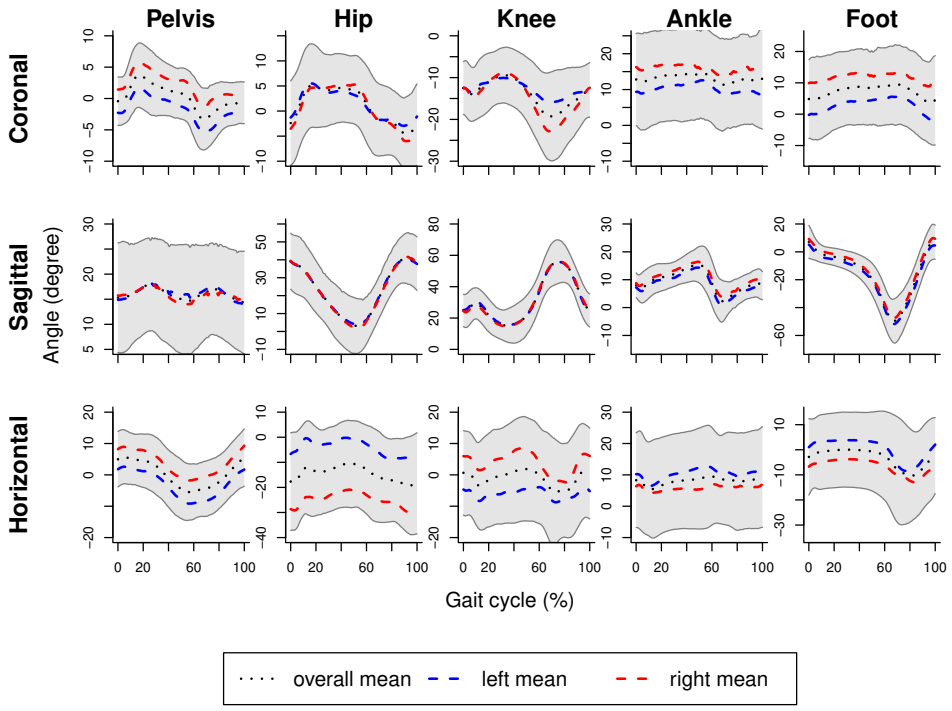

Figure 4.7: Gait with AFO in 14 children with cerebral palsy. Data are normalised to percentage (%) of the gait cycle and grey areas represent intervals [mean−s.d., mean+s.d.] at every point.

Pointwise F tests

We first examined effects of AFO on different segmental rotations by using the multiple pointwise F tests and results are shown in Figure 4.8. All individual tests used a significance level of $\alpha = 0.05$. In the figure, AFO have significant effects when the value of the F statistic exceeds the critical value, which is the same at all time points ($F_{0.05}(1,13) = 4.67$). We can see that there is no panel where the whole curve of statistic values exceed the critical values. However, we detect significant effects at some specific points.

In certain parts of the gait cycle AFO have significant effects on pelvis in the coronal and horizontal planes; hip joint in the coronal and sagittal planes; knee joint in all three planes; ankle joint in the coronal and sagittal planes and foot in the sagittal and horizontal planes (Figure 4.8). Moreover, for different segments significant effects of AFO occur at different time points along the gait cycle conferring a temporal effect. Referring to Figures 4.6 and 4.7, we can see that for the pelvis in the coronal and horizontal planes, hip joint and ankle joint in the sagittal plane, AFO have significant effects roughly around the minimal angles, whereas for the hip in the coronal plane and the knee in the sagittal plane effects of AFO tend to occur near maximal angles.

The nominal significance level of every individual pointwise F test is $\alpha = 0.05$. However, in every panel of Figure 4.8 many of those tests are performed on a grid of $m = 201$ points. Consequently, the familywise error rate, which is the probability of at least one incorrect rejection of the null hypothesis, of this multiple testing procedure can be much higher than the nominal significance level if one looks at an interval rather than a single time point. For instance, AFO affect hip rotation in the sagittal plane between 50-60% of the gait cycle (see Figure 4.8). This section of the gait cycle contains approximately 20 grid points. At each of these points the probability of a type I error is 0.05. However, an approximate calculation under the simplifying (and surely not correct) assumption that the tests are independent shows that the familywise error rate for the 20 tests in the 50-60% interval of the

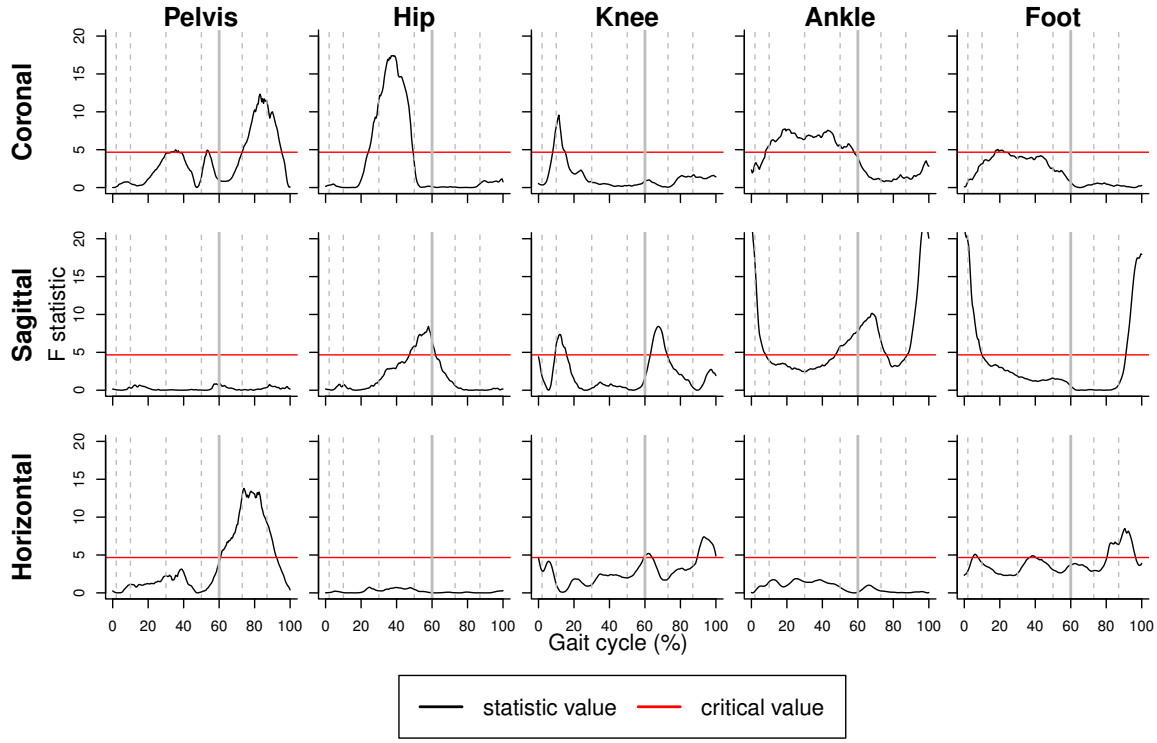

Figure 4.8: Multiple pointwise F tests at significance level $\alpha = 0.05$ for effects of AFO on segmental rotations. Grey dashed and solid lines are used to divide the whole gait cycle into phases: initial contact, loading response, mid-stance, terminal stance, pre-swing, initial swing, mid-swing and terminal swing (from left to right).

gait cycle can be as high as $1-(1-0.05)^{20} \approx 0.64$. This example illustrates that results of pointwise tests need to be interpreted with care, since the "significance" of the results may be overstated. Pointwise tests may suggest the presence of effects where there are actually none.

Functional F test and univariate F tests

The first part of Table 4.2 presents the functional F test for each of the segments and planes. The values of the test statistic F and the corresponding p-values are shown in the second column of the table and the degrees of freedom of the approximate null distribution of F in the first column. The degrees of freedom are reported in the form $(df_{AFO}, df_{residual})$ and

Table 4.2: Functional F tests for the whole gait cycle and F tests from the univariate ANOVA for minimal and maximal angles. Degrees of freedom for the univariate ANOVA are $(1, 13)$ and * indicates significance at 0.05 significance level.

		Functional F test		Univariate ANOVA (F value (p.))	
		degrees of freedom	F value (p.)	minimal angle	maximal angle
Pelvis	coronal	$(1.47, 19.06)$	$2.80(0.10)$	$0.03(0.86)$	$0.34(0.57)$
	sagittal	$(1.16, 15.04)$	$0.21(0.69)$	$0.20(0.66)$	$0.01(0.93)$
	horizontal	$(2.11, 27.48)$	$3.45(0.04)$*	$8.32(0.01)$*	$1.19(0.30)$
Hip	coronal	$(2.79, 36.27)$	$1.32(0.28)$	$0.03(0.87)$	$0.29(0.60)$
	sagittal	$(1.92, 24.92)$	$1.69(0.20)$	$4.28(0.06)$	$0.27(0.61)$
	horizontal	$(1.27, 16.48)$	$0.15(0.76)$	$0.08(0.79)$	$0.08(0.79)$
Knee	coronal	$(1.89, 24.59)$	$1.11(0.34)$	$1.43(0.25)$	$1.14(0.31)$
	sagittal	$(3.21, 41.68)$	$2.29(0.09)$	$1.68(0.22)$	$1.91(0.19)$
	horizontal	$(1.52, 19.76)$	$2.90(0.09)$	$0.34(0.57)$	$7.45(0.02)$*
Ankle	coronal	$(1.11, 14.45)$	$4.37(0.05)$*	$5.50(0.04)$*	$1.65(0.22)$
	sagittal	$(1.49, 19.43)$	$6.44(0.01)$*	$19.3(< 0.01)$*	$3.35(0.09)$
	horizontal	$(1.27, 16.46)$	$0.82(0.40)$	$2.52(0.14)$	$0.97(0.34)$
Foot	coronal	$(1.15, 14.97)$	$2.24(0.15)$	$2.52(0.17)$	$0.45(0.51)$
	sagittal	$(2.20, 28.54)$	$2.63(0.08)$	$1.67(0.22)$	$13.37(< 0.01)$*
	horizontal	$(1.69, 21.99)$	$3.98(0.04)$*	$2.02(0.18)$	$4.81(0.05)$*

depend on the actual data. At a significance level of $\alpha = 0.05$, the functional F tests detect significant effects of AFO on the pelvis rotation in the horizontal plane, ankle rotation in the coronal and sagittal planes and foot rotation in the horizontal planes. These results indicate that AFO have significant effects on the overall motion of these segments over the whole gait cycle.

The second part of Table 4.2 reports results of a univariate ANOVA with minimal angle as the response variable in the third column of the table, and corresponding results for maximal angle as the response variable in the fourth column. The F values in the table are computed as for the pointwise F test with the only modification that all sums of squares are

calculated at the time points of the gait cycle at which the minimum (respectively maximum) angles occur. These time points do vary within and between patients. For both response variables, the null distribution of the test statistic is an $F(1,13)$ distribution and thus the same as for the pointwise F test.

With significance level $\alpha = 0.05$ as before, the F tests from the univariate ANOVA detect effects of AFO on minimal pelvis angle in the horizontal plane, ankle angle in the coronal and sagittal planes, which agrees with the results of the functional F tests. For maximal angle, the F tests from the univariate ANOVA find a significant effect on foot in the horizontal plane, which is again in agreement with the result of the functional F test. Moreover, the F test detects an effect on maximal knee angle in the horizontal plane and maximal foot angle in the sagittal plane, where the corresponding functional F test for the whole gait cycle is not significant.

Functional F test for gait phases

Besides the whole gait cycle, we are also interested in effects of AFO during the stance phase (0-60% of gait cycle) and swing phase (60-100% of gait cycle) separately. In Figure 4.8, the stance and swing phases are divided by grey solid lines.

In order to perform functional F tests for these phases, it is only necessary to replace the interval $[0,1]$ in the formula for F in Equation (4.12) with appropriate subintervals. For the stance phase we replace $[0,1]$ with $[0,0.6]$ and for the swing phase we use $(0.6,1]$. For simplicity, we continue to denote the resulting test statistics by F.

Results for the stance and gait phases are shown in Table 4.3. For significance level $\alpha = 0.05$, AFO only have significant effects during the stance phase on the ankle rotation in the coronal and sagittal planes. In the swing phase, there are significant effects on pelvis rotation in the coronal and horizontal planes, knee rotation in the horizontal plane, ankle rotation in the sagittal plane and foot rotation in the horizontal plane.

Table 4.3: Functional F tests for stance and swing phases of gait cycle with * indicating significance at 0.05 significance level

		Stance phase (F value (p.))	Swing phase (F value (p.))
Pelvis	coronal	$1.69(0.21)$	$4.41(0.04)^*$
	sagittal	$0.17(0.72)$	$0.27(0.64)$
	horizontal	$1.14(0.33)$	$7.47(<0.01)^*$
Hip	coronal	$2.44(0.09)$	$0.28(0.74)$
	sagittal	$3.39(0.13)$	$0.98(0.37)$
	horizontal	$0.24(0.68)$	$0.06(0.86)$
Knee	coronal	$1.38(0.27)$	$0.97(0.37)$
	sagittal	$1.21(0.32)$	$2.96(0.07)$
	horizontal	$2.04(0.17)$	$3.83(0.05)^*$
Ankle	coronal	$6.00(0.03)^*$	$1.65(0.22)$
	sagittal	$5.15(0.02)^*$	$8.42(<0.01)^*$
	horizontal	$1.12(0.32)$	$0.28(0.65)$
Foot	coronal	$3.27(0.09)$	$0.26(0.64)$
	sagittal	$2.95(0.09)$	$2.31(0.13)$
	horizontal	$3.34(0.08)$	$4.65(0.03)^*$

4.2.5 Comparison of statistical results

Results from the functional F test are also detected by pointwise F test and univariate F test. As can be seen from Figure 4.8 and Table 4.2, significant effects of AFO on the pelvis in the horizontal plane, ankle joint in the coronal and sagittal planes and on the foot in the horizontal plane are detected by functional F tests as well as pointwise F tests and univariate F tests.

In addition to these unequivocal findings, the pointwise F tests detect significant results for certain parts of the gait cycle where the functional F test for the whole gait cycle and the F tests in the univariate ANOVA do not show significant effects. More specifically, only the pointwise F tests find effects on the pelvis in the coronal plane, on the hip in the

coronal and sagittal planes, on the knee in all three plane and on the foot in the sagittal plane. Significant results of pointwise F tests for the knee rotation in the sagittal and horizontal planes and the foot rotation in the sagittal plane agree with the weakly significant effects from the functional F test. Moreover, some of significant pointwise results are consistent with results of functional F tests for the stance and swing phases. In particular, the significant pointwise effects on the pelvis in the coronal and horizontal planes are also detected by the functional F test for the swing phase. The significant pointwise effects on the hip in the coronal plane at around 40% of the gait cycle agree with the weakly significant effects detected by the functional F test for the stance phase.

With the univariate ANOVA, we can see that the significant effects on minimal ankle angle in the coronal and sagittal planes are detected by the functional F tests in the stance phase; the significant effect on the minimal pelvis angle in the horizontal plane, on the maximal knee angle in the horizontal plane, on the maximal foot angle in the horizontal plane are also revealed by the functional F tests in the swing phase. Overall, the results from the different approaches seem to inform each other.

4.2.6 Discussion

Gait data of 28 lower limbs in 14 patients with cerebral palsy, typically hemiplegia, were modelled by a functional mixed-effects model. The effects of wearing AFO on 3-dimensional joint rotations were assessed by three different methods: multiple testing with pointwise F tests performed at separate points of a fine grid, a new functional F test which was applied to entire gait curves, and univariate F tests, which were performed separately on minimal and maximal joint angles. By comparing statistical results, we can see that the proposed functional F tests provided additional information to pointwise F tests and univariate F tests.

Although this study showed the applicability of functional ANOVA in gait analysis, we did not have any further clinical information about patients in this retrospective study, such as

the AFO configuration, GMFCS level and cerebral palsy type (spastic hemiplegia or spastic diplegia cerebral palsy) of each patient. Moreover, there are some limitations of this study due to the retrospective data collection, such as the data quality. As pointed out in another retrospective study that using barefoot walking as the control condition was not ideal since footwear affected the gait pattern (Brehm et al., 2008). In addition, the influences of footwear on gait kinematics and on the effects of AFO have been investigated in Desloovere et al. (2006), which found significant differences of maximum ankle dorsiflexion and maximum knee flexion in the stance phase between barefoot and shod walking, while no difference was found for the maximum hip extension in the stance phase and mean pelvic rotation. Desloovere et al. (2006) also examined the effects of two types of AFOs and had different results between the shod walking compared to walking with AFOs and the barefoot walking compared to walking with AFOs, with respect to ankle and knee kinematics. Therefore, it is difficult to distinguish whether the significant differences we found in this study are caused by the effect of AFO or footwear. Furthermore, Abel et al. (1998) discussed the issue of non-randomised design in the retrospective study, which is also a limitation in the present study.

Another controversial issue of this study is the experimental structure, as shown in Figure 4.5 and Table 4.1, which is proper from a statistical perspective. However, the statistical test based on this structure is equivalent to a paired two-sample test for the average of the left and right limbs. From a clinical perspective, the diagnoses of recruited patients include both hemiplegia cerebral palsy and diplegia cerebral palsy. Spastic hemiplegia implies the paralysis on one side of the body, while spastic diplegia affects both legs although two sides of the body may perform asymmetrically (Whittle, 2007, p. 197). Therefore, hemiplegia always and diplegia may result in asymmetric gait patterns. Averaging the gait data from the left and right legs may conceal the effects of AFO to some extent. Menz (2004) discussed whether each subject or each leg of each subject should be considered as an observation but concluded a lack of statistical solutions to this problem.

4.3 Functional F test for gait data from a split-plot design

4.3.1 Introduction

In this section we consider gait data collected from healthy subjects in a split-plot design. In order to achieve a successful orthotic management it is necessary first to understand the biomechanics of normal gait (Owen, 2010), although we focus more on statistical techniques rather than clinical interpretation.

The effects of AFO and walking speeds on gait patterns of healthy subjects are tested by functional F tests. The use of AFO, which partially corrects gait patterns of patients, may constrain the gait of a healthy subject (Opara et al., 1985; Guillebastre et al., 2009). Thus, we explore potential utilisations of the proposed functional F test to gait analysis, however, do not make any clinical recommendation.

4.3.2 Experimental design

We consider two treatment factors in this experiment: AFO and $speeds$. During the data collection, each participant was asked to walk on an instrumented treadmill under three conditions: barefoot (BF), wearing one orthosis around the left leg (unilateral AFO) and wearing two orthoses around both legs (bilateral AFO). Furthermore, under each orthotic condition, gait data were collected at three different speeds that had been set for the treadmill: the self-selected speed (medium), the speed which is $1km/h$ faster than the self-selected speed (fast) and the speed which is $1km/h$ slower than the self-selected speed (slow).

In this experiment, each subject walked more than once and block factors are subjects and time-periods. Within each subject, each level of treatment factor AFO is randomly allocated to one of three time-periods. Moreover, each time-period is split into three sub-periods, when the participant walked at different speeds. The total number of recruited participants is 9 and the experimental structure is illustrated by Hasse diagrams (Figure 4.9)

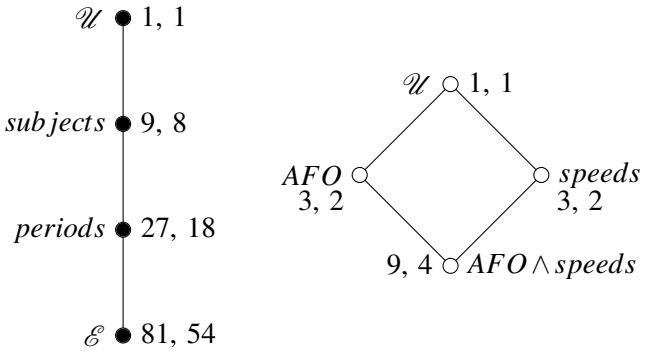

Figure 4.9: Hasse diagrams for the block structure (left) and the treatment structure (right) of the experiment where gait data of healthy subjects were collected

Table 4.4: Skeleton ANOVA table for the experiment where gait data of healthy subjects were collected

Stratum	Source	$d_{\mathbb{W}}$
$\mathscr{U}$	$\mathscr{U}$	1
subjects	*subjects*	8
periods	*AFO*	2
	residual	16
	total	18
$\mathscr{E}$	*speeds*	2
	$AFO \wedge speeds$	4
	residual	48
	total	54
Total		81

and a skeleton ANOVA table (Table 4.4), where the treatment factor AFO is located in the *periods*-stratum, whereas the treatment factor *speeds* and the interaction term are located in the $\mathscr{E}$-stratum.

4.3.3 Data collection

The present study was performed in accordance with the ethical guidelines of the Declaration of Helsinki and was approved by Queen Mary University of London Ethics of Research Committee (REF QMREC2014/24/48). The written informed consent was obtained from all participants. The ethical application form for approval including the Participant Information Sheet and Informed Consent are enclosed in Appendix B.

During the experiment, each recruited participant was asked to walk on an instrumented treadmill (Gaitway 2, h/p/cosmos sports & medical gmbh, Nussdorf-Traunstein, Germany) under different walking conditions, which are combined by three AFO conditions crossed with three speeds. Each trial under one walking condition lasts 30 - 60 seconds. Additionally,

Figure 4.10: Ankle-foot orthoses (AFO)

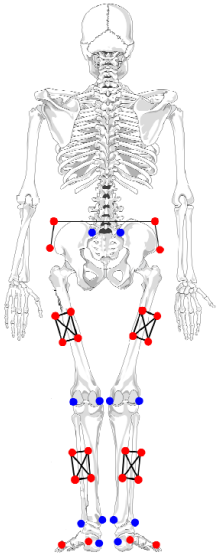

Figure 4.11: Back view of the marker set with red dots as infra-red markers and blue dots as digitised virtual markers (Codamotion ODIN user Guide, 2016)

the orthosis (medium size, footplate length 160mm and brace height 340mm) used in this study is shown in Figure 4.10 and AFO were placed within participants' own shoes. When the subject walked with the unilateral AFO, the orthosis was always placed around the left leg.

Furthermore, data were collected by using a modified CAST marker protocol (Richards, 2008), whereby a combination of 4 marker clusters were placed above and beneath the knees on the lateral aspects of the thighs and shanks. Active infra-red markers were placed on the anterior sacro-iliac spine and posterior sacro-iliac spine bilaterally, lateral aspect of the heel and fifth metatarsal, which are indicated by red dots in Figure 4.11. In addition, digitised virtual markers at the lateral and medial malleolus and epicondyles of the knees, which are indicated by blue dots in Figure 4.11, were used to construct a gait model for the analysis of human movement.

Gait data were measured and analysed by Codamotion ODIN (CX-1 system, Charn-

wood Dynamics, Rotheley, Leicestershire, U.K.). Gait events of each trial, including initial contact, toe off and the next initial contact, were marked according to the velocity of calcaneous marker. Data were retrieved and stored for offline analysis by using Matlab (version R2016a, The Mathworks, Natick, MA, USA). In this study, we again focus on the kinematic data, which were calculated from the gait model constructed by the Codamotion ODIN analysis software. Raw kinematic data are rough and missing values exist in the dataset. Therefore we smoothed the gait data by using the non-parametric smoothing technique (Zhang, 2013).

4.3.4 Statistical analysis

Based on the experimental structure introduced in Section 4.3.2, we apply the following functional mixed-effects model

$$\mathbf{y}(t) = \boldsymbol{\beta}_0(t) + \mathbf{X}_1\boldsymbol{\beta}^A(t) + \mathbf{X}_2\boldsymbol{\beta}^B(t) + \mathbf{X}_3\boldsymbol{\beta}^{A\wedge B}(t) + \boldsymbol{\delta}_0(t) + \mathbf{Z}_1\boldsymbol{\delta}^L(t) + \mathbf{Z}_2\boldsymbol{\delta}^S(t) + \boldsymbol{\varepsilon}(t), \tag{4.13}$$

to study the effects of AFO and speeds. Model equation (4.13) is an extension of Equation (3.16) which is the model for the null experiment of the split-plot design in Example 3.3. The main effects of AFO, speeds and their interaction are indicated by $\boldsymbol{\beta}^A(t) = [\beta_1^A(t), \beta_2^A(t), \beta_3^A(t)]^T$, $\boldsymbol{\beta}^B(t) = [\beta_1^B(t), \beta_2^B(t), \beta_3^B(t)]^T$ and $\boldsymbol{\beta}^{A\wedge B}(t) = [\beta_1^{A\wedge B}(t), \ldots, \beta_9^{A\wedge B}(t)]^T$, respectively. The random-effect terms $\boldsymbol{\delta}^L(t)$ and $\boldsymbol{\delta}^S(t)$ indicate random effects for block factors *subjects* and *periods*. All assumptions are the same as those in Equation (3.16).

Functional F test for AFO

In order to test the effects of AFO under the hypotheses:

$$H_0 : \beta_1^A(t) = \beta_2^A(t) = \beta_3^A(t) \text{ for all } t \in [0,1] \quad \text{versus} \quad H_1 : \neg H_0,$$

we apply a functional F test with test statistic:

$$F = \frac{\int_0^1 SS_{AFO}(t)dt/2}{\int_0^1 SS_{res_1}(t)dt/16} \overset{approx.}{\sim} F(df_{AFO}, df_{res_1}),$$

where res_1 indicates the residual in the *periods*-stratum. Moreover, the adjusted degrees of freedom are calculated by:

$$df_{AFO} = 2 \times \frac{(\sum_{r=1}^{\infty} \lambda_r)^2}{\sum_{r=1}^{\infty} \lambda_r^2} \quad \text{and} \quad df_{res_1} = 16 \times \frac{(\sum_{r=1}^{\infty} \lambda_r)^2}{\sum_{r=1}^{\infty} \lambda_r^2},$$

where $\lambda_1 \geq \lambda_2 \geq \cdots \geq 0$ are the eigenvalues of the covariance operator that is associated with the *periods*-stratum-based covariance function $\Lambda_{periods}(s,t)$.

Functional F tests for speeds and interaction

Similarly, in order to test the effects of speeds under the hypotheses:

$$H_0 : \beta_1^B(t) = \beta_2^B(t) = \beta_3^B(t) \text{ for all } t \in [0,1] \quad \text{versus} \quad H_1 : \neg H_0,$$

we apply a functional F test with test statistic:

$$F = \frac{\int_0^1 SS_{speeds}(t)dt/2}{\int_0^1 SS_{res_2}(t)dt/48} \overset{approx.}{\sim} F(df_{speeds}, df_{res_2}),$$

and in order to test the interaction under the hypotheses:

$$H_0 : \beta_1^{A\wedge B}(t) = \cdots = \beta_9^{A\wedge B}(t) \text{ for all } t \in [0,1] \quad \text{versus} \quad H_1 : \neg H_0,$$

we apply a functional F test with test statistic:

$$F = \frac{\int_0^1 SS_{AFO\wedge speeds}(t)dt/4}{\int_0^1 SS_{res_2}(t)dt/48} \overset{approx.}{\sim} F(df_{AFO\wedge speeds}, df_{res_2}),$$

where res_2 indicates the residual in the $\mathscr{E}$-stratum. Moreover, the adjusted degrees of freedom are calculated by:

$$df_{speeds} = 2 \times \frac{(\sum_{r=1}^{\infty} \lambda_r^*)^2}{\sum_{r=1}^{\infty} \lambda_r^{*2}}, \quad df_{AFO \wedge speeds} = 4 \times \frac{(\sum_{r=1}^{\infty} \lambda_r^*)^2}{\sum_{r=1}^{\infty} \lambda_r^{*2}} \text{ and } df_{res_2} = 48 \times \frac{(\sum_{r=1}^{\infty} \lambda_r^*)^2}{\sum_{r=1}^{\infty} \lambda_r^{*2}},$$

where $\lambda_1^* \geq \lambda_2^* \geq \cdots \geq 0$ are the eigenvalues of the covariance operator that is associated with the $\mathscr{E}$-stratum-based covariance function $\Lambda_{\mathscr{E}}(s,t)$.

Contrast analysis for AFO

In the previous test for AFO, we considered whether there is a difference among walks barefoot, wearing unilateral AFO and wearing bilateral AFO. However, such a test is sometimes not very informative, since one may be more interested in which treatment is different from others (Hinkelmann and Kempthorne, 1994). Therefore, we also compare the barefoot walking with walks wearing AFO by applying the contrast analysis. A new Hasse diagram for the treatment structure is shown in Figure 4.12. We can see that the treatment factor AFO is partitioned into two parts: the comparison of walks barefoot with wearing AFO, which is indicated by $L_1 : BF \; vs. \; AFO$, and the comparison of walks wearing the unilateral AFO with bilateral AFO, which is indicated by $L_2 : Unilateral \; AFO \; vs. \; Bilateral \; AFO$. Moreover, the interaction term is also split into two parts: $L_1 \wedge speeds$ and $L_2 \wedge speeds$.

The block structure and the test for speeds remain the same in the contrast analysis, whereas we use new functional F tests for the partitioned treatments and interactions, as will be introduced later.

4.3.5 Results

Observational results

In this example, we focus on the kinematics of the pelvis, hip joint, knee joint, ankle joint and foot in the sagittal plane. Mean gait curves of all subjects for walks under different walking

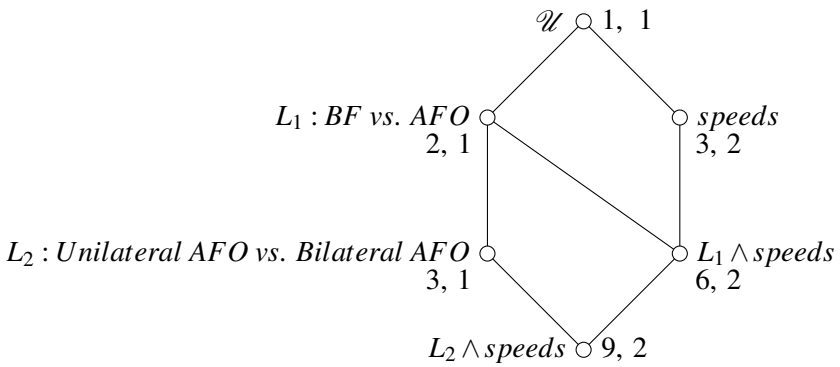

Figure 4.12: Hasse diagram for the treatment structure in the orthogonal contrast analysis

conditions are shown in Figure 4.13.

Clinical visual analysis of these plots was carried out, as might often be the case with individual case analysis, albeit without a normal database plot and no visual indication of variance. In summary, the plots are found to indicate little effect of walking speeds on pelvis movement, but a possible differential effect of AFO conditions that varies with speed - with the unilateral AFO altering pelvis movement more at higher speed, the bilateral more at medium speed and little effect at low speed, possibly due to there being enough flexibility in the musculoskeletal system to allow for compensation at low but not medium or high speed. There is a general trend of range of motion being higher at faster speeds at the hip, knee, ankle and foot but not pelvis. Little effect of AFO conditions is seen at the hip but an interesting interaction between speed and AFO is seen lower down the kinetic chain. Specifically, the effect of the AFO at fast speed is especially seen at the foot and ankle, whereas it is more seen at the knee for medium speed and minimally seen at slow speed. Whether these results would be clinically meaningful would depend on the patient's presenting complaint and other assessment findings - such as the effect of lower limb dysfunction on everyday life activities. This subjective interpretation is useful to compare with the statistical analysis.

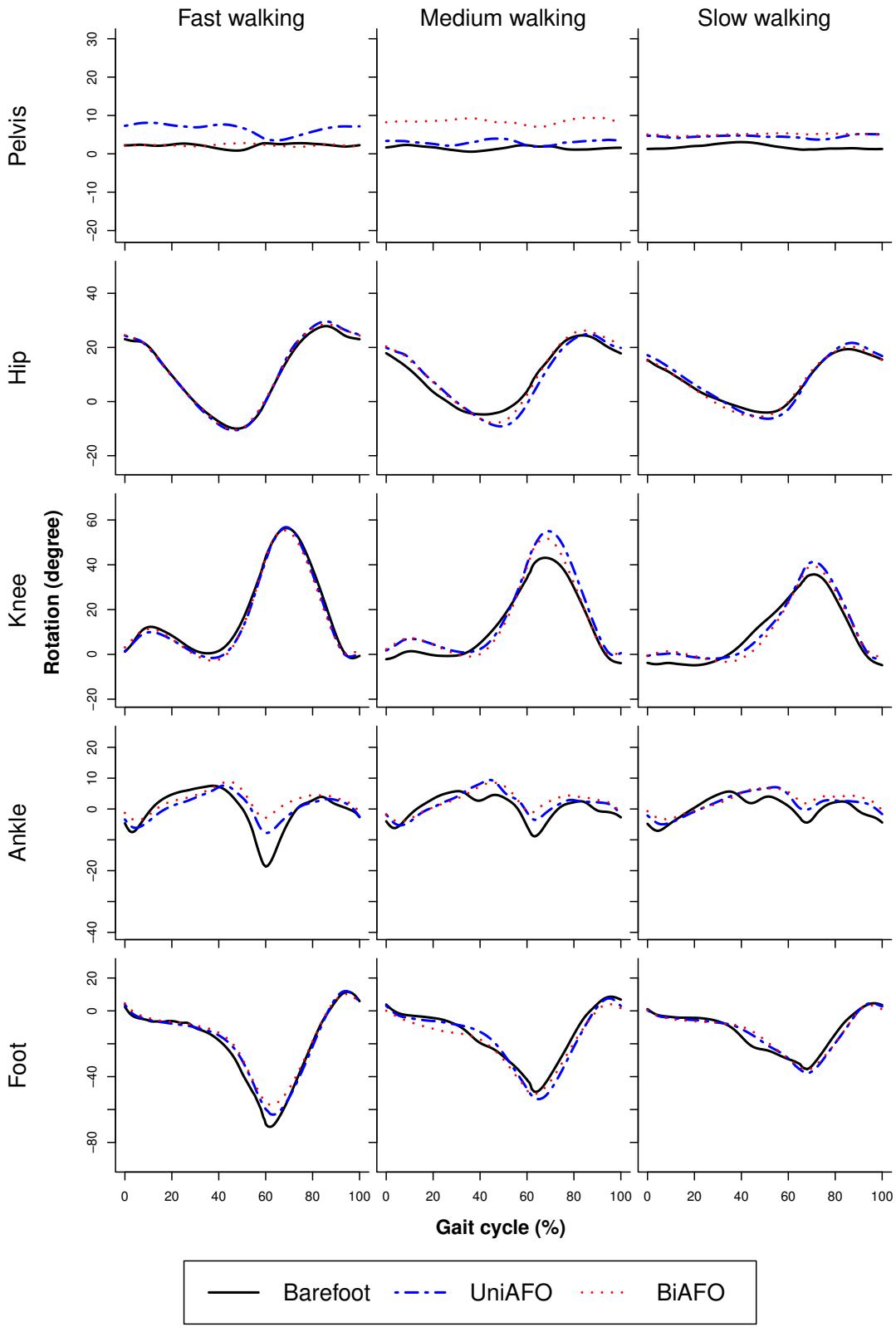

Figure 4.13: Mean gait curves of 9 healthy subjects during walking under different AFO conditions at different walking speeds. UniAFO indicates the walk wearing the unilateral AFO and BiAFO indicates the walk wearing the bilateral AFO.

Functional F tests for all segments

For each of the pelvis, hip joint, knee joint, ankle joint and foot in the sagittal plane, we constructed functional F tests for AFO, speeds and their interation. Results are summarised in Table 4.5 and we can see that the walking speeds have statistically significant effects on the hip joint, knee joint, ankle joint and foot at significance level $\alpha = 0.05$. Moreover, no significant difference has been found among the walks barefoot, wearing unilateral AFO and bilateral AFO on all five segments at significance level $\alpha = 0.05$. This may be caused by the fact that we measured gait in healthy subjects instead of patients. Although AFO provide sagittal plane support for abnormal gait, healthy subjects have sufficient joint flexion range and control during walking due to normal coordination and musculature of the lower limbs (Whittle, 2007). Therefore, any effects of AFO in gait on healthy subjects are minimal. Finally, in the last column of the table, there is no significant effect of interaction on all five segments. Since we only collected gait data of 9 subjects, the study may be somewhat underpowered for the small sample size.

Table 4.5: Functional F tests for AFO, speeds and the interaction with * indicating significance at 0.05 significance level

	F value (p.)		
	AFO	$speeds$	$AFO \wedge speeds$
Pelvis	2.07 (0.15)	0.12 (0.91)	1.38 (0.25)
Hip	0.52 (0.69)	13.12 (< 0.01)*	0.49 (0.90)
Knee	0.87 (0.69)	17.95 (< 0.01)*	0.88 (0.58)
Ankle	2.06 (0.1)	9.67 (< 0.01)*	0.94 (0.52)
Foot	0.50 (0.77)	19.86 (< 0.01)*	0.94 (0.50)

Results from functional F tests are consistent with the clinical interpretation of Figure 4.13. At the pelvis there is a higher p value for the effect of the walking speeds and lower p value for the effects of AFO and the interaction term. We found strong effects of the walking speeds on joints below pelvis according to p values which are smaller than 0.01. Functional

F tests reveal no effects of AFO and the interaction term for the movements of the hip, knee joints and foot, whereas there is a weak effect of AFO on ankle joint movement with the p value of functional F test equal to 0.1. Due to the important role that the ankle joint plays in the assessment of AFO, we explore additional influences of AFO on the ankle rotation.

Additional analysis for the ankle joint

We explore further effects of AFO on the ankle joint by using the pointwise F tests and functional F tests in the orthogonal contrast analysis. Figure 4.14 shows results of the pointwise F tests of the hypotheses:

$$H_0 : \beta_1^A(t_\ell) = \beta_2^A(t_\ell) = \beta_3^A(t_\ell) \quad \text{versus} \quad H_1 : \neg H_0,$$

for each of m equally spaced points $t_\ell \in [0,1]$, $\ell = 1,\ldots,m$ in the gait cycle. The test statistic of the pointwise F test at t_ℓ and its distribution under the null hypothesis H_0 are given by

$$F(t_\ell) = \frac{SS_{AFO}(t_\ell)/2}{SS_{res_1}(t_\ell)/16} \sim F(2,16).$$

We can see in Figure 4.14 that at the significance level $\alpha = 0.05$, AFO affect the ankle rotation during the transition from the stance to swing phase, which is from the 55% to 65% of the gait cycle. This period is around the gait event of toe off (60% of gait cycle), when the peak of ankle plantar flexion, that is the minimum of the ankle rotation, occurs for the normal gait (Whittle, 2007).

Furthermore, from the ankle rotations that are shown in Figure 4.13 we can see that gait curves during walking with unilateral and bilateral AFO are similar, however, in barefoot gait, joint rotations for the ankle are more pronounced. In order to compare barefoot walking with wearing AFO, we use the orthogonal contrast analysis with the treatment structure shown in Figure 4.12. Results from the contrast analysis are summarised in Table 4.6. We can see that functional F tests detect a significant difference between walks barefoot and

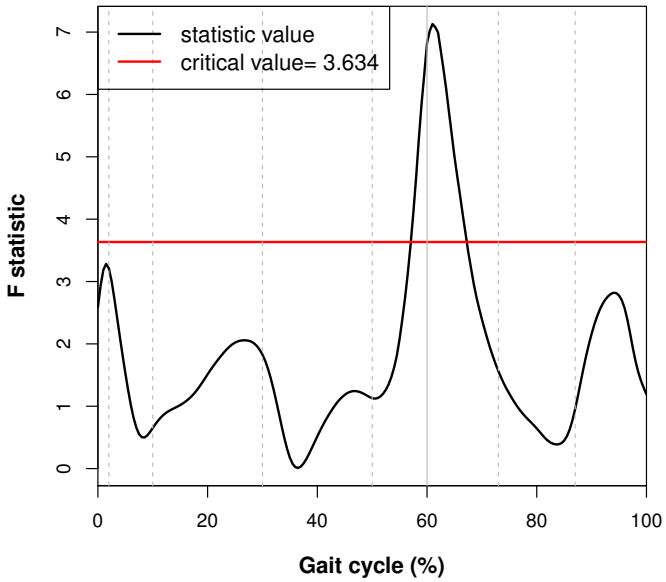

Figure 4.14: Multiple pointwise F tests for effects of AFO on ankle joints at the significance level $\alpha = 0.05$. Grey dashed lines and the grey solid line are used to divide the whole gait cycles into phases: initial contact, loading response, mid-stance, terminal stance, pre-swing, initial swing, mid-swing and terminal swing phases (from left to right).

wearing AFO on the ankle joint, which is indicated by L_1, whereas there is no difference between walks wearing unilateral and bilateral AFO, which is indicated by L_2. However, neither interaction of contrasts and speeds is significant at 0.05 significance level.

4.3.6 Discussion

We consider a split-plot design to collect time-dense gait data from 9 healthy subjects. The effects of AFO, speeds and their interaction on kinematics of the pelvis, hip joint, knee joint, ankle joint and foot in the sagittal plane have been examined by functional F tests, which detect significant effects of the walking speeds on segments lower than the pelvis at 0.05 significance level and a weak effect of AFO on the ankle joint at 0.1 significance level. Additional analysis is considered for rotations of the ankle joint. Pointwise F tests detect significant effects of AFO on the ankle rotations around the gait event of toe off. The

Table 4.6: ANOVA table for the orthogonal contrast analysis to compare the differences between walks barefoot and wearing AFO on the ankle joint. * indicates significance at 0.05 significance level.

Stratum	Source	$d_{\mathbb{W}}$	F value (p.)
$\mathscr{U}$	$\mathscr{U}$	1	
subjects	*subjects*	8	
periods	L_1	1	3.56 (0.03)*
	L_2	1	0.56 (0.59)
	residual	16	
	total	18	
$\mathscr{E}$	*speeds*	2	9.67 (< 0.01)*
	$L_1 \wedge$ *speeds*	2	1.49 (0.18)
	$L_2 \wedge$ *speeds*	2	0.39 (0.90)
	residual	48	
	total	54	
Total		81	

orthogonal contrast analysis identifies the difference between walks wearing and not wearing AFO, whereas no significant difference has been found between gait with the unilateral and bilateral AFO.

This example illustrated how our proposed approach could be applied to analyse gait curves observed from a complex experiment. However, the use of healthy subjects limits the clinical utility of the present study, due to the differences between abnormal and normal gait patterns. Thus this study will not provide clinical recommendation. Furthermore, there is a limitation of this study with respect to the data processing procedure. Raw gait curves which last 30 - 60 seconds were chopped by identifying gait events of initial contact and toe off manually. Since there was no force plate on the treadmill, gait events were identified by using data from markers of the heel and fifth metatarsal. The precision of data processing is probably not as good as those in Section 4.2, where ground reaction force and data from

markers were used to identify gait events.

Another concern is that gait data from the left and right lower limbs were averaged for each participant during walking barefoot and with bilateral AFO, while only gait data from the lower limb where the unilateral orthosis was placed were used during walking with unilateral AFO. The statistical issue related to these calculations is that the variance of averaged responses may vary from the variance of a single response. There are two possible solutions to deal with this issue. One possibility is to analyse 15 instead of 9 gait curves for each participant, that is, under each of three walking speeds there are two gait curves from barefoot walking, one gait curve from walking with unilateral AFO and two gait curves from walking with bilateral AFO. However, there is a non-uniform block factor in such experimental structure, for which our proposed method is not applicable, and more details can be found in Appendix C. Therefore, we consider another solution. We repeated the analyses based on Model (4.13) but only used gait data from left lower limbs, where the unilateral AFO was placed, under all three orthotic conditions. Results are similar to those in Section 4.3.5, as shown in Appendix D.

4.4 Conclusions

Based on the experimental structure and functional mixed-effects model introduced in Chapter 3, the functional F test has been developed to examine treatment effects in an orthogonal design with functional responses. The test statistic is equal to the ratio of the integrated treatment mean square and the corresponding integrated residual mean square. The null distribution of such statistic is derived by the Welch-Satterthwaite χ^2-approximation. To summarise, under the null hypothesis the test statistic in a functional F test approximately follows an F distribution with adjusted degrees of freedom, which can be calculated by using eigenvalues of the estimated stratum-based covariance function.

Functional F tests are applied to examine the effects of AFO in gait studies of patients

with cerebral palsy and healthy subjects in Section 4.2 and 4.3. In the first example, where gait data were collected from patients with cerebral palsy, results from the functional F tests are compared with pointwise F tests and F tests in the univariate ANOVA. Functional F tests provide additional information to the traditional statistical tests. The analyses in Zhang et al. (2017) where legs instead of patients are considered as independent observations, are useful for clinical interpretation.

In the second example, where gait data were collected from healthy subjects in a split-plot design, the effects of AFO, speeds and their interaction are examined in different strata. The functional F tests detect significant effects of the walking speeds on four segments that are lower than the pelvis and a weak effect of AFO on the ankle joint. In addition, the pointwise F tests detect that significant effects of AFO on the ankle joint occur around the transition from the stance phase to swing phase. Moreover, the orthogonal contrast analysis identifies the significant differences of the ankle rotations between walking barefoot and with AFO.

Chapter 5

The influence of gait analysis on clinicians' management of cerebral palsy: a qualitative study

5.1 Introduction

The analysis of gait data in Chapter 4 illustrates how, by using the tests developed in this thesis, statistical inferences about treatment effects can be drawn with confidence. In particular, gait patterns of patients with cerebral palsy were studied in Section 4.2. Although similar to most statistical analyses in gait studies, the present statistical method has been designed for the research purpose and targets a group or population of patients, it is possible to apply functional ANOVA and functional F test proposed in previous chapters to clinical gait analysis, such as assessing the effect of a therapy by using intra individual gait curves or assessing the reliability of gait curves for individuals (Duhamel et al., 2006). However, exploring the potential applications of novel statistical tools should be based on preliminary research assessing stakeholder requirements and important to help researchers define the required specifications for improved assessment tools, such as analytical approaches (Toro

et al., 2003).

There is a long history of gait analysis, which dates back to Giovanni Alfonson Borelli in the 1680s, but more accurate gait analysis with kinematics started in the late 19th century (Richards, 2008, p. 51). It was not until the invention of the force plate (Elftman, 1939) that kinetics was considered in gait analysis. Now, gait analysis usually refers to 3-dimensional instrumented gait analysis (IGA) and is composed of kinematics, kinetics and electromyography (EMG). Since 3-dimensional IGA requires advanced technology and equipment, it is usually conducted in a gait laboratory. When clinicians do not have access to a full gait laboratory, 2-dimensional gait analysis or visual (observational) gait analysis is considered. Kirtley (2006, p. 299) provided a list of suggestions, including ten assessments and the corresponding technical requirements, such as the simple observational gait analysis which requires a large area or the complex joint moments and powers analysis which requires a 3-dimensional motion analysis system. Clinicians could choose appropriate gait analysis from the list according to technology and time that they have.

Gait analysis in this thesis indicates *instrumented gait analysis* (or quantitative gait analysis). To avoid confusion, we use the term *visual gait analysis* to indicate visual inspection of walking and the term *video gait analysis* to indicate visual assessment augmented with video capture. Although IGA is supplemented by computer-based video capture as well, video gait analysis can be simply conducted by cameras (e.g. phone or ipad) without data being collected. Furthermore, according to Whittle (2007) clinical gait assessment is typically based on history, physical examinations and special investigations. Figure 5.1 illustrates components of clinical gait assessment, in which we particularly focus on 3-dimensional IGA.

The clinical assessment of patients focuses on the individual patient and the report from a gait laboratory provides useful information for clinical decision making. However, the clinical use of gait analysis is difficult, which has already been discussed in the literature. Cimolin and Galli (2014) and Baker et al. (2016) explored the difficulties of clinical gait

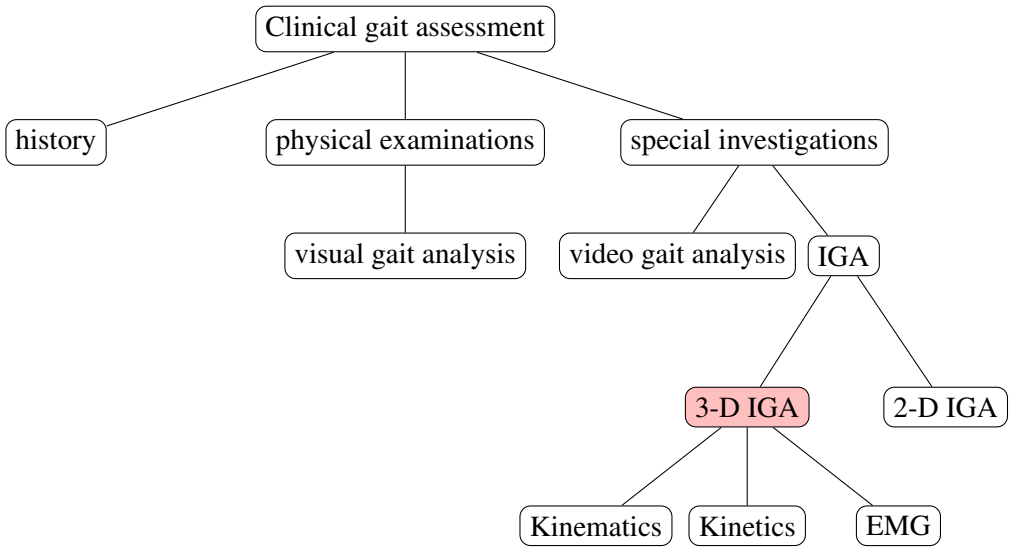

Figure 5.1: Clinical gait assessment and gait analysis (IGA = instrumented gait analysis, 3-D = 3-dimensional, 2-D = 2-dimensional)

analysis from a technical perspective. Toro et al. (2003) investigated clinical gait application amongst UK physiotherapists and emphasised the importance of finding a balance between the clinical utility and scientific merit for gait assessment tools.

Moreover, Toro et al. (2003) found physiotherapists' need for gait analysis varied. For instance, physiotherapists with degrees focused more on the reliability of gait analysis than physiotherapists with diplomas. Hart et al. (1990) stated that physiotherapists' roles affected their professional attitudes and behaviors, such as the frequency of using more complex procedures, like gait analysis or EMG, in routine clinical practice. Hart et al. (1990) distinguished whether physiotherapists involved in roles that allowed more professional judgement, personal responsibility, decision making and self-direction in contrast to those whose roles were more subordinate and structured. It is not clear whether the conclusions in Toro et al. (2003) and Hart et al. (1990) can be generalised to other clinicians who are involved in gait analysis rather than physiotherapists.

In this study we consider the following research question: the interaction between clinicians' ability to utilise information from gait analysis and the requirements of the role that

they are in. To answer this question, we therefore explored clinical gait analysis by collecting and analysing interview data from a group of clinicians who might be potential audiences for and users of gait analysis which would be the context in which novel statistical tools developed in this thesis are deployed. Qualitative information from a group of clinicians with different clinical roles in the management of cerebral palsy has been gathered, since the qualitative research has advantages in identifying processes, distinguishing factors that lead to different perspectives and teasing out attitude, decisions and outcomes (Ritchie et al., 2014).

5.2 Method

This qualitative study was approved by Queen Mary University of London Ethics of Research Committee (REF QMREC2014/24/99) and written informed consent was obtained from all participants. The ethical application form, Participant Information Sheet and Informed Consent are enclosed in Appendix E.

Data were collected using semi-structured interviews with participants recruited using a purposive sampling strategy. Subjects were recruited by emails that were sent to possible candidates in Southeastern and Eastern London. Participants were only included if they had clinical experience of working with patients with cerebral palsy for a minimum of six months and if their professional roles involved gait assessments.

The sampling framework is shown in Table 5.1. In total twelve clinicians were interviewed, including five physiotherapists, four orthotists, two clinical scientists and one specialist orthopaedic surgeon. Moreover, there were seven males and five females and ten of the participants had over 5 years of clinical experience. The sample covers clinicians who are most frequently involved in the gait assessment for patients with cerebral palsy. Among these clinicians, clinical scientists usually collect and analyse instrumented gait data in laboratories and provide recommendations to other clinicians. Orthotists in the clinical team are

Table 5.1: Classifications of 12 participants portrayed in relation to the purposive sampling frame

	Clinical experience $\geq$ 5 years		Clinical experience $<$ 5 years	
	Male	Female	Male	Female
Clinical scientists				
Orthotists				
Physiotherapists				
Specialist orthopaedic surgeons				

responsible for orthotic management, such as designing measure, fitting orthoses and follow-up (Hsu et al., 2008). Physiotherapists are considered to be the "mainstay" and "team leader" in the rehabilitation management of the movement disorder for patients with cerebral palsy, whose roles include assessing gross motor skills and functional mobility, performing therapy and recommending equipment (Papavasiliou, 2009). Specialist orthopaedic surgeons are usually involved in the treatment to improve musculoskeletal function and ambulation for patients with cerebral palsy (Sharan, 2017). Moreover, as pointed out by Papavasiliou (2009) that the treatment of the motor problems in patients with cerebral palsy used to be solely orthopaedic surgeons' responsibility, but now the treatment recommendations require an interprofessional team (IPT) evaluation.

An initial topic guide for the interviews (see Table 5.2) was developed after discussions within the research team and adjusted after a mock interview between the interviewer and a clinician who met the inclusion criteria within the team. The mock interview was not used in data analysis. Semi-structured face-to-face interviews, each of which lasted approximately 60 minutes, were conducted either at the participants' work place or at Queen Mary University of London. All interviews were recorded using a smart phone, anonymised and transcribed by the investigators and a transcription company.

The qualitative data from the interviews were analysed using the framework approach described in Ritchie et al. (2014, p. 281) and the analysis process for this qualitative study is

Table 5.2: Headings of interview topic guide

Background
Clinical experience (job title, description of current role, professional experience)
Patient group (diseases, age group)
Training about gait analysis
- Sample gait report showed as discussion prompt
Experience of using gait analysis
Gait assessment of patients with cerebral palsy in practice
Applications of 3-dimensional IGA
Collaboration with gait laboratory
Opinions of using gait analysis
Benefits
Barriers

illustrated in Figure 5.2.

All audio records were listened and all transcripts were read for the familiarisation of the qualitative data. Then the initial framework with themes and sub-themes was constructed based on the research objectives and data. Phrases, sentences and paragraphs of raw textual data were located to particular themes or sub-themes (indexing) and then material for the same theme or sub-theme was gathered together (sorting). The computer-assisted analysis software (CAQDA) NVivo 11 was applied to construct the initial thematic framework and to code the raw data under the themes and sub-themes.

Then, a framework matrix with each column for one theme or sub-theme and each row for one participant to summarise the data was created by using Microsoft Excel. At this stage, the language of participants was retained. The thematic framework was refined by reviewing data extracts and categories were developed. A new framework matrix with updated themes and subthemes was created in another Excel sheet. In this framework matrix, descriptive and summative categories were used instead of participants' own language. Finally, the linkage

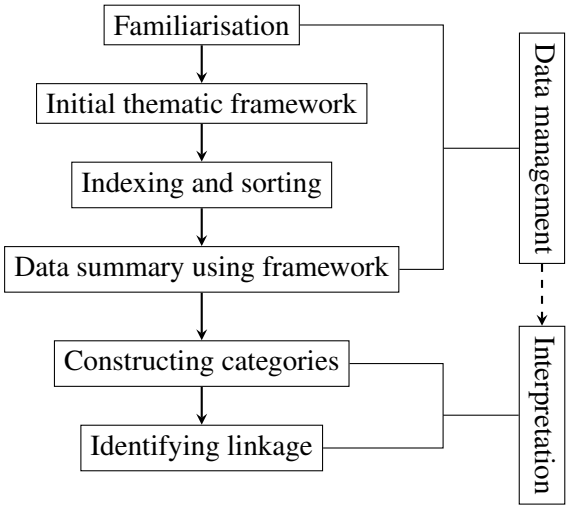

Figure 5.2: The process to analyse the qualitative data

which indicates the relation between phenomena with respect to the subgroups of the sample was identified.

5.3 Results

The data yielded 21 sub-themes, grouped under 4 themes: *Group characteristics and gait assessment*; *Instrumented gait analysis*; *Gait report* and *Gait laboratory*. The thematic framework is shown in Table 5.3, where themes and sub-themes are listed in the first column while main findings for each sub-theme are summarised in the second column along with illustrative quotes in the last column. Under the theme of *Group characteristics and gait assessment*, we summarised the patient group and the clinical gait assessments of patients with cerebral palsy. Then we focused on *Instrumented gait analysis*, particularly 3-dimensional IGA. Under this theme, we considered clinicians' knowledge about IGA, clinical experience of applying IGA to manage cerebral palsy and their opinions on IGA. Then, clincians' feedback about the gait report and gait laboratory is summarised under the *Gait report* and *Gait laboratory* themes.

Table 5.3: Clinicians' experience and views on gait analysis in the management of cerebral palsy

Themes	Main findings	Illustrative quotes
Group characteristics and gait assessment		
Patient group	Diagnosis: cerebral palsy; age: most patients are from 4 to 19 years old; GMFCS levels: most patients are GMFCS 1-3	"I would say predominately children with cerebral palsy. I think they make about 75%-80% " (A0525)
		"Normally from about age four to ... we have nineteen, probably the oldest" (C0427)
		"[GMFCS levels] one to three...we have very very ocassionally four, as you can understand gait analysis, by four really struggling " (R0608)
Contrast of clinical gait assessment	Gait analysis in the gait lab: time-consuming; clinical appointments: brief and short	"The data collection takes long time; it's about one and a half to two hours" (A0525)
		"The clinic I work at the moment, I got 15 minutes for everything"; "you have to do everything quickly, you can miss things" (C0331)
Features to examine during a clinical gait assessment	Clinicians examine abnormalities during walking and some other activities; assess gait with and without orthosis; assess movement balance	"Watching them do walking with and without orthosis" (P0518)
		"Do they have reasonable sitting balance? When they start crawling, are they symmetrical in movment or are they dragging in one leg?" (V0413)
		"we would do a couple of walks, up and down...we do balance assessment...we often do video analysis on the splints" (R0608)
Common tools used for clinical gait assessments	Vision, video, IGA	"Usually we get the information by either using vision or using a camera" (M0608)
		"We do clinical examination... video in two orientations...then there are markers on them, sometimes we don't have kinetic data but we pretty much always get kinematic data" (R0608)

Continued on next page

Table 5.3 – *Continued from previous page*

Themes	Main findings	Illustrative quotes
Main outcomes of clinical gait assessments	Recommendations of footwear, planning treatments for the next year, prescription of an orthosis	"I would advice what kind of footware" (C0427)
		"We have developed to report about their walking and so they have that every year"; "we make a plan for the next year" (M0518)
Instrumented gait analysis		
Ways to gain knowledge about IGA	University, training courses, books, peer review, developed with time and experience	"Obviously we studied at university to begin" (M0608)
		"I have done various gait analysis courses in the past" (P0518)
		"From colleagues, physiotherapist helped me" (R0329)
		"You need to sit down, I think, and do some background reading" (C0608)
Referrals to IGA	Frequent access: most referrals are from orthopaedic surgeons; restricted access for physiotherapists and orthotists	"I say more than 50% from orthopaedic surgeons" (A0525)
		"I referred three recently" (C0427)
		"It's a bit shame that as a practitioner in the community we don't have any access to that at all, I mean we don't have means to refer" (V0413)
Purposes of referrals	Surgical decision, complicated patients, pre- and post operation analysis	"Generally people are seeking...some of these orthopaedic surgeons are considering an intervention. Rare...is about baseline measurement"(A0525)
		"It tends to be ones that are very complicated" (M0608)
		"So after we get the opinion from the gait lab, we do the operation. It is essential and vital that the patient go back, a year, 6 months, 2 years, to be analysed to see if that is actually better or worse" (R0329)

Continued on next page

Table 5.3 – *Continued from previous page*

Themes	Main findings	Illustrative quotes
Impact of IGA	Benefits patients who have intervention; clinicians tend to make better surgical decisions and be more confident	"Data sources analysis are accurate and reliable on when you got clinicians looking at these together, they make a better decision" (A0525)
		"Highlight your reason behind doing something that also instills a lot of confidence" (C0608)
Factors that may influence the reliability of IGA	Technique factor: poor marker set; patient factor: patients' walking patterns for gait analysis may be different from their usual gait	"There are some measures with poor marker set. We may estimate about where their joint centres are" (R0608)
		"You ask a child to do gait analysis, for instance, they will do their very best walk that doesn't represent what they do day to day, 'catwalk' walk" (P0518)
Comparisons with the visual and video gait analysis	Visual gait analysis is practical, easy, subjective, quick, not quantitative; IGA is accurate, reliable, comprehensive, informative, objective, expensive and time-consuming	"I do a video...slow it down and have a look at all the stages of the gait as best as we can but it is not going to be as good obviously as a proper gait analysis lab" (D0330)
		"You've actually got kinematics and it's brilliant...you are not lacking in any information, you've got everything you can possible conceive, it is slow, it's exceptionally expensive and the data isn't always available immediately, you know, the analysis can take a fair amount of time" (M0608)
Barriers of IGA	Money, time, knowledge, space, communication between clinicians, guidance of referral, increasing number of patients and equity of selecting patients to gait analysis	"I would definitely say money is an issue and I think where money is an issue and you can't refer lots of children, the problem is deciding who you refer, so inequity...how you make that fair and that's a big problem" (M0518)
		"We try to communicate with the tertiary centre the best we can...sometimes they don't communicate back to us" (V0413)

Continued on next page

Table 5.3 – *Continued from previous page*

Themes	Main findings	Illustrative quotes
Gait report		
Information of gait reports	Report for IGA: patients' history, findings of gait analysis, recommendations, graphs and data; report for visual gait analysis: descriptive information, observed gait patterns and weakness	"We will start words with history...and we write our opinion which is backup with some evidence...and final might be supported by recommendations"; "I think a typical gait report have at least 18 graphs, often double that or triple that" (R0608)
		"We put all those assessment appointments together in one report, so it's a lot of information, we try to summarise it, the report is just a summary"; "it was hightlighted areas of weakness" (M0518)
Knowledge to understand an instrumented gait report	Couldn't understand and never use in practice; understand but never use in practice, understand but not use a lot; really familiar	"Never seen before, don't know where to start" (C0427)
		"I have never seen one in practice"; " Once I have the graphs, I am pretty sure that I can do the job of interpreting" (C0331)
		"Some of us have experience of looking at gait reports. I imagine there are a lot of places where they would find it quite difficult because they haven't been shown as part of training. They haven't experienced in looking at gait reports" (M0518)
Impact of instrumented gait reports	Clinicians tend to follow a gait report; impact clinicians' decision about whether to have surgery or not; not always being followed by clinicians	"When everything is written down...it gives you a good idea and I think they can lead you to the right conclusion" (C0608)
		"Generally if I get a report from them, I will kind of follow." (D0330)
		"Sometimes we would recommend something and the recommendations weren't being followed, but that's up to the clinicians' preference." (R0608)
Patients'/parents' feedback	Parents tend to follow the recommendations	"Obviously parents get that as well and parents want to follow because this comes from a big hospital" (D0330)

Table 5.3 – *Continued from previous page*

Themes	Main findings	Illustrative quotes
Comments on gait report	Much information, complex, comprehensive, time-consuming to generate and read; not routine in clinical replacement; not always matched up with practicality; some clinicians prefer descriptive information	"Sometimes the clinical decision...you can see the clinical decision, all the theory behind that, but the practicality in term of that child is not always married up all the time" (D0330)
		"I prefer things that are more descriptive" (C0427)
		"They are intimidating because if you don't come from a mathematical background or you haven't really looked at graphs since potential 6 years and there are a lot of them" (R0608)
Gait laboratory		
Local gait labs	Know gait labs in this area; don't know gait lab	"In London itself, there are 3 clinical gait labs that will serve cerebral palsy population" (A0525)
		"In St. Thomas? ... St. Mary? " (V0413)
Access to gait labs	Have access; know gait labs in this area but don't have access	"I started at a very well established gait lab"; "learn about the surgical procedures that were available in centain presentations in the laboratory" (C0608)
		"Not the clinic I work ... not very accessible" (C0331)
Advantages of gait labs	Great facility, good views of gait; learn skills; centralise information	"You can pick up skills there that's transferable and you know you can see it"; "I think that would be a valuable tool for prosthetics, orthotics and physio rehab"; "I think having a gait lab...you know it's a great facility to have (C0608)
		"I think being able to do that just gives you really good kind of lab show, anterior, posterior views as well" (D0330)
		"You don't need a highly specialised gait lab in every hospital. If having one or two, you can actually centralise the data in one place" (R0329)

Continued on next page

Table 5.3 – *Continued from previous page*

Themes	Main findings	Illustrative quotes
Disadvantages of gait labs	Children are only seen for a short time at a gait lab; patients wait long time for appointments; patients' requests may be neglected	"I'm thinking that sometimes people can read too deeply into that data and they don't consider the patient's needs and requests" (A0525)
		"It is hard...you only see them once a year or six months" (D0330)
		"I've got two children waiting for appointments for about one and half years" (V0413)

5.3.1 Clinical gait assessment of cerebral palsy

For a patient with cerebral palsy, the clinical gait assessment is usually undertaken in a clinic, community or gait laboratory. Common procedures usually start with the history taking and physical examination, followed by visual gait analysis and, possibly, IGA. Clinicians may select some or all of these procedures, according to the purpose of an assessment, the output that they need, the time and staffing levels. However, due to the lack of a standard protocol, clinicians sometimes evaluate patients in their own ways. More details of clinical gait assessment are displayed in Figure 5.3, where the gait assessment for a clinical appointment usually contains the history taking, physical examinations and basic visual gait assessment. At this stage, clinicians initially identify the gait pattern of a patient and based on these findings a specific treatment may be prescribed. More details and subtle features of gait patterns are usually examined in the community, where physiotherapists probably have more time and space to observe gait visually and using a video record. In addition, video may be slowed down and current gait may be compared with previous records. Some communities produce gait assessment reports for patients, which are used to make annual plans of treatment. Copies of a report may be sent to the patient/parents and other clinicians that are involved in the treatment of the patient. Physiotherapists' opinions are appreciated by other clinicians

since it is likely that they have the most contact with patients over a period of months or years.

> *...which we couldn't able to know without the physio. Apparently, they really know the kids well. (C0331, orthotist)*

> *We run groups that children can go to as well as physios, it is an extra twenty-six appointments a year if they go to; we do a sport club once every fortnight plus they have hydrotherapy plus they can go to the gym plus they have one-to-one [appointments]; so we can see children fifty...sixty appointments in a year. (M0518, physiotherapist)*

When a patient needs a more accurate gait assessment, he/she would be referred to a gait laboratory, where usually procedures are carried out by clinical scientists or those who have an equivalent role in IGA IPT. After the examination, most gait laboratories generate a gait analysis report to send to the clinician who referred the patient. A typical gait analysis report is composed of the history of the patient, IPT opinions based on evidence gathered from the assessment, and recommendations. Graphs are used as evidence in the IGA and data are sometimes provided in the appendix of the report. Once the leading clinician receives the report, the treatment plan may be altered and therapeutic decisions adjusted accordingly.

An aspect which initially complicated the data analysis was the realisation that some professionals may carry out multiple roles, and that the interaction of role and profession differs according to the care delivery structure and skill-mix at any given facility. For example, some laboratories have physiotherapists with high levels of technical ability who carry out detailed gait analysis while that role may be fulfilled by a clinical scientist in another laboratory. This was a major learning point for me in performing this study, and an illustration of exactly why the qualitative study was needed, for instance, for the researcher to understand the context in which innovations will be applied, who by and where in the process their work will be utilised.

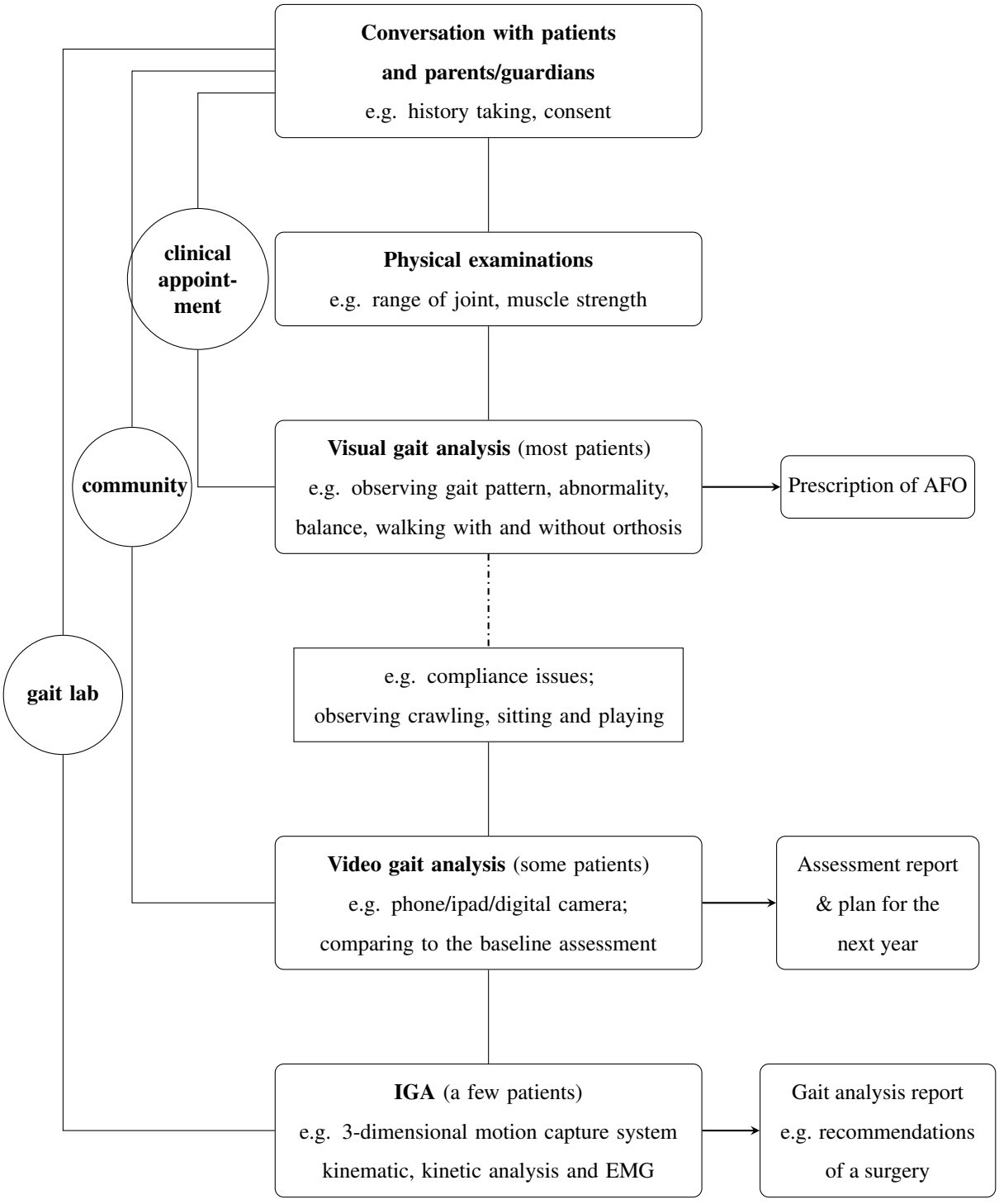

Figure 5.3: Processes of clinical gait assessment in the management of cerebral palsy

5.3.2 Instrumented gait analysis

Although most clinicians learn about IGA through either modules at university or short training courses, IGA is not a routine part of management of cerebral palsy for some clinicians. IGA is commonly considered for a complicated patient or a difficult therapeutic decision and some clinicians use IGA as a tool to assess whether the treatment is likely to improve a patient's condition. Moreover, the decision of patient referral to IGA is mainly made by orthopaedic surgeons, although sometimes senior orthotists or physiotherapists also refer patients to a gait laboratory or may initiate the referral process, whereas junior clinicians are seldom involved in IGA. However, the situation of referrals can vary, depending on the local health care resource and the experience of relevant clinical teams. In some clinical settings, even senior physiotherapists have little experience with IGA.

It is commonly agreed by interviewed clinicians that IGA is useful, particularly for a patient with cerebral palsy undergoing orthopaedic surgery. Based on the evidence from IGA, clinicians tend to be more confident and make better clinical decisions. Although IGA is more reliable, accurate and informative, some clinicians still prefer visual gait analysis, which is quicker and easier to conduct and less challenging to interpret albeit far more subjective. Most interviewees pointed out that visual gait analysis was "good enough", considering the high cost of IGA. In addition, clinical observation is currently supplemented by digital camera and computer-based video systems, which allow clinicians to slow videos down and identify more subtle abnormalities of gait patterns.

However, visual gait analysis is subjective and the quality of assessment largely depends on the experience and knowledge of clinicians. Because of complexity of cerebral palsy, heterogeneity of this population and variety of manifestations, the surgical decision-making can be very difficult in patients with cerebral palsy.

Cerebral palsy is a very heterogeneous group so what works for one kid will not

necessarily work for another. (R0608, clinical scientist)

Hence, when the treatment of cerebral palsy is prescribed without objective gait analysis, sub-optimal decisions of intervention are thought to be quite common (Whittle, 2007).

While most clinicians stated that the quality of IGA is better than visual gait analysis and video gait analysis, some other clinicians raised doubts about the reliability of the technique. One clinical scientist mentioned that the poor marker setting occasionally occurred during data collection, which affected the quality of 3-dimensional gait data. Another concern about IGA that was commonly mentioned by interviewees is whether the gait pattern of a patient in the gait laboratory can represent the patient's real walking pattern. The way a patient walks in a clinical room is sometimes referred to as a "catwalk" by clinicians. In order to eliminate or reduce the "catwalk" effect, clinicians use games to distract patients' attention and make the environment of the clinical room more friendly. However, interviewees have different opinions on whether "catwalk" affects IGA or not, as will be discussed later.

Apart from these concerns, most interviewed clinicians considered the high cost as the biggest barrier which prevented them from referring patients to IGA. It is difficult for a gait laboratory to reduce cost since gait analysis is consuming with respect to time, human resource and equipment. One gait laboratory may only have two appointments, each of which needs the engagement of several technicians and clinical scientists. Furthermore, the numbers of patients with cerebral palsy are increasing, while there are only *"3 [gait labs] in London and 14 labs in total in the UK" (A0525, clinical scientist)*. Thus, it is not surprising that there are patients *"waiting for appointments for about one and half years" (V0413, physiotherapist)*. Although there is a lack of resource for gait analysis, some equipment is idle in communities or hospitals, such as force plates. Besides money and knowledge, the criterion of referrals is another barrier of IGA. Inequity in selecting patients for IGA results from a lack of clear referral criteria.

5.3.3 Gait report

As can be seen in Figure 5.3, the report from a gait laboratory is the outcome of IGA. In addition, some communities also produce reports for clinical gait assessment based on visual gait analysis. Both reports contain information about the patient, such as history and findings of gait assessments. However, the report of clinical gait assessment from a community is usually more descriptive, while the report of IGA is technical and systematic, including gait graphs and data generated by computers.

Generally, it requires moderate knowledge and some experience with IGA to understand gait reports generated from a gait laboratory. Thus, the report of IGA can be difficult for many junior clinicians, who may have had fewer opportunities to attend training courses or to access gait analysis outputs. During the interview, participants were shown a sample gait report. Clinical scientists and orthopaedic surgeons were more familiar with the report than orthotists and physiotherapists. In particular, some clinicians had seen a report of IGA in training courses but never used one in practice. Some clinicians mentioned that they would follow recommendations if they received a gait report, while others pointed out that recommendations in the report did not always agree with the clinical decision, which should be made by combining all information together, rather than simply following a gait analysis report. Moreover, some interviewed clinicians argued that it was difficult to extract information from gait graphs and they preferred a more descriptive report. Meanwhile, the IGA IPT has realised the extent of this issue and are exploring better ways to communicate IGA findings. However, there is no simple solution to this problem so far. Furthermore, generating a report of IGA is time-consuming. It may take six weeks or even longer for clinicians to receive the report, which sometimes results in clinical decisions being made without the gait report.

5.3.4 Gait laboratory

We first consider accessibility under the *Gait laboratory* theme. It is obvious that clinical scientists have access to gait laboratories. Since orthopaedic surgeons usually refer patients to gait laboratories, they have more access than many other clinicians. For some senior orthotists or physiotherapists, they may not have direct access to a gait laboratory but can refer patients through other clinicians who have a closer collaboration with gait laboratories. However, some other orthotists or physiotherapists, particularly those in more isolated communities, would rarely have contact with a gait laboratory. Clinicians who have a better perception about the gait laboratory tend to have a more positive view of IGA. For instance, some interviewees thought a frequent attendance of a gait laboratory would help clinicians to maintain knowledge.

From a clinical perspective, the gait laboratory also has some disadvantages. For example, it was mentioned that clinical scientists usually saw a patient once every six months or year in the gait laboratory. In order to better identify the gait pattern of a patient, it was argued that physiotherapists involved in usual care, who were usually more familiar with the patient, should be involved more in gait analysis. Some interviewed clinicians thought the communication between clinical scientists and physiotherapists was insufficient. Furthermore, some clinicians were concerned that too much concentration on the quantitative analysis might result in relative neglect of patients' needs and requests. It was also mentioned that IGA had sometimes been considered as a marketing tool to attract patients.

We summarise the linkage between the need and knowledge of IGA and the access to gait laboratories with respect to the classification of clinicians in Figure 5.4, where the distinction made between clinicians by profession is based on the most common role that these professions undertake, while recognising that there is much variety. The need for IGA is judged based on clinical roles that participants described during the interviews, although we concluded that the data saturation may not have been reached by detecting 7 out of 12 empty

	User/potential user of IGA		No clinical use of IGA	
	Sufficient knowledge	**Insufficient knowledge**	**Sufficient knowledge**	**Insufficient knowledge**
Frequent access to gait lab	**Clinical scientists** - degree in science - working in gait labs - producing the reports - IPT meeting	**Orthopaedic surgeons & senior orthotists** - training courses, books & peer review - frequently refer patients - frequently read a report - IPT meeting		
Occasional access to gait lab		**Senior orthotists & senior physios** - training courses - occasionally refer patients - may never see a report in practice		
No access to gait lab		**Junior orthotists & senior physios** - never have access to a gait lab / see a report - design orthoses - make plan for a patient		**Junior physios** - never have access to a gait lab / see a report

Figure 5.4: A linkage from the qualitative analysis between the need and knowledge of IGA and the access to gait laboratories for clinicians. In this case, the roles are represented by professions although it is clear that roles vary independent of profession.

panels in Figure 5.4. Clinicians are considered as potential users if the clinical assessment and treatment may be improved by IGA. To assess whether a clinician has sufficient knowledge about IGA or not, we consider training and understanding of the sample gait analysis report. Therefore, we conclude that clinical scientists have sufficient knowledge about IGA, since they usually have the scientific background to understand biomechanics. As mentioned before, orthopaedic surgeons frequently refer patients to a gait laboratory and they have high

needs for IGA to make surgical decisions. Sometimes orthopaedic surgeons need clinical scientists' or specialist physiotherapists' help to fully understand IGA or a gait report. Whether an orthotist or physiotherapist has access to a gait laboratory largely depends on the community and his/her position in the community. According to the information we have gathered, IGA is useful for orthotists to design an orthosis and for senior physiotherapists to make better plans for a patient. Thus more training or more routine use of IGA should be considered for them. Finally, it may not be necessary for junior physiotherapists to engage in IGA, since their clinical role requires basic gait assessment and they may need more clinical experience before they can benefit from using IGA.

5.4 Extension of results

In this thesis, I explored how the proposed statistical method could be utilised to improve the analyses of 3-dimensional gait data and the goal of a further step is to explore whether the gait analysis with the novel statistical analysis can potentially benefit patients with cerebral palsy. This may be achieved through clinicians who have direct contact with patients or engage in the IPT meeting for the management of cerebral palsy. In an IPT, which may consist of paediatricians, neurologists, orthopaedic surgeons, physiotherapists, occupational therapists, etc., the gait assessment is usually conducted by physiotherapists, orthotists, specialist orthopaedic surgeons and clinical scientists. I consulted an academic clinician within the research team, who helped to identify clinical roles that may be improved by IGA as follows: (1) assessment, (2) monitoring, (3) surgical decision-making, (4) liaison, (5) recommendation, (6) orthotic prescription and (7) therapy prescription. Roles of clinicians with different job titles are summarised in Table 5.4. Among all these roles, gait analysis with the proposed statistical method is possibly applied to improve recommendation, orthotic prescription and therapy prescription. For instance, functional F test may be applied to assess the effect of an orthosis or a therapy on intra individual gait curves. Therefore, physiotherapists, orthotists, orthopaedic surgeons and clinical scientists may benefit from the proposed statistical

Table 5.4: Roles of interviewed clinicians with respect to reasons for gait analysis

Job title	Reasons for gait analysis within clinical roles
Physiotherapists	assessment, monitoring, liaison, recommendation, therapy prescription, orthotic prescription
Orthotists	assessment, recommendation, orthotic prescription
Specialist orthopaedic surgeons	assessment, monitoring, surgical decision-making, liaison, recommendation, therapy prescription
Clinical scientists	assessment, liaison, recommendation

analysis, albeit the person responsible for writing analysis code may be the primary direct beneficiary. It may be that equipment manufacturers, who often provide proprietary gait analysis software, would also benefit from novel statistical approaches.

5.5 Discussion

We have collected and analysed qualitative data from 12 clinicians who had experience of gait assessment in patients with cerebral palsy. According to results of the qualitative data analysis, we concluded that clinicians with different roles had different levels of knowledge and experience on IGA, which had influences on the clinical applications of IGA.

Some findings agree with the conclusions of previous studies. Our results support that IGA has been underutilised to some extent (Simon, 2004) and the main usage of IGA is still to identify key problems for orthopaedic surgery (Franki et al., 2014). Although the need for orthopaedic surgery probably motivated the development of IGA in the early stages, it now prevents wider applications of IGA to some extent. Some clinicians consider IGA more for multi-level surgeries and neglect other potential uses.

Furthermore, according to both the literature and our study, the cost of IGA is an important barrier. It is impossible for communities and hospitals to refer more patients to a gait laboratory when the budget is limited. Therefore, it may be more efficient for clinicians to

better utilise existing facilities. For instance, 2-dimensional gait data, collected by simpler equipment, may provide sufficient information for some patients. However, basic knowledge of the data collection and analysis is required, which is also a big barrier. The knowledge of gait analysis can be obtained from training courses and is also developed with clinical experience. We found that senior clinicians are more knowledgeable about gait analysis than junior clinicians, which contradicts the statement in Franki et al. (2014), which mentioned that younger therapists might be more familiar with 3-dimensional IGA than older therapists due to engagement in courses about gait analysis in recent postgraduate paediatric rehabilitation programs without evidence of the statement or further exploration.

Apart from these conclusions, two controversial issues were articulated during the interviews. One of the issues is whether gait analysis should be considered as a second opinion. Clinical scientists, or those who have an equivalent role in IGA IPT, apparently have different views from clinicians outside the immediate IGA IPT, who usually consider gait analysis to be a second opinion. Clinical scientists argued that other clinicians should trust interpretations more in the gait report. Another issue is the "catwalk" effect. Some clinicians considered this a serious limitation of gait analysis, while some other clinicians argued that gait analysis was to examine patients' ability and hence it was not a big problem if patients walked well in a gait laboratory. These two questions could be explored more in future study.

There are some limitations to this study. We cover a wide range of clinicians, including physiotherapists, orthotists, orthopaedic surgeons and clinical scientists in this study. Thus, the sample size of each group is not yet large enough to reach data saturation. For example, we only interviewed one orthopaedic surgeon and two clinical scientists. Some other clinicians in an IPT, such as paediatricians, may also be involved in the clinical gait assessment or IGA. However, we excluded paediatricians, since they may not consider the gait assessment as frequently as clinicians in the sample framework. During the initial analysis of this data, a focus was put on professions with the underlying assumption that this reflected role. However, there is more diversity in the roles-profession interaction than that assumption suggests.

Sampling was by profession, gender and experience level so analysis initially followed suit. It is important to recognise that the characteristic professional role will not be consistent between different IPT who deliver IGA.

The qualitative study will be continued and interviews will be conducted with more orthopaedic surgeons and clinical scientists. Based on the analysis results summarised in this chapter, the topic guide will be amended. Although it is usually difficult for statistical analysis to benefit patients directly, this study has explored the potential and it is possible for statistical analysis to improve patient outcome if communication with clinicians, in particular, clinical scientists and specialist orthopaedic surgeons, is enhanced.

There are indications that clinical scientists or those in an equivalent IGA IPT role, are the key, but not only, audiences to reach with novel statistical techniques such as those developed in this thesis. Amendment of testing protocols from applications of design of experiments principles in conjunction with FDA may also be worthwhile exploring further to enhance the decision-making return from limited data sets and maximisation of gait laboratory efficiency. When considered alongside the potential changes in interpretation indicated in Chapter 4 and my published paper (Zhang et al., 2017), there is every possibility that statistical innovations will impact patient care if carefully disseminated.

Chapter 6

Discussion

6.1 Main findings

In this thesis, functional ANOVA has been developed to analyse data from complex designs where the responses are curves and the proposed methods have been applied to time-dense data depicting segmental rotations during gait.

6.1.1 Methodology development

The methodological research in the thesis generalises the classical univariate analysis of experiments which use an orthogonal design to functional data. In a classical orthogonal design, the block structure with random-effect block factors contributes to the covariance between responses, and thus affects the hypothesis test which is used to compare "mean responses" determined by the treatment structure. Similarly, in a complex design with functional responses, the primary goal is to test treatment effects which are now however functions and functional responses are correlated due to the block structure. To analyse such data, techniques for orthogonal designs, hypothesis tests for functional data and correlated functional data are combined. Figure 6.1 summarises the methodology development based on these techniques, among which orthogonal designs developed by Bailey (2008), the func-

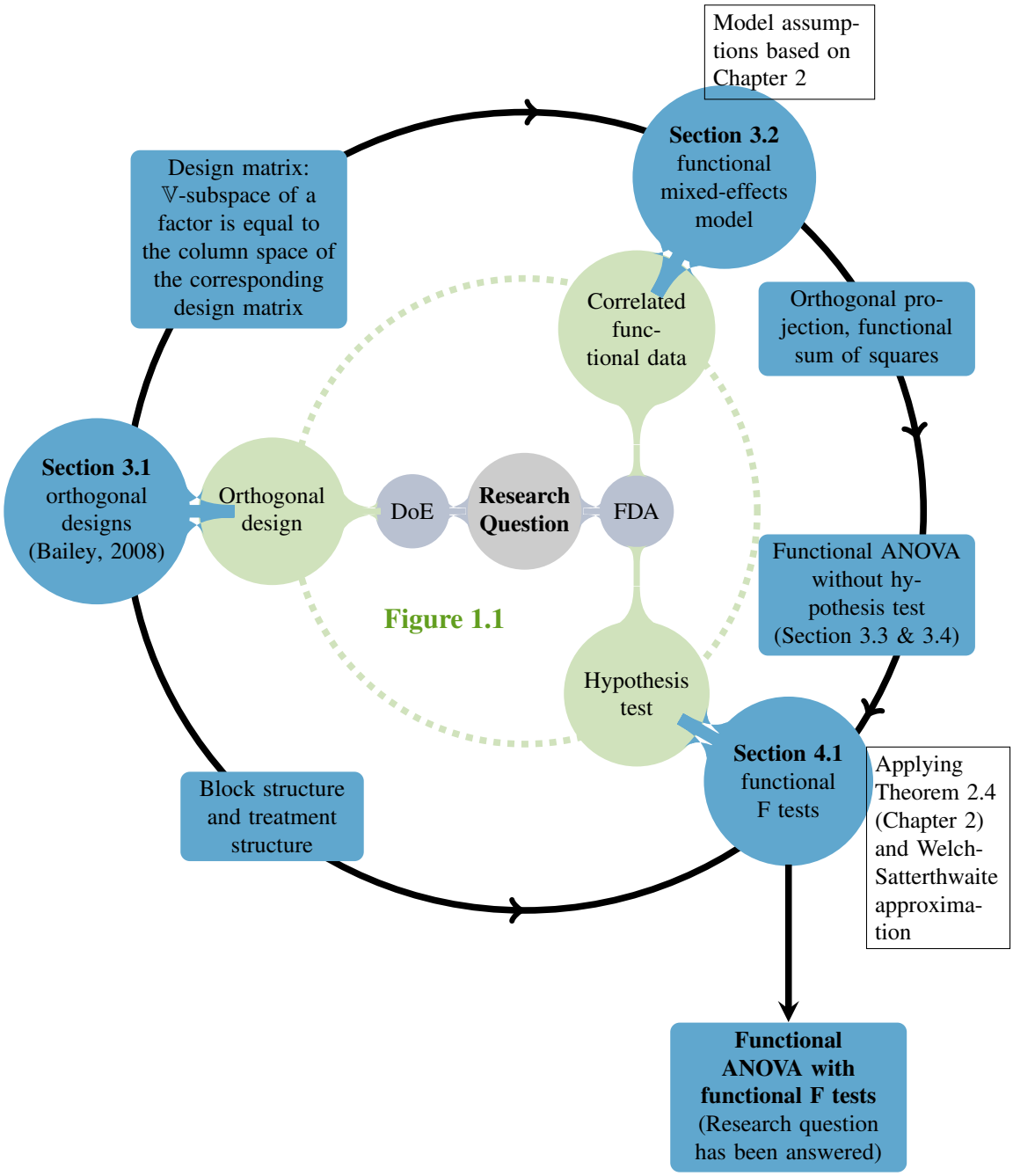

Figure 6.1: Summary of methodology development (blue). DoE = design of experiment, FDA = functional data analysis, Research Question: how to analyse data from complex experiments when responses are curves. In Section 3.1: orthogonal designs, Section 3.2: functional mixed-effects model and Section 4.1: functional F tests, white boxes show inputs, and blue boxes show outputs of the relevant sections. As indicated by arrows, outputs of previous sections are inputs to the following sections.

tional mixed-effects model used to study correlated functional data, and functional F tests serve as the main building blocks.

The methodology development starts with orthogonal designs in Section 3.1, where methods in Bailey (2008) are applied to study the block and treatment structures. Then in Section 3.2, with design matrices determined by the experimental structure, functional responses are considered in a functional mixed-effects model which is similar to the model proposed by Morris and Carroll (2006). As illustrated in Figure 6.1, assumptions of the functional mixed-effects model are based on Chapter 2. More specifically, in addition to modelling functional responses by using jointly measurable mean-square continuous stochastic processes that are also random elements in $\mathbb{L}^2(T, \mathscr{B}(T), \mu)$ space, all random-effect terms and error terms are independent Gaussian processes. Under these assumptions, the functional sum of squares for a factor can be represented as a sum of squared independent Gaussian processes $\{R_1(t) : t \in T\}$, $\{R_2(t) : t \in T\}$, ..., $\{R_d(t) : t \in T\}$ with d being the degrees of freedom for the factor, as introduced in Section 3.3 and 3.4. Sums of squares are derived by using orthogonal projections. In Chapter 3, the ANOVA table summarises the analyses of block and treatment structures, sums of squares and expected mean squares. In particular, the expected mean square for a factor is derived from the mean and covariance function, which is called the stratum-based covariance function, of independent Gaussian processes $\{R_1(t) : t \in T\}$, $\{R_2(t) : t \in T\}$, ..., $\{R_d(t) : t \in T\}$, as used to represent the functional sum of squares.

Functional F tests for treatment comparisons which were previously proposed for completely randomised designs (Shen and Faraway, 2004; Zhang, 2013) are developed for general orthogonal designs in Section 4.1. The general idea is similar to F tests for a classical orthogonal designs, where a treatment factor is tested in the relevant stratum by using an F ratio of treatment and residual sums of squares divided by degrees of freedom (Bailey, 2008). Since functional sums of squares are random functions themselves, the F statistic of a functional F test is calculated as a ratio of integrals of functional sums of squares (*integrated sums*

of squares) divided by appropriate degrees of freedom. By applying Theorem 2.4 in Chapter 2, it was shown that an integrated sum of squares is a random variable whose distribution is the same as that of a linear combination of independent χ^2 random variables. The distribution of such a linear combination of independent χ^2 random variables can be approximated by using the Welch-Satterthwaite approximation. Consequently, under the null hypothesis of no treatment effect the F statistic of the functional F test is approximately F distributed with degrees of freedom that are calculated from the stratum-based covariance function.

The methods in Chapter 3 and the functional F test in Section 4.1 can be used to analyse complex experimental designs with functional responses in situations where previously proposed tests (Cuevas et al., 2004; Cuesta-Albertos and Febrero-Bande, 2010; Zhang, 2013) cannot be used.

6.1.2 Applications

The proposed functional ANOVA was applied to gait data from patients with cerebral palsy and healthy subjects in Sections 4.2 and 4.3 respectively, as summarised in Figure 6.2. Moreover, results of a qualitative study to investigate the clinical application of gait analysis were reported in Chapter 5.

In Section 4.2, the effects of AFO on 3-dimensional kinematics of patients with cerebral palsy were examined. Gait curves which represent joint rotations during walking barefoot and with AFO were compared by functional F tests, in addition to pointwise F tests and univariate F tests which used maximal and minimal angles as responses. Functional F tests were also used to examine gait data in the stance phase and swing phase, respectively. Although results from functional F tests, pointwise F tests and univariate F tests are not identical, these approaches complement each other to provide a better statistical interpretation of gait analysis.

In Section 4.3, the split-plot design that was introduced in Example 3.2 was used to

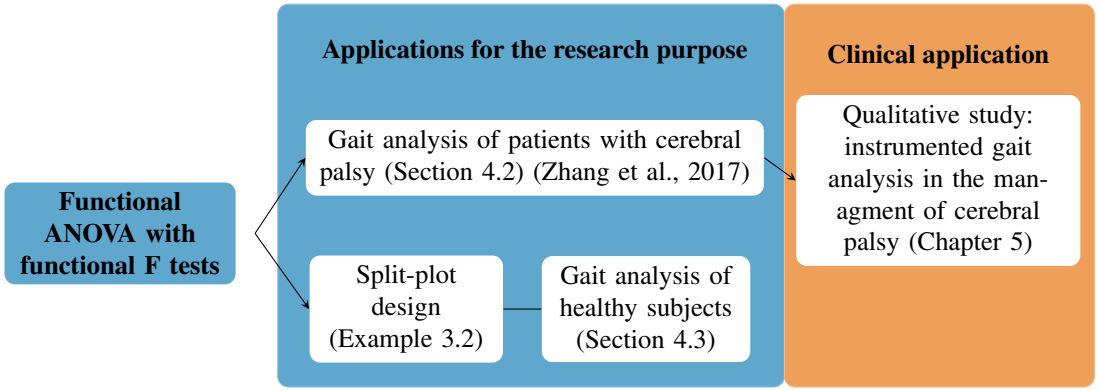

Figure 6.2: Applications of functional ANOVA to gait analysis

collect gait data from healthy subjects. Three different orthosis conditions and three different speeds were considered as two treatment factors, which were tested in different strata by functional F tests. Significant effects of speed were detected on the rotations of hip, knee and ankle joints and foot, whilst the ankle rotations were only weakly affected by the application of AFO. Furthermore, an orthogonal contrast analysis with the ankle rotations as responses was considered to split the treatment factor AFO into two parts: wearing or not wearing AFO and wearing unilateral or bilateral AFO. Although walks were not significantly different between wearing unilateral AFO around one leg and wearing bilateral AFO around both legs, a significant difference between barefoot walking and walks with AFO was found by the functional F test.

In Chapter 5, the clinical application of gait analysis was explored by using qualitative data that were collected from semi-structured interviews conducted with clinical scientists, a specialist orthopaedic surgeon, physiotherapists and orthotists. Instrumented gait analysis has not played a prominent role in clinical routine due to barriers, such as the high cost of gait analysis and the limited budget for patients being referred to instrumented gait analysis. Although some clinicians have insufficient knowledge of gait analysis, which is likely due to limited access to gait laboratories, benefits of instrumented gait analysis to patients are recognised by clinicians. Furthermore, instrumented gait analysis is currently conducted in gait laboratories by clinical scientists, who usually have a strong scientific background and a

good understanding of statistics. Advanced statistical techniques, such as functional ANOVA proposed in the current study, are likely to be implemented via clinical scientists to improve gait analysis.

6.2 Conclusions

In this thesis, the ANOVA has been generalised to functional data and the functional F test for completely randomised designs has been generalised to general orthogonal designs. These approaches have been applied to gait data and these applications were further explored in a qualitative study with scientists and clinicians.

The complexity of correlated functional data generated from a complex experiment arises from the correlation existing both between and within functional responses. While the correlation between functions is determined by the experimental structure, individual functions are explored using FDA (Hsing and Eubank, 2015), where each function is viewed as a sample path of a stochastic process and under specific conditions (detailed in Chapter 2) also realisation of a random element. The two types of correlation were considered separately in this thesis. First, the correlation between responses was handled as in a classical orthogonal design with univariate responses, where the vector space of observations can be decomposed into a direct sum of orthogonal subspaces and sums of squares were derived by using the orthogonal projections of responses onto relevant subspaces. Likewise, in designs with functional responses, sums of squares were also calculated by using orthogonal projections, but they are functions. According to the singular value decomposition of the orthogonal projection matrix, each functional sum of squares was expressed as a sum of squared independent stochastic processes. Furthermore, to analyse these stochastic processes individually, a useful tool is the Karhunen-Loève expansion which represents a stochastic process by a series of uncorrelated random variables and orthonormal eigenfunctions of the relevant covariance operator.

The distributions of functional sums of squares are complicated, but under assumptions expressed in the functional mixed-effects model integrating a functional sum of squares gives a random variable, whose approximate distribution can be derived. Accordingly, the integrated sums of squares were used in the development of functional F tests.

The functional ANOVA with the associated functional F tests was applied to gait analysis. I mainly considered two aspects of such data, that are, the structure of experiments where gait data were collected and to compare entire gait curves collected under different conditions. Hasse diagrams and skeleton ANOVA tables were useful to illustrate the experimental structures regardless of whether the gait comparison was considered for selected characteristics of gait curves, such as maximal rotations, or the entire gait curves. Functional F tests were applied to compare gait curves. Although it is difficult to conclude whether the functional F test is preferable to the traditional univariate F test since conclusions may vary depending on the specific research interest, the functional F tests have provided additional results to the univariate statistical tests in this study. Furthermore, functional ANOVA can be applied flexibly in gait analysis. According to specific research questions, functional F tests can be applied to either the whole gait cycle or specific gait phases.

The qualitative study in Chapter 5 indicates that better application of gait analysis in the management of cerebral palsy can be achieved by strengthening communication between gait laboratories and physiotherapists and orthotists. Moreover, it is possible for the advanced statistical methods proposed in this study, which have been shown to be useful for gait comparison, to be applied to clinical gait assessment and possibly to improve patient outcome, with particular relevance to groups of patients.

6.3 Future work

Both the theoretical and practical results presented in this thesis can be extended for the future study.

Throughout this study, the methodology has been developed for orthogonal designs where all block factors are uniform. However, as mentioned in Section 4.3, to analyse gait data from both legs during walking barefoot and with bilateral AFO and gait data from the single leg during walking with unilateral AFO, block factors of the experiment are non-uniform. Thus, the experimental structure does not fulfil conditions of orthogonal design summarised in Chapter 3 and the present method is not applicable. In the classical univariate analysis of experiments, a mixed model can be used to analyse experiments which are non-orthogonal or lack of uniformity (Brien and Bailey, 2006). Piepho et al. (2003) provided the guidance of applying mixed models to analyse randomised experiments, which can be extended to experiments where functional data are collected. Therefore, it is possible to develop a functional mixed-effect model approach to analyse more general experiments with functional responses. However, the present method for the covariance function estimation can not be used in the functional mixed-effects model for non-orthogonal designs and the Bayesian approach proposed by Morris and Carroll (2006) may be applied for the parameter estimation.

The applications of functional ANOVA to gait analysis can be extended from two aspects. First, although functional ANOVA was only applied to gait analysis of a group of patients in Chapter 4, this method may also be used to analyse gait patterns of individual patients. One possibility, as mentioned in Chapter 5, is for the reliability analysis. To assess the intrasubject reliability of gait analysis, statistical tools of intra-class correlation coefficient (ICC) and coefficient of multiple correlation (CMC) are commonly used (Kadaba et al., 1989; Steinwender et al., 2000; Maynard et al., 2003; McGinley et al., 2009). However, the within-curve correlation has yet taken into account for the reliability analysis. It is possible to use the proposed functional ANOVA to improve the reliability analysis of gait curves. Second, the present functional ANOVA and functional F test were applied to 1-dimensional gait data and gait data in the coronal, sagittal and horizontal planes were analysed separately in Section 4.2. Therefore, I have considered to extend functional ANOVA and functional F

test to multi-dimensional data in the future work. This may be achieved either by applying the Karhunen-Loève expansion for multiple stochastic processes (Balakrishnan, 1960; Kelly and Root, 1960) or by combining the proposed methods with statistical parametric mapping (Pataky et al., 2013).

Appendix A

Zhang et al. (2017)

The published paper *Testing Gait with Ankle-Foot Orthoses in Children with Cerebral Palsy by Using Functional Mixed-Effects Analysis of Variance*

SCIENTIFIC REPORTS

OPEN

Received: 26 January 2017
Accepted: 17 August 2017
Published online: 11 September 2017

Testing Gait with Ankle-Foot Orthoses in Children with Cerebral Palsy by Using Functional Mixed-Effects Analysis of Variance

Bairu Zhang[1], Richard Twycross-Lewis[2], Heiko Großmann[3] & Dylan Morrissey[2,4]

Existing statistical methods extract insufficient information from 3-dimensional gait data, rendering clinical interpretation of impaired movement patterns sub-optimal. We propose an alternative approach based on functional data analysis that may be worthy of exploration. We apply this to gait data analysis using repeated-measurements data from children with cerebral palsy who had been prescribed fixed ankle-foot orthoses as an example. We analyze entire gait curves by means of a new functional F test with comparison to multiple pointwise F tests and also to the traditional method - univariate repeated-measurements analysis of variance of joint angle minima and maxima. The new test maintains the nominal significance level and can be adapted to test hypotheses for specific phases of the gait cycle. The main findings indicate that ankle-foot orthoses exert significant effects on coronal and sagittal plane ankle rotation; and both sagittal and horizontal plane foot rotation. The functional F test provided further information for the stance and swing phases. Differences between the results of the different statistical approaches are discussed, concluding that the novel method has potential utility and is worthy of validation through larger scale patient and clinician engagement to determine whether it is preferable to the traditional approach.

Functional data analysis[1–4] (FDA) is an umbrella term for statistical methods that are applicable when the measured responses are not numbers but functions of time, space or some other domain. When the domain is time, responses are typically represented by curves. Data of this kind arise commonly, for instance, in laboratory settings where measurements can be taken almost continuously at densely spaced time points. Human gait research is an important clinical and experimental setting where functional data are collected to guide intervention decisions. In this field, the curves of interest often depict the rotation of a joint during a stride, across a standardized time interval between one foot contact to the next by the same foot.

Early work on FDA for human gait data developed methods for estimating mean and covariance functions[5] and for calculating prediction regions for entire curves[6], and applied these to samples of curves that were collected on healthy children. Other researchers[1,7–9] used the data[5,6] to illustrate various types of FDA techniques, including functional principal components analysis, functional canonical correlation analysis and functional regression. Data from an experiment[10] where volunteers were stepping in place have served as an example to demonstrate the use of functional analysis of variance[10–12] (ANOVA) for investigating the effects of different orthosis conditions on moments at the knee. Despite these examples and the fact that the FDA approach appears to be particularly useful for studying gait curves[13], only a few gait studies[14–16] have used FDA to investigate questions of genuine clinical interest. Moreover, only relatively basic FDA methods[1] seem to have been used in clinical applications. Possible reasons for this are that more advanced FDA techniques are less widely known and theoretically and computationally more complex.

This paper proposes a new method of functional mixed-effects ANOVA for studying gait data of children with cerebral palsy, who have abnormal gait patterns leading to fixed ankle-foot orthoses prescription. We analyze gait curves that were collected from a repeated-measurements design in which barefoot walking preceded walks

[1]School of Mathematical Sciences, Queen Mary University of London, London, E1 4NS, UK. [2]Sports and Exercise Medicine, Queen Mary University of London, London, E1 4DG, UK. [3]Fakultät für Mathematik, Otto-von-Guericke-Universität Madgeburg, 39106, Madgeburg, Germany. [4]Physiotherapy Department, Barts Health NHS Trust, London, E1, UK. Correspondence and requests for materials should be addressed to D.M. (email: d.morrissey@qmul.ac.uk)

with ankle-foot orthoses. The use of ankle-foot orthoses to control movements of patients with cerebral palsy has a long history[17] and the main purpose of an ankle-foot orthosis is to enhance function by improving motion of lower limb body segments during the gait cycle[18]. Ambulatory function, such as walking ability, balance and stability, is qualitatively assessed by physiotherapists. Quantitative gait analysis occurs in specialist centres when critical decisions, such as orthosis prescription or operative intervention consideration, are being made and require interpretation of complex data sets. In this study we investigate the effects of ankle-foot orthoses on quantitatively measured lower limb 3-dimensional joint rotation during gait, also known as the study of kinematics[19].

The effects of ankle-foot orthoses on kinematic gait data of patients with cerebral palsy have previously been examined in several studies[20–26]. However, in these studies gait curves were not treated as analyzable entities and kinematic parameters reflecting particular characteristics of the curves were used as the response variable in a univariate analysis. Examples of such response parameters include joint rotation values at specific gait events such as heel strike or toe-off[23–25], maximal or minimal rotation during the gait cycle or midpoints of identifiable gait phases such as stance[21,23–25], and mean and range of rotation for the whole or parts of the gait cycle[26]. Integrating findings that are based on different kinds of parameters is not always straightforward. Moreover, considering the effects of ankle-foot orthoses throughout the gait cycle has been recommended to ensure important findings are not neglected[27] and the FDA approach would meet this criterion.

In what follows, we present a novel application of FDA to entire gait curves from children with cerebral palsy which allows us to test the effect of ankle-foot orthoses while accounting for the repeated-measurements nature of the data. Repeated measurements are modeled by a special case of a functional mixed-effects model[28], although we avoid the complex computations that are involved when the model is fitted in a Bayesian manner[28–31]. We propose a new functional F test which integrates information over the whole gait cycle and compare the results of its application with those of multiple pointwise F tests that are performed at equally spaced time points in the gait cycle. In addition, the functional F test is also compared with the traditional univariate F test in a one-way repeated-measurements ANOVA[32], which is commonly used in gait studies[22–24].

The main purpose of this study is to explore suitable FDA techniques that can be applied to complex data by developing a better tool for testing functional data collected from repeated-measurements experiments, in which multiple curves are collected from each subject. In the specific case considered here, the functional F test is applied to examine the global effects of ankle-foot orthoses at a group level to guide clinicians. This application will also facilitate utilization of functional F tests in other domains with similar data.

Tests for functional mixed-effects models have only been considered in a few reports[33,34]. The new test generalizes previous work on functional F tests[3,35] for independent curves, to repeated measurements in which the curves are correlated. The proposed functional F test preserves the nominal significance level, whereas the multiple testing approach based on pointwise tests is subject to a potentially large familywise error probability. Moreover, the functional test can be easily modified to test the effect of the orthoses for different well-defined phases of the gait cycle[36,37], thereby enabling the researcher to tailor the analysis to specific research questions. We report corresponding results for the stance and swing phases respectively.

Method

Data collection. The present study was performed in accordance with the ethical guidelines of the Declaration of Helsinki and was approved by East London NHS Research Ethics Committee (Ethics REF 09/H0806/56). Written informed assent and consent, from all children and parents respectively, was collected.

Time-dense gait data were collected from fourteen children (mean age $12.3 \pm 2.88 years$, mean height $1.44 \pm 0.15\, m$, mean weight $39.57 \pm 11.78\, kg$) at the Human Performance Laboratory, Queen Mary University of London. All recruited children had been diagnosed with spastic cerebral palsy and prescribed fixed ankle-foot orthoses (see Fig. 1) for a minimum of six months. Children were initially assessed by a paediatric orthopaedic consultant and only included if they were independently ambulatory and considered to have sufficient muscular endurance for gait measurements. This study was designed after the clinical assessment had taken place, and hence we were not approved to access the medical records of patients nor was the direct clinical interpretation our primary focus. Nonetheless, we consulted the physiotherapist who accompanied patients for data collection and she confirmed that most recruited children were classified to the Gross Motor Function Classification System (GMFCS)[38] level 2 and 3 and few children were classified at level 4.

Data collection followed the commonly used protocol[20,25,39] whereby each patient was instructed to perform a series of walks both barefoot and wearing ankle-foot orthoses placed within shoes. Order was not randomised and barefoot walking was conducted first[20,25]. While walking with ankle-foot orthoses, patients were shod, owing to the importance of footwear in the orthotic prescription that ankle-foot orthoses modify kinematics of segments only with appropriate footwear[27]. More specifically, anthropometric information, including pelvic width and depth and bilateral knee and ankle width, was obtained. Then kinetic data were collected while the patient walked barefoot at a self selected pace along a 6-meter walkway with two ground embedded force plates (Type 9281B Multicomponent Force Plate, Kistler Instruments Ltd, Winterthur, Switzerland) that measured 3-dimensional ground reaction force. After 10–20 walks, patients then repeated walking tests whilst wearing their ankle-foot orthoses over the same force plates.

Kinematic data were collected using four 3D Cartesian Optoelectric Dynamics Anthropometer systems (Charnwood Dynamics, Rotheley, Leicestershire, UK) that were placed at distances of 2–3 meters from the force plates, oblique to the centre of the laboratory in order to create a data collection volume. A modified Helen Hayes marker set protocol[19] was used, whereby active infra-red markers were placed bilaterally on the anterior sacro-iliac spine (ASIS); posterior sacro-iliac spine (PSIS); lateral epicondyle of the knee and the lateral malleolus; lateral aspect of the calcaneous and the 5th metatarsal. Instrumented marker wand sets were also placed superior and inferior to the knees. Joint centers for the pelvis, hips, knees and ankles were calculated using Codamotion Analysis software (version 6.76.2-CX1/mpx30, Charnwood Dynamics, Rotheley, Leicestershire, UK) based on

Figure 1. Bespoke, fixed ankle-foot orthoses for children with cerebral palsy.

subject specific anthropometric data. Gait events in each trial, from initial contact to toe off to the following initial contact, were marked using the vertical component of ground reaction force and velocity of the calcaneous marker for both the ipsilateral and contralateral limbs. Standardized gait graphs were then extracted by analyzing the kinematic data offline using Matlab (version 2009a, The Mathworks, Natick, MA, USA).

Statistical model. For testing the effect of ankle-foot orthoses, we consider the functional mixed-effects ANOVA model

$$y_{ijk}(t) = \mu(t) + \alpha_i(t) + \beta_{j(i)}(t) + \gamma_k(t) + \varepsilon_{ijk}(t), \quad t \in \mathcal{T} = [0, 1], \tag{1}$$

where $\mu(t)$ is the overall mean function; $\alpha_i(t)$ for $i = 1, \ldots, 14$ is the i th subject-specific random effect; $\beta_{j(i)}(t)$ for $j = 1, 2$ is the random effect for the j th lower limb nested within the i th subject; $\gamma_k(t)$ for $k = 1, 2$ is the fixed effect for wearing (or respectively not wearing) ankle-foot orthoses and $\varepsilon_{ijk}(t)$ is the error term. The total number of response curves $y_{ijk}(t)$ is $n = 56$. The random effect terms $\alpha_i(t)$, $\beta_{j(i)}(t)$ and the error term $\varepsilon_{ijk}(t)$ are assumed to be independent zero-mean Gaussian processes, each with its own covariance function. More specifically, by using the generic notation $GP(0, \theta)$ for a zero-mean Gaussian process with covariance function $\theta \equiv \theta(s, t)$, it is assumed that $\alpha_i(t) \sim GP(0, \theta_a)$, $\beta_{j(i)}(t) \sim GP(0, \theta_b)$ and $\varepsilon_{ijk}(t) \sim GP(0, \theta_e)$ for $i = 1, \ldots, 14, j = 1, 2$ and $k = 1, 2$, all independent.

Since for all curves $y_{ijk}(t)$, $\mu(t)$, $\alpha_i(t)$, $\beta_{j(i)}(t)$, $\gamma_k(t)$ and $\varepsilon_{ijk}(t)$ we use the same time points of the gait cycle, at every fixed time point $t \in \mathcal{T}$ equation (1) can be regarded as the model equation of a univariate repeated-measurements ANOVA model. Hence, at every fixed t, pointwise sums of squares $SS(t)$ and expected mean squares $EMS(t)$ for the different terms in the model can be calculated as for the univariate model. However,

	Degrees of freedom	$SS(t)$	$EMS(t)$
mean	1	$\sum_{i=1}^{14}\sum_{j=1}^{2}\sum_{k=1}^{2}\bar{y}_{...}(t)^2$	
subjects	13	$\sum_{i=1}^{14}\sum_{j=1}^{2}\sum_{k=1}^{2}\{\bar{y}_{i..}(t)-\bar{y}_{...}(t)\}^2$	
limbs	14	$\sum_{i=1}^{14}\sum_{j=1}^{2}\sum_{k=1}^{2}\{\bar{y}_{ij.}(t)-\bar{y}_{i..}(t)\}^2$	
AFO	1	$\sum_{i=1}^{14}\sum_{j=1}^{2}\sum_{k=1}^{2}\{\bar{y}_{..k}(t)-\bar{y}_{...}(t)\}^2$	$14\times 2\times\sum_{k=1}^{2}\gamma_k(t)^2+\theta_\epsilon(t,t)$
residual	27	by subtraction	$\theta_\epsilon(t,t)$
Total	56	$\sum_{i=1}^{14}\sum_{j=1}^{2}\sum_{k=1}^{2}y_{ijk}(t)^2$	

Table 1. Pointwise ANOVA table with "AFO" indicating the factor for wearing/not wearing ankle-foot orthoses.

when t traverses the whole gait cycle, both $SS(t)$ and $EMS(t)$ become functions of t, which we refer to as the functional sum of squares and the functional expected mean squares respectively.

The pointwise ANOVA table for fixed $t \in \mathcal{T}$ is presented in Table 1 in which the various means are given by

$$\bar{y}_{...}(t)=\frac{1}{n}\sum_{i,j,k}y_{ijk}(t),\quad \bar{y}_{i..}(t)=\frac{1}{2\times 2}\sum_{j,k}y_{ijk}(t),\quad \bar{y}_{ij.}(t)=\frac{1}{2}\sum_{k}y_{ijk}(t)\quad\text{and}\quad \bar{y}_{..k}(t)=\frac{1}{14\times 2}\sum_{i,j}y_{ijk}(t). \tag{2}$$

The breakdown of the total sum of squares in the table into sums of squares for the different sources of variation is valid at every point t and, hence, also for the functional sums of squares. Equation (1) together with the usual constraint $\gamma_1(t)+\gamma_2(t)=0$ for all $t\in\mathcal{T}$ implies that for every t the expected mean squares for the sums of squares $SS_{AFO}(t)=\sum_{i,j,k}\{\bar{y}_{..k}(t)-\bar{y}_{...}(t)\}^2$ and $SS_{residual}(t)=\sum_{i,j,k}\{y_{ijk}(t)-\bar{y}_{ij.}(t)-\bar{y}_{..k}(t)+\bar{y}_{...}(t)\}^2$ come out as shown in Table 1.

The ANOVA in Table 1 provides the basis for testing if ankle-foot orthoses have an effect. Both types of test, the pointwise F tests and the functional F test, use the sums of squares in the table. However, whereas the pointwise F tests also use the degrees of freedom in the table in order to assess the significance of the results, this is not the case for the functional F test.

Pointwise F tests. The effect of ankle-foot orthoses may be tested by adopting a multiple testing approach. This amounts to performing a series of separate F tests of

$$H_0\colon \gamma_1(t_\ell)=\gamma_2(t_\ell)\quad\text{versus}\quad H_1\colon \gamma_1(t_\ell)\neq\gamma_2(t_\ell) \tag{3}$$

at each of m equally spaced points $t_\ell\in\mathcal{T}$, $\ell=1,\ldots,m$, in the gait cycle. We refer to these tests as pointwise F tests. The test statistic of the pointwise F test at t_ℓ and its distribution under the null hypothesis H_0 are given by

$$F(t_\ell)=\frac{SS_{AFO}(t_\ell)/1}{SS_{residual}(t_\ell)/27}\sim F(1,27). \tag{4}$$

The resulting values $F(t_\ell)$ are plotted against t_ℓ for $\ell=1,\ldots,m$ and can be assessed for statistical significance at every time point.

Pointwise F tests do not take the functional nature of the data into account. Moreover, this approach faces the usual problems surrounding multiple testing[40]. In particular, the familywise error probability can be much higher than the nominal significance level of the individual tests as will be illustrated later.

Functional F test. As an alternative to multiple testing with pointwise F tests we propose a new functional F test. The functional F test summarizes information across the whole gait cycle by integrating the functional sums of squares $SS_{AFO}(t)$ and $SS_{residual}(t)$ over $\mathcal{T}$ and uses the ratio of the integrals as the test statistic. Contrary to the pointwise F tests, the hypotheses tested by the functional F test refer to the whole curves $\gamma_k(t)$, $k=1,2$, in Equation (1). More specifically, the testing problem is given by

$$H_0\colon \gamma_1(t)=\gamma_2(t)\text{ for all }t\in\mathcal{T}\quad\text{versus}\quad H_1\colon \gamma_1(t)\neq\gamma_2(t)\text{ for some }t\in\mathcal{T}. \tag{5}$$

The null hypothesis H_0 states that the two functions $\gamma_1(t)$ and $\gamma_2(t)$ are equal, whereas the alternative hypothesis H_1 says that they are different. In order to test H_0 against H_1, the functional F test uses the single statistic

$$\mathcal{F}=\frac{\int_{\mathcal{T}}SS_{AFO}(t)dt/1}{\int_{\mathcal{T}}SS_{residual}(t)dt/27}. \tag{6}$$

Under the null hypothesis H_0 of no effect, by using arguments similar to the case of independent curves[3,35], the distributions of the integrated sums of squares in (6) can be shown to be mixtures of independent chi square distributions[34]. More precisely, under H_0 it holds that

$$\begin{aligned}\int_{\mathcal{T}} SS_{AFO}(t)dt &= \int_{\mathcal{T}} \sum_{i,j,k} \{\bar{\varepsilon}_{..k}(t) - \bar{\varepsilon}_{...}(t)\}^2 dt \sim \sum_{r=1}^{\infty} \lambda_r \chi_1^2,\\ \int_{\mathcal{T}} SS_{residual}(t)dt &= \int_{\mathcal{T}} \sum_{i,j,k} \{\varepsilon_{ijk}(t) - \bar{\varepsilon}_{ij.}(t) - \bar{\varepsilon}_{..k}(t) + \bar{\varepsilon}_{...}(t)\}^2 dt \sim \sum_{r=1}^{\infty} \lambda_r \chi_{27}^2.\end{aligned} \tag{7}$$

In (7), the means $\bar{\varepsilon}_{...}(t)$, $\bar{\varepsilon}_{ij.}(t)$ and $\bar{\varepsilon}_{..k}(t)$ of the random errors $\varepsilon_{ijk}(t)$ in equation (1) are computed like the corresponding means of the responses in (2). Moreover, $(\lambda_r)_{r\geq 1}$ is the sequence of eigenvalues of the covariance operator[4] associated with the covariance function $\theta_\varepsilon(s, t)$ and $\sum_{r=1}^{\infty} \lambda_r \chi_1^2$ denotes the distribution of a mixture of independent random variables, each of which has a chi square distribution with 1 degree of freedom, while $\sum_{r=1}^{\infty} \lambda_r \chi_{27}^2$ represents a similar mixture of independent random variables, each having a chi square distribution with 27 degrees of freedom.

The sums of squares $SS_{AFO}(t)$ and $SS_{residual}(t)$ are independent for every $t \in \mathcal{T}$ and it can be shown that this property carries over to the integrals $\int_{\mathcal{T}} SS_{AFO}(t)dt$ and $\int_{\mathcal{T}} SS_{residual}(t)dt$. The same arguments[35] as in the derivation of the functional F test for the functional linear fixed-effects-only model then show that under H_0 the distribution of $\mathcal{F}$ in (6) can be approximated by an F distribution as follows

$$\mathcal{F} \overset{approx.}{\sim} F(df_{AFO}, df_{residual}), \tag{8}$$

with degrees of freedom equal to $df_{AFO} = \frac{(\sum_{r=1}^{\infty} \lambda_r)^2}{\sum_{r=1}^{\infty} \lambda_r^2}$ and $df_{residual} = 27 \times \frac{(\sum_{r=1}^{\infty} \lambda_r)^2}{\sum_{r=1}^{\infty} \lambda_r^2}$, respectively.

The practical application of the functional F test requires the approximation of the integrals in the numerator and denominator of $\mathcal{F}$ and also the approximate computation of the eigenvalues that are needed for calculating the degrees of freedom df_{AFO} and $df_{residual}$. To this end, we adapt the approaches[3,35] that have been used for the case of independent curves and which essentially amount to turning the functional problem into a multivariate problem.

More precisely, the interval $\mathcal{T} = [0, 1]$ representing the gait cycle is discretized by superimposing a fine grid of m equally spaced points t_ℓ, $\ell = 1, \ldots, m$, where $t_1 = 0 < t_2 < \ldots < t_{m-1} < t_m = 1$. The integral $\int_{\mathcal{T}} SS_{AFO}(t)dt$ is then approximated by the sum $\sum_{\ell=1}^{m} SS_{AFO}(t_\ell)$. Likewise, as an approximation to the integral $\int_{\mathcal{T}} SS_{residual}(t)dt$ the sum $\sum_{\ell=1}^{m} SS_{residual}(t_\ell)$ is used. In the calculation of df_{AFO} and $df_{residual}$, the sequence $(\lambda_r)_{r\geq 1}$ of eigenvalues is replaced by m estimated eigenvalues $\hat{\lambda}_1, \ldots, \hat{\lambda}_m$ which are obtained as the eigenvalues of the $m \times m$ matrix $\hat{\Sigma} = (\hat{\theta}_\varepsilon(t_\ell, t_q))$, where for $\ell, q = 1, \ldots, m$

$$\hat{\theta}_\varepsilon(t_\ell, t_q) = \frac{\sum_{i,j,k} \{y_{ijk}(t_\ell) - \bar{y}_{ij.}(t_\ell) - \bar{y}_{..k}(t_\ell) + \bar{y}_{...}(t_\ell)\}\{y_{ijk}(t_q) - \bar{y}_{ij.}(t_q) - \bar{y}_{..k}(t_q) + \bar{y}_{...}(t_q)\}}{27}. \tag{9}$$

is an estimate of $\theta_\varepsilon(t_\ell, t_q)$. Hence, in practice the degrees of freedom of the approximate null distribution of $\mathcal{F}$ are calculated as $df_{AFO} = \frac{(\sum_{\ell=1}^{m} \hat{\lambda}_\ell)^2}{\sum_{\ell=1}^{m} \hat{\lambda}_\ell^2}$ and $df_{residual} = 27 \times \frac{(\sum_{\ell=1}^{m} \hat{\lambda}_\ell)^2}{\sum_{\ell=1}^{m} \hat{\lambda}_\ell^2}$. Simple linear algebra shows, that the sums in the numerator and denominator of df_{AFO} and $df_{residual}$ can be calculated respectively as the sum of the diagonal elements of the matrix $\hat{\Sigma}$ and the sum of the diagonal elements of $\hat{\Sigma}^2 = \hat{\Sigma}\hat{\Sigma}$. In what follows, we use the value $m = 201$ which corresponds to splitting the gait cycle into two hundred intervals of equal width.

An attractive feature of the functional F test is that the integration over $\mathcal{T}$ can be replaced with integration over subsets of $\mathcal{T}$. This opens up the possibility to test the effect of ankle-foot orthoses in specific phases of the gait cycle as will be illustrated below.

Results

Observational results. Figures 2 and 3 show descriptive information for 3-dimensional segmental rotations for the lower body in 14 children with cerebral palsy during both barefoot and shod with ankle-foot orthoses walking respectively. In the figures, gait data are presented as a standardized gait report where columns show the pelvis, hip joint, knee joint, ankle joint and foot and rows are the coronal plane, sagittal plane and horizontal plane of rotation respectively. Differences can be seen in the overall kinematics with the application of the ankle-foot orthoses: there is an overall increase in maximal dorsiflexion from 10° to 15° of the ankle joint in the sagittal plane in gait with ankle-foot orthoses, however the magnitude of joint rotation does not change. Differences in the mean curves shown in Figs 2 and 3 are not immediately apparent.

Pointwise F tests. We first examined effects of ankle-foot orthoses on different segmental rotations by using the multiple pointwise F tests shown in Fig. 4. All individual tests used a significance level of $\alpha = 0.05$. In the figure, ankle-foot orthoses have significant effects when the value of the F statistic exceeds the critical value, which is the same at all time points ($F_{0.05}(1, 27) = 4.21$).

Effects of ankle-foot orthoses are more evident in the sagittal plane than in the coronal and horizontal planes. Generally, ankle-foot orthoses affect ankle joint and foot more than other segments, although there are also effects on the pelvis and the knee and hip joints. More specifically, in certain parts of the gait cycle ankle-foot orthoses have significant effects on pelvis in the coronal and horizontal planes; hip joint in the sagittal plane; knee joint in the sagittal and horizontal planes; ankle joint in the coronal and sagittal planes and foot in all three planes (Fig. 4). Moreover, for different segments significant effects of ankle-foot orthoses occur at different time points along

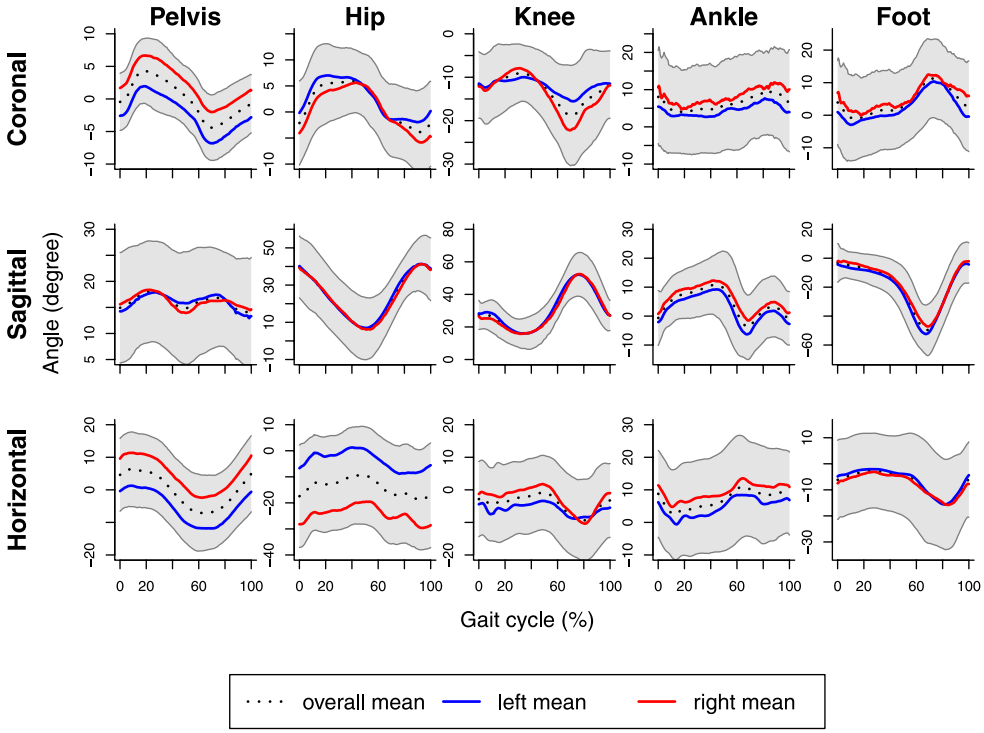

Figure 2. Barefoot walking in 14 children with cerebral palsy. Data are normalized to percentage (%) of the gait cycle, which starts from heel strike. Grey areas represent intervals [mean − s.d., mean + s.d.] at every point.

the gait cycle conferring a temporal effect. Referring to Figs 2 and 3, we can see that for the pelvis in the coronal and horizontal planes, hip joint and ankle joint in the sagittal plane, ankle-foot orthoses have significant effects roughly around the minimal angles, whereas for the knee in the sagittal plane effects of ankle-foot orthoses tend to occur near maximal angles.

The nominal significance level of every individual pointwise F test is $\alpha = 0.05$. However, in every panel of Fig. 4 many of those tests are performed on a grid of $m = 201$ points. Consequently, the familywise error rate[40], which is the probability of at least one incorrect rejection of the null hypothesis, of this multiple testing procedure can be much higher than the nominal significance level if one looks at an interval rather than a single time point. For instance, ankle-foot orthoses affect hip rotation in the sagittal plane between 40–63% of the gait cycle (see Fig. 4). This section of the gait cycle contains approximately 46 grid points. At each of these points the probability of a type 1 error is 0.05. However, an approximate calculation under the simplifying (and surely not correct) assumption that the tests are independent shows that the familywise error rate for the 46 tests in the 40–63% interval of the gait cycle can be as high as $1 - (1 - 0.05)^{46} \approx 0.90$. This example illustrates that results of pointwise tests need to be interpreted with care, since the "significance" of the results may be overstated. Pointwise tests may suggest the presence of effects where there are actually none.

Functional F test and univariate repeated-measurements analysis. The first part of Table 2 presents the functional F test for each of the segments and planes in Fig. 4. The values of the test statistic $\mathcal{F}$ and the corresponding p-values are shown in the second column of the table and the degrees of freedom of the approximate null distribution of $\mathcal{F}$ in the first column. The degrees of freedom are reported in the form $(df_{AFO}, df_{residual})$ and depend on the actual data. At a significance level of $\alpha = 0.05$, the functional F tests detect significant effects of ankle-foot orthoses on knee rotation in the sagittal plane ($\mathcal{F} = 3.07$, $p = 0.02$); ankle rotation in the coronal ($\mathcal{F} = 5.95$, $p = 0.02$) and sagittal ($\mathcal{F} = 8.25, p < 0.01$) planes and foot rotation in the sagittal ($\mathcal{F} = 3.61$, $p = 0.03$) and horizontal planes ($\mathcal{F} = 5.27$, $p = 0.01$). These results indicate that ankle-foot orthoses have significant effects on the overall motion of these segments over the whole gait cycle.

The second part of Table 2 reports results of a univariate repeated-measurements ANOVA with minimal angle as the response variable in the third column of the table, and corresponding results for maximal angle as the response variable in the fourth column. The F values in the table are computed as for the pointwise F test with the

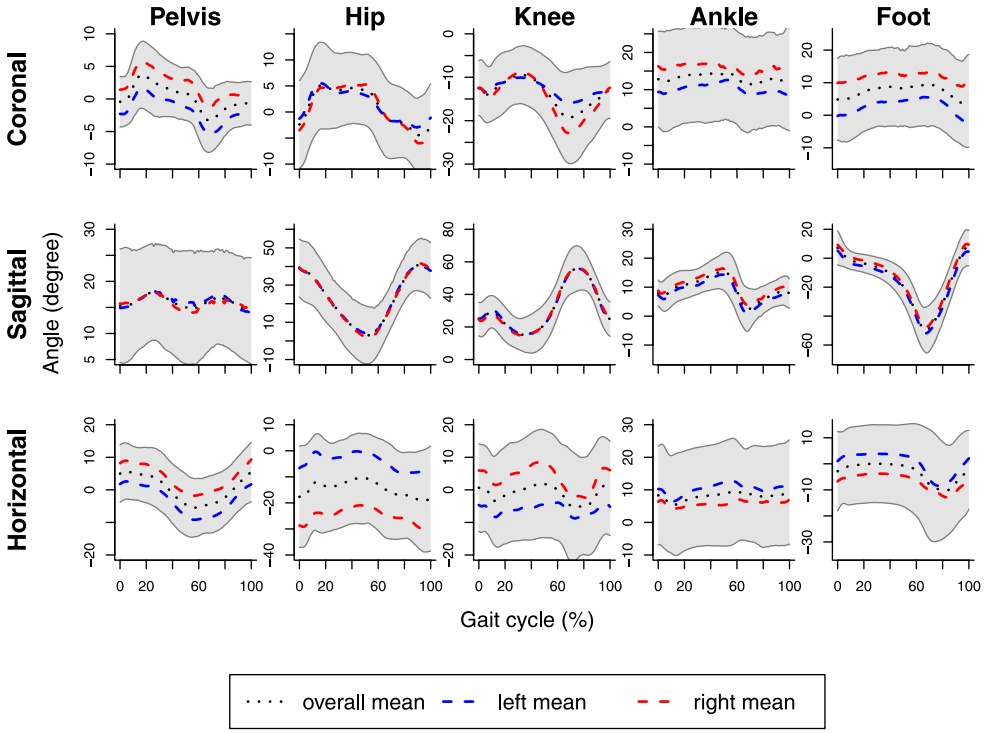

Figure 3. Gait with ankle-foot orthoses in 14 children with cerebral palsy. Data are normalized to percentage (%) of the gait cycle, which starts from heel strike. Grey areas represent intervals [mean − s.d., mean + s.d.] at every point.

only modification that all squared differences that enter the sums of squares in Table 1 are calculated at the time points of the gait cycle at which the minimum (respectively maximum) angles occur. These time points do vary within and between patients. For both response variables, the null distribution of the test statistic is an $F(1, 27)$ distribution and thus the same as for the pointwise F test.

With significance level $\alpha = 0.05$ as before, the F tests from the univariate repeated-measurements ANOVA detect effects of ankle-foot orthoses on minimal ankle angle in the coronal and sagittal planes, which agrees with the results of the functional F test, and, contrary to the functional F test, an effect on minimal hip angle in the sagittal plane. For maximal angle, the F tests from the univariate repeated-measurements ANOVA find significant effects on foot in the sagittal and horizontal planes as well as on ankle in the sagittal plane and these results are again in agreement with those of the functional F tests. Moreover, the repeated-measurements F test detects an effect on maximal knee angle in the horizontal plane where the corresponding functional F test for the whole gait cycle is not significant. Contrary to the functional F test, the repeated-measurements F tests with both minimal and maximal angle as the response do not detect a significant effect of ankle-foot orthoses on the knee joint in the sagittal plane.

Functional F test for gait phases. Besides the whole gait cycle, we are also interested in effects of ankle-foot orthoses during the stance and swing phases separately. In normal gait, the stance phase accounts for the first 60% of the gait cycle and is defined as the period when the foot is in contact with the ground. Conversely, the swing phase accounts for approximately 40% of the gait cycle and is defined as the period when the foot does not have contact with the ground and is propelled forward ready for the next step[41]. This can also be seen in Fig. 4, where the stance and swing phases are divided by grey solid lines.

In order to perform functional F tests for these phases, it is only necessary to replace the interval $\mathcal{T} = [0,1]$ in the formula for $\mathcal{F}$ in (6) with appropriate subintervals. For the stance phase we replace $\mathcal{T}$ with $\mathcal{T}_1 = [0, 0.6]$ and for the swing phase we use $\mathcal{T}_2 = (0.6, 1]$. Previous comments regarding the discretization of the interval $\mathcal{T}$ apply analogously to $\mathcal{T}_1$ and $\mathcal{T}_2$. For simplicity, we continue to denote the resulting test statistics by $\mathcal{F}$.

Results for the stance and gait phases are shown in Table 3. For significance level $\alpha = 0.05$, ankle-foot orthoses have significant effects during the stance phase on hip rotation in the sagittal plane, ankle rotation in the coronal

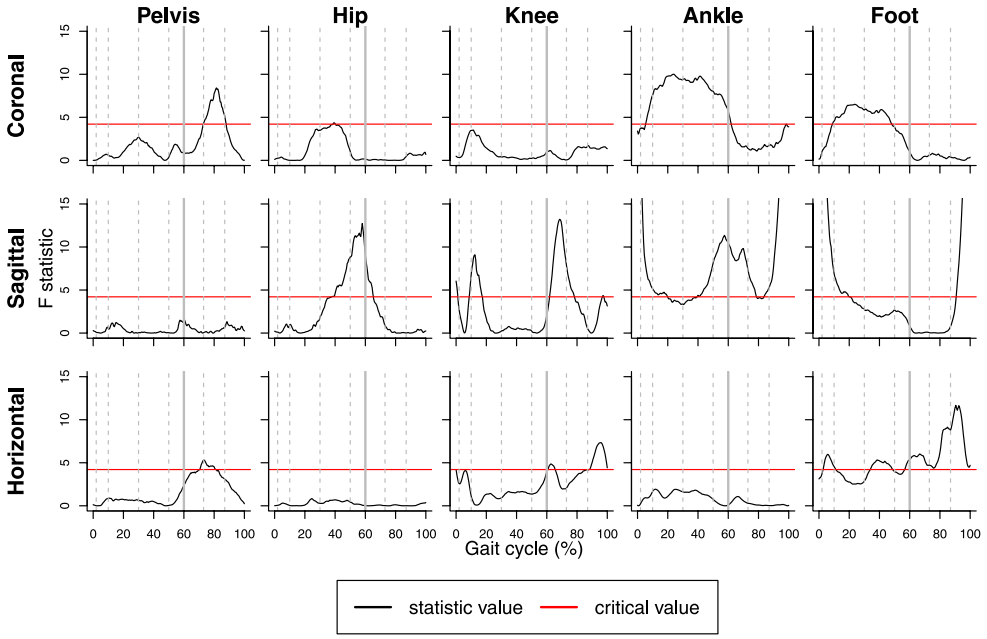

Figure 4. Multiple pointwise F tests at significance level $\alpha = 0.05$ for effects of ankle-foot orthoses on segmental rotations. Grey dashed and solid lines are used to divide the whole gait cycle into phases: initial contact, loading response, mid-stance, terminal stance, pre-swing, initial swing, mid-swing and terminal swing (from left to right).

		Functional F test		Univariate R-M ANOVA (F value (*p.*))	
		degrees of freedom	$\mathcal{F}$ value (*p.*)	minimal angle	maximal angle
Pelvis	coronal	(2.12, 57.30)	1.89(0.16)	0.02(0.88)	0.16(0.69)
	sagittal	(1.41, 38.02)	0.38(0.61)	0.39(0.54)	0.02(0.89)
	horizontal	(1.77, 47.83)	1.61(0.21)	0.58(0.07)	0.51(0.48)
Hip	coronal	(2.77, 74.76)	0.98(0.40)	0.02(0.88)	0.24(0.63)
	sagittal	(2.37, 63.99)	2.53(0.08)	7.21(0.01)*	0.48(0.49)
	horizontal	(1.29, 34.98)	0.18(0.74)	0.08(0.77)	0.09(0.77)
Knee	coronal	(1.66, 44.82)	1.04(0.35)	1.06(0.31)	1.00(0.33)
	sagittal	(3.53, 95.36)	3.07(0.02)*	2.08(0.16)	3.42(0.08)
	horizontal	(1.38, 37.39)	2.60(0.10)	0.26(0.61)	8.02(<0.01)*
Ankle	coronal	(1.12, 30.23)	5.95(0.02)*	6.85(0.01)*	2.71(0.11)
	sagittal	(1.42, 38.44)	8.25(<0.01)*	21.1(<0.01)*	4.15(0.05)*
	horizontal	(1.21, 32.72)	0.87(0.38)	2.45(0.13)	0.95(0.34)
Foot	coronal	(1.15, 30.96)	3.10(0.08)	2.85(0.10)	0.68(0.42)
	sagittal	(2.29, 61.80)	3.61(0.03)*	2.49(0.12)	21.5(<0.01)*
	horizontal	(1.72, 46.39)	5.27(0.01)*	3.05(0.09)	7.09(0.01)*

Table 2. Functional F tests for the whole gait cycle and F tests from univariate repeated-measurements (R-M) ANOVA for minimal and maximal angles. Degrees of freedom for the univariate R-M ANOVA are (1, 27) for all segments and *indicates significance at the 0.05 significance level.

and sagittal planes, as well as on foot rotation in all three planes. In the swing phase, there are significant effects on knee rotation in the sagittal and horizontal planes, ankle rotation in the sagittal plane and foot rotation in the horizontal plane.

Comparison of statistical results. As can be seen from Fig. 4 and Table 2, all three methods of analysis consistently detect statistically significant effects of ankle-foot orthoses on the ankle joint in the coronal and

		Stance phase $\mathcal{F}$ value (p.)	Swing phase $\mathcal{F}$ value (p.)
Pelvis	coronal	1.10(0.33)	3.12(0.07)
	sagittal	0.31(0.65)	0.49(0.54)
	horizontal	0.55(0.54)	3.26(0.07)
Hip	coronal	1.49(0.24)	0.26(0.75)
	sagittal	3.46(0.05)*	1.52(0.23)
	horizontal	0.28(0.65)	0.07(0.86)
Knee	coronal	1.09(0.33)	1.01(0.35)
	sagittal	1.35(0.27)	4.51(0.01)*
	horizontal	1.59(0.22)	4.11(0.04)*
Ankle	coronal	8.19(<0.01)*	2.23(0.14)
	sagittal	7.06(<0.01)*	9.80(<0.01)*
	horizontal	1.19(0.29)	0.29(0.62)
Foot	coronal	4.65(0.04)*	0.35(0.58)
	sagittal	4.61(0.03)*	2.80(0.08)
	horizontal	4.03(0.05)*	6.85(<0.01)*

Table 3. Functional F tests for stance and swing phases of gait cycle with * indicating significance at 0.05 significance level.

sagittal planes and on the foot in the sagittal and horizontal planes. With the repeated-measurements ANOVA the former effects are significant when one looks at minimal angles (for maximal angles significance occurs only in the sagittal plane), while the latter effects are only significant for maximum angles. These results are also corroborated by the functional F tests for the stance and swing phases in Table 3.

In addition to these unequivocal findings, the pointwise F tests detect significant results for certain parts of the gait cycle where the functional F test for the whole gait cycle and the repeated-measurements ANOVA do not show significant effects. In particular, only the pointwise F tests find effects on the pelvis in the coronal and horizontal planes and on the foot in the coronal plane. For the pelvis in the horizontal plane, the significant pointwise F tests at around 80% of the gait cycle may be regarded as a false rejection due to the increased familywise error probability of the multiple testing approach or may be attributed to potential effects on minimal angles during the swing phase, although the corresponding p-values in Tables 2 and 3 are equal to $p = 0.07$ in both cases. Similarly, for the pelvis in the coronal plane, the visual impression from Fig. 4 is supported by the p-value of $p = 0.07$ of the corresponding functional F test for the swing phase (Table 3). A similar statement applies to the foot in the coronal plane and the corresponding functional F test for the stance phase.

By looking at the sagittal plane for the hip and knee joints in Fig. 4 one can see that the pointwise F tests detect significant effects just before and just after the point of transition from the stance to the swing phase. For the hip joint, these effects are also identified by the repeated-measurements ANOVA on minimal angles (Table 2) and the functional F test for the stance phase (Table 3). For the knee, the effect in the sagittal plane is detected by the functional F test for the swing phase and also by the functional F test for the whole gait cycle, although changes of the angles at around 20% may also have contributed to the latter result. For the knee joint in the horizontal plane the pointwise F tests signal some effect toward the end of the gait cycle, and this effect is also detected by the repeated-measurements ANOVA on maximal angles (Table 2) and the functional F test for the swing phase (Table 3). Overall, the results from the different approaches seem to inform each other.

Discussion

We collected time-dense gait data for 28 lower limbs in 14 children with cerebral palsy, typically hemiplegia, in a repeated-measurements design where every individual was measured while walking both barefoot and shod with ankle-foot orthoses. Gait curves depicting rotations for lower limb segments in different planes were modeled by a functional mixed-effects model. The data were analyzed by using three different methods: multiple testing with pointwise F tests performed at separate points of a fine grid, a new functional F test which uses entire gait curves, and univariate repeated-measurements ANOVA, which was performed separately on minimum and maximum rotations. The results obtained by these approaches had many fundamental commonalities, but there were also some differences which warrant further explanation. In what follows, we first interpret the results and discuss some limitations of the approach and the current study. We then discuss some methodological issues and extensions of the proposed functional F test to more complicated experimental designs.

Biomechanical effects of ankle-foot orthoses, including direct effects to the limb segments contained within the orthoses and indirect effects to the rest of the body, mainly shank kinematics[27], are consistent with the results from functional F tests. Moreover, ankle-foot orthoses can be seen to have a greater effect on sagittal joint rotations as compared to coronal and horizontal planes. This is likely due to the design of bespoke ankle-foot orthoses for patients with cerebral palsy (Fig. 1). The rigid L shaped ankle-foot orthoses with an upright portion behind the calf greatly limits plantar flexion and dorsiflexion of the ankle and foot. Moreover, the distal anterior ankle strap and the foot plate have a joint fixing effect which is associated with decreased orthogonal plane rotations. Thus, effects on ankle rotation in the coronal plane and foot rotation in the horizontal plane, which were detected by the functional F tests, are possibly due to some compensatory mechanism.

There are some limitations to this study. One of the issues we debated at length was that of using each leg of each subject as an independent observation. The literature is divided on this issue[42], however we felt this was justified because the between limb correlation was low, subjects typically had hemiplegia and therefore moved asymmetrically and the purpose of the study was to compare different models rather than make definitive clinical or applied scientific recommendations. Moreover, depending on severity of spasticity, children with cerebral palsy are prone to fatigue after short bouts of low to medium intensity activity[43]. In order to minimize patient fatigue and to maximize data output, patients were asked to walk barefoot and without walking aids, if possible, before walking with ankle-foot orthoses. As a consequence, the effect of wearing/not wearing ankle-foot orthoses is confounded with a potential effect of the walking condition testing order. To strengthen the study design, the order of walking conditions should be randomized to eliminate or reduce potential systematic biases[44–47], if possible.

Another limitation of this study is that we only studied a sample of 14 patients. While this is considered small for many statistical applications, it is not uncommon for studies of this type, in this patient population, to have similar sample sizes[48]. This issue has been commonly addressed in gait study reports investigating cerebral palsy[49–51] and is mainly due to the restricted inclusion criteria necessary for enrolment, necessary due to the extremely heterogeneous nature of movement impairments in people with cerebral palsy[51]. Other studies to assess the effects of ankle-foot orthoses in patients with cerebral palsy[22–24, 52–61] have used sample sizes that are similar to that of the current study, and our approach and findings are therefore justifiable and comparable respectively. Furthermore, in the present study we examined retrospective data but have not explored clinical patient information (i.e. gait type, severity of spasticity). Our focus was to quantitatively validate the functional mixed-effects ANOVA as a means of determining differences in gait between barefoot walking versus the use of ankle-foot orthoses in a relatively homogeneous but clinically relevant patient group. Therefore, at this stage we have excluded detailed clinical discussion.

We now give possible reasons why there are sometimes discrepancies between the statistical results. Differences between the functional F tests and the repeated-measurements ANOVA for minimal and, respectively, maximal angles may arise from the fact that the former tests consider the whole gait cycle, whereas the repeated-measurements ANOVA provides a univariate analysis in which the values of the response variable correspond to the most extreme observations that occur throughout the gait cycle. These extremes, e.g. minimal angles, occur at points of the gait cycle that vary within and between patients. For example, for the hip joint in the sagittal plane we examined the data and found that for most patients and most walks minimal angles occurred well before the end of the stance phase, but there were also two patients for whom minimal angles occurred during the swing phase.

Regarding differences in the results between the pointwise F tests and the repeated-measurements ANOVA, we note that with respect to comparing the conditions of wearing and not wearing ankle-foot orthoses every single pointwise F test as well as the repeated-measurements F test is mathematically equivalent to a standard paired t test[62] on 28 pairs of observations, where every pair consists of observations for a single leg that is observed with and without orthoses. If, for example, the minimal angle always occurred at the same time point, then the F test of the repeated-measurements ANOVA on minimal angles would coincide with the pointwise F test at this particular point in time. However, since minimal angles occur at different time points, results from both tests will be different. Put differently, although all pointwise F tests and the repeated-measurements F test use the same formula for calculating the test statistic, the tests apply this formula to different data with a difference in results of findings.

Differences in the results of pointwise F tests and functional F tests may be caused by the fact that the familywise error probability[63] for the whole or parts of the gait cycle of the multiple testing approach exceeds the nominal significance level of the individual pointwise tests. One way to alleviate this problem would be to apply a Bonferroni correction to the nominal significance level of the pointwise F tests. If this were to be done for the whole gait cycle, each of those tests would need to use a significance level that was equal to, for instance, 0.05 divided by the number of tests. In the current study, we used 201 separate pointwise tests and hence, in Fig. 4, the critical value represented by the line would need to be adjusted from $F_{0.05}(1, 27) = 4.21$ to $F_{0.05/201}(1, 27) = 17.78$[64] with the consequence that only the effects in the sagittal plane on the ankle joint and foot would remain significant. Thus the Bonferroni correction would be overly conservative which is one reason why it is not recommended in the FDA literature[65]. Notwithstanding, some adjustment of the nominal significance level that is used for the pointwise F tests would seem to be appropriate in order to avoid too many type I errors. Although not designed for this purpose, the functional F tests appear to achieve this goal by integrating information over the whole or parts of the gait cycle while maintaining the pre-specified significance level.

We believe that the different types of analysis considered in this paper should be regarded as being complementary rather than competing. Although we would not recommend pointwise testing alone, we nevertheless find this approach useful since from results like those in Fig. 4 one can see very easily where in the gait cycle effects occur. However, we think of pointwise tests as more of an exploratory rather than a confirmatory tool, so when reporting an effect as being significant we would prefer to base this decision on a functional F test. With respect to detecting effects in specific parts of the gait cycle very little seems to be lost by this approach, since, as shown in Table 3, the functional F test can be flexibly applied to different phases of the gait cycle. Analyzing specific gait features, like the minimum and maximum angles in the current study, may also be useful but we believe this type of analysis should be motivated by biomechanical considerations or specific clinical questions and not be used for the reason that it sidesteps the difficult analysis of entire curves.

The functional mixed-effects ANOVA model in this paper and the method for obtaining functional F tests can be generalized to more complex experimental designs in which, like in the present study, there is correlation between entire curves. More precisely, the methodology can be applied to experiments with an orthogonal block structure[66–68] and to general orthogonal designs[47]. These designs include, for example, randomized complete

block designs, row-column and split-plot designs. Current treatments[3] of testing problems for functional ANOVA models appear to only consider experiments whose layout is given by a completely randomized design.

Further validation, including structured clinician and patient engagement, is warranted to clarify whether our interpretation of the individually or collectively applied statistical analyses in this paper adds value in practice. Ultimately, the litmus test of whether this novel statistical analysis is truly useful would be improved patient outcomes, a subject for future work.

Data Availability. The datasets generated and analysed during the current study are available from the corresponding author on reasonable request.

References

1. Ramsay, J. O. & Silverman, B. W. *Functional Data Analysis* (Springer, New York, 2005), 2 edn.
2. Horváth, L. & Kokoszka, P. *Inference for Functional Data with Applications* (Springer, New York, 2012).
3. Zhang, J.-T. *Analysis of Variance for Functional Data* (CRC Press, New York, 2013).
4. Hsing, T. & Eubank, R. *Theoretical Foundations of Functional Data Analysis, with an Introduction to Linear Operators* (Wiley, Chichester, 2015).
5. Rice, J. A. & Silverman, B. W. Estimating the mean and covariance structure nonparametrically when the data are curves. *J R Stat Soc Series B Stat Methodol* **53**, 233–243 (1991).
6. Olshen, R. A., Biden, E. N., Wyatt, M. P. & Sutherland, D. H. Gait analysis and the bootstrap. *Ann Stat* **17**, 1419–1440 (1989).
7. Leurgans, S. E., Moyeed, R. A. & Silverman, B. W. Canonical correlation analysis when the data are curves. *J R Stat Soc Series B Stat Methodol* **55**, 725–740 (1993).
8. Rice, J. A. & Wu, C. O. Nonparametric mixed effects models for unequally sampled noisy curves. *Biometrics* **57**, 253–259 (2001).
9. Rice, J. A. Functional and longitudinal data analysis: perspectives on smoothing. *Stat Sin* **14**, 631–647 (2004).
10. Abramovich, F. & Angelini, C. Testing in mixed-effects FANOVA models. *J Stat Plan Inference* **136**, 4326–4348 (2006).
11. Antoniadis, A. & Sapatinas, T. Estimation and inference in functional mixed-effects models. *Comput Stat Data Anal* **51**, 4793–4813 (2007).
12. Cuesta-Albertos, J. A. & Febrero-Bande, M. A simple multiway ANOVA for functional data. *Test* **19**, 537–557 (2010).
13. Duhamel, A. *et al*. Functional data analysis for gait curves study in Parkinson's disease. *Stud Health Technol Inform* **124**, 569–574 (2006).
14. Donoghue, O. A., Harrison, A. J., Coffey, N. & Hayes, K. Functional data analysis of running kinematics in chronic Achilles tendon injury. *Med Sci Sports Exerc* **40**, 1323–1335 (2008).
15. Røislien, J. *et al*. Simultaneous estimation of effects of gender, age and walking speed on kinematic gait data. *Gait Posture* **30**, 441–445 (2009).
16. Ryan, W., Harrison, A. & Hayes, K. Functional data analysis of knee joint kinematics in the vertical jump. *Sports Biomech* **5**, 121–138 (2006).
17. Miller, F. *Cerebral Palsy* (Springer, New York, 2005).
18. Wingstrand, M., Hägglund, G. & Rodby-Bousquet, E. Ankle-foot orthoses in children with cerebral palsy: a cross sectional population based study of 2200 children. *BMC Musculoskelet Disord* **15**, 327 (2014).
19. Richards, J. *Biomechanics in Clinic and Research* (Churchill Livingstone/Elsevier, New York, 2008).
20. Abel, M. F., Juhl, G. A., Vaughan, C. L. & Damiano, D. L. Gait assessment of fixed ankle-foot orthoses in children with spastic diplegia. *Arch Phys Med Rehabil* **79**, 126–133 (1998).
21. Thompson, N. S., Taylor, T. C., McCarthy, K. R., Cosgrove, A. P. & Baker, R. J. Effect of a rigid ankle-foot orthosis on hamstring length in children with hemiplegia. *Dev Med Child Neurol* **44**, 51–57 (2002).
22. Buckon, C. E. *et al*. Comparison of three ankle-foot orthosis configurations for children with spastic diplegia. *Dev Med Child Neurol* **46**, 590–598 (2004).
23. Lam, W. K., Leong, J. C. Y., Li, Y. H., Hu, Y. & Lu, W. W. Biomechanical and electromyographic evaluation of ankle foot orthosis and dynamic ankle foot orthosis in spastic cerebral palsy. *Gait Posture* **22**, 189–197 (2005).
24. Radtka, S. A., Skinner, S. R. & Johanson, M. E. A comparison of gait with solid and hinged ankle-foot orthoses in children with spastic diplegic cerebral palsy. *Gait Posture* **21**, 303–310 (2005).
25. Brehm, M.-A., Harlaar, J. & Schwartz, M. Effect of ankle-foot orthoses on walking efficiency and gait in children with cerebral palsy. *J Rehabil Med* **40**, 529–534 (2008).
26. Danino, B. *et al*. Influence of orthosis on the foot progression angle in children with spastic cerebral palsy. *Gait Posture* **42**, 518–522 (2015).
27. Hsu, J. D., Michael, J. W. & Fisk, J. R. *AAOS Atlas of Orthoses and Assistive Devices* (Mosby/Elsevier, Philadelphia, 2008), 4 edn.
28. Morris, J. S. & Carroll, R. J. Wavelet-based functional mixed models. *J R Stat Soc Series B Stat Methodol* **68**, 179–199 (2006).
29. Berhane, K. & Molitor, N.-T. A bayesian approach to functional-based multilevel modeling of longitudinal data: applications to environmental epidemiology. *Biostatistics* **9**, 686–699 (2008).
30. Zhu, H., Brown, P. J. & Morris, J. S. Robust, adaptive functional regression in functional mixed model framework. *J Am Stat Assoc* **106**, 1167–1179 (2011).
31. Zhu, H., Brown, P. J. & Morris, J. S. Robust classification of functional and quantitative image data using functional mixed models. *Biometrics* **68**, 1260–1268 (2012).
32. Myers, J. L. & Well, A. D. *Research Design and Statistical Analysis* (Lawrence Erlbaum Associates, Mahwah, 2003), 2 edn.
33. Staicu, A.-M., Lahiri, S. N. & Carroll, R. J. Significance tests for functional data with complex dependence structure. *J Stat Plan Inference* **156**, 1–13 (2015).
34. Zhang, B. & Großmann, H. Functional data analysis in designed experiments. In *mODa 11-Advances in Model-Oriented Design and Analysis*, 235–242 (Springer, 2016).
35. Shen, Q. & Faraway, J. An F test for linear models with functional responses. *Stat Sin* **14**, 1239–1257 (2004).
36. Hegarty, A. K., Petrella, A. J., Kurz, M. J. & Silverman, A. K. Evaluating the effects of ankle-foot orthosis mechanical property assumptions on gait simulation muscle force results. *J Biomech Eng* **139**, 031009 (2017).
37. Boudarham, J., Pradon, D., Roche, N., Bensmail, D. & Zory, R. Effects of a dynamic-ankle-foot orthosis (liberté) on kinematics and electromyographic activity during gait in hemiplegic patients with spastic foot equinus. *NeuroRehabilitation* **35**, 369–379 (2014).
38. Palisano, R. *et al*. Development and reliability of a system to classify gross motor function in children with cerebral palsy. *Dev Med Child Neurol* **39**, 214–223 (1997).
39. Ounpuu, S., Gage, J. R. & Davis, R. B. Three-dimensional lower extremity joint kinetics in normal pediatric gait. *J Pediatr Orthop* **11**, 341–349 (1991).
40. Hochberg, Y. & Tamhane, A. C. *Multiple Comparison Procedures* (John Wiley & Sons, New York, 1987).
41. Whittle, M. W. *Gait Analysis: an Introduction* (Elsevier, Oxford, 2007), 4 edn.
42. Menz, H. B. Two feet, or one person? Problems associated with statistical analysis of paired data in foot and ankle medicine. *The Foot* **14**, 2–5 (2004).

43. Stackhouse, S. K., Binder-Macleod, S. A. & Lee, S. C. K. Voluntary muscle activation, contractile properties, and fatigability in children with and without cerebral palsy. *Muscle Nerve* **31**, 594–601 (2005).
44. Mead, R., Gilmour, S. G. & Mead, A. *Statistical Principles for the Design of Experiments: Applications to Real Experiments* (Cambridge University Press, Cambridge, 2012).
45. Cox, D. R. Randomization in the design of experiments. *Int Stat Rev* **77**, 415–429 (2009).
46. Hinkelmann, K. & Kempthorne, O. *Design and Analysis of Experiments, Volumn I: Introduction to Experimental Design and Analysis* (Wiley, New York, 1994).
47. Bailey, R. A. *Design of Comparative Experiments* (Cambridge University Press, Cambridge, 2008).
48. Ridgewell, E., Bobson, F., Bach, T. & Baker, R. A systematic review to determine best practice reporting guidelines for AFO interventions in studies involving children with cerebral palsy. *Prosthet Orthot Int* **34**, 129–145 (2010).
49. Ballaz, L., Plamondon, S. & Lemay, M. Ankle range of motion is key to gait efficiency in adolescents with cerebral palsy. *Clin Biomech* **25**, 944–948 (2010).
50. Ridgewell, E., Sangeux, M., Bach, T. & Baker, R. A new method for measuring AFO deformation, tibial and footwear movement in three dimensional gait analysis. *Gait Posture* **38**, 1074–1076 (2013).
51. Kerkum, Y. L. *et al*. An individual approach for optimizing ankle-foot orthoses to improve mobility in children with spastic cerebral palsy walking with excessive knee flexion. *Gait Posture* **46**, 104–111 (2016).
52. Crenshaw, S. *et al*. The efficacy of tone-reducing features in orthotics on the gait of children with spastic diplegic cerebral palsy. *J Pediatr Orthop* **20**, 210–216 (2000).
53. Romkes, J. & Brunner, R. Comparison of a dynamic and a hinged ankle-foot orthosis by gait analysis in patients with hemiplegic cerebral palsy. *Gait Posture* **15**, 18–24 (2002).
54. Romkes, J., Hell, A. K. & Brunner, R. Changes in muscle activity in children with hemiplegic cerebral palsy while walking with and without ankle–foot orthoses. *Gait Posture* **24**, 467–474 (2006).
55. Balaban, B. *et al*. The effect of hinged ankle-foot orthosis on gait and energy expenditure in spastic hemiplegic cerebral palsy. *Disabil Rehabil* **29**, 139–144 (2007).
56. Jagadamma, K. C. *et al*. Effects of tuning of ankle foot orthoses-footwear combination using wedges on stance phase knee hyperextension in children with cerebral palsy - preliminary results. *Disabil Rehabil Assist Technol* **4**, 406–413 (2009).
57. Smith, P. A. *et al*. Brace evaluation in children with diplegic cerebral palsy with a jump gait pattern. *J Bone Joint Surg Am* **91**, 356–365 (2009).
58. Jagadamma, K. C. *et al*. Optimising the effects of rigid ankle foot orthoses on the gait of children with cerebral palsy (CP) - an exploratory trial. *Disabil Rehabil Assist Technol* **10**, 445–451 (2015).
59. Kerkum, Y. L. *et al*. Acclimatization of the gait pattern to wearing an ankle–foot orthosis in children with spastic cerebral palsy. *Clin Biomech* **30**, 617–622 (2015).
60. Kerkum, Y. L. *et al*. The effects of varying ankle foot orthosis stiffness on gait in children with spastic cerebral palsy who walk with excessive knee flexion. *Plos One* **10**, 1–19 (2015).
61. Wren, T. A. L. *et al*. Comparison of 2 orthotic approaches in children with cerebral palsy. *Pediatr Phys Ther* **27**, 218–226 (2015).
62. Montgomery, D. C. *Design and Analysis of Experiments* (Wiley, Hoboken, 2013), 8 edn.
63. Goeman, J. J. & Solari, A. Multiple hypothesis testing in genomics. *Stat Med* **33**, 1946–1978 (2014).
64. Simes, R. *J*. An improved Bonferroni procedure for multiple tests of significance. *Biometrika* **73**, 751–754 (1986).
65. Vsevolozhskaya, O. A., Greenwood, M. C., Powell, S. L. & Zaykin, D. V. Resampling-based multiple comparison procedure with application to point-wise testing with functional data. *Environ Ecol Stat* **22**, 45–59 (2015).
66. Nelder, J. A. The analysis of randomized experiments with orthogonal block structure. I. Block structure and the null analysis of variance. *Proc R Soc Lond A* **283**, 147–162 (1965).
67. Nelder, J. A. The analysis of randomized experiments with orthogonal block structure. II. Treatment structure and the general analysis of variance. *Proc R Soc Lond A* **283**, 163–178 (1965).
68. Tjur, T. Analysis of variance models in orthogonal designs. *Int Stat Rev* **52**, 33–65 (1984).

Acknowledgements

Dr Morrissey is part funded by the NIHR/HEE Senior Clinical Lecturer scheme. This report presents independent research part-funded by the National Institute for Health Research (NIHR) CAT SCL-2013-04-003. The views expressed are those of the authors and not necessarily those of the NHS, the NIHR or the Department of Health. The data were collected in a study funded by The Nancie Finnie Charitable Trust.

Author Contributions

B.Z. and H.G. proposed the statistical methodology, R.T.-L. and D.M. conceived the experiment of gait data collection, R.T.-L. collected and pre-processed the gait data of patients with cerebral palsy, B.Z. analyzed the gait data. All authors contributed to the writing and reviewed the manuscript.

Additional Information

Competing Interests: The authors declare that they have no competing interests.

Publisher's note: Springer Nature remains neutral with regard to jurisdictional claims in published maps and institutional affiliations.

Appendix B

Ethics application form 1

Approved ethical application for the gait data collection in healthy subjects including the Participant Information Sheet and the Informed Consent.

For Office Use Only:
Rec Reference ……
Date received: ……

Queen Mary
University of London

Application form – Queen Mary Ethics of Research Committee

1 Name, department and email address of applicant
Bairu Zhang, School of Mathematical Sciences, bairu.zhang@qmul.ac.uk
2 Title of study
The application of experimental design and functional mixed-effects ANOVA model in healthy gait data.
3 Investigators
Bairu Zhang (School of Mathematical Sciences, QMUL): bairu.zhang@qmul.ac.uk Tel: +44 7547807008 Dr Richard Twycross-Lewis (Sports & Exercise Medicine, School of Engineering and Material Science, QMUL): r.twycross-lewis@qmul.ac.uk Tel: +44 2078826072 Dr Dylan Morrissey (Sports & Exercise Medicine, QMUL): d.morrissey@qmul.ac.uk Tel: ＋44 7941710273 Dr Heiko Grossmann (School of Mathematical Sciences, Otto-von-Guericke-University Magdeburg): heiko.grossmann@ovgu.de Tel: +49 2514841774 Dr Wolfram Just (School of Mathematical Sciences, QMUL): w.just@qmul.ac.uk
4 Proposed timetable
13/July/2015- 20/July/2015: Ethics approval 13/July/2015- 20/July/2015: Experimental design and priori analysis July/2015- September/2016: collect and process the data October/2016: data analyses
5 Other organisations involved
Not applicable
6 Other REC approval
Not applicable
7 Nature of project e.g. undergraduate, postgraduate

This data collection is part of the PhD project.

8 Purpose of the research

Purpose from gait study perspective:
Gait analysis is a powerful tool to study the human movement (Whittle 2007). The primary propose of the project is to study the abnormal gait patterns of cerebral palsy (CP) patients. Gait data for CP children have already been collected by Dr Richard Twycross-Lewis in the Human Performance Laboratory. We have tried data analysis using the existing CP gait data. In previous study, we focused on two aspects: how does the Ankle-Foot Orthosis (AFO) change the gait patterns of CP patients? Do the bilateral lower limbs of CP patients perform synchronously during walking?

In order to compare and detect the abnormality of the CP gait patterns, the study of healthy gait is also crucial. In this part of study. We aim to find out both the common features and differences between healthy and CP gait patterns. More specifically, we will concentrate on the effects of AFO on healthy subjects and the synchronization of the normal walking patterns. After this research, we may have a better understanding of the gait patterns and are able to give good interpretations to results from data analysis.

Purpose from experimental design perspective:
Randomization is not always considered carefully in the complicated data collection. However, we can construct completely randomized designs to avoid the some bias (systematic bias, selection bias, accidental bias and cheating) of the data (Baily 2008) and increase the power of analysis. Theoretically, another way to increase the power of data analysis is to consider the effect of blocking, which is how the observational units are grouped. There will be more than one type of blocks applied in this study.

Therefore, the data collected in this study will not only used in the gait analysis, but also to measure the effect of randomization and blocking on the experiment.

9 Study design, methodology and data analysis

This is an observational study to measure the effect of AFO on lower limb when healthy subjects are walking under different conditions.

We will use 3D Cartesian Optoelectronic Dynamic Anthropometer (CODA) motion system to measure coronal, sagittal, and transverse plane kinematic data. Two experimenters (A and B) will affix the CODAmotion markers on different subjects respectively to study the effect of blocking. Markers are infra-red and the protocol for marker placement is the Helen Hayes protocol.

About 20 healthy subjects will be recruited for this study. The specific sample

size will be determined by the priori power analysis later. General information, including gender, date of birth, height, weight, pelvic width and depth, knee width, ankle width and foot length, will be recorded. The experimenter, who will be randomly selected from the two, will affix markers on subjects.

Each subject will be required to walk on a treadmill under three conditions: normal walking, walking with AFO on one foot and walking with AFO on both feet. The order of three different trials for each subject will be randomized by 3×3 Latin squares. In addition, the one AFO walking condition is not limited to one side of the body but will be done both left and right sides and order will be randomised as well.

Kinematic data including pelvis, hip, knee, ankle, foot rotations in different planes will be measured by CODAmotion system. The data will be stored on the hard disc and standardized by an existing program. Several different methods such as continuous relative phase and functional mixed ANOVA model will be applied to analyse the data.

10 Participants to be studied

Healthy young adults; age=18-50 years. Subjects should be free from systemic injury and disease. The sample should contain both male and female.

11 Selection criteria

Inclusion criteria: 1) Subjects must be between the ages of 18 to 50 years.

Exclusion criteria are: 1) subjects who suffer from neurological or musculoskeletal disease which would cause movement disorder, 2) subjects who had lower limb injuries that affected walking for >2 weeks in the past 6 months, 3) subjects who had lower limb surgeries in the past 1 years, 4) pregnant women, 5) subjects who had problems of drug abuse or alcohol abuse in the past 3 months, 6) subjects whose cognitive functions prevent them from understanding the study.

12 Recruitment (including incentives and compensation)

Subjects will be recruited by posted adverts through emails and at the notice board in the student union building, mile end library and accommodation buildings at Queen Mary, University of London.

13 Ethical considerations and risks to participants

There are no known risks for the CODAmotion system. It has been successfully used in the Human Performance Laboratory without any record of harm. Anthropometric measurements will be done with standardised lab equipments, which have no known risks to subjects.

The treadmill walking will be done under the instruction of investigators. Subjects will have a short period to practice walking on the treadmill with lower speed. There are risks of losing balance or falling down, but risks of walking on the treadmill are low for healthy young adults. In addition, subjects can practice walking on the treadmill before experiments and will walk under the instruction of investigators.

Subject will be required to walk with adult AFO, which will be borrowed from the hospital. The orthosis is used to support walking and fixed between foot and ankle. It is widely applied among patients with movement disorder and no known adverse effect for short term wearing.

14 Confidentiality, anonymity, and data storage

The data will only be used on research and names of subjects will not be recorded. The date of data collection will be used to identify the data in the computer. Only the research team will have the access to the data. Usually the data will be stored in the Bairu and Dr Richard Twycross-Lewis's USB stick and computer.

15 Information for participants

See attached

16 Consent

See attached

17 Signature of applicant and authorising signatories.

Principal Investigator

Other Applicant(s)

(Head of Department)

Pro forma information sheet and consent form

Information sheet

Research study: The application of experimental design and functional mixed-effects ANOVA model in healthy gait data

We would like to invite you to be part of this research project, if you would like to. If you choose not to take part there won't be any disadvantages for you and you will hear no more about it. Please read the following information carefully as it will tell you why the research is being done and what you will be asked to do if you take part. Please ask if there is anything that is not clear or if you would like more information. If you decide to take part you will be asked to sign the attached form to say that you agree.

You are still free to withdraw at any time and without giving a reason.

We are studying the movement of the legs during walking. More specifically, we aim to detect any unusual walking features in patients who have movement disorders to improve clinical treatments. To do this, we want to compare existing information on walking patterns of people with problems to more regular walking patterns in healthy subjects.

In this study we will also test the effect of Ankle-Foot Orthoses (AFO) on your walking. An AFO is a plastic brace placed around the ankle and foot but fitting inside the shoe. This is widely applied to patients with walking problems, such as people with cerebral palsy who we are particularly interested in. Walking patterns can be studied by using CODAmotion system, which is an instrumental 3D system, in the Human Performance Laboratory at Queen Mary, University of London.

We would like to collect gait data in healthy young subjects 18 to 50 years old, and are interested in both males and females. Any gait differences between genders will also be analyzed in the study.

Accepted subjects will be required to come to the Human Performance Laboratory at Queen Mary, University of London at an agreed time and date. Subjects will be expected to wear or bring shorts and a tee shirt. There is a changing room in the laboratory. Subjects will be required to sign the consent form before beginning data collection.

We will measure your height, weight, and lower limb sizes. Before the main test, you can walk on the treadmill freely for around 3 to 5 minutes to make sure you are comfortable. Then we will ask you to walk on the treadmill under three conditions -normal walking in shoes, walking with an AFO on one foot and walking with AFOs on both feet.

We will attach small light emitting markers with tape to your legs and pelvis. Each trial will last 5 minutes. For each subject, the whole process should take 1-1.5 hours.

All the instruments and orthoses are safe with minimal risk of injury. However, you may find it difficult in walking on the treadmill if this is unfamiliar to you. We can stop at any time if you are not comfortable.

The data will only be used for the research purpose. Names of subjects will not be recorded along with the data and dates of data collection will be used to identify the data in the computer. Only the research team will have the access to the data. Additional information sheet such as signed consent forms will be stored in the Center of Sports & Exercise Medicine at Queen Mary, University of London. Data will be stored in accordance with the Data Protection Act.

It is up to you to decide whether or not to take part. If you do decide to take part you will be given this information sheet to keep and be asked to sign a consent form.

If you have any questions or concerns about the manner in which the study was conducted please, in the first instance, contact the researcher responsible for the study. If this is unsuccessful, or not appropriate, please contact the Secretary at the Queen Mary Ethics of Research Committee, Room W117, Queen's Building, Mile End Campus, Mile End Road, London or research-ethics@qmul.ac.uk.

Contact details:

Bairu Zhang (School of Mathematical Sciences, QMUL): bairu.zhang@qmul.ac.uk Tel: +44 7547807008

Dr Richard Twycross-Lewis (Sports & Exercise Medicine, School of Engineering and Material Science, QMUL): r.twycross-lewis@qmul.ac.uk Tel: +44 2078826072

Queen Mary
University of London

Consent form

Please complete this form after you have read the Information Sheet and/or listened to an explanation about the research.

Title of Study: the application of experimental design and functional mixed-effects ANOVA model in healthy gait data.

Queen Mary Ethics of Research Committee Ref: _____

. • Thank you for considering taking part in this research. The person organizing the research must explain the project to you before you agree to take part.

. • If you have any questions arising from the Information Sheet or explanation already given to you, please ask the researcher before you decide whether to join in. You will be given a copy of this Consent Form to keep and refer to at any time.

. • *I understand that if I decide at any other time during the research that I no longer wish to participate in this project, I can notify the researchers involved and be withdrawn from it immediately.*

. • *I consent to the processing of my personal information for the purposes of this research study. I understand that such information will be treated as strictly confidential and handled in accordance with the provisions of the Data Protection Act 1998.*

Participant's Statement:

I _____ agree that the research project named above has been explained to me to my satisfaction and I agree to take part in the study. I have read both the notes written above and the Information Sheet about the project, and understand what the research study involves.

Signed: Date:

Investigator's Statement:

I _____ confirm that I have carefully explained the nature, demands and any foreseeable risks (where applicable) of the proposed research to the volunteer

Sports & Exercise Medicine
Queen Mary, University Of London

RECRUITMENT OF STUDY PARTICIPANTS
(July/2015 – September/2016)
18 years or older

Title of study:	the application of experimental design and functional mixed-effects model in healthy gait data
Purpose of project:	we are studying the movement of the leg during walking and the effect of Ankle-Foot Orthoses (AFO).
Experimenter:	Dr Richard Twycross-Lewis, Bairu Zhang
Location of study:	**Human Performance Laboratory** (Mile end campus, Queen Mary University of London)
Type of activity:	walking on the treadmill will small light infra-red markers on pelvis and legs
Approx. time:	1-1.5 hours
Contact Details:	Bairu Zhang Email: bairu.zhang@qmul.ac.uk Tel: + 44 (0)7547807008 Dr Richard Twycross-Lewis Email: r.twycross-lewis@qmul.ac.uk

Appendix C

Hasse diagram for an alternative block structure of the experiment in Section 4.3

In Section 4.3, I also consider an alternative structure of experiment, where 15 gait curves rather than 9 gait curves are included for each participant. More specifically, gait data from both left and right lower limbs are used during walking barefoot and with bilateral AFO, while gait data from only the relevant left lower limbs are used during walking with unilateral AFO.

The block structure of the experiment, where 15 responses for each participant are used, is shown in Figure C.1. Compare to the Hasse diagram for the block structure of the experiment (Figure 4.9), where only 9 responses for each participant are used, an additional block factor *limbs* is included in Figure C.1. The block factor *subperiods* indicates the sub-periods when participants walked at different speeds. The infimum of block factors *periods* and *limbs* is indicated by $periods \wedge limbs$, which is not a uniform factor. Moreover, the block factor *subperiods* in Figure C.1 is the same as the block factor $\mathscr{E}$ in Figure 4.9, while the factor $\mathscr{E}$ in Figure C.1 is the infimum of *subperiods* and $periods \wedge limbs$.

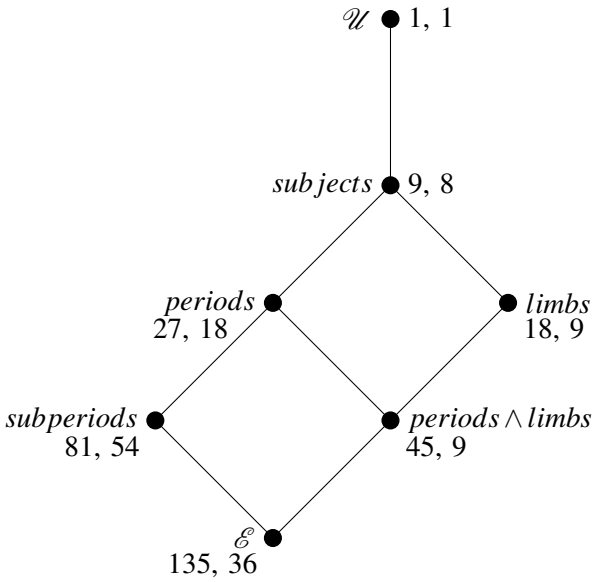

Figure C.1: Hasse diagram for the block structure of the experiment, where 15 gait curves rather than 9 gait curves are included for each participant, in Section 4.3

Appendix D

Additional analysis for gait data in Section 4.3

The analysis in Section 4.3 were repeated by using data from left lower limbs of subjects only. In what follows, we will show that there are only slight changes in results compared to results in Section 4.3.5.

Mean gait curves under different walking conditions can be seen in Figure D.2, which is similar to Figure 4.13. Although in some panels, such as rotations of the ankle joint and foot at the fast and medium speeds, we can see gait curves collected during walking with unilateral AFO (blue, dashed) and bilateral AFO (red, dotted) are closer to each other in Figure D.2 than Figure 4.13, it is difficult to distinguish further differences. Moreover, similar to Table 4.5, results from functional F tests, where only data collected from left lower limbs were used, are shown in Table D.1. Although F values and p values have slight changes compared to Table 4.5, the significance of factors remains the same.

Likewise, since the p value in Table D.1 to assess the effect of AFO on the ankle joint is 0.09, which implies a weak significance, we repeated the pointwise F tests and orthogonal contrast analysis to the ankle joint. Results are shown in Figure D.1 and Table D.2, which

are again close to those in Section 4.3.5.

Table D.1: Functional F tests for AFO, speeds and the interaction with * indicating significance at 0.05 significance level

	F value (p.)		
	AFO	$speeds$	$AFO \wedge speeds$
Pelvis	2.00 (0.16)	0.13 (0.91)	1.33 (0.27)
Hip	0.51 (0.69)	12.30 (< 0.01)*	0.33 (0.97)
Knee	0.71 (0.61)	16.04 (< 0.01)*	0.69 (0.72)
Ankle	2.16 (0.09)	8.68 (< 0.01)*	0.93 (0.53)
Foot	0.38 (0.86)	18.13 (< 0.01)*	0.93 (0.52)

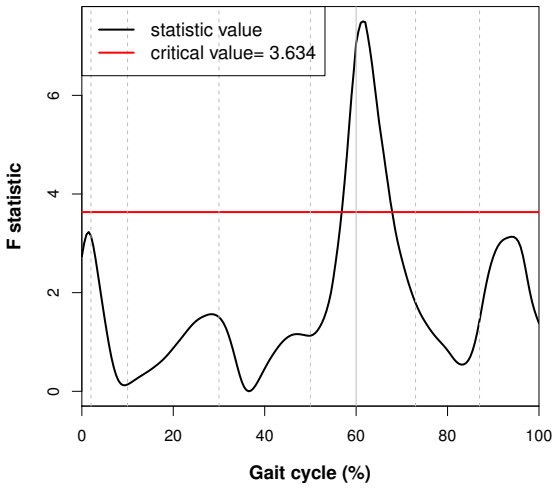

Figure D.1: Multiple pointwise F tests for effects of AFO on ankle joints at the significance level $\alpha = 0.05$. Grey dashed lines and the grey solid line are used to divide the whole gait cycles into phases: initial contact, loading response, mid-stance, terminal stance, pre-swing, initial swing, mid-swing and terminal swing phases (from left to right).

Table D.2: ANOVA table for the orthogonal contrast analysis to compare the differences between walks barefoot and wearing AFO on the ankle joint. * indicates significance at 0.05 significance level.

Stratum	Source	$d_{\mathbb{W}}$	F value (p.)
$\mathscr{U}$	$\mathscr{U}$	1	
$subjects$	$subjects$	8	
$periods$	L_1	1	4.00 (0.03)*
	L_2	1	0.32 (0.74)
	$residual$	16	
	$total$	18	
$\mathscr{E}$	$speeds$	2	9.67 (< 0.01)*
	$L_1 \wedge speeds$	2	1.60 (0.14)
	$L_2 \wedge speeds$	2	0.25 (0.97)
	$residual$	48	
	$total$	54	
$Total$		81	

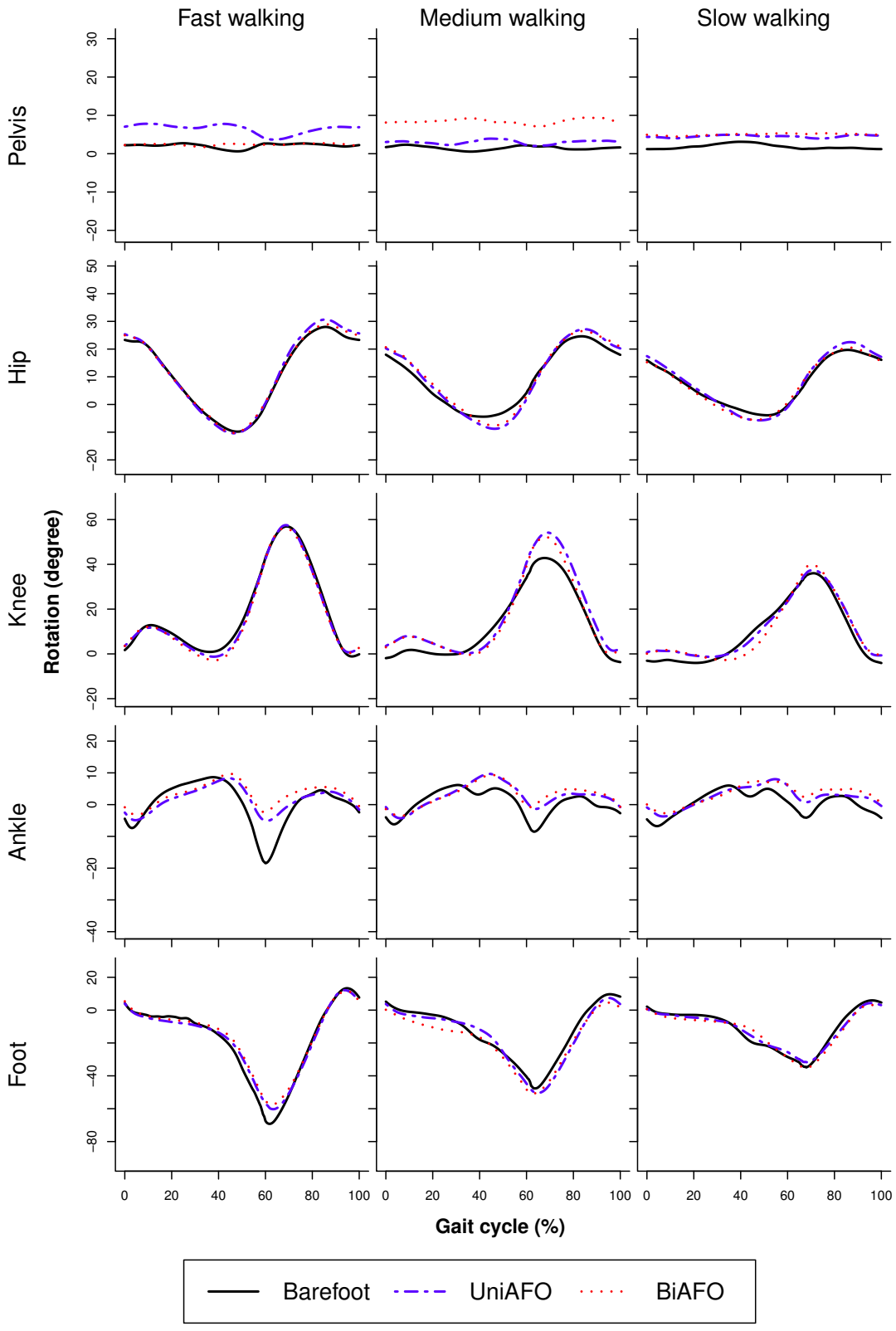

Figure D.2: Mean gait curves of 9 healthy subjects during walking under different AFO conditions at different walking speeds. UniAFO indicates the walk wearing the unilateral AFO and BiAFO indicates the walk wearing the bilateral AFO. All data are from left lower limbs of subjects.

Appendix E

Ethics application form 2

Approved ethical application for the study *The influence of gait analysis in the management of cerebral palsy: a qualitative exploration of clinicians' perspectives* including the Participant Information Sheet and the Informed Consent.

For Office Use Only:
Rec Reference …….
Date received: ……

Queen Mary
University of London

Application form – Queen Mary Ethics of Research Committee

1 Name, department and email address of applicant
Augustine Adu-Amankwah, Sports & Exercise Medicine, QMUL a.adu-amankwah@smd14.qmul.ac.uk, Tel: +44(0)7946679673
2 Title of study
The influence of gait analysis on decision making in the management of Cerebral Palsy: a qualitative exploration of clinicians' perspectives
3 Investigators
Principal Investigator: Augustine Adu-Amankwah, Sports & Exercise Medicine, QMUL Anna Hebda-Boon, Royal London Hospital, Hebda-Boon.Anna@bartshealth.nhs.uk, Tel: +44(0)7595264209 Research Supervisors: Bairu Zhang, School of Mathematical Sciences, QMUL bairu.zhang@qmul.ac.uk, Tel: +44(0)7547807008 Dr Dylan Morrissey, Sports & Exercise Medicine, QMUL d.morrissey@qmul.ac.uk , Tel: +44 (0)7941710273
4 Proposed timetable

Queen Mary Research Ethics Committee sitting: 12 January 2017 Proposed Recruitment: 16/Jan/2017 - 28/April/2017 Data Collection: 1/Mar/2017 – 31/May/2017 Data Analysis and Triangulation: 1/Jun/2017 – 30/Jun/2017 Write and Submission: 1/Jul/2017 – 31/Aug/2017 Completion date: 31 August 2018
5 Other organisations involved
N/A organizations involved. Research undertaken as part of fulfilment for MSc in Sports & Exercise Medicine
6 Other REC approval
None
7 Nature of project e.g. undergraduate, postgraduate
Postgraduate MSc research project
8 Purpose of the research
Overall aims: To explore the effects of the use of gait laboratory analysis in the management of patients with Cerebral Palsy (CP) from clinicians' perspectives in order to improve the patient's outcome. Subsidiary aims: a) This project will investigate clinicians' experience and opinions of applying gait data including barriers and facilitators. b) Using semi-structured interview, explore the utilisation of gait analysis in

clinical assessment and treatment of CP.

c) Identify the applicable barriers to gait analysis and bridge the gap between gait laboratory data and clinical application.

Why this study?

CP is a common neurology disorder often affecting paediatric patient. CP is characterised by loss of muscle selectivity spasticity, motor and sensory disturbance, and premature muscle firing. The gait of children with CP is often asymmetric and less stable.

In recent years, the use of laboratory based gait analysis has increased over the last three to four decades to help clinicians' decision-making. The effects of gait analysis on clinical decision-making are widely known among orthopaedic surgeons. However, the effects of gait analysis for clinical treatment are still controversial.

Despite the recent advancement in technology and better quality data, the role of laboratory based gait analysis among clinicians is widely variable depending on locations practice, resources available and access to gait laboratory. As a result, clinician's application of gait analysis data in their daily clinical practice is variable and not regarded to some extent as essential component of clinical practice.

Null Hypothesis: n/a

9 Study design, methodology and data analysis

Qualitative research with semi-structured interview

1) Face-to-face interviews with participants.
2) Sample size is 10 initially and we continue the data collection until data saturation, likely 20 overall.

3

3) Topic guide will be used to guide the interview whilst adopting a predominantly open style to allow participants to feel at ease and express themselves freely in order to capture the true meaning of what they are saying.

4) Interviews will last about one hour.

5) Interviews will be recorded by using two electronic devices to avoid the technical problem of the recording equipment. This would be checked immediately before and after interviews.

6) Interviews will be outside of clinical time.

7) Interviews will be within the premises convenient to the participant (their place of work) or at Queen Mary University London (QMUL).

Analysis:

Recording of each interview would be transcribed verbatim on the computer using Microsoft Word software. We will take the text line by line to generate a code or categories and framework approach will be utilised to analyse the data.

Participants will have the opportunity to see their transcribed interviews before writing up the final project, providing a further opportunity to debrief and for participants to air any views.

All participants will be made aware of my supervisors' details, should they wish to contact them about a concern they do not wish to discuss with me directly.

10 Participants to be studied

Participants will be Health Professionals (Physiotherapist, Orthotics, Prosthetics and Consultant) who has had practical application of gait analysis.

Participants would be recruited across 4 locations in London:

- Royal London Hospital

4

- Kaleidoscope Child Development Centre
- Sunshine House Specialist Child Development Centre
- Bowley Close Rehabilitation centre

11 Selection criteria

Inclusion Criteria:

1) Health Professionals who have experience of working children with CP
2) Clinicians whose professional roles involve gait analysis as part of their assessment or treatment

Exclusion Criteria:

1) Clinical staff who does not practice within paediatric sector or patient diagnosed with CP
2) Clinical staff who has less than six months' clinical experience working with such patient groups
3) Clinical staff that has no experiences or practical of performing gait analysis or of applying their results, either laboratory based or through their day-to-day patient assessment

12 Recruitment (including incentives and compensation)

1) Participants will be recruited across four London based paediatric services who specialise in assessment and treatment of patients diagnosed with CP.
2) Purposive sampling is applied and participants are selected according to: gender, profession and experience of working with CP.
3) No incentives (e.g. financial incentives) will be offered to the participants and no coercion, payments to participate or other financial incentives will occur.

5

13 Ethical considerations and risks to participants

1) There will be no physical risk or career risks to the participants.
2) The study is not expected to touch on topics that are highly emotive, however, there is the need to be sensitive due to the fact that the information is still personal to the participant.
3) In event that a participant suffers any psychological stress, they will be able to stop the interview at any time.
4) The participants will be informed they can terminate the interview at any time or opt out of the study at any time.
5) The interview will take place away from the members of the public or colleagues of the participant.

14 Confidentiality, anonymity, and data storage

The data will only be used for research and full names of participants will not be recorded. Initials of participants will be used to identify the data. The principal investigator will keep accurate records throughout the period of study.

Data storage and access:

1) Signed consent form will be kept in a locked cabinet in the Centre for Sports and Exercise Medicine at QMUL. They will be kept under Participant's data protection and research data gathering guidelines after completion of the study.
2) Participants identifiable data will be anonymized and kept separate from study data in a secure locked cabinet located at QMUL.
3) Electronic data will be stored on a password protected PC.
4) Access will be restricted to research team members. The principal investigator

will act as custodian of the data.
15 Information for participants
See attached
16 Consent
See attached
17 Signature of applicant and authorising signatories.
Principal Investigator…….. **Other Applicant(s)…….…...** **(Head of Department)……..**

7

Pro forma information sheet and consent form

Queen Mary
University of London

Information sheet

Study Title: **The influence of gait analysis in decision making in the management of Cerebral Palsy: a qualitative exploration of clinicians' perspectives.**

We would like to invite you to be part of this research project. You should only agree to take part if you want to, it is entirely up to you. If you choose not to take part, there won't be any disadvantages for you and will hear no more from me.

Please read the following information carefully before you decide to take part; this will tell you why the research is being done and what you will be asked to do if you take part. Please ask if there is anything that is not clear or if you would like more information.

If you decide to take part, you will be asked to sign the attached form to say that you agree. **You can withdraw at any time from the study and without giving a reason, although once your data has been anonymously combined with that of others it will not be possible to exact it.**

In recent years, the use of laboratory based gait analysis has increased to help clinical decision-making. However, sometimes clinicians feel they do not know how to fully make sense of the data. Through face-to-face interviews, this research will explore the effects of laboratory gait analysis in the management of patient with Cerebral Palsy from clinicians' perspectives. More specifically, the research will investigate clinicians' experience and opinions of applying gait data including barriers and facilitators. This study is expected to help improve clinicians understanding of gait analysis and contribute

to the clinicians' decision making in the management of children diagnosed with Cerebral Palsy. Finally, we will make recommendations that might improve communication about laboratory based gait analysis between clinicians and scientist.

What will happen? This would involve an interview at location of your choice, where it is familiar to you (work place office) or at Queen Mary University of London. The interview would last for approximately one hour. The experience and opinion shared will be recorded by using digital mobile device. The opinions and experience shared will be annonymised and kept in the strictest of confidence. After the interview, the information would be fully transcribed to develop theme that arises out of the interview.

There will be no physical or career risk to you. The data will only be used for the research purpose. Full name will not be recorded along with the data and initials will only be used to identify the data in the computer. The information would be not shared with anyone other than those participating on the research. The identity information will be stored in a secure locked cabinet located at Queen Mary University of London and only accessible to the research team.

What happens if there is a problem or you have a question?

If you have any questions or concerns about the manner in which the study was conducted please, in the first instance, contact the researcher responsible for the study: Augustine Adu-Amankwah, a.adu-amankwah@smd14.qmul.ac.uk +44(0)7946679673

or Anna Hebda-Boon, Hebda-Boon.Anna@bartshealth.nhs.uk +44(0)7595264209.

If this is unsuccessful, or not appropriate, please contact the Secretary at the Queen Mary Ethics of Research Committee, Room W104, Queen's Building, Mile End Campus, Mile End Road, London or research-ethics@qmul.ac.uk.

Queen Mary
University of London

Consent form

Please complete this form after you have read the Information Sheet and/or listened to an explanation about the research.

Title of Study: the influence of gait analysis on decision making in the management of Cerebral Palsy (CP): A qualitative exploration of the clinicians' Perspective.

Queen Mary Ethics of Research Committee Ref: _____

Thank you for considering taking part in this research. Please read the statements below and initial the boxes if you are happy to proceed:

Please initial box

1. I confirm that I have read the Participant Information sheet for the above study. I have had the opportunity to consider the information and ask questions which have been satisfactorily answered. ☐
2. If you have any questions arising from the Information Sheet or explanation already given to you, please ask the researcher before you decide whether to join in. You will be given a copy of this Consent Form to keep and refer to at any time. ☐
3. I understand that my participation is voluntary and that I am free to withdraw at

10

any time, without giving a reason and without any consequences to my care or legal rights, although once my data has been anonymously combined with that of others it will not be possible to extract it. ☐

4. I consent to the processing of my personal information for the purposes of this research study. I understand that such information will be treated as strictly confidential and handled in accordance with the provisions of the Data Protection Act 1998. ☐

5. I agree to take part in the above named study. ☐

Participant's Statement:

I _____ agree that the research project named above has been explained to me to my satisfaction and I agree to take part in the study. I have read both the notes written above and the Information Sheet about the project, and understand what the research study involves.

Signed: Date:

Investigator's Statement:

I _____ confirm that I have carefully explained the nature, demands and any foreseeable risks (where applicable) of the proposed research to the volunteer.

Signed: Date:

11

Bibliography

Abd El-Kafy, E. M. (2014). The clinical impact of orthotic correction of lower limb rotational deformities in children with cerebral palsy: a randomized controlled trial. *Clinical Rehabilitation*, 28:1004–1014.

Abel, M. F., Juhl, G. A., Vaughan, C. L., and Damiano, D. L. (1998). Gait assessment of fixed ankle-foot orthoses in children with spastic diplegia. *Archives of Physical Medicine and Rehabilitation*, 79:126–133.

Abramovich, F. and Angelini, C. (2006). Testing in mixed-effects FANOVA models. *Journal of Statistical Planning and Inference*, 136:4326–4348.

Ash, R. B. and Gardner, M. F. (1975). *Topics in Stochastic Processes*. Academic Press, New York.

Aston, J. A. D., Chiou, J.-M., and Evans, J. P. (2010). Linguistic pitch analysis using functional principal component mixed effect models. *Journal of the Royal Statistical Society, Series C*, 59:297–317.

Bailey, R. A. (2008). *Design of Comparative Experiments*. Cambridge University Press, Cambridge.

Baker, R., Esquenazi, A., Benedetti, M. G., and Desloovere, K. (2016). Gait analysis: clinical facts. *European Journal of Physical and Rehabilitation Medicine*, 52:560–574.

Baladandayuthapani, V., Mallick, B. K., Hong, M. Y., Lupton, J. R., Turner, N. D., and Carroll, R. J. (2008). Bayesian hierarchical spatially correlated functional data analysis with application to colon carcinogenesis. *Biometrics*, 64:64–73.

Balakrishnan, A. V. (1960). Estimation and detection theory for multiple stochastic processes. *Journal of Mathematical Analysis and Applications*, 1:386–410.

Bernardi, M. S., Sangalli, L. M., Mazza, G., and Ramsay, J. O. (2017). A penalized regression model for spatial functional data with application to the analysis of the production of waste in Venice province. *Stochastic Environmental Research and Risk Assessment*, 31:23–38.

Bosq, D. (2000). *Linear Processes in Function Spaces: Theory and Applications*. Springer, New York.

Brehm, M.-A., Harlaar, J., and Schwartz, M. (2008). Effect of ankle-foot orthoses on walking efficiency and gait in children with cerebral palsy. *Journal of Rehabilitation Medicine*, 40:529–534.

Brien, C. J. and Bailey, R. A. (2006). Multiple randomizations (with discussion). *Journal of the Royal Statistical Society, Series B*, 68:571–609.

Buckon, C. E., Thomas, S. S., Jakobson-Huston, S., Moor, M., Sussman, M., and Aiona, M. (2004). Comparison of three ankle-foot orthosis configurations for children with spastic diplegia. *Developmental Medicine & Child Neurology*, 46:590–598.

Cheng, C.-S. (2014). *Theory of Factorial Design: Single- and Multi-Stratum Experiments*. CRC Press, Boca Raton.

Christensen, R. (2011). *Plane Answers to Complex Questions: the Theory of Linear Models*. Springer, New York, Fourth edition.

Cimolin, V. and Galli, M. (2014). Summary measures for clinical gait analysis: a literature review. *Gait & Posture*, 39:1005–1010.

Crainiceanu, C. M., Staicu, A.-M., Ray, S., and Punjabi, N. (2012). Bootstrap-based inference on the difference in the means of two correlated functional processes. *Statistics in Medicine*, 31:3223–3240.

Crane, E. A., Cassidy, R. B., Rothman, E. D., and Gerstner, G. E. (2010). Effect of registration on cyclical kinematic data. *Journal of Biomechanics*, 43:2444–2447.

Cuesta-Albertos, J. A. and Febrero-Bande, M. (2010). A simple multiway ANOVA for functional data. *Test*, 19:537–557.

Cuevas, A. (2014). A partial overview of the theory of statistics with functional data. *Journal of Statistical Planning and Inference*, 147:1–23.

Cuevas, A., Febrero, M., and Fraiman, R. (2004). An anova test for functional data. *Computational Statistics & Data Analysis*, 47:111–122.

Danino, B., Snir, E., Kfir, M., Khamis, S., Batt, R., Hemo, Y., Wientroub, S., and Hayek, S. (2016). Are gait indices sensitive enough to reflect the effect of ankle foot orthosis on gait impairment in cerebral palsy diplegic patients? *Journal of Pediatric Orthopaedics*, 36:294–298.

Derrick, B., Toher, D., and White, P. (2016). Why Welch's test is Type I error robust. *The Quantitative Methods for Psychology*, 12:30–38.

Desloovere, K., Molenaers, G., Van Gestel, L., Huenaerts, C., Van Campenhout, A., Callewaert, B., Van de Walle, P., and Seyler, J. (2006). How can push-off be preserved during use of an ankle foot orthosis in children with hemiplegia? A prospective controlled study. *Gait & Posture*, 24:142–151.

Di, C.-Z., Crainiceanu, C. M., Caffo, B. S., and Punjabi, N. M. (2009). Multilevel functional principal component analysis. *Annals of Applied Statistics*, 3:458–488.

Donoghue, O. A., Harrison, A. J., Coffey, N., and Hayes, K. (2008). Functional data analysis of running kinematics in chronic Achilles tendon injury. *Medicine and Science in Sports and Exercise*, 40:1323–1335.

Duhamel, A., Bourriez, J. L., Devos, P., Krystkowiak, P., Destée, A., Derambure, P., and Defebvre, L. (2004). Statistical tools for clinical gait analysis. *Gait & Posture*, 20:204–212.

Duhamel, A., Devos, P., Bourriez, J. L., Preda, C., Defebvre, L., and Beuscart, R. (2006). Functional data analysis for gait curves study in Parkinson's disease. *Studies in Health Technology and Informatics*, 124:569–574.

Elftman, H. (1939). Forces and energy changes in the leg during walking. *American Journal of Physiology*, 125:339–356.

Fan, J. and Lin, S.-K. (1998). Test of significance when data are curves. *Journal of the American Statistical Association*, 93:1007–1021.

Faraway, J. J. (1997). Regression analysis for a functional response. *Technometrics*, 39:254–261.

Franki, I., De Cat, J., Deschepper, E., Molenaers, G., Desloovere, K., Himpens, E., Vanderstraeten, G., and Van den Broeck, C. (2014). A clinical decision framework for the identification of main problems and treatment goals for ambulant children with bilateral spastic cerebral palsy. *Research in Developmental Disabilities*, 35:1160–1176.

Gohberg, I. C. and Kreĭn, M. G. (1969). *Introduction to the Theory of Linear Nonselfadjoint Operators*. American Mathematical Society, Rhode Island.

Górecki, T. and Smaga, Ł. (2015). A comparison of tests for the one-way ANOVA problem for functional data. *Computational Statistics*, 30:987–1010.

Großmann, H. (2014). Automating the analysis of variance of orthogonal designs. *Computational Statistics and Data Analysis*, 70:1–18.

Guillebastre, B., Calmels, P., and Rougier, P. (2009). Effects of rigid and dynamic ankle-foot orthoses on normal gait. *Foot & Ankle International*, 30:51–56.

Guo, W. (2002). Functional mixed effects models. *Biometrics*, 58:121–128.

Hart, E., Pinkston, D., Ritchey, F. J., and Knowles, C. J. (1990). Relationship of professional involvement to clinical behaviors of physical therapists. *Physical Therapy*, 70:179–187.

Hinkelmann, K. and Kempthorne, O. (1994). *Design and Analysis of Experiments, Volume I: Introduction to Experimental Design*. Wiley, New York.

Hochberg, Y. and Tamhane, A. C. (1987). *Multiple Comparison Procedures*. John Wiley & Sons, New York.

Hsing, T. and Eubank, R. (2015). *Theoretical Foundations of Functional Data Analysis, with an Introduction to Linear Operators*. Wiley, Chichester.

Hsu, J. D., Michael, J. W., and Fisk, J. R. (2008). *AAOS Atlas of Orthoses and Assistive Devices*. Mosby/Elsevier, Philadelphia, Fourth edition.

Johnson, R. A. and Wichern, D. W. (2007). *Applied Multivariate Statistical Analysis*. Pearson, New Jersy, Six edition.

Kadaba, M. P., Ramakrishnan, H. K., Wootten, M. E., Gainey, J., Gorton, G., and Cochran, G. V. B. (1989). Repeatability of kinematic, kinetic and electromyographic data in normal adult gait. *Journal of Orthopaedic Research*, 7:849–860.

Karatzas, I. and Shreve, S. E. (1998). *Brownian Motion and Stochastic Calculus*. Springer, New York, Second edition.

Kelly, E. J. and Root, W. L. (1960). A representation of vector-valued random processes. *Journal of Mathematics and Physics*, 39:211–216.

Kerkum, Y. L., Buizer, A. I., van de Noort, J. C., Becher, J. G., Harlaar, J., and Brehm, M.-A. (2015). The effects of varying ankle foot orthosis stiffness on gait in children with spastic cerebral palsy who walk with excessive knee flexion. *Plos One*, 10:1–19.

Kirtley, C. (2006). *Clinical Gait Analysis: Theory and Practice*. Churchill Livingstone, London.

Koenig, L. L., Lucero, J. C., and Perlman, E. (2008). Speech production variability in fricatives of children and adults: results of functional data analysis. *The Journal of the Acoustical Society of America*, 124:3158–3170.

Kokoszka, P. and Reimherr, M. (2017). *Introduction to Functional Data Analysis*. CRC Press, Boca Raton.

Lenhoff, M. W., Santner, T. J., Otis, J. C., Peterson, M. G. E., Williams, B. J., and Backus, S. I. (1999). Bootstrap prediction and confidence bands: a superior statistical method for analysis of gait data. *Gait & Posture*, 9:10–17.

Loève, M. (1977). *Probability Theory II*. Springer-Verlag, New York, Fourth edition.

Maynard, V., Bakheit, A. M. O., Oldham, J., and Freeman, J. (2003). Intra-rater and inter-rater reliability of gait measurements with CODA mpx30 motion analysis system. *Gait & Posture*, 17:59–67.

McGinley, J. L., Baker, R., Wolfe, R., and Morris, M. E. (2009). The reliability of three-dimensional kinematic gait measurements: A systematic reivew. *Gait & Posture*, 29:360–369.

Menz, H. B. (2004). Two feet, or one person? Problems associated with statistical analysis of paired data in foot and ankle medicine. *The Foot*, 14:2–5.

Mercer, J. (1909). Functions of positive and negative type, and their connection with the theory of integral equations. *Philosophical Transactions of the Royal Society of London*, 209:415–446.

Miller, F. (2005). *Cerebral Palsy*. Springer, New York.

Morris, J. S. (2015). Functional regression. *Annual Review of Statistics and Its Application*, 2:321–359.

Morris, J. S. and Carroll, R. J. (2006). Wavelet-based functional mixed models. *Journal of the Royal Statistical Society, Series B*, 68:179–199.

Nelder, J. A. (1965a). The analysis of randomized experiments with orthogonal block structure. I. block structure and the null analysis of variance. *Proceedings of the Royal Society of London, Series A*, 283:147–162.

Nelder, J. A. (1965b). The analysis of randomized experiments with orthogonal block structure. II. treatment structure and the general analysis of variance. *Proceedings of the Royal Society of London, Series A*, 283:163–178.

Olshen, R. A., Biden, E. N., Wyatt, M. P., and Sutherland, D. H. (1989). Gait analysis and the bootstrap. *The Annals of Statistics*, 17:1419–1440.

Opara, C., Levangie, P. K., and Nelson, D. L. (1985). Effects of selected assistive devices on normal distance gait characteristics. *Physical Therapy*, 65:1188–1191.

Ounpuu, S., Gage, J. R., and Davis, R. B. (1991). Three-dimensional lower extremity joint kinetics in normal pediatric gait. *Journal of Pediatric Orthopedics*, 11:341–349.

Owen, E. (2010). The importance of being earnest about shank and thigh kinematics especially when using ankle-foot orthoses. *Prosthetics and Orthotics International*, 34:254–269.

Palisano, R., Rosenbaum, P., Walter, S., Russell, D., Ellen, W., and Galuppi, B. (1997). Development and reliability of a system to classify gross motor function in children with cerebral palsy. *Developmental Medicine & Child Neurology*, 39:214–223.

Papavasiliou, A. S. (2009). Management of motor problems in cerebral palsy: a critical update for the clinician. *European Journal of Paediatric Neurology*, 13:387–396.

Pataky, T. C., Robinson, M. A., and Vanrenterghem, J. (2013). Vector field statistical analysis of kinematic and force trajectories. *Journal of Biomechanics*, 46:2394–2401.

Perry, J. (1992). *Gait Analysis: Normal and Pathological Function*. SLACK Incorporated, Thorofare.

Piepho, H. P., Büchse, A., and Emrich, K. (2003). A hitchhiker's guide to mixed models for randomized experiments. *Journal of Agronomy and Crop Science*, 189:310–322.

Ramsay, J. O. (1982). When the data are functions. *Psychometrika*, 47:379–396.

Ramsay, J. O. and Silverman, B. W. (2005). *Functional Data Analysis*. Springer, New York, Second edition.

Richards, J. (2008). *Biomechanics in Clinic and Research*. Churchill Livingstone/Elsevier, New York.

Riesz, F. and Szökefalvi-Nagy, B. (1955). *Functional Analysis*. Frederick Ungar, New York.

Ritchie, J., Lewis, J., McNaughton Nicholls, C., and Ormston, R. (2014). *Qualitative Research Practice: a Guide for Social Science Students & Researchers*. SAGE, London, Second edition.

Ryan, W., Harrison, A., and Hayes, K. (2006). Functional data analysis of knee joint kinematics in the vertical jump. *Sports Biomechanics*, 5:121–138.

Saks, S. and Banach, S. (1937). *Theory of the Integral*. Stechert, New York.

Satterthwaite, F. E. (1941). Synthesis of variance. *Psychometrika*, 6:309–316.

Satterthwaite, F. E. (1946). An approximate distribution of estimates of variance components. *Biometrics Bulletin*, 2:110–114.

Sharan, D. (2017). Orthopedic surgery in cerebral palsy: Instructional course lecture. *Indian Journal of Orthopaedics*, 51:240–255.

Shen, Q. and Faraway, J. (2004). An F test for linear models with functional responses. *Statistica Sinica*, 14:1239–1257.

Shou, H., Zipunnikov, V., Crainiceanu, C. M., and Greven, S. (2015). Structured functional principal component analysis. *Biometrics*, 71:247–257.

Simon, S. R. (2004). Quantification of human motion: gait analysis - benefits and limitations to its application to clinical problems. *Journal of Biomechanics*, 37:1869–1880.

Song, J. J., Deng, W., Lee, H.-J., and Kwon, D. (2008). Optimal classification for time-course gene expression data using functional data analysis. *Computational Biology and Chemistry*, 32:426–432.

Staicu, A.-M., Crainiceanu, C. M., and Carroll, R. J. (2010). Fast methods for spatially correlated multilevel functional data. *Biostatistics*, 11:177–194.

Staicu, A.-M., Lahiri, S. N., and Carroll, R. J. (2015). Significance tests for functional data with complex dependence structure. *Journal of Statistical Planning and Inference*, 156:1–13.

Staicu, A.-M., Li, Y., Crainiceanu, C. M., and Ruppert, D. (2014). Likelihood ratio tests for dependent data with applications to longitudinal and functional data analysis. *Scandinavian Journal of Statistics*, 41:932–949.

Steinwender, G., Saraph, V., Scheiber, S., Zwick, E. B., Uitz, C., and Hackl, K. (2000). Intrasubject repeatability of gait analysis data in normal and spastic children. *Clinical Biomechanics*, 15:134–139.

Sutherland, D. H., Olshen, R. A., Biden, E. N., and Wyatt, M. P. (1988). *The Development of Mature Walking*. Mac Keith Press, Oxford.

Tjur, T. (1984). Analysis of variance models in orthogonal designs. *International Statistical Review*, 52:33–65.

Toro, B., Nester, C. J., and Farren, P. C. (2003). The status of gait assessment among physiotherapists in the United Kingdom. *Archives of Physical Medicine and Rehabilitation*, 84:1878–1884.

Ullah, S. and Finch, C. F. (2013). Applications of functional data analysis: a systematic review. *BMC Medical Research Methodology*, 13:43.

Vsevolozhskaya, O. A., Greenwood, M. C., Powell, S. L., and Zaykin, D. V. (2015). Resampling-based multiple comparison procedure with application to point-wise testing with functional data. *Environmental and Ecological Statistics*, 22:45–59.

Wang, J.-L., Chiou, J.-M., and Müller, H.-G. (2016). Functional data analysis. *Annual Review of Statistics and Its Application*, 3:257–295.

Welch, B. L. (1947). The generalization of 'Student's' problem when several different population variances are involved. *Biometrika*, 34:28–35.

Whittle, M. W. (2007). *Gait Analysis: an Introduction*. Elsevier, Oxford, Fourth edition.

Wingstrand, M., Hägglund, G., and Rodby-Bousquet, E. (2014). Ankle-foot orthoses in children with cerebral palsy: a cross sectional population based study of 2200 children. *BMC Musculoskeletal Disorders*, 15:327.

Zhang, B. and Großmann, H. (2016). Functional data analysis in designed experiments. In *mODa 11-Advances in Model-Oriented Design and Analysis*, pages 235–242. Springer.

Zhang, B., Twycross-Lewis, R., Großmann, H., and Morrissey, D. (2017). Testing gait with ankle-foot orthoses in children with cerebral palsy by using functional mixed-effects analysis of variance. *Scientific Reports*, 7:11081.

Zhang, J.-T. (2005). Approximate and asymptotic distributions of chi-squared-type mixtures with applications. *Journal of the American Statistical Association*, 100:273–285.

Zhang, J.-T. (2013). *Analysis of Variance for Functional Data*. CRC Press, New York.

Zhang, J.-T. and Chen, J. (2007). Statistical inferences for functional data. *The Annals of Statistics*, 35:1052–1079.

Zhang, J.-T. and Liang, X. (2014). One-way ANOVA for functional data via globalizing the pointwise F-test. *Scandinavian Journal of Statistics*, 41:51–71.